Auditory Processing Deficits in Mouse Models of Developmental Disorders

Jane Mattley

UCL Ear Institute

Declaration

I, Jane Mattley, confirm that the work presented in this thesis is my own. Where information has been derived from other sources, I confirm that this has been indicated in the thesis.

Signed  ……..

11th March 2020

Date ……

Abstract

BXSB/MpJ-*Yaa* mice are a model of neurodevelopmental disorders where some animals have cortical malformations, called ectopia. Mice with ectopias are impaired at detecting short gaps in noise compared to the mice without ectopias both behaviourally and neurally in auditory thalamus (Anderson & Linden, 2016; Clark, et al., 2000; Frenkel et al., 2000). We made auditory brainstem recordings (ABRs) and extracellular recordings in the inferior colliculus (IC). Central IC cells were found to have shorter gap-detection thresholds in ectopic compared to non-ectopic mice. ABRs suggest there is no difference between auditory processing in early area of the auditory pathway. Histological analysis suggests the deficit does not arise in auditory cortex or thalamus. So the deficit appears to arise in the IC or between IC and thalamus.

Additionally, we investigate auditory processing in KO mice for two genes associated with the neurodevelopmental disorder, dyslexia. We performed ABRs on these mice and found suprathreshold changes in some ABR waves which appears to be more severe in a KO mouse for both candidate genes. So in some animal models of neurodevelopmental disorders deficits in auditory processing can arise early in the auditory pathway below the level of IC.

Acknowledgements

Many thanks to my supervisor, Professor Linden, for the support, patience and never ending enthusiasm to help me complete this dissertation. Thanks also to Lucy Anderson for training me in electrophysiology and histology and letting constantly quote her work. Thank you to Luiz Guidi for a productive 'short' collaboration. Thank you to Fraya Harrison for her contribution to the cortical thickness analysis. Finally, thank you to my family for 'putting-up with me'.

Impact Statement

The findings in this thesis ultimately provide further understanding on disruptions of auditory processing in neurodevelopmental disorders. This work is important in trying to understand the exact disruption in auditory processing in neurodevelopmental disorders may then lead to the development of drugs or devices to help elevate the issues. Furthermore, this work is a further demonstration of auditory processing other than deafness per se. and how and why these can occur in animal models of neurodevelopmental disorders

Ethics

All animal work contained within this dissertation was completed under the United Kingdom Animals (Scientific Procedures) Act of 1986. A personal licence from the UK Home Office was held by all researchers involved and all work was conducted under a Project Licence held by Professor Jennifer F. Linden.

Contents

Introduction

Hearing difficulties affect around 1 in 6 people in the UK (Facts and Figures, 2018), however this number is based on the idea that people with a hearing loss have an abnormal audiogram. We know it is possible from conditions such as hidden hearing loss and auditory processing disorder (APD), that it is possible to have a normal audiogram but have problems hearing and this number is likely to be much higher and more importantly is likely to be detrimental factor in the education of a significant number of children and therefore an important area of investigation. Moreover, studying these conditions in humans can be complicated, has to use indirect measures and can therefore lead to variable results. This is why in this thesis I have chosen to study mouse models neurodevelopmental disorders in order to try to understand the changes in the auditory brain that may underlie these disorders.

In this thesis I mostly focus on a mouse model of neurodevelopmental disorders called BXSB/MpJ-*Yaa* mouse, which was chosen as it is known to spontaneously develop cortical laminar abnormalities similar to those observed in humans with dyslexia and other developmental disorders. The use of a mouse model allows direct investigation using extracellular recordings and histological techniques which would not be possible in humans. Finally, I will investigate a genetic mouse model(s) for 2 candidate genes associated with dyslexia (a neurodevelopmental disorder) using auditory brainstem response (ABR) recordings in order to identify any abnormalities in the auditory brainstem of these mice.

Overview of the auditory system

The ability of the auditory system to not only hear a sound but to extract information from that sound extraordinary. For example, imagine I told you to close your eyes, while I drop an unknown object. Hearing only a brief sound of impact, you are likely to estimate the location, size, weight and composition of the object, all from the noise alone.

As the object is dropped, upon impact, the object will vibrate creating rarefactions and compressions in the molecules in the air resulting in sound waves which travel through the air and enter your ear, being amplified and filtered by the convolutions of the pinna and enter the meatus (ear canal; figure 1). The initial transfer of information from the ear to the brain can be thought of a series of dominos falling. As the sound travels down the meatus it reaches the tympanic membrane (ear drum) and causes it to vibrate which, in turn, moves the ossicles (small bones in the inner ear) which deflect the round window of the cochlea. This deflection moves the fluid within the cochlea, activating the receptive cells, called hair cells, which, in turn, activate the auditory nerve fibres.

From the auditory nerve, information is transferred to the brainstem nuclei and in turn sends the information to the midbrain and eventually to the auditory cortex; each of these central auditory processing stages is discussed further below. From the auditory cortex the information is also send to other cortical and non-cortical areas, including feeding back to the ascending brain areas. Below is a more detailed description of this brief overview.

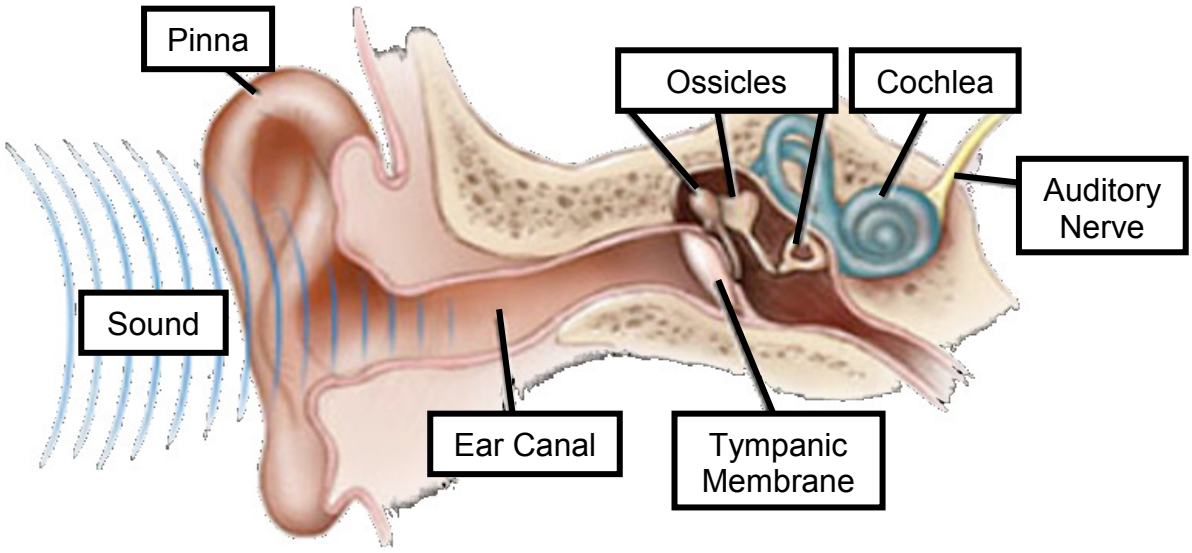

Figure 1: Diagram showing cross-section of the ear. Sound enters the ear via the ear canal which is funnelled by the pinna. The sound vibrations (fluctuations in air pressure) cause the tympanic membrane to vibrate resulting in movement of the ossicles. This movement of the ossicles, result in movement of the fluids inside the cochlea and ultimately activation of the auditory nerve which connects to the higher auditory nuclei of the auditory pathway within the brain. Modified from: http://www.ohniww.org/acoustic-trauma-how-loud-noises-can-damage-hearing/

The Inner Ear

As the sound hits the tympanic membrane of the inner ear, the deflections of the air cause it to vibrate. This vibration causes a chain reaction within the ear. The movement of the tympanic membrane causes the small bones of the inner ear, call the ossicles, to move which, in turn, press on the round window (a small round membrane) of the main structure of the inner ear, called the cochlea. The cochlea is a coiled structure encased in a bony labyrinth. The properties of the cochlea mean it acts as a frequency analyser, where frequencies are separated with each frequency having a place of maximal vibration along the cochlea, with high frequencies towards the base of the cochlea and low frequencies towards the apex. As the sound activates the cochlea vibrations of the basilar membrane within the cochlea lead to activation of the cochlea's sensory hair cells which in turn send the information to the

brain via the auditory nerve, where the frequency separation of the cochlea is preserved.

The auditory brainstem

From the auditory nerve the first stop, within the brain, is the cochlear nucleus (figure 2). The cochlear nucleus is made up of different cell types which have distinct morphology and are grouped in location within the cochlear nucleus. These different cell types are thought to be important in determining information from different parts of the sound; for example, octopus cells are detect sound onsets whereas sperical bushy cells enhance phase locking.

The cochlear nucleus is primarily divided into two main subdivisions: ventral and dorsal cochlea nuclei each of which process the sound information from the auditory nerve and project to different brain areas. The ventral cochlea nucleus can be further divided, based cell type, into the anteroventral cochlea nucleus (AVCN) and posteroventral cochlea nucleus. Since the auditory nerve fibres preserve the frequency separation of the cochlea, the fibres terminate in the cochlea nucleus in a tonotopic manner. The ventral and dorsal subdivisions project onto different areas of the brain, with the ventral subdivision projecting to superior olivary nucleus and the dorsal subdivision projecting to the inferior colliculus.

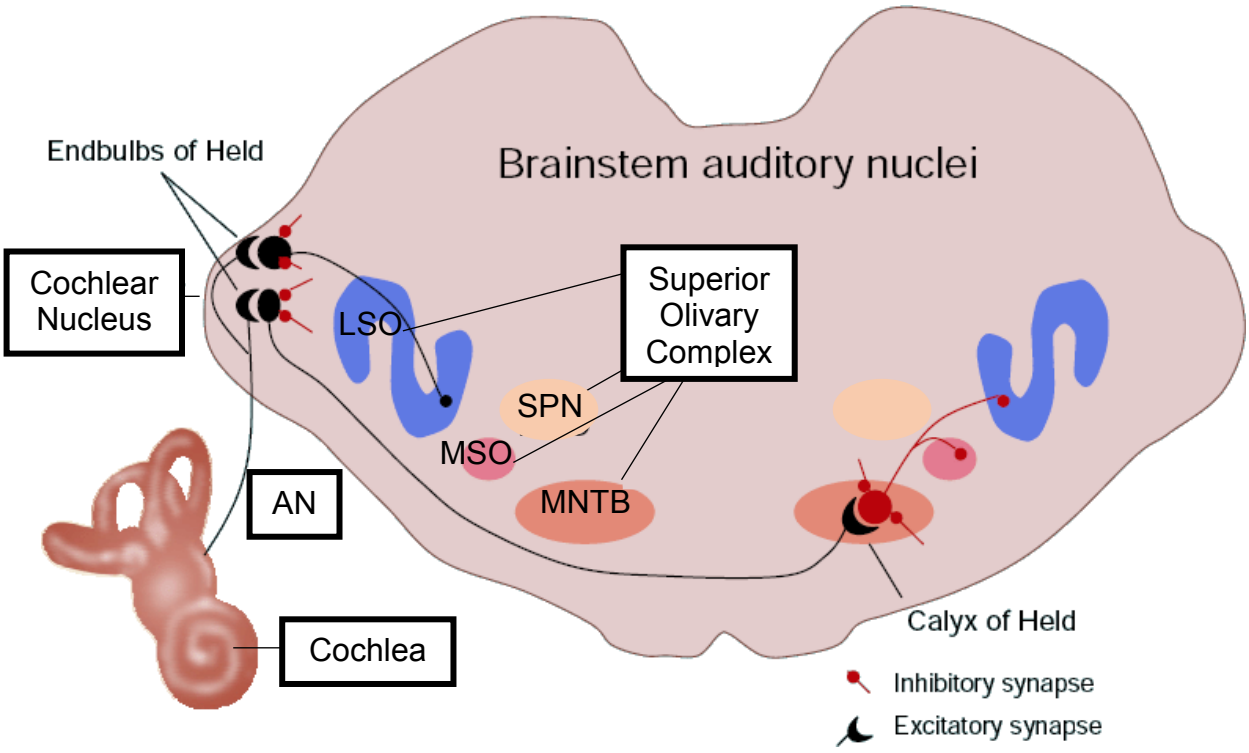

Figure 2: Diagram showing auditory brainstem nuclei. Auditory nerve (AN) signals resulting from transduction of the cochlea to the cochlear nucleus via excitatory connections. After the cochlear nucleus, excitatory neurons connect to the superior olivary complex. The superior olivary complex is comprises the lateral superior olivary nucleus (LSO), medial superior olivary nucleus (MSO), superior paraolivary nucleus (SPN) and the medial nucleus of the trapezoid body (MNTB). These nuclei are involved in sound localisation and project to the inferior colliculus in the midbrain. Adapted from: http://www.cs.stir.ac.uk/~bpg/research/syntran.html.

Superior olivary nucleus

The superior olivary nucleus is the first binaural nucleus. Sound information converges from inputs from both ears in both the lateral superior olivary nucleus (LSO) and medial superior olivary nucleus (MSO; figure 2). The LSO is important for processing interaural level differences, where differences in sound levels between the two ear whereas the MSO processes interaural time differences which is the differencing the timing of between the two ears, both of which are used to identify the location of a sound source. MSO projects to the ipsilateral inferior colliculus and LSO projects bilaterally to the central IC nuclei.

Inferior Colliculus

The information which has been processed by the lower auditory areas converge on the Inferior Colliculus (IC). The IC is functionally important in sound localisation and for the detection of pitch. Like other areas of the brain, the inferior colliculus can be divided into subdivisions, the main ones are central IC which is surrounded by dorsal and lateral IC subdivisions (Duque, et al. 2015). Although, the exact borders of the subdivisions are disputed and differ across species (Loftus et al., 2008). As well as receiving inputs from lower auditory brain nuclei, the IC also receives inputs from higher brain areas such as auditory cortex (figures 3 and 4). Central IC tends to have mostly inputs from lower brain areas whereas dorsal IC tends to be most influenced by descending projections. IC projects to the auditory thalamus and also has descending projections to SOC and CNC. Central IC projects mostly to ventral MGB in mostly a tonotopic manner.

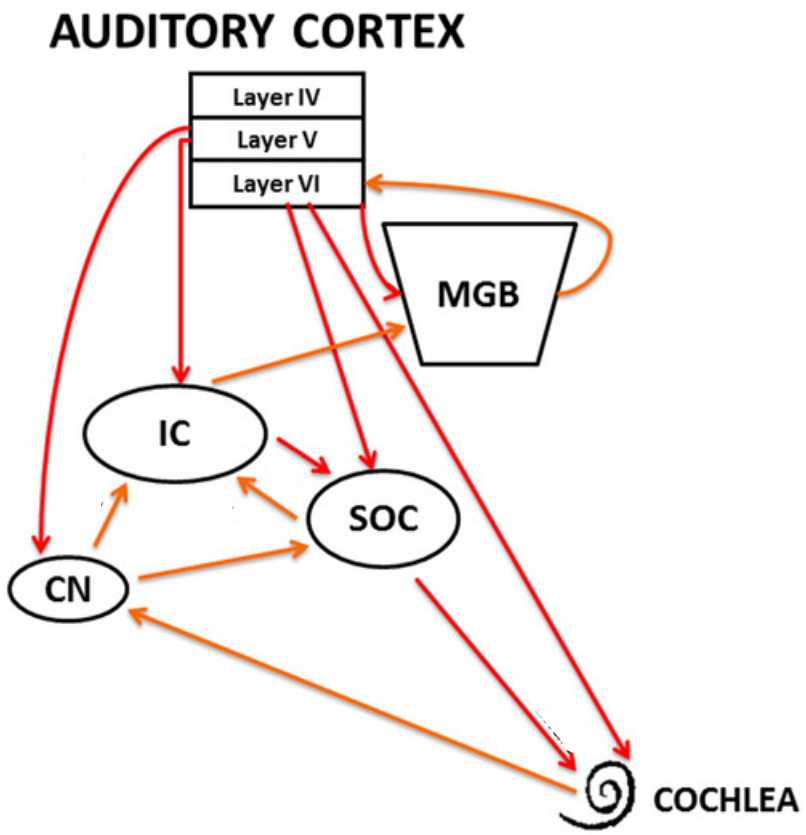

Figure 3: Schematic showing auditory pathway nuclei together with main feedforward and feedback connections. When auditory information has reached the cochlear nucleus (CN) from the cochlea via the auditory nerve. The CN then projects to the superior olivary complex (SOC), feedforward connections transport the information the inferior colliculus within the midbrain which, in turn, projects to the auditory thalamus (medial geniculate body; MGB). The MGB then projects to layer VI of the auditory cortex. Auditory cortex projects to higher auditory and non-auditory areas of the brain. Feedback connections exist throughout the auditory pathway mostly from the auditory cortex to the lower areas of the auditory pathway. Adapted from: http://journals.plos.org/plosone/article?id=10.1371/journal.pone.0155991

Medial Geniculate Body

The medial geniculate body (MGB) acts as a gate between IC and auditory cortex (figures 3 and 4). MGB has 3 main subdivisions: ventral, dorsal and medial (Anderson et al. 2011). Ventral MGB is organised tonotopically and thought to be important for relaying frequency, intensity and binaural information to the cortex. Dorsal MGB is thought to be important for processing complex stimuli and medial MGB is thought to process multi modal information (Weiner, 1992).

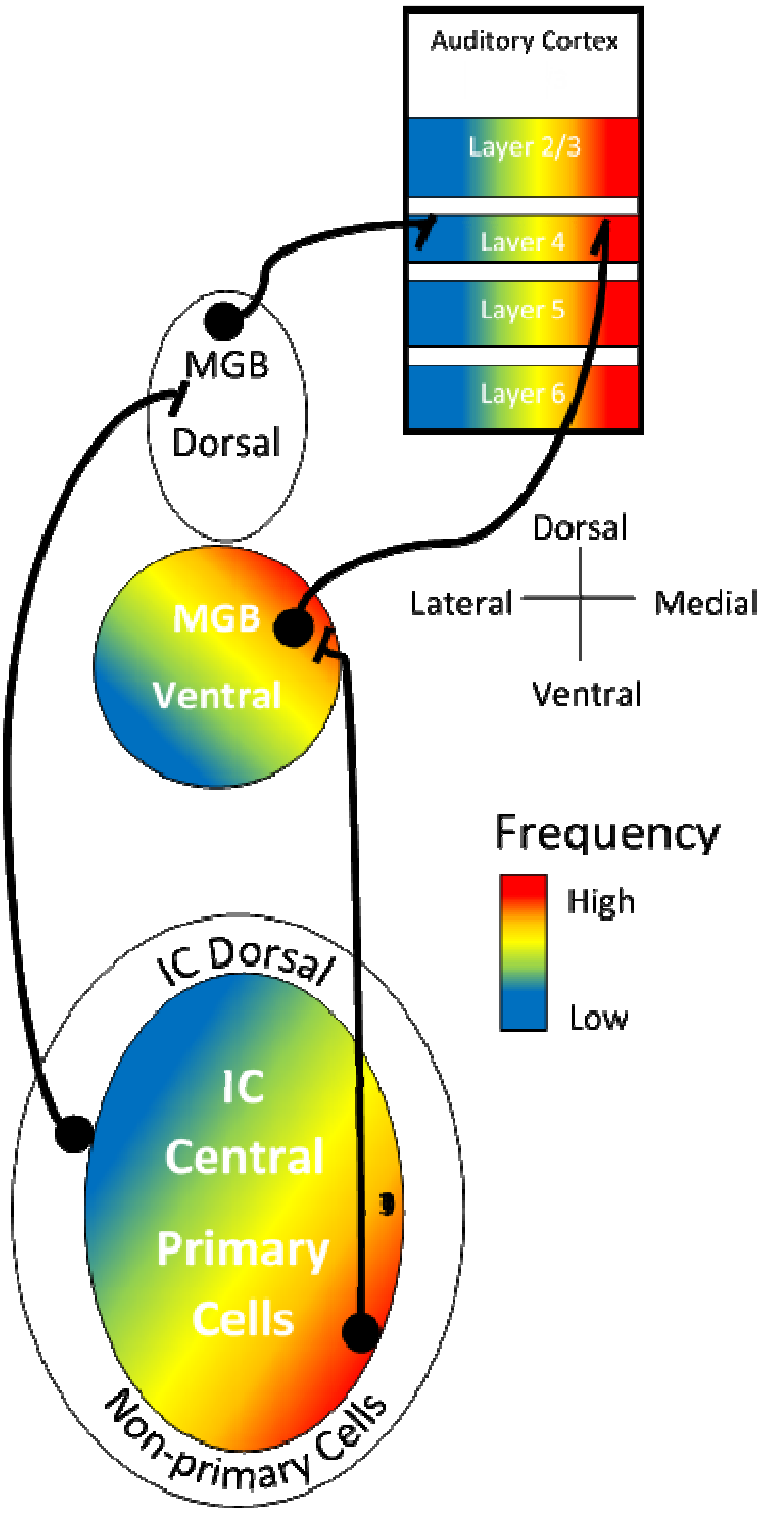

Figure 4: Schematic showing auditory pathway from IC to auditory cortex together with main connections.
Information in IC is forwarded to MGB. With central IC projecting to ventral MGB and later IC connecting to dorsal MGB. MGB then connects to auditory cortex via layer 4. Tonotopy is preserved throughout the central IC -> ventral MGB -> auditory cortex route and is indicated in coloured shading on the schematic.

Auditory cortex

Auditory cortex consists of areas that are specialised for a particular function. It is made up of core, belt and parabelt areas. Auditory cortex has a number of descending projections to areas lower in the auditory pathway (figures 3 and 4). Core auditory cortex is activated mostly by simple sounds whereas complex sounds

mostly activate belt and parabelt areas. Core auditory cortex primarily received inputs from auditory thalamus and is tonotopically organised. It connects to both core and belt areas. The belt area of auditory cortex receives primary thalamic input and is also tonoptically organised and connects to all auditory cortex areas. The parabelt region of auditory cortex does not receive primary thalamic input and is tonotopic. It connects to the belt, parabelt and other cortical areas (King et al. 2018). Like other areas of the cortex, the auditory cortex has 6 clearly defined layers which can be identified using Nissl stained sections (Sakata and Harris, 2009).

Auditory Brainstem Response

The auditory brainstem response (ABR) is an EEG measurement which can be used to quickly and minimally invasively record the voltages produced by neural activity in the brainstem nuclei of the auditory pathway. These small voltages are often buried in other non-auditory voltage changes and are therefore typically detected by presenting a stimulus many times and averaging the result. ABRs are measured using 3 subdermal electrodes which are used as 2 recording channels and a ground (Akil, 2016; figure 5).

In response to a stimulus an ABR waveform is obtained (figure 5), from this waveform a number of measures can be made in order to determine the functioning of the early parts of the auditory pathway. The waveform is made up of a number of waves but the most easily seen and most commonly measured waves are waves I-V. The origin of each of these waves is thought to represent different nuclei within the early auditory system. In mice, wave I is thought to arise in the cochlea or auditory nerve, wave II in the cochlea nucleus, wave III in the trapizoid body or superior olivary complex, wave IV in the superior olivary complex to IC and wave V

in the IC (Henry J. Am. Aud. Soc 1979). Although the exact origin of the waves is controversial and seems to defer between species.

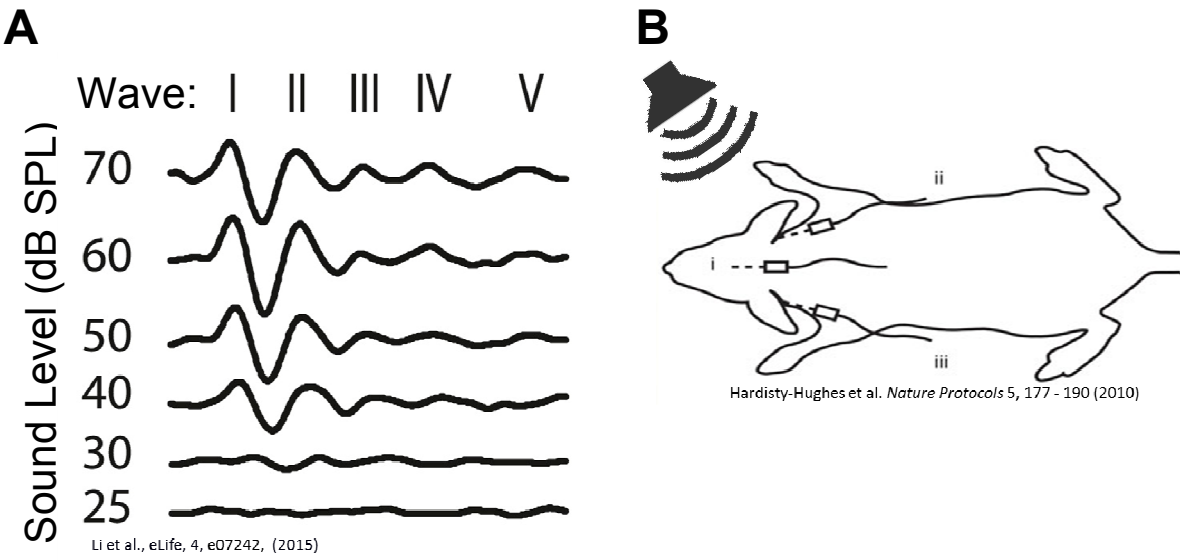

Figure 5: Auditory brainstem response (ABR) wave locations and ABR electrode placement. (A) Demonstrates ABR at different sound levels together with location of waves I-V of the ABR. The earlier ABR waves (waves I and II) are usually the largest deflections when the ABR electrodes are in the positions indicated (B). The ABR threshold is determined by looking at the ABR with the responses plotted at different sound levels (as in A) and identifying the lowest sound level where 2 clear waves can be seen. In this example the threshold would be set at 30dB SPL. Wave I of the ABR is thought to arise from the auditory nerve; wave II from the cochlear nucleus; wave III from the superior olivary complex; wave IV from the connection between the superior olivary complex and inferior colliculus and wave V from the inferior colliculus itself (Henry J. Am. Aud. Soc 1979). (B) Schematic showing ABR electrode placement in relation to the mouse. Three electrodes are used for the ABR recordings consisting of two recording electrodes (i and ii) and a ground (iii).

From the recorded data, the most common measure is the ABR threshold which is used as a determinant of hearing sensitivity. Most commonly for this measurement many trials of clicks are played at different sound levels and the threshold is the lowest sound level where a response to the stimulus can be detected. The exact method of doing this varies, for example, some people define the threshold as two clear ABR waves, whereas others identify the first significant wave 1 response.

As well as ABR thresholds, the individual wave amplitudes and latencies can be measured in order to give an estimate of the amount of firing or amount of synchronous firing within the particular nucleus (Zhou et al., 2006).

Temporal processing within the auditory system (gap detection)

Many biologically relevant sounds have a temporal component, for example speech, music and animal vocalisations. There are a number of commonly used stimuli that researchers use in order to probe how the auditory system processes temporal information. One of the main stimuli used is gap detection task, which is a sound where a gap, usually silence, is presented. Usually, gaps of different lengths are presented in order to determine the short gap that can be detected, the gap-detection threshold. Gap detection seems to rely on the frequency of the sound and the intensity of the sound, with longer gap-detection threshold in animals as the sound intensity is decreased (Radziwon et al. 2009).

Studies in rats have shown that if the auditory cortex is inactivated either through lesioning or chemical inactivation, the animal's behavioural gap-detection threshold is elevated or extinguished (Syka et al., 2003). Although there was some recovery after one or two months, the gap-detection thresholds remained elevated.

When salicylate was used to inactivate GABA neurons, the authors found elevated behavioural gap detection thresholds 1 hour after injection and the gap-detection thresholds recovered to normal levels 1 day after injection for low but not high sound intensities. Also, auditory cortical responses to gap-in-noise stimuli showed elevated neural gap-detection thresholds 1-3 hours after salicylate injection with full recovery after one day; however the thresholds were not elevated within IC (Deng, et al.,

2010). These results provide further evidence for a key role for auditory cortex in gap detection.

Furthermore, gap-detection ability is known to decline with age in humans (Humes et al., 2009; Poth et al. 2001), mice (Barsz et al. 2002) and gerbils (Hamann et al. 2004) although not in rats; see Friedman et al.(Friedman et al. 2004). This decline in gap-detection ability with age is thought to be due to abnormal age-related changes in brain levels of GABA. When Gleich et al. gave gerbils a drug to prevent the break-down of GABA they found that the gap-detection thresholds were reduced, meaning increasing the amount of GABA allows the animals to detect smaller gaps in noise (Gleich et al. 2003). However, when this group gave a GABA mimetic drug to old and young gerbils, they found no effect on gap-detection and forward-masking thresholds in the old animals and no effect on gap-detection thresholds in the young animals, but elevated forward masking thresholds in young animals, meaning the animals needed a louder probe following the masker to detect the probe. This result is contradictory to the idea of increased GABA levels leading to better performance on gap-detection and forward-masking tasks. The authors suggest the difference in these studies is due to the amount of increase GABA in the brain using the drug used in the previous study being around 88% (in rats) and in latter study the increase being only approximately 12%(Gleich and Strutz 2011); however this explanation does not account for the contradictory findings.

Gap-detection ability is thought to be reduced in neurodevelopmental disorders including autism (Bhatara et al. 2013), dyslexia (Van Ingelghem et al. 2001) and auditory processing disorders (Phillips, Comeau, and Andrus 2010). Some of the results of these studies are mixed; for example, in humans with dyslexia compared to controls, 7 out of 10 different studies found no significant difference for gap-

detection thresholds (Hämäläinen, Salminen, and Leppänen 2012). However, the variability in the results may be due to differences in gap-detection ability with age, as one study found a difference in gap-detection thresholds for dyslexic versus control subjects at 6-8 years old but not 10-11 years old (Hämäläinen, Salminen, and Leppänen 2012).

In short, behavioural studies in both humans and animals have suggested that gap detection involves central auditory processing, that inhibitory neurotransmission may play a particularly important role and that mechanisms of dap detection are somehow disrupted in neurodevelopmental disorders and aging.

Neuroanatomical abnormalities in humans

In 1979 Albert Galaburda wrote a case study on a male patient with a history of developmental dyslexia who had subsequently died, and whose brain had been stained for histological analysis. In this paper Galaburda reported the presence of polymicrogyria and dysplasia in the areas of the brain known to be involved in language processing.(Galaburda and Kemper 1979). Galaburda then went on to show similar cytoarchitectural abnormalities in other brains from humans with developmental dyslexia in both males and females (Galaburda et al. 1985, Humphreys, Kaufmann, and Galaburda 1990). It should be noted, however, that some of these patients also had specific language impairments (SLI) as well as dyslexia. Moreover, similar cortical malformations have since been observed in brains of patients with other neurodevelopmental disorders including epilepsy (Ramus 2004) . Therefore the most accurate interpretation of the previous work is likely to be that cortical microabnormalitites are commonly associated with neurodevelopmental disorders in general, not specifically with dyslexia.

Animal models of human neuroanatomical abnormalities

Spontaneously occurring neuroanatomical abnormalities

Spontaneously occurring ectopias are found in several strains of mice including the common laboratory strains C57Bl/6 and C57Bl/10 (Sherman and Holmes 1999; Lipoff et al. 2011). A number of inbred stains of mice have been shown to exhibit ectopias more frequently. In the immune-defective New Zealand Black (NZB) strain, approximately 40% of the mice have ectopias which can be found in somatosensory or motor cortices (Sherman et al. 1992; Sherman et al. 1985). Work on this animal model has shown these mice have abnormal radial glial fibres in and around the ectopic areas of the cortex. Around the ectopia the radial glial cells were found to be less numerous and in the ectopia they were found to be disorganised. This study further showed that the glial membrane was breached in the ectopic cortex and this may explain why the cell bodies from lower layers 'over-migrate' to cortical layer I (Sherman et al. 1992). Tracing studies on this mouse model (and a different mouse model: NXSM-D/EiJ) show that fibres from the ectopia extend to deep layers of the cortex and then divide into projections to the corpus callosum and internal capsule together with connections to several areas of the thalamus. They also found ipsilateral but not contralateral connections from the ectopia to somatosensory and motor cortex (Jenner et al., 2000).

One paper on NZB mice indicates that auditory processing may be impaired in ectopic animals. Fitch et al. showed the NZB mice with ectopias have a behavioural impairment in detecting short but not long embedded tones (Peiffer et al. 2001). Another paper on the NZB model has also shown that the behavioural deficits in ectopic animals can be eliminated or at least ameliorated by raising the mice in an enriched environment (Schrott et al. 1992).

An important mouse model of spontaneously occurring neocortical abnormalities is the BXSB/MpJ-*Yaa* mouse. BXSB/MpJ-*Yaa* mice are males of the BXSB/MpJ strain; these animals carry the Y-chromosome-associated autoimmune acceleration gene that accelerates the autoimmune disease existent within the strain (Sherman et al. 1987, Schrott et al. 1993). Approximately half of the BXSB/MpJ-*Yaa* mice (and 20% of female BXSB/MpJ mice) develop cortical ectopias. This means this strain of mouse has a built-in control the 'mutant' animals being the animals with ectopias ('ectopic mice') and the remaining animals without ectopias ('non-ectopic mice').

BXSB/MpJ-Yaa mice with ectopias have been shown to have differences in performance on learning tasks compared to their non-ectopic littermates (Hyde et al. 2001). Ectopic animals actually perform better on spatial and non-spatial reference memory tasks than non-ectopic littermates, but if the ectopia is located in prefrontal cortex (which is known to be involved in behavioural flexibility) then the ectopic mice have a deficit in ability to switch between the two tasks (Hyde et al. 2002). However, since there was a two-day gap in testing, the observed deficit could have arisen from a problem with memory rather than behavioural flexibility although another study has shown that ectopic mice can have greater retention on some memory tasks, supporting the interpretation of the deficit as arising from impaired behavioural flexibility (Boehm et al. 1996).

Previous work suggests the presence of ectopias is also associated with deficits in auditory processing. BXSB/MpJ-*Yaa* mice with ectopia have been found to have a behavioural deficit when processing short gaps but not long gaps in noise compared to non-ectopic BXSB/MpJ-Yaa mice (Clark, et al. 2000). Similarly Frenkel et al. showed BXSB/MpJ-Yaa mice with ectopia have reduced auditory evoked potentials

compared to non-ectopic mice, for stimuli consisting of tones separated by a short-duration tone of a different frequency (Frenkel et al. 2000).

Recent work from the Anderson and Linden revealed ectopic BXSB/MpJ-*Yaa* mice have a deficit in thalamic responses to brief gaps in noise, with fewer cells in MGB responding to short gaps in noise in ectopic compared to non-ectopic mice (Anderson and Linden 2016). Interestingly, this work shows that while it was previously thought gap-detection deficits reflect an overall sluggishness in auditory processing of rapidly changing sounds, the thalamic gap-detection deficit is not arising from a problem with rapid temporal processing, as there is no deficit in thalamic responses to rapid click trains. Instead the thalamic gap-detection deficit appears to arise from a more specific problem: reduced neural activity following noise offsets. Consistent with this conclusion, thalamic responses to clicks and other stimuli presented in a silent background are normal but ectopic mice do have reduced neural responses to a click following noise.

Induced neuroanatomical abnormalities

As well as naturally occurring neuroanatomical abnormalities a form of induced microgria in rats has been studied and suggested to be analogous to the spontaneously occurring cortical microabnormalities in the mouse models. An induced microgyria is created by taking a freezing probe and placing it on the skull cap of a rat pup (Threlkeld et al. 2006). In adulthood these animals have microgyria near the site of the freezing lesions induced during development. Behavioural work with this animal model has demonstrated that animals with induced microgyria have impaired rapid auditory processing compared to sham controls (Threlkeld et al. 2006, Herman et al. 1997, Clark, et al. 2000, Fitch et al. 1980) and the behavioural effects were not limited to working memory as spatial memory has also been shown to be

affected in lesioned rats (Threlkeld et al. 2012). Furthermore, neurophysiological deficits in auditory cortical processing of rapidly changing sounds have been demonstrated in rats with induced microgyria (Escabí et al. 2007).

Study of this animal model also showed male lesioned animals had more small and fewer large neurons within dorsal MGB (Herman et al. 1997). In another study looking at the effects of induced cortical lesions, the ventrobasal area of the thalamus was found to show a decrease in the number and nuclear volume of neurons in the animals with induced lesions compared to sham controls; interestingly, there were no differences in overall number or volume of neurons in the dorsal lateral geniculate nucleus (LGN) and MGB (Rosen et al. 2006). However, the study did report more small cells and fewer large cells within both ventrobasal complex and MGB but not dorsal LGN (Rosen et al. 2006). Interestingly, these changes seem to be associated with the male steroid hormone testosterone; androgenised females (which have been treated with testosterone) exhibit the same MGB shift to more small cells and fewer large cells when they have a freezing lesion whereas untreated female mice do not show this shift (Rosen et al., 1999).

These effects did not seem to be evident in non-androgenised females with induced microgyria, suggesting perhaps that testosterone might make the central auditory system more vulnerable to developmental perturbations. However an alternative explanation is that the gender-specific results may be due to age at which the lesions were induced, since male and female brains may have a different developmental trajectory (Fitch et al. 1997).

Importantly, these experiments show that the age of the freezing injury determines the outcome; lesions induced at P1-3 produce microgyria and alterations in brain

weight (Peiffer et al. 2003) and cortical volume, while lesions induced on P5 did not result in such alterations (Threlkeld et al. 2007). Moreover, while P1-3 animals had impaired processing of rapidly changing sounds as juveniles, this deficit did not last into adulthood except in the animals that were lesioned on P1 (Threlkeld et al. 2007).

Project Aims

The work contained in this report aims to investigate the BXSB/MpJ-*Yaa* mouse model in order to further explore the finding of shorter gap-detection thresholds within MGB (Anderson and Linden 2016). This will be achieved by both histological and extracellular techniques. First, I will examine the anatomy of the thalamus for changes in cell density and nuclei volume, together with layer thickness within auditory cortex, I will attempt characterise the ectopics, in size, number, location and cell types. In the extracellular studies I will record from inferior colliculus which projects to MGB in order to investigate potential deficits lower down in the auditory pathway. I will used the ABR to investigate lower areas of the auditory pathway. Finally, I use the ABR in order to probe potential auditory deficits in a genetic knockout mouse model(s) for key dyslexia genes to further examine auditory processing in other mouse models of neurodevelopmental disorders.

Chapter 1 - Characterisation of Ectopias

Abstract

BXSB/MpJ-Yaa mice have been shown to develop neocortical abnormalities called ectopias, which are small nests of neurons most evident in cortical layer I. Here we attempt to characterise ectopias in BXSB/MpJ-Yaa mice by measuring the location, volume and number of ectopia together with the type of cells they contain. We found that approximately 50% of male BXSB/MpJ-Yaa mice have ectopias and that most ectopic animals had a single ectopia in the motor cortex and the cells contained with the ectopia are a mix of both neurons and glia. Cortical layer markers indicated the cells in the ectopia are formed from the more superficial of the cortex, not from the deeper cortical layers indicating the ectopia is formed by a bursting up of cells probably as a result of some small injury to the limiting membrane during neuronal migration.

Introduction

Spontaneously occurring ectopias are found in several strains of mice including the common laboratory strains C57Bl/6 and C57Bl/10 (Lipoff et al. 2011). A number of inbred stains of mice have been shown to exhibit ectopias more frequently. In the immune-defective New Zealand Black (NZB) strain, approximately 40% of the mice have ectopias which can be found in somatosensory or motor cortices (Schrott et al. 1992). Work on this animal model has shown these mice have abnormal radial glial fibres in and around the ectopic areas of the cortex. Around the ectopia the radial glial cells were found to be less numerous and in the ectopia they were found to be

disorganised (Sherman et al. 1992). This study further showed that the glial membrane was breached in the ectopic cortex and this may explain why the cell bodies from lower layers 'over-migrate' to layer I. Tracing studies on this mouse model (and a different mouse model: NXSM-D/EiJ) show that fibres from the ectopia extend to deep layers of the cortex and then divide into projections to the corpus callosum and internal capsule together with connections to several areas of the thalamus (Gabel, 2011). They also found ipsilateral but not contralateral connections from the ectopia to somatosensory and motor cortex.

Ectopias or ectopia-like malformations can also be induced, for example in newborn rats placing a freezing probe on the skull leads to an ectopia-like cortical abnormality (Humphreys et al. 1991; Threlkeld et al. 2006). Induced as well as spontaneously occurring ectopias are thought to arise from damage to the external glial limiting membrane or superficial plexiform layer, resulting in the barrier to migration being disrupted and hence the cells 'over migrate' (Rosen et al. 1992).

Another mouse model of spontaneously occurring neocortical abnormalities is the BXSB-MpJ mouse model. BXSB/MpJ-Yaa mice are males of the BXSB/MpJ strain; these animals carry the Y-chromosome-associated autoimmune acceleration gene that accelerates the autoimmune disease existent within the strain. Approximately half of the BXSB/MpJ-Yaa mice (and 20% of female BXSB/MpJ mice) develop cortical ectopias. There has been limited research on the cell type composition of the ectopias within this stain and the work completed in this chapter is an attempts to start to address this problem. Here we analysis the cells origins of ectopias in BXSB/MpJ-Yaa mice, together with frequency, cell numbers, location and size of ectopias. We find around 50% of BXSB/MpJ-Yaa mice have a single ectopia although they can be multiple in a single brain. The ectopias are always frontal in

origin and generally located around the motor cortex. The cells found in the ectopias seems to be from the upper cortical layers consistent with the idea that the ectopia is formed by a 'bursting' up of the superficial layers into layer I but different to the findings from the NXSMD/EiJ mouse where ectopias in this mouse model are formed from cells from the both supragranualar and infragranular layers (Gabel, 2011).

Note the immunohistochemical staining detailed in this chapter was performed by Jane Mattley together with Luiz Guidi from Oxford University. Sectioning was performed by Jane Mattley. Staining was performed by both Luiz Guidi and Jane Mattley. Imaging of the immunohistochemical staining was performed by Luiz Guidi. Analysis and presentation of the images was performed by Jane Mattley. All other work detailed in the chapter was performed by Jane Mattley.

Methods

Histological processing

Animals were overdosed with sodium pentobarbital and perfused transcardially with 4% paraformaldehyde. The brain was removed and post-fixed in 4% paraformaldehyde for 12 hours, then sliced on a vibratome into 50 µm sections. The alternate sections were mounted on polarised glass slides (SuperPlus Frost) and Nissl substance was revealed using cresyl violet after defatting with a mixture of chloroform, rising in Histoclear and dehydrating through a series of alcohol rises. After staining and rehydrating, slides were cover-fixed, using DPX as a mounting medium. The remaining alternate sections were stored free-floating in 1xPBS at 4℃ until immunohistochemical staining as described below.

The brains of 26 BXSB/MpJ-Yaa (males) were used for ectopia incidence, location, areas and cell counts.

Immunohistochemistry

Alternate sections containing an ectopia were identified from 4 mice in the previously stained Nissl sections. These sections were then double immunological stained using the antibodies listed in table 1. All sections were also counterstained with DAPI.

Table 1: Primary antibodies used in immunohistochemical staining.

Target	**Marker**	**Host species**	**Dilution**	**Supplier**
Cux1	Layer II-IV	rabbit	1:500	Santa Cruz, sc-28185
Brn2	Layer II/II + L5b	goat	1:500	Santa Cruz sc-6029
Foxp2	L6	rabbit	1:500	Abcam, ab16046
PV	Parvalbumin interneurons	rabbit	1:500	Swant PV28
Iba1	Microglia	goat	1:500	ab5076; Abcam
GFAP	Astrocytes	rabbit	1:500	Sigma, G9269

For immunohistochemical preparation, 50µm coronal free-floating sections were rinsed in 1XPBS followed by 2 hours in blocking solution (donkey serum (3%), 1XPBS with 0.1% Triton-X). This was followed by further rinsing in 1XPBS (3 times for 10 minutes each). The sections were then incubated in primary antibody, diluted in blocking solution (primary antibody details and concentration given in table 1) for 24 hours at 4℃ with light shaking. Following primary antibody incubation the sections were rinsed in 1XPBS 3 times for 10 minutes. The sections were then incubated in the appropriate secondary antibody (table 2) for 2 hours at room

temperature. Finally the sections were rinsed in 1XPBS, 3 times for 10 minutes, mounted on slides, covered with mounting solution containing DAPI and cover-slipped (ProLong Gold mounting medium Molecular Probes).

Table 2: Secondary antibodies used for immunohistochemical staining.

Secondary antibody	**Supplier**	**Dilution**
Donkey α Goat IgG Alexa 568	Alexa Fluor A-11057	1:500
Donkey α Rabbit IgG*Alexa 488	Alexa Fluor A-21206	1:500

Image Processing

After staining, sections stained for Nissl were imaged on a Zeiss AxioPlan 2 Imaging microscope at 100 times magnification. An RGB image of each section showing the ectopia was acquired using a Zeiss AxioCam HRc camera. Immunostained images were captured using a confocal laser-scanning microscope at 200 times magnification (Leica TCP SP8).

Ectopia volumes

For the ectopic animals, the ectopia volume was calculated from the individual areas using the Nissl stained section using ImageJ to mark the borders of the neocortical ectopia using the polygon selection tool, this selection was then used to obtain the area of the ectopia for each section using the ImageJ routine for measuring areas (figure 6). From the areas and thickness of each section was used for the calculation of the ectopia volume and was corrected for overestimation using Cavaleri's rule (Rosen and Harry 1990).

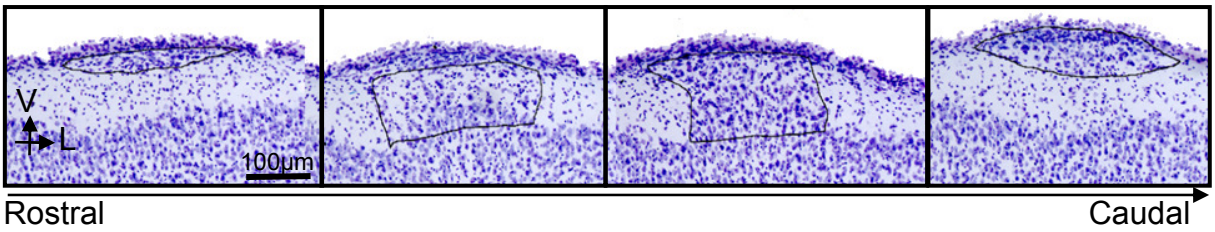

Figure 6: Sections of single neocortical ectopia with border drawn for area calculation. Image shows ventral most layers of cortex, mostly layer I where the ectopia is most visible as a dense collection of cell bodies and the surrounding layer I is mostly free of cell bodies compared to the lower layers. Coronal sections, 50µm thick, were taken throughout the cortex. Each section was stained for Nissl bodies which reveal the cell bodies of cells. After sectioning, staining and mounting, all sections were analysed under a microscope to check for the presence of an ectopia. If an ectopia was found in a section(s), the observation was noted and images were acquired and saved (at 100 times magnification) for all the sections where the ectopia was visible. These images were then analysed in ImageJ which was used to draw and borders from which the areas were measured. The area of visible ectopia from each section was used to determine the volume of the ectopic using Cavaleri's rule.

Ectopia cell counts

Manual cell counts were performed on 7 of the 13 ectopic brains. ImageJ was used to track the manually identified cells from the Nissl sections (figure 7).

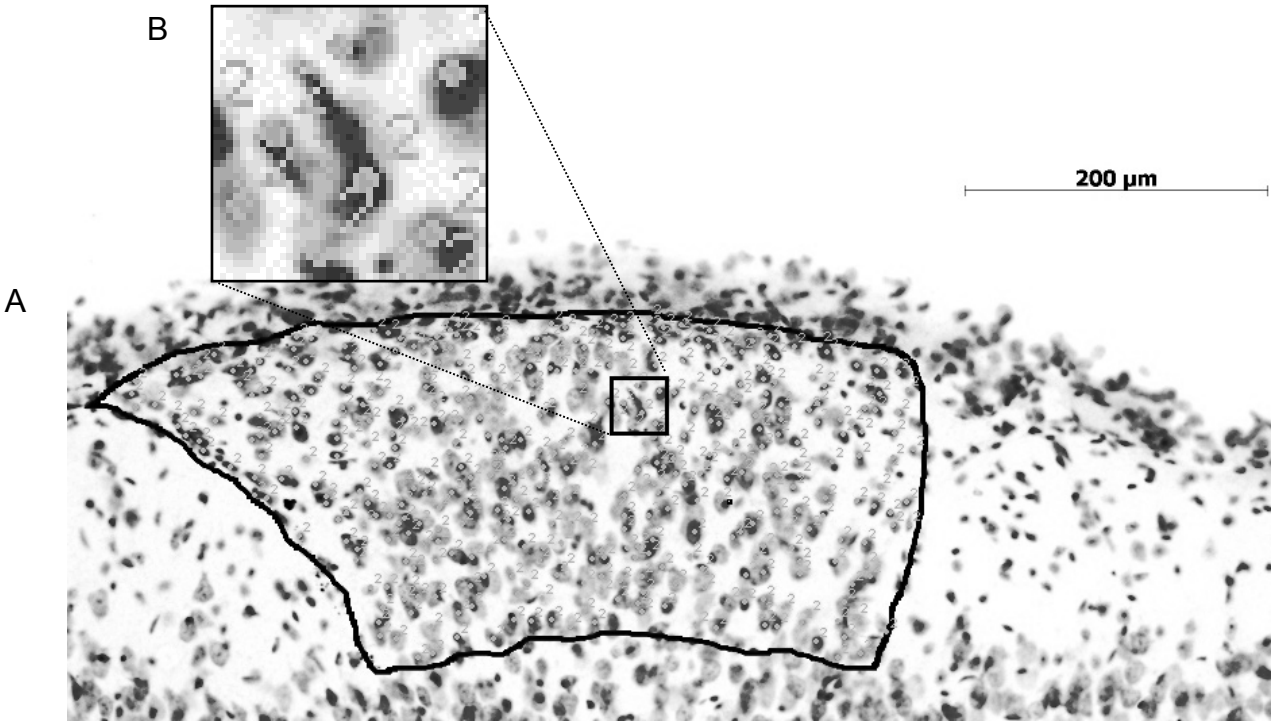

Figure 7: Ectopia with border drawn for area calculation and cells counted for cell counts. A) Entire counted ectopia. B) Enlarged section showing of ectopia showing cell bodies marked for cell counts. Images were obtained into ImageJ as in figure 6. Images were manually inspected and each potential cell body was marked and counted using an inbuilt ImageJ routine which gave a final overall cell count for that section. This was performed on each section where the ectopia was visible and the total across sections was used as an estimate of the total number of cells within the ectopia.

Analysis

All data was exported from ImageJ into Microsoft Excel spreadsheets and read into Matlab, which was used to plot and analyse the data.

Results

Brains from 26 male BXSB/MpJ mice were processed for histology to obtain 50-micron coronal sections spanning the entire neocortex. Alternate sections stained for Nissl substance were examined for evidence of ectopic cell bodies in layer I of the neocortex.

Ectopias found in approximately 50% of BXSB male mice

Out of 26 male BXSB/MpJ mice used for this study, 13 were found to have at least one neocortical ectopia, suggesting an incidence of approximately 50%. Further analysis of ectopia characteristics was performed on data from 10 ectopic animals.

Mostly one ectopia per animal but a single animal can have multiple ectopias

In almost all cases (9 of 13 animals), ectopic mice were found to have a single ectopia (Figure 1). Three ectopic mice were found to have two ectopia and only one ectopic animal had six ectopia.

Ectopias found mostly in or around motor cortex but vary in exact location

In all animals with a single ectopia, the ectopia was located within primary motor cortex (M1; Figure 1). In the ectopic mice with two ectopia one ectopia from each animal was found in motor cortex and the other ectopias were found in other frontal locations. In the one animal with six ectopias three ectopic were found in M1 and three were found in dorsolateral orbital cortex, piriform cortex and somatosensory cortex. In this animal three ectopia were found in the left hemisphere (two in M1 and one in somatosensory cortex) and three ectopic were found in the right hemisphere

(one in M1, one in dorsolateral orbital cortex and one in piriform cortex). In the remaining ectopic animals half had ectopias in left hemisphere and half had ectopias in right hemisphere

Ectopias vary in size between different ectopic mice

Note 2 of the 13 ectopic mice had damaged to some of the ectopic sections and were therefore excluded from the subsequently volume and cell count analysis. Also brains with more than one ectopia included giving total number of volumes from of 20 ectopias. Ectopia volume was quantified as described in Methods, by outlining areas of layer I encompassing ectopic cell bodies in sections stained for Nissl substance, and computing volume from areas in successive sections. Ectopia volume ranged from 0.001 to 0.036 mm^3, with the largest ectopia occurring in the one animal with multiple ectopias. For animals with only one ectopia, mean ± SE of ectopia volume was 0.013 ± 0.004 mm^3. In the animal with multiple ectopia, the mean volume of these ectopia was 0.013 mm^3 (figure 8).

Larger ectopias contain a larger number of cells

Note cells counts were performed from Nissl sections therefore may include glia as well as neurons in the cell counts. Also, cells counts were only performed on 7 of the 13 ectopic brains (9 ectopias cell counted). We found a correlation between ectopia cells counts and volume (figure 9; pairwise linear correlation p=0.016) as might be expected the number of cells found in an ectopia increases in line with the volume of the ectopia. This indicates the ectopia volume provides a good measure of cell displacement for an ectopia.

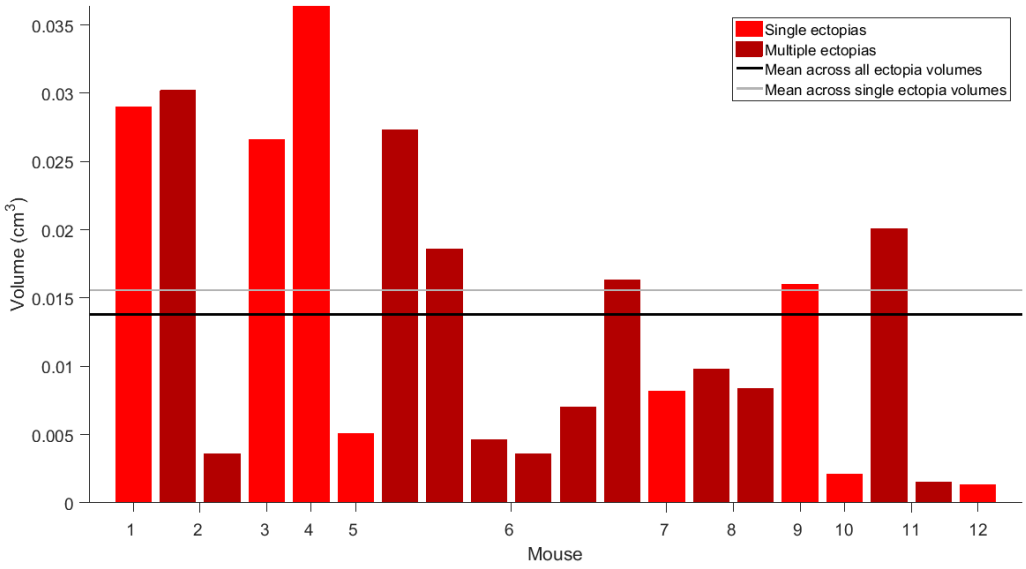

Figure 8: Range of ectopic sizes found in BSXB ectopic mice. Bar chart showing ectopia volumes obtained from each ectopic BXSB/MpJ-*Yaa* mouse used in the ectopic volume calculations. Ectopia volumes were obtained as described in figure 6 (n=12). Most mice were found to have a single ectopia but some mice were found to have multiple ectopias. Ectopia volumes ranged sized from 0.001 to 0.036 mm^3. Mice with a single ectopia are shown in bright red, mice with multiple ectopias are shown in dark red. Grey line indicates the mean ectopia volume calculated across all mice with a single ectopia. Black line indicates the mean ectopia volume across all mice.

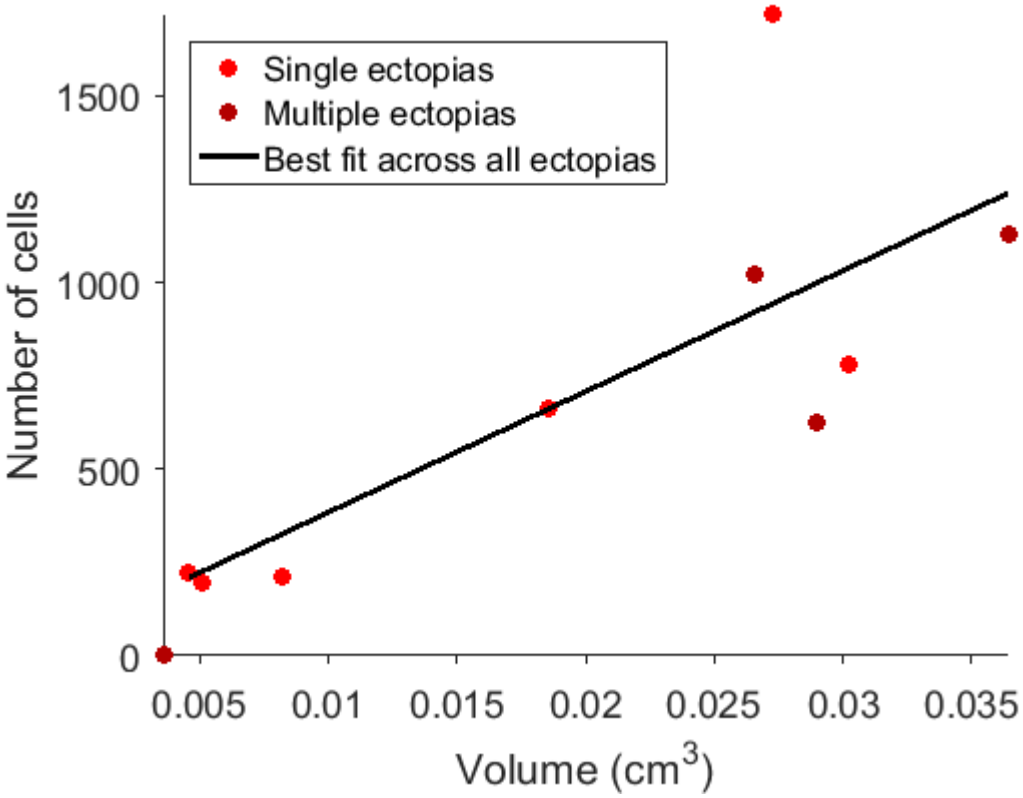

Figure 9: Plot showing there is a significant correlation between ectopia volume and ectopia cell counts. As the volume of the ectopia increases, the number of cells found within the ectopia increased. This indicates a larger ectopia means a larger number of cells rather than each ectopia containing a fixed number of cells with increased spacing between them. Volume and cell number estimates were obtained as described in figure 6 and 7 respectively. Light red indicates ectopias from animals with a single ectopia. Dark red indicates ectopias from animals with multiple ectopias. Black line indicates line of best fit.

Ectopias contain a mix of both glia and neurons from the underlying superficial cortical layers

PV+ cells were found within the ectopia (see figure 10). This section shows the presence of PV+ interneurons within the ectopia. These PV+ cells co-localised well with DAPI indicating they are actual cells and not just artefacts. This is consistent with the idea that in an ectopia lower layers are 'burst-up' into upper layers.

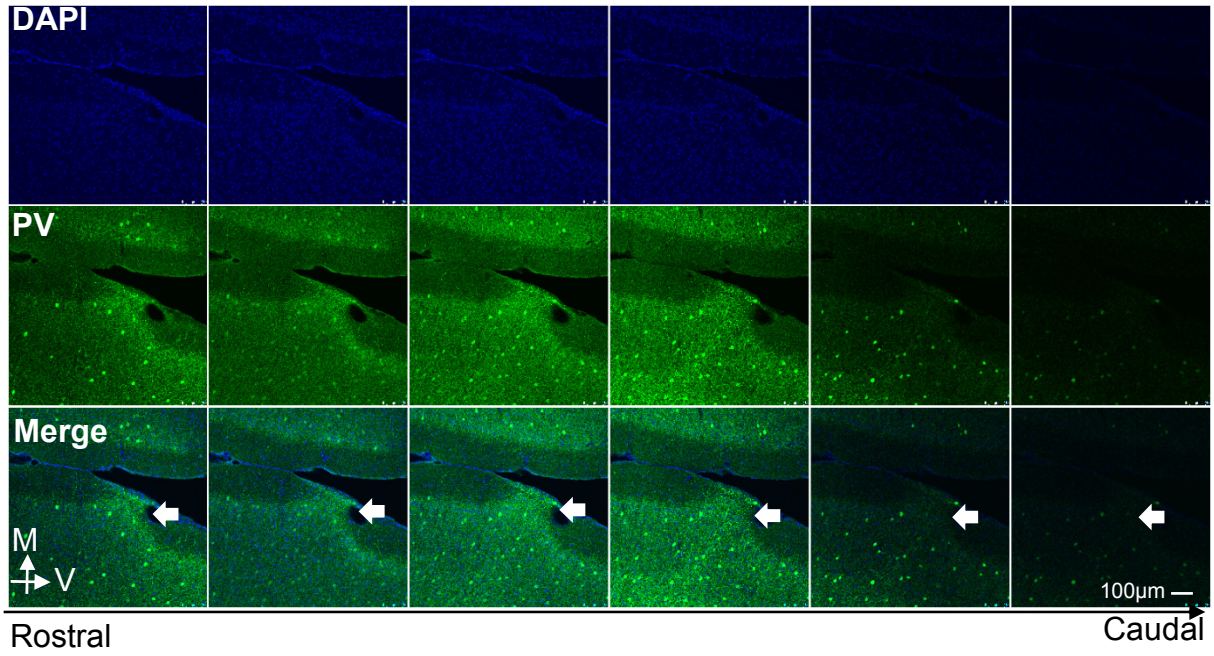

Figure 10: PV cells are found in ectopia. Immunohistochemical images of coronal sections showing the presence of an ectopia correlates with the presence of interneurons in layer I of the cortex which is typically free from of interneurons. Successive images from 50µm section containing ectopia stained for DAPI (top row; a marker for DNA found within cell bodies), PV+ cells (middle row; a marker for interneurons) and the merge of these images (bottom row) showing the PV staining correlates with the DAPI so the staining is from actual cells rather than histological artefacts. White arrows indicate ectopia location on merged images. Note contrast of images increased 40% to aid visualisation.

Stained sections containing Iba1+ cells (indicating microglia) were obtained from one ectopia sections (figure 11). These figures show that there seems to be an increased number of microglia within (and possibly surrounding) the ectopia compared with the adjacent layer I. This and the previous result provides evidence that ectopias contain a mixture of both glia and neurons.

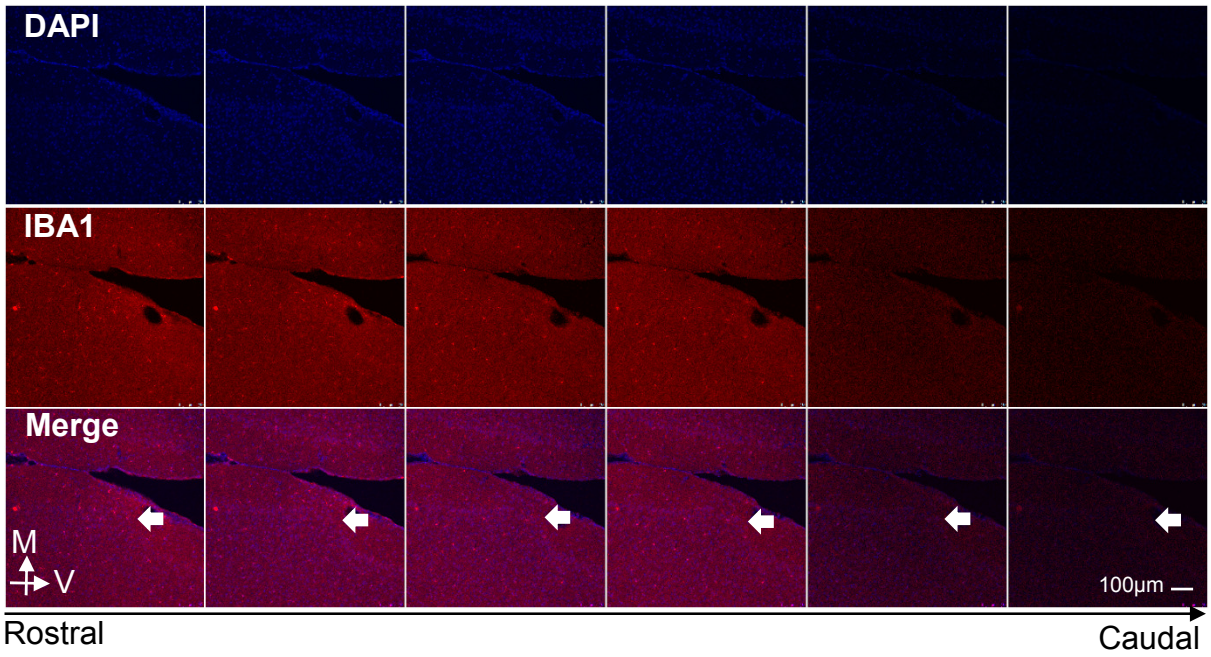

Figure 11: Microglia found in ectopia. Immunohoistochemical images showing the presence of microglia within an ectopia. Successive images from 50µm section containing ectopia stained for DAPI (top row; stains DNA), Iba1+ cells (middle row; marker for microglia) and the merge (bottom row) indicating the microglia correlate with the DAPI staining and are therefore are actual cells rather than artefacts. White arrow indicates ectopia location on merged images. Note brightness of images increased 20% and contrast reduced 40% to aid visualisation.

One ectopic section was stained for Cux1+ cells indicating cortical layers II-IV neurons are found within the ectopia (see figure 12). The Cux1+ cells can be seen as a pushing up of layer II into layer I in support of the hypothesis that ectopic cells are 'pushed-up' from lower layers.

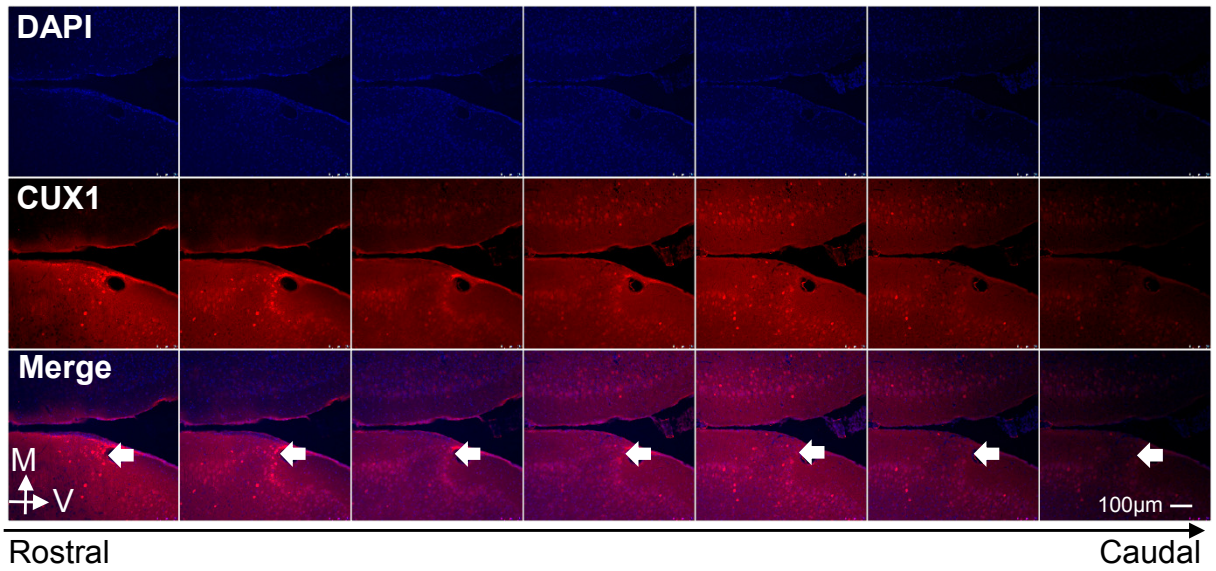

Figure 12: Layer II-IV cells found in ectopia. Immunohistochemical images showing the presence of layer II-IV cells within layer I of an ectopia which is normal free from these cells. Top row shows coronal sections stained for DAPI (marker for DNA), middle row shows same sections counter stained for Cux1+ cells (maker for layer II-IV cells). Bottom row shows merge of DAPI and Cux1 staining. White arrow indicates ectopia location on merged images. Note brightness of images increased 20% and contrast reduced 40% to aid visualisation.

One ectopic section was stained for GFAP+ cells indicating the presence of astrocytes within the ectopia (see figure 13). This indicates there are also astrocytes present within the ectopia.

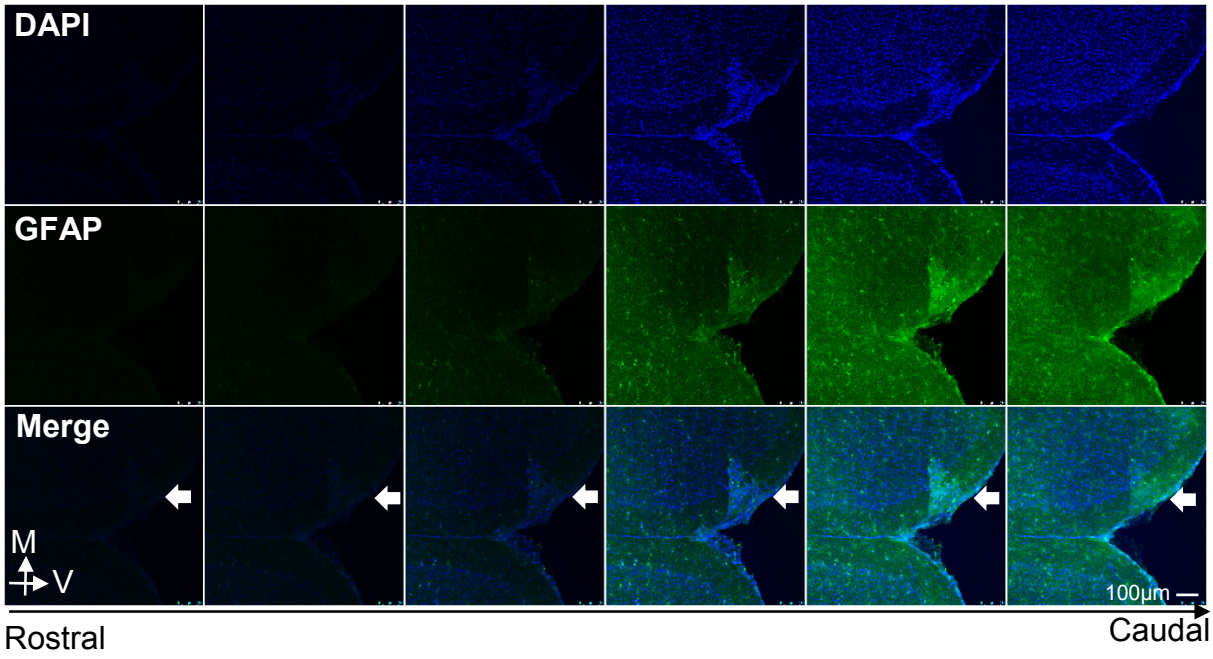

Figure 13: Astrocytes found in ectopia. Successive immunohistochemical images from 50µm coronal sections showing the presence of astrocytes cells within the ectopia. Top row shows DAPI stained sections (marking DNA), middle row indicates GFAP staining (marker for astrocytes) and bottom row shows a merge indicating that the GFAP staining is correlated with DAPI staining and therefore stains astrocytes rather than histological artefacts. White arrow indicates ectopia location on merged images. Note the presence of background staining which may affect the conclusions from this figure and brightness of images increased 40% to aid visualisation.

One section was stained for Brn2+ cells indicating the presence of layer II/III/5b neurons within the ectopia (see figure 14).

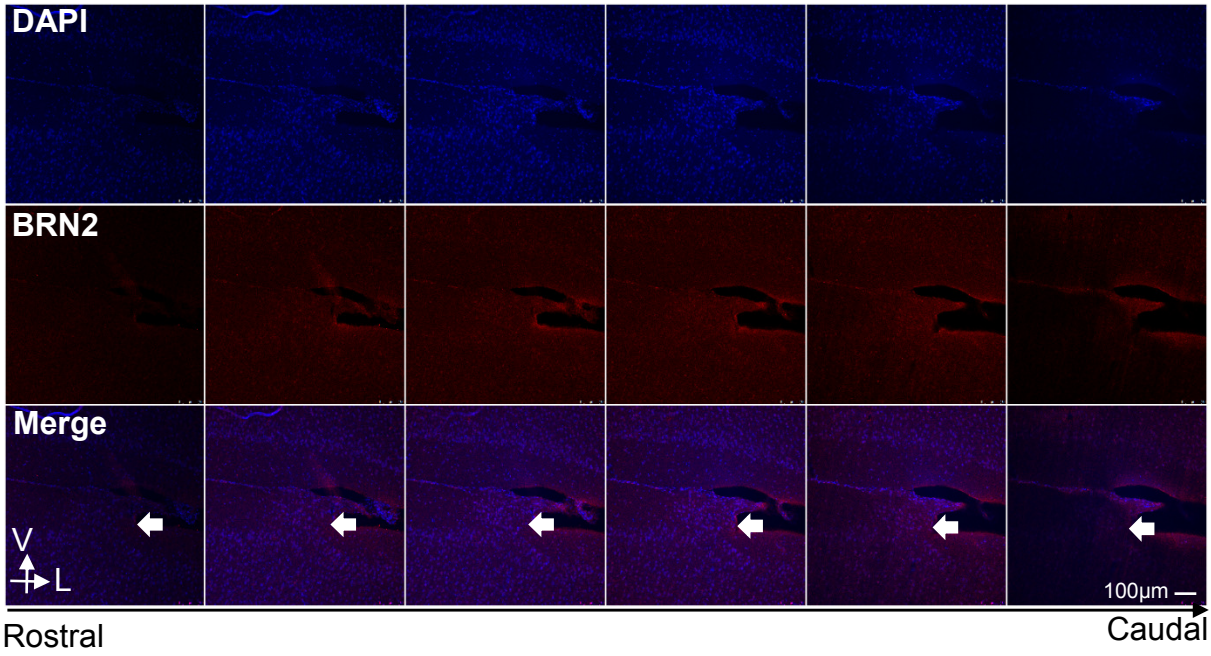

Figure 34: Layer II/III/5B cells found in ectopia. Immunohistochemical images from successive 50µm coronal sections showing the presence of LII/III/5B cells are found within an ectopia. Top shows staining for DAPI (DNA marker), middle row shows staining for Brn2 (a marker for layer II/III/5b cells) and bottom row shows a merge demonstrating the Brn2 staining is correlated with cell bodies. White arrow indicates ectopia location on merged images.

Two sections which were stained for FOXP2+ (cell which are usually found within layer 6) and showed an absence of FOXP2+ cells within the region of the ectopia (see figures 15). An absence of FOXP2+ cells within the region of the ectopia suggests the lower layers of the cortex are not present in the ectopia and confirm the hypothesis that the ectopia is a 'pushing-up' of only the upper layers.

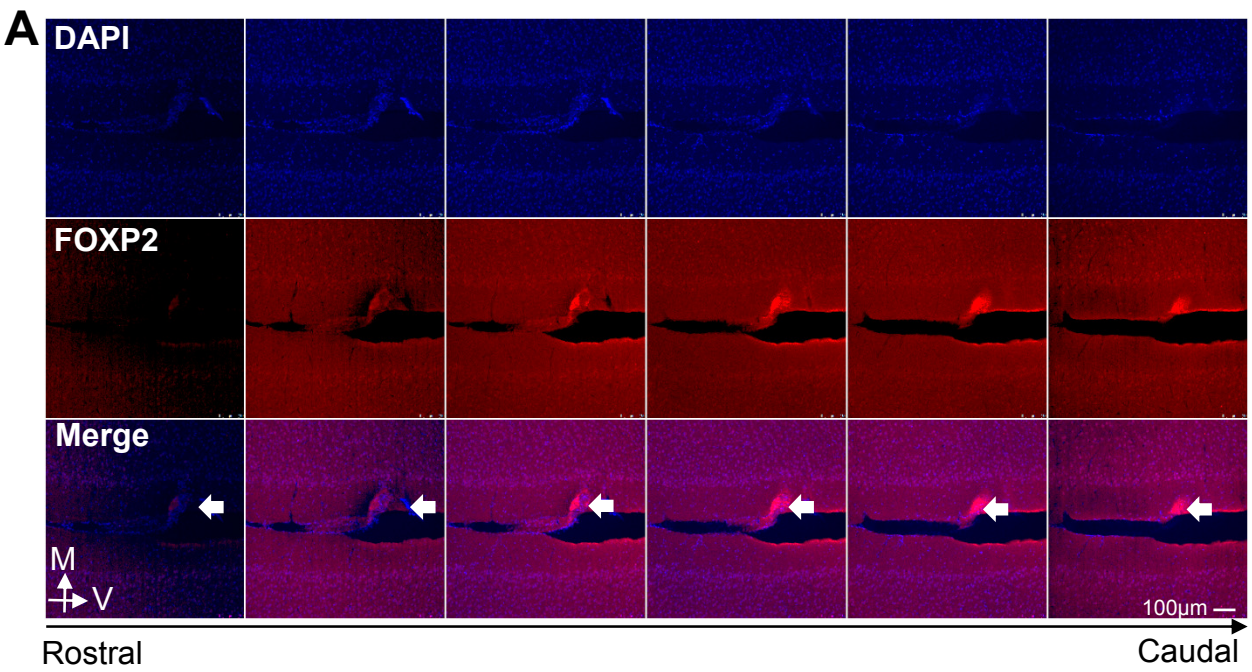

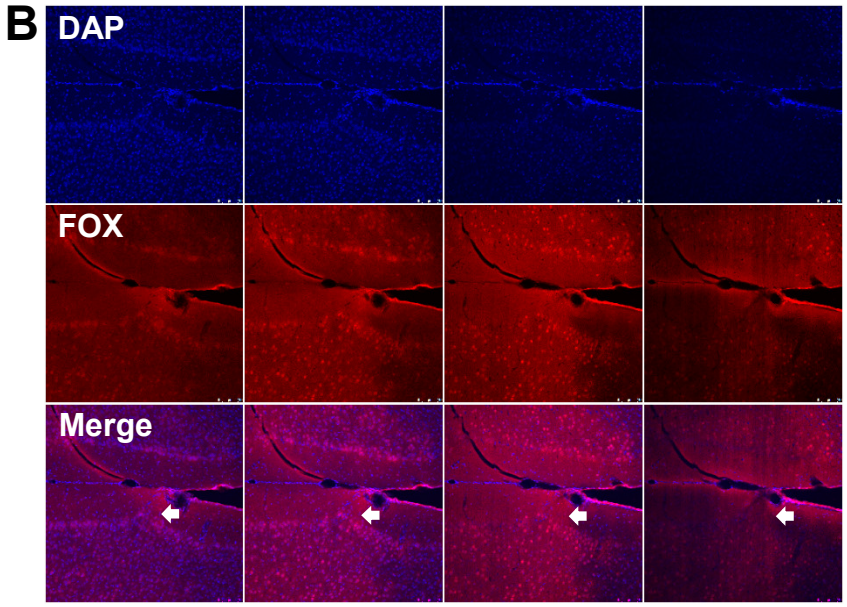

Figure 15: Absence of layer 6 cells in ectopia. Immunohistochemical images from two ectopic mice showing the absence of layer 6 cells in an ectopia. (A) and (B) show successive images from 50µm coronal sections containing ectopia stained for DAPI (top row; DNA marker) FOXP2+ (middle row; marker for layer 6) and merge (bottom row). White arrow indicates ectopia location on merged images. Sections in A and B are taken from different mice. Note brightness of images increased 20% and contrast reduced 40% to aid visualisation.

Discussion

In this chapter we investigate the characteristic features of ectopias. We found most ectopic mice have a single ectopia but an individual mouse can have more than one ectopia. The ectopias were found to occur in approximately 50% of male BXSB mice and tended to be located in or around motor cortex. The volume of ectopias ranged from 0.001 to 0.036 mm^3, with larger the ectopias having a larger number of cells.

The ectopias themselves were found to contain a mix of glia and neurons: PV, microglia, layer II-IV cells, astrocytes, layer II/III/5b cells. The finding that there is an absence of layer 6 cells within ectopias suggests the very lower layers of the cortex are not affected.

This is one of the first studies to specifically look at the characterisation of ectopias in BXSB/MpJ mice. We found ectopic BXSB/MpJ mice generally have a single ectopia though multiple ectopias in the same animal can occur but not as often. Interestingly, ectopia are known to exist in the approximately 10% human brains without dyslexia or other neurological disorders but in the dyslexia brain ectopias are found in higher numbers particularly around the perisylvian gyrus near the language areas of the brain (Ramus, 2004).

Most of the ectopias seem to be located within the M1 though in one animal multiple ectopia were found with half of them existing outside of M1. Ramus has suggested the location of ectopia has an effect on which deficits are present and suggest this could explain the high rate of dyslexia with other neurological disorders such as epilepsy and specific language impairment (Ramus, 2004). Since the previous study on the BXSB/MpJ-Yaa mice had found the ectopic mice have longer neural gap-detection thresholds in the auditory thalamus than the mice without ectopias (Anderson and Linden, 2016), is it possible that a different deficit would be found if the ectopias were located in a different area of the brain? The NZB mice have been found to have ectopias located in somatosensory or motor cortex (Schrott et al., 1992), would the mice with ectopias in motor cortex be impaired in gap-detection whereas the mice ectopias in somatosensory cortex not?

Ectopic cells numbers correlates with volume therefore more displaced cells in larger ectopia not same number of cells but more densely packed. Volume therefore gives a good guide to amount of displacement.

We also found 4 mice had multiple ectopias. A study using freezing lesions to induce ectopia-like malformations showed multiple injuries can arise from a single insult (Rosen and Galaburda, 2000) suggesting the mice with multi-ectopias not be that different to mice with single ectopias, having been exposed to the same genetic or epigenetic insult.

Induced as well as spontaneously occurring ectopias are thought to arise from damage to the external glial limiting membrane or superficial plexiform layer, resulting in the barrier to migration being disrupted and hence the cells 'over migrate' (Rosen et al., 1992). The immunohistochemical results support this idea as were found mostly upper cortical layers within the ectopia but not the deeper cortical layers.

The primary aim of the work presented in this chapter was to perform an initial study into ectopias and their characteristic features. We conclude that male BXSB have a 50% chance of having at least one ectopia and that it will generally be located around motor cortex. Immunohistochemistry reveal the ectopia to contain a both neurons and glia which seem to be from the more superficial layers of the underlying cortex consistent with the theory from other similar animal models of a 'bursting-up' of cells.

Chapter 2 – Macro anatomy

Abstract

In order to try to explain previous observations of differences in gap-detection responses in BXSB/MpJ-Yaa mice, anatomy of two key areas of the auditory pathway were analysed to look for differences in cell size and number. We analysed MGB volumes and pixel density (to give a measure of cell numbers) together with layer thickness of auditory cortex between ectopic and non-ectopic mice and found there were no differences in any of these areas. These results suggest that cell numbers and sized do no differ between ectopic and non-ectopic mice in both MGB and auditory cortex.

Introduction

Previous studies have shown a subsection BXSB/MpJ-Yaa mice experience behavioural deficits when performing gap-detection tasks involving very short but not long gaps in noise (Clark et al., 2000). The mice that exhibit these behavioural deficits have been found to have neocortical migration abnormalities called ectopias where the laminar structure of the outer layers of cortex is disrupted. These ectopia are thought to arise through a developmental thalamocortical abnormality and it has recently been shown that ectopic BXSB/MpJ-Yaa mice have shorter neural gap-detection thresholds to short gaps-in-noise compared to BXSB/MpJ-Yaa mice without ectopias (non-ectopic) within the medial geniculate body (MGB; Anderson and Linden 2016). Interestingly, in humans, ectopias have been associated with neurodevelopmental disorders including dyslexia and have been shown to have a difference in cell density in the MGB of the left hemisphere compared to control

brains where the dyslexic brains were found to have more small cells and fewer large cells (Galaburda et al., 1994). Do these MGB morphological differences also occur within the ectopic animal model?

Previous studies have looked at induced microgyria, which are similar to ectopia but generally involve a much larger disruption of the underlying layers. Microgyria were induced using a freezing probe in neonatal Wistar rats in order to disrupt thalmocortical development (Rosen et al., 1995). These studies have shown that male rats with induced microgyria have deficits in processing gaps in noise for short intervals and a difference in MGB morphology with more small cells and fewer large cells within dorsal MGB (Herman et al., 1997; Escabí et al., 2007; Rosen et al., 1999) and ventrobasal complex in lesioned compared to sham animals (Rosen et al. 2006). Peiffer et al. also found alterations in white matter and overall brain weight in this model (Peiffer et al., 2003).

Whether these morphometric changes also occur within MGB of ectopic BXSB/MpJ-Yaa mice has not yet been studied. This particular model is interesting because the ectopias arise spontaneously compared to the lesion model and is therefore more analogous to the human condition. We aim to look for MGB morphology differences and differences in auditory cortex layer thickness in these animals by comparing MGB volume and cell packing density and auditory cortex layer thickness between ectopic and non-ectopic BXSB/MpJ-Yaa mice. We also look at LGN volumes and cell density as a control, non-auditory, brain area. We found no significant difference between ectopic and non-ectopic animals in MGB or LGN volume, cell packing density or auditory cortex layer thickness either as overall or for any individual cortical layer so the observed difference in gap-detection thresholds between ectopic and non-ectopic BXSB/MpJ-Yaa mice cannot be explained by a difference in cell

size or number in MGB or auditory cortex suggesting neither of these areas in the origin of the deficit.

Methods

Histological processing

Animals were prepared for histological analysis as described in Anderson et al. (2009). In brief, mice were overdosed with sodium pentobarbital and perfused transcardially with 0.1 M phosphate buffer followed by 4% paraformaldehyde. The brain was removed and post-fixed in 4% paraformaldehyde for 12 hours, then sliced on a vibratome into 50 µm sections. The sections were mounted on slides in two alternate series which were stained for either cytochrome oxidase (CYO) or Nissl substance.

To reveal the expression of CYO, slide-mounted sections (within 24 hours of perfusion and slicing) were incubated at 37°C for 3-5 hours in a bath containing 20mg diaminobenzidine hydrochloride in 10ml distilled water together with 30mg cytochrome c, 3g of sucrose in 30ml of 0.1M phosphate buffer. Nissl substance was revealed using cresyl violet, after defatting in a chloroform/alcohol mixture (1:1), and dehydration in a series of alcohols, after cresyl violet and rehydration through a further series of alcohols. All stained sections were cover-slipped using DPX as a mounting medium.

Volume analysis

MGB and LGN subdivision volumes were estimated in 8 ectopic and 8 non-ectopic mice by drawing around the subdivisions in ImageJ on 50µm sections stained for cytochrome oxidase which has been previously used to reveal the MGB subdivisions (Anderson et al., 2007). These borders were used to calculate the area of each

subdivision on each section (figure 18A). All of the areas collected were then used with the section thickness to calculate the volume of the subdivision using Cavalieri's rule to compensate for overestimation (Rosen and Harry, 1990). Subdivision volumes were added to give the total volume. MGB and LGN analysis was completed on 8 ectopic mice and 8 non-ectopic mice for MGB analysis and 7 ectopic and 7 non-ectopic mice for LGN analysis. The researcher was blind to the ectopic status of the mouse during analysis.

Pixel density analysis

Cell density estimation was completed using the density of pixels within an image to make an estimate. A 218 x 172 μm rectangle from Nissl stained sections was photographed at high magnification images (x40) of ventral MGB and a lateral and medial portion of dorsal MGB on three sections from each animal (the caudal most, rostral most and middle sections containing MGB; figure 16) also LGN subdivisions (dorsal and ventral) was completed on the rostral most, caudal most and middle section of the two LGN subdivisions. Pixel density analysis of MGB was performed on 8 ectopic and 8 non-ectopic mice and for LGN on 7 ectopic and 7 non-ectopic mice.

The images were all converted to black and white, the pixel values were normalised to eliminate any background effects and the median of these normalised values were calculated (figure 16). The mean of these medians for each subdivision gave a value defined as the 'tissue density index' which was used to compare the cell densities between ectopic and non-ectopic animals. The researcher was blind to the ectopic status of the mouse during analysis.

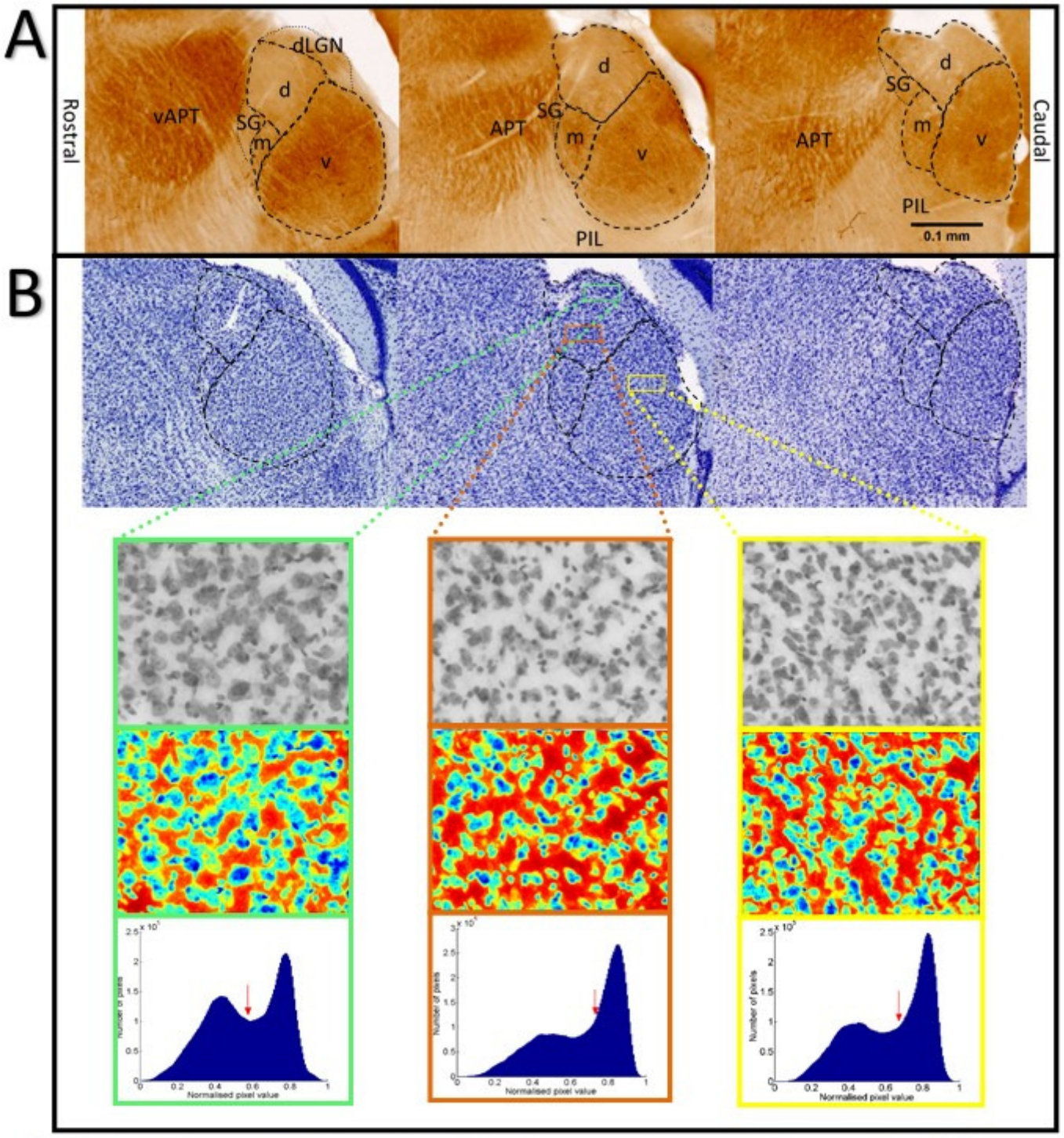

Figure 56: Example of images used for border and cell density estimation. Example images used for cell density estimations showing MGB section borders on CYO images and the borders transferred onto Nissl stained sections together with image portions transformed for pixel density analysis and location of medium pixel density which is used as the cell density measure. (A) Dashed lines indicate different MGB subdivisions (d=dorsal MGB, v=ventral MGB, m=Medial MGB). Note volume estimation was performed on all alternative sections containing MGB/LGN but only 3 sections are shown for ease of display. (B) Top panel example Nissl sections used for pixel density estimation, lower panels shown example conversion to black and white, normalised pixel conversions and histograms of pixels with tissue density index (median value) marked with red arrow.

Cortical Layer thicknesses

For the cortical layer thickness estimations, Nissl stained sections containing auditory cortex were identified and imaged, these images were given to a BSc student who identified the different cortical layers within auditory cortex and used ImageJ to make measurements of the layer thickness. We used 3 sections containing auditory cortex per mouse (rostral most section, middle most sections and caudal most section). Images were taken using Zeiss Axioscan at 10x and 20x resolution. ImageJ was used by the research for the layer thickness estimation. The researcher was blind to the ectopic status of the mouse during analysis.

Results

No difference in MGB volumes between ectopic and non-ectopic mice

The volume of each left-hand MGB subdivision volume was not found to be significantly different between ectopic compared to non-ectopic mice (ranksum; dorsal, ventral and medial all $p > 0.05$; Figure 17; table A1). Total MGB volume (calculated as a sum of the ventral, medial and dorsal subdivision volumes) also showed no significant difference between ectopic and non-ectopic animals (ranksum; $p > 0.05$; Figure 17; table A1).

Although we found no difference between ectopic and non-ectopic mice for any MGB subdivision or overall MGB volume we did, however, find a significant difference between the volumes of the different subdivisions, which acts as a positive control (ranksum; all $p>0.001$; figure 17; table A1) indicating a difference can be found using this method.

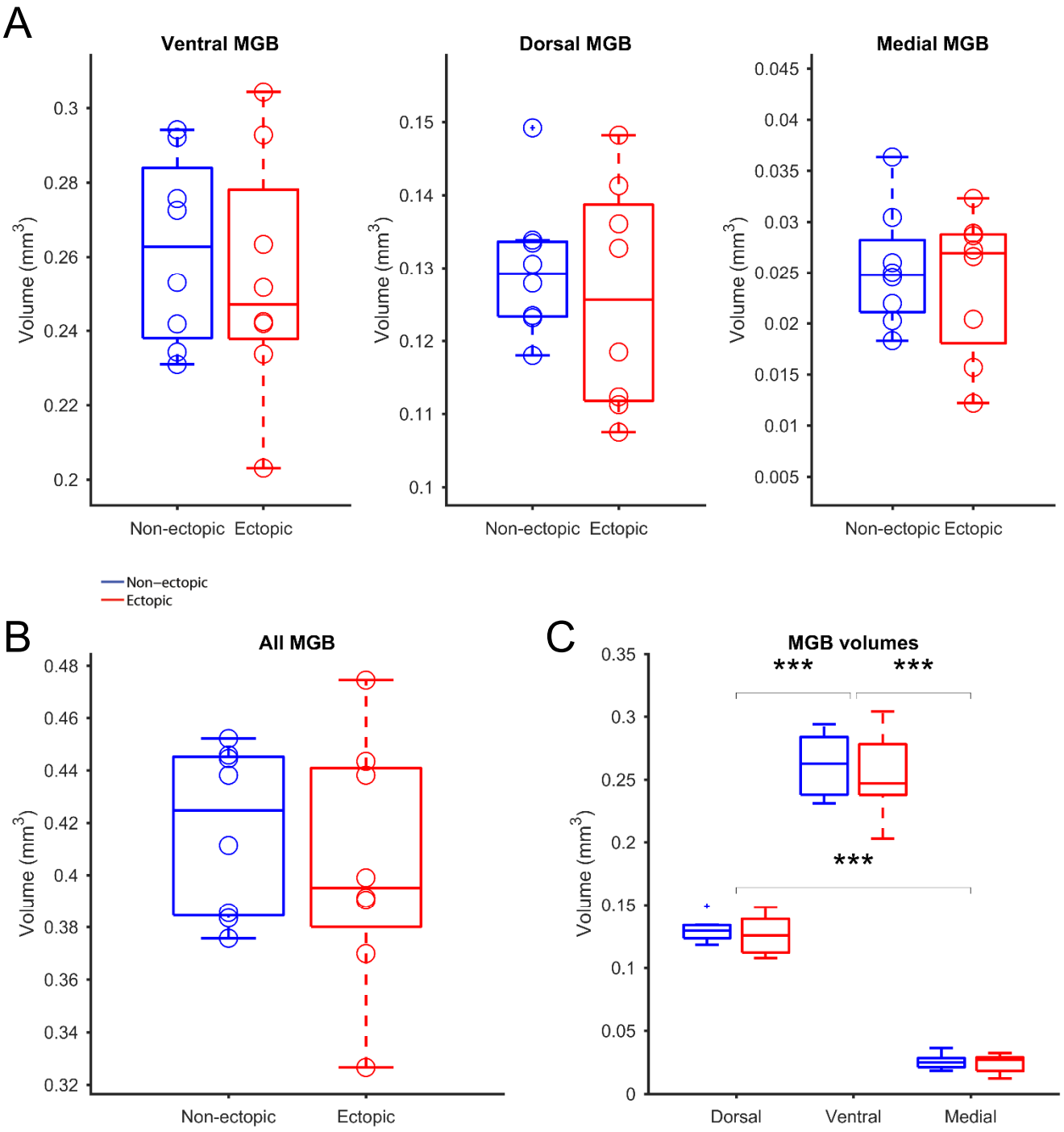

Figure 17: No difference in MGB size between ectopic and non-ectopic mice. Ectopic animals are shown in red, non-ectopic animals in blue. Data points indicate volumes from individual animals, box plots are across animals and indicate the median (line within box), 25% interquartile ranges (box) and minimum and maximum data ranges (whiskers). Outliers are marked with a cross. (A) Comparison across MGB subdivisions demonstrating no significant difference between ectopic and non-ectopic subdivision areas (ranksum; all $p>0.05$). (B) No difference in total MGB volume between ectopic and non-ectopic mice regardless of subdivision (all $p>0.05$). (C) Comparison between MGB subdivisions reveals volume differences between the MGB areas (within groups and pooled across groups) can be detected (acting as a positive control; all $p<0.001$).

Overall, these results show a significant effect for the positive control of difference between the subdivisions but between ectopic and non-ectopic animals, however, there is no significant difference in any of the individual MGB subdivisions or in the total MGB volumes between ectopic and non-ectopic mice suggesting the presence of an ectopia does not lead to a reduction in MGB size in BXSB/MpJ-Yaa mice.

MGB cell density does not differ between ectopic and non-ectopic mice

Since there was no difference in MGB volumes between ectopic and non-ectopic mice further analysis was performed in order to estimate cell density with MGB to determine if there was a difference in cell number between ectopic and non-ectopic mice. In order to perform a consistent analysis cell density estimation was obtained using the density of pixels within an image as described in the methods section. The tissue density index from each animal was compared to determine if there is difference in cell density between ectopic and non-ectopic mice. As with the MGB volume results, there was a significant difference between the lateral and medial portions of dorsal MGB which forms a positive control indicating the pixel density analysis method is sufficiently sensitive to detect differences in cell density (ranksum, $p>0.001$; figure 18; table A1). However, there was no significant difference between ectopic and non-ectopic animals in ventral or dorsal MGB subdivisions or in the total cell density estimates of these subdivisions (ranksum all $p>0.05$; figure 18; table A1). Note we compared to different areas of dorsal MGB as the cell density within dorsal MGB varies. Also we did not analyse the medial MGB subdivision due to its small size.

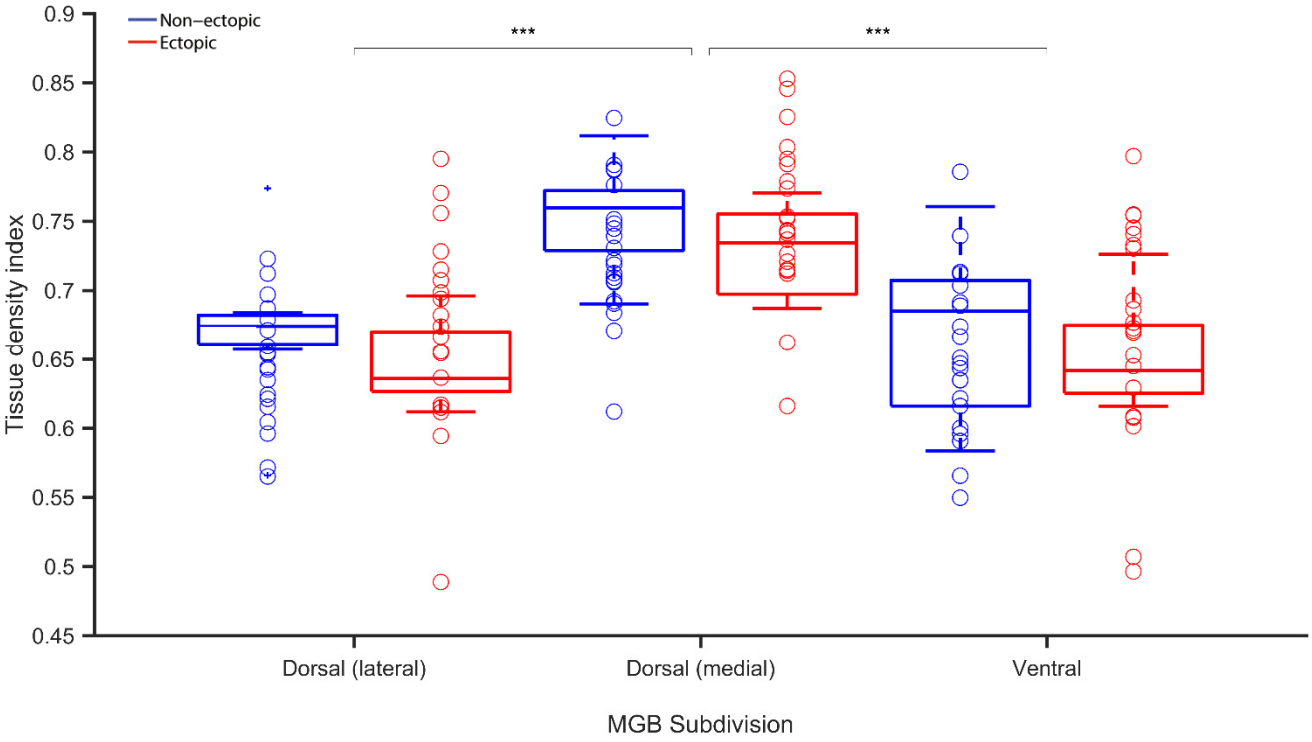

Figure 18: No significant difference in cell density in MGB between ectopic and non-ectopic mice. Plot showing there is no significant difference ectopic and non-ectopic mice in cell density of ventral and two sections of dorsal MGB (ranksum; all $p>0.05$). A tissue density index was obtained from analysis of the pixel shading within particular image. Dorsal MGB is known to vary in cell size and therefore two areas of dorsal MGB (lateral and medial aspects) were analysed. Comparisons between areas demonstrates a significant difference using this cell density measure (ranksum; $p<0.001$) for the lateral and medial aspects of dorsal MGB and between dorsal medial and ventral MGB indicating a difference in cell density can be detected using this measure. Nb. a tissue density index of 0 means there are more dark pixels and therefore likely to be more/larger cells.

LGN volumes similar between ectopic and non-ectopic mice

In order to add further controls to the work completed as part MSc Neuroscience thesis LGN volume estimation was completed since this area has also been found to differ anatomically between dyslexics and controls in humans (Livingstone et al., 1991) and as a non-auditory control area.

Using the same methods as with the MGB volume analysis described above, LGN volumes were estimated including for subdivisions (dorsal and ventral where ventral can be further split into parvocellular and magnocellular subdivisions) in 7 ectopic

and 7 non-ectopic BXSB/MpJ-Yaa mice. The results revealed no significant difference between ectopic and non-ectopic mice for the LGN subdivisions (ranksum all; $p > 0.05$; figure A1; table A1). Nor was there any significant difference between ectopic and non-ectopic mice for the total LGN volume estimation, as shown in (ranksum $p > 0.05$; figure A1; table A1). Note ventral LGN was spilt into magnocellular and parvocellular subdivisions. There was a positive control where we found as significant difference in volumes between the ventral and dorsal LGN subdivisions (ranksum all $p < 0.001$; figure A1; table A1) and a significant difference between ectopic and non-ectopic mice in the volumes of magnocellular and parvocellular portions of ventral LGN (ranksum $p=0.017$). These results suggest the size of both the visual and auditory areas of the thalamus are similar between ectopic and non-ectopic mice.

LGN cell density similar between ectopic and non-ectopic mice

As with the pixel density analysis from the MGB described above, analysis of pixel density from the LGN subdivisions (dorsal and ventral) was completed on the rostral most, caudal most and middle section of the two LGN subdivisions in 7 ectopic and 7 non-ectopic BXSB/MpJ-Yaa mice. The results show no significant difference between ectopic and non-ectopic animals in pixel density for any of the LGN subdivisions (ranksum all $p>0.05$; figure A2; table A1). Positive controls showed a significant difference between ventral magnocullar subdivision and dorsal LGN tissue density indexes and ventral magnoceullar subdivision and parvocellular subdivision tissue indexes (ranksum; all $p>0.05$; figure A2; table A1). These results indicate there is no difference in the cell packing density between ectopic and non-ectopic mice. So the ectopic mice do not appear to have less cells within the visual or auditory areas of the thalamus compared to the non-ectopic mice.

No difference between ectopic and non-ectopic mice in auditory cortex layer thicknesses

In order to determine whether there is any evidence for a difference in auditory cortex layer thickness between ectopic and non-ectopic mice, estimates of cortical layer thickness were made for each layer. The results showed no difference in layer thickness for any layer between ectopic and non-ectopic mice (ranksum; all $p>0.05$; figure 19; table A1). We did however find a significant difference between the different layer thickness which act as a positive control (ranksum; all $p<0.05$; table A1).

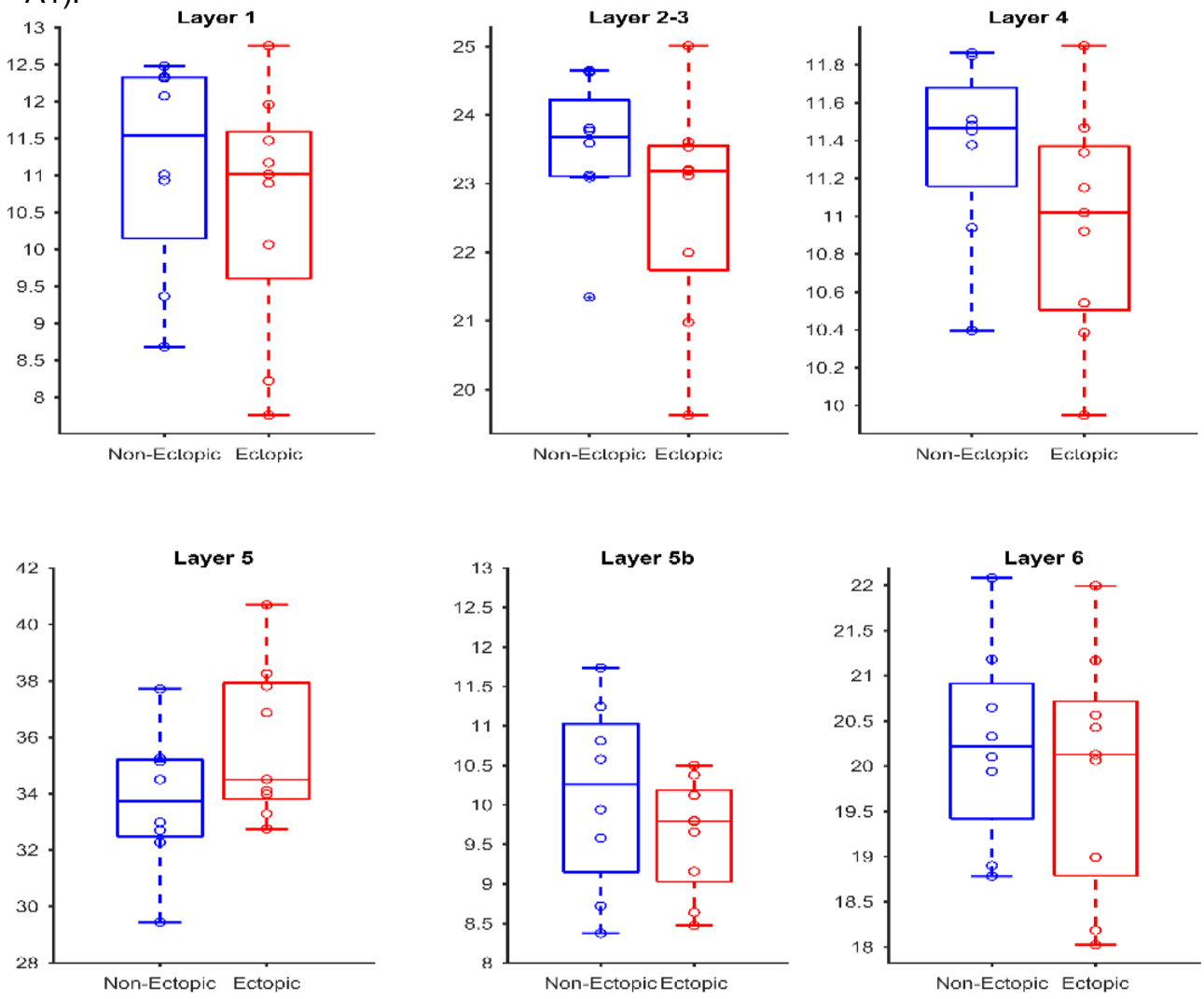

Figure 19: No significant difference in auditory cortex layer thickness between ectopic and non-ectopic mice. There is no difference between ectopic and non-ectopic mice in auditory cortex layer thicknesses (ranksum; $p>0.05$). Measurements on cortical layers were taken from images of auditory cortex in both ectopic and non-ectopic mice using ImageJ. Each layer was compared for differences in layer thickness.

These results indicate as with the results from the thalamus there is no difference in the thickness of the auditory cortex layers between ectopic and non-ectopic mice. This suggests auditory cortex is a similar size in both ectopic and non-ectopic mice.

Discussion

This chapter looked for differences between ectopic and non-ectopic mice histologically. We found no difference in MGB or LGN and (their subdivisions) volume or cell density between ectopic and non-ectopic mice. So the size and cell number/size does not seem to be different between ectopic and non-ectopic mice in these areas. We also looked at cortical layer thickness in auditory cortex and again found no difference between ectopic and non-ectopic mice indicating auditory size does not differ between ectopic and non-ectopic mice.

MGB volumes results revealed there are no significant differences in volume size between ectopic and non-ectopic animals that could explain the previously observed neural deficits in response to fast auditory processing. A case study in humans with dyslexia found there was a difference between the size of the hemispheres with the patient having a wider left than right hemisphere suggesting there may be a difference in volume in the left hemisphere in people with dyslexia (Galaburda and Kemper, 1979). Also previous studies looking at the effects of induced microgyria discovered decreased brain weight in animals with microgyria compared to sham animals (Peiffer et al., 2003) and since a previous study revealed a neural deficit in gap-detection in the auditory thalamus of ectopic compared to non-ectopic mice it is reasonable to have expected a possible morphological difference in these nuclei (Anderson and Linden, 2016).

The possibility that the methods used in this paper were not sensitive enough to detect a true difference in volume between ectopic and non-ectopic animals has to be considered. In this study we used sections stained for cytochrome oxidase in order to delineate the MGB borders as it has previously been shown to be to be the recommended method for revealing MGN borders (Anderson and Linden, 2011; Anderson et al., 2009) however there is still a large amount of subjectivity to this process. Since all borders were completed blind to the ectopic status of the animal and by the same researcher together with the repeated measures score completed on 8 and the fact that the data is lacking any kind of trend does provide some confidence in the results. However the possibility that a volume difference does exist but could not be revealed either due to too small a number of animals or incorrect placement of the borders or a combination of these factors cannot be ruled out.

One of the current prevailing theories of dyslexia is that from a deficit in large cells that process fast information. This theory originates from literature on the visual system where it has been found that dyslexics show a deficit in the magnocellular system and problems processing fast, high contrast stimuli which the magnocellular system is thought to process (Galaburda and Kemper, 1979; Stein, 2001; Ramus, 2003; Ramus, 2004). Since it has been shown that human dyslexics have a deficit in processing rapidly changing sound an analogue deficit has been sought in the auditory pathway as well.

A study using a small number of brains for dyslexics and non-dyslexics showed the dyslexic brain may have some differences in cell packing density in the thalamus particularly the MGB. Galaburda et al. found in the dyslexic brains there were more small and fewer large cells in the left compared to the right MGB. Also, the induced microgyria studies found a difference in cell packing density with induced microgyria

animals having more small and fewer large neurons in MGB compared to shams (Herman et al., 1997; Rosen, 1993; Rosen et al., 1995).

So on the basis of the human data, freezing lesion studies and magnocellular theory, we expected to see some difference in the cell packing analysis for MGB however we were unable to find any difference in ectopic compared to non-ectopic animals on either the left or right MGB. We did demonstrate that the method we were using was able to detect a difference in between two areas of dorsal suggesting the method is able to detect a known difference providing some confidence in the method and the results. Of course this does not rule out the magnocellular theory of dyslexia as it may exist in a different part of the auditory pathway however it does not seem to exist at the level of auditory thalamus. Since the medial MGB is known to contain magno-cells (Winer et al., 1999) it is disappointing that we were not able to include this area in our analysis however since the previous freezing lesion studies found a difference between microgyritic and sham animals the lack of any difference between ectopic and non-ectopic animals is still of interest. However, since the LGN is known to contain mangnocellular and parvocellular subdivisions within the ventral subdivisions, the fact that we found no difference in either volume or pixel density further rules out the theory of the a reductions in magno-cells in the case of the BXSB/MpJ-Yaa mice.

The fact that the previous studies did not use a more reliable technique and our failure to replicate their findings in the BXSB/MpJ mouse model weakens the results of the previous studies. Moreover, since most of these studies come from work on induced freezing lesions the possibility that the difference is real but the induced freezing lesion is an accurate model of naturally occurring ectopias exists. This idea is support by a study completed by Rosen et al. which found a difference in

behavioural effects of spontaneous ectopia compared to induced microgyria (Rosen et al., 1995). It is known that the freezing lesion technique involves the destruction of cell whereas the naturally occurring ectopia involves the displacement of cells. Also in humans one study revealed, when looking at 4 brains of known dyslexics, found all 4 brains had multiple ectopia and dysplasia whereas only 2 of the brain were found to have microgyria (Galaburda et al., 1995). The question is then raised as to how similar these two models actually are and whether the freezing lesion model is the most appropriate model for studying the effects of dyslexia.

Since we found no difference in either the auditory or visual areas of the thalamus it is possible that the previously noted deficit in auditory gap-detection in BXSB/MpJ-Yaa mice was inherited from another area of the auditory cortex. We found no difference in auditory cortex layer thicknesses suggesting the auditory cortex is similar in both ectopic and non-ectopic mice which may indicate the deficit is not inherited from the auditory cortex through feedback connections.

Since there does not seem to be any difference in auditory cortex or auditory thalamus future studies should look to areas lower in the auditory pathway, such as the inferior colliculus. Also, future analysis would be better focused towards micro analysis such as synapses or dendrites in central IC and ventral MGB.

Overall the aim of this chapter was to determine if there were any difference in volume or cell number/size similar to those previous reported in induced microglia studies (Herman et al., 1997; Escabí et al., 2007; Rosen et al., 1995/1999). We found there was no difference between ectopic and non-ectopic mice in size or cell density of the measured areas so this is in contrast the rat lesion studies where they did find differences. Of course, it is possible there are differences between ectopic

and non-ectopic which are more subtle than the methods used in this chapter can determine but future experiments should focus on understanding the differences between ectopic and non-ectopic mice eletrophysiologically before further histological experiments are performed in order that the full details of the difference can be more fully understood.

Chapter 3 – Inferior colliculus extracellular recordings

Abstract

Previous work has shown that mice with ectopias demonstrate impairment in detecting short gaps in noise compared to mice without ectopias (Clark et al., 2000). Extracellular recordings from the medial geniculate body (MGB) have indicated that neural gap-detection thresholds (defined as the minimum gap duration required to elicit a significant change in firing rate) are longer in ectopic than non-ectopic mice, particularly in the ventral MGB (Anderson and Linden, 2016). The proportion of cells with offset responses is also reduced in ventral MGB of ectopic mice, suggesting that the thalamic gap-detection deficit might arise from an offset-response abnormality (Anderson and Linden, 2016). To determine whether neural deficits in gap-in-noise sensitivity and sound-offset responses in ventral MGB of BXSB/MpJ-*Yaa* mice are inherited from the auditory midbrain, we made extracellular recordings from the inferior colliculus (IC) in 10 ectopic and 10 non-ectopic mice. We found that in contrast to the previous results from ventral MGB recordings, neural gap-detection thresholds were *shorter* in ectopic than non-ectopic mice for neurons with V-shaped tuning curves typical of the central IC (ranksum $p<0.001$; ectopic n=133, non-ectopic n=79). However, in agreement with previous results from the ventral MGB, we also found that the proportion of offset-responsive cells in IC was reduced in ectopic mice (15% in ectopic, 23% in non-ectopic across all IC recordings; Fisher exact test $p<0.01$). Thus, in the same mouse were have a deficit in gap-detection in the auditory thalamus but an enhanced gap-detection ability in the IC yet in both brain areas we a see a reduction in the number of offset sensitive cells. Understanding the mechanisms of how this arises may help reveal how the brain detects short gaps in noise which is important to understand as it underlies speech processing.

Introduction

Previous work suggests the presence of ectopias in BXSB/MpJ-Yaa mice is associated with deficits in auditory processing. Clark et al. 2000, showed BXSB/MpJ-Yaa mice with ectopia have a behavioural deficit when processing short gaps but not long gaps in noise compared to non-ectopic BXSB/MpJ-Yaa mice (Clark et al. 2000). Similarly Frenkel et al. 2000, showed BXSB/MpJ-Yaa mice with ectopia have reduced auditory evoked potentials compared to non-ectopic mice, for stimuli consisting of tones separated by a short-duration tone of a different frequency (Frenkel et al. 2000).

As well as naturally occurring neuroanatomical ectopias, a form of induced microglia in rats has been studied and suggested to be analogous to the spontaneously occurring cortical micro-abnormalities in the mouse models. An induced microgyria is created by taking a freezing probe and placing it on the skull cap of a rat pup. In adulthood these animals have microgyria near the site of the freezing lesions induced during development. Behavioural work with this animal model has demonstrated that animals with induced microgyria have impaired rapid auditory processing compared to sham controls and that the behavioural effects were not limited to working memory as spatial memory has also been shown to be affected in lesioned rats (Threlkeld et al., 2012). Furthermore, neurophysiological deficits in auditory cortical processing of rapidly changing sounds have been demonstrated in rats with induced microgyria (Threlkeld et al., 2012).

This work in animal models has been said thought to be analogous to work in humans, for example work by Paula Tallal, who demonstrated people with dyslexia are impaired at gap detection tasks (Tallal, 1980) since work by Galaburda et al. found an increased number of ectopia and other neuroanatomical abnormalities in

brains of people with dyslexia. Note a number of these patients also had other conditions particularly speech and language deficits also a number have also shown there to be no difference in gap detection between dyslexias and controls (Galaburda et al., 1985).

However, recent work from the Linden lab revealed ectopic BXSB/MpJ-Yaa mice have a deficit in thalamic responses to brief gaps in noise; fewer cells in MGB respond to short gaps in noise in ectopic compared to non-ectopic mice (Anderson & Linden 2016). Interestingly, this work demonstrates that while it was previously thought gap-detection deficits reflects an overall sluggishness in auditory processing of rapidly changing sounds, the thalamic gap-detection deficit is not arising from a problem with rapid temporal processing, as there is no deficit in thalamic responses to rapid click trains. Instead the thalamic gap-detection deficit appears to arise from a more specific problem: reduced neural activity following noise offsets. Consistent with this conclusion, thalamic responses to clicks and other stimuli presented in a silent background are normal but ectopic mice do have reduced neural responses to a click *following* noise.

As previously detailed in the introduction of this thesis, a main aim of this PhD research is to address the question of where in the auditory pathway the neural gap-detection deficit and reduced noise-offset sensitivity arises in ectopic BXSB/MpJ-Yaa mice. In an attempt to start to answer this question, extracellular recordings were made from the inferior colliculus (IC). We found in contrast to the previous extracellular recording results in MGB, in the IC cells typical of central IC, the ectopic mice have shorter, not longer, neural gap-detection thresholds than non-ectopic mice.

Additionally, as was found in the MGB study, in the IC there was a reduction in the number of cells with noise-offset responses in the ectopic compared to non-ectopic mice (Anderson & Linden 2016). There was no difference between ectopic and non-ectopic mice in characteristic frequencies of the IC recordings nor in click-train synchronisation thresholds in either the primary or non-primary cells. However, we did find a difference between ectopic and non-ectopic mice in spontaneous firing rates in the non-primary (likely recorded from dorsal/external IC) but not primary IC cells.

In light of the IC recording results, we performed additional analysis on the previous MGB recordings. We found a difference between ectopic and non-ectopic for spontaneous firing rates only in ventral MGB. Furthermore, ventral MGB recordings were also found to have differences in the sustained response to a noise (after the initial onset response to the noise) where the rate of decline in the response is increased in the ectopic compared to the non-ectopic mice and also differences in the variability of responses across individual trials over this time period in ectopic and non-ectopic mice.

Methods

Mice

20 BXSB/MpJ-Yaa male mice were used in the experiments IC aged 109-165 days, median age of 133 days. The symptoms of accelerated autoimmune disease in BXSB/MpJ-Yaa mice usually arise around 140 days of age. Histological examination (see Histological Analysis section below for details) revealed 10 mice as ectopic and 10 mice as non-ectopic All data collection was necessarily performed blind to the ectopic status of the animal, which was only discovered by *post-mortem*

histological analysis. Data analysis was also performed blind to ectopic status of the animal using MatLab code as detailed below.

The previously recorded MGB data was performed on 27 BXSB/MpJ-Yaa male mice where histological examination found 13 of these mice were ectopic and 14 non-ectopic as detailed in Anderson & Linden (2016).

Recording strategy

Recording strategy as in Anderson & Linden (2016), briefly all auditory stimuli was presented free-field to the left ear, contralateral to the recording location through a FF1, Tucker-Davis Technologies speaker which was approximately 45° and 20cm apart and similar height to the presenting ear. Acoustic calibration was performed at the start of each experiment, with the microphone placed in the similar location to animal's left ear canal. The system was used to correct the sound system frequency responses to be flat with 2dB from 2 to 90 kHz.

A craniotomy of approximately 2mm by 2mm was made over the right hemisphere along lambda and 0.5mm to the right of bregma to enable access to the inferior colliculus for recording. The cortical surface was kept moist with regular application of saline through the experiments. All recordings with made multi-channel silicon probes (Neuronexus Technologies A1x16-5mm-100-177-A16) with a 5mm single shank of 16 channels spaced 100µm apart.

Electrode placement was determined by visual examination since the IC is visible from the surface in the mouse. Probe depth was measured using a hydraulic probe drive (FHC 50-12-1C) controlled outside the sound attenuated booth, which was zeroed with the electrode at the tip of the brain (confirmed microscopically and by acoustic changes in electrode signal). Experiments typically started with placement

of the probe in the rostro-medial corner of the craniotomy; subsequent penetrations were made in a zig-zag pattern, caudal to the first penetration followed by placement to right of the original penetration then caudal to this etc. Neural responses to experiment stimuli were recorded when there was found to be a visible response (on the raster plots) to continuous 50μs square-wave clicks with 500ms inter-stimulus-interval on at least 10 electrodes (not recorded). As in Anderson & Linden (2016), all recordings were made under urethane anaesthesia (1.9g/kg in 20% solution, i.p.) with atropine (0.1ml at 0.06 mg/ml, s.c.) to reduce bronchial secretions. Ringer's solution was supplied hourly (0.1-0.2ml s.c.) to maintain hydration. Typically a tracheotomy was made at the start of the experiment to aid breathing. Temperature was maintained throughout the experiment using a homeothermic blanket (Harvard Aparatus) and monitored via a rectal probe at around 37.5 ± 0.5 ℃. Supplemental warmth was provided as needed, using a glove filled with warm water as an additional heating pad.

Stimuli

All stimuli were preceded by 100ms silent onset delay and unless otherwise indicated 20 repetitions of each condition were recorded. Frequency response areas (FRAs) were recorded using 3 repetitions of tone pips of 100ms length (including 5ms rise/fall time) at 4000-60000Hz with 8 tones per octave and sound intensity of 10-80dB SPL in 10dB steps. Tones were followed by 300ms silences making the sweep duration 500ms.

Click trains were 200ms in length followed by 200ms silence making the sweep duration 500ms. Click trains were recorded with a sound intensity of 60dB SPL and inter-click intervals of 1, 1.4142, 2, 2.8284, 4, 5.6569, 8, 16, 32, 64 and 128ms. These intervals were chosen to be densely logarithmically spaced from 1 to 8ms,

then more sparsely logarithmically spaced from 8 to 128ms, in order to optimise both coverage of a wide interval range and sampling of the shortest intervals.

Gap-in-noise stimuli were designed using white noise (0ms rise/fall time) of 20, 40 or 60dB SPL always with a 200ms first noise, followed by a varying length gap, followed by a 50ms noise. Gap durations were the same as the click-train inter-click intervals with the addition of 0ms gap condition. Gap-in-noise stimuli were recorded with a 750ms sweep duration regardless of gap length including the 100ms initial silent delay.

Histological analysis

Histological analysis was used to determine the ectopic status of animals. The extracellular recordings were followed by transcardial perfusion using chilled 4% paraformaldehyde (PFA) following overdose with pentobarbital. Brains were removed and place in PFA for at least 24 hours following which the forebrains were washed in 0.1M phosphate buffered solution and sectioned coronally into 50µm sections. Sections were mounted on alternate slides (Superfrost Plus) and stained to reveal Nissl bodies using creysl violet (see Chapter 1 for staining methods). The stained slides were scanned using a slide scanner (Zeiss Axioscan Z1) at 20x magnification (objective: Plan-Apochromat 20x/0.8 M27) captured using a Hitachi camera (HV-F202SCL). Alternate sections were checked for the presence of an ectopia(s). If no ectopia was found the remaining sections were checked for the presence of the ectopia and if still not found the mouse was deemed ‘non-ectopic’.

Recording location

Since histological analysis of the forebrain was needed to determine the ectopic status of each mouse and due to the large number of penetrations (up to 6) made in

the IC, recording sites were not reconstructed histologically. Instead, an estimate of recording location was obtained from analysis of the tuning curve for each recorded cell, by blind-manual inspection. Cells with V-shaped tuning curves were determined as likely recorded form central IC and are referred to throughout as 'primary IC cells'. Cells without a V-shaped tuning curve (mostly with multi-peaked W shaped tuning curves) were deemed to be recorded from non-central nuclei such as dorsal or external IC and are referred to as 'non-primary IC cells'. There was a further group of cells which had a significant response to a noise but no clear tuning and since these could have been recorded from any area, they are referred to throughout simply as 'untuned cells'.

Data analysis

All data analysis was performed using custom made scripts in MATLAB (MathsWorks) and blind to ectopic status of the animal. Statistically significant was defined as $p<0.01$. Unless otherwise stated the statistical test used was the non-parametric Wilcoxon rank-sum test ('rank-sum'). Gap threshold analysis used a repeated measure ANOVA on ranked thresholds which allows non-parametric data to be analysed using a parametric test. The repeated measure was the sound level (dB SPL). All IC PSTH data was analysed using 1ms bin width.

Cells were only included in further analysis if they met two inclusion criteria. Firstly, the response to a particular stimulus was required to be 2 x standard deviation of the spontaneous rate; secondly a threshold on the Fano factor analysis (standard deviation of number of spikes for each trial square and divided by the mean) on a responses to a 250ms white noise was applied to reject any recording which showed a large amount of instability. For IC recordings, a threshold value of 5 was chosen from inspection of the Fano factors obtained from all cells as shown in figure 20A.

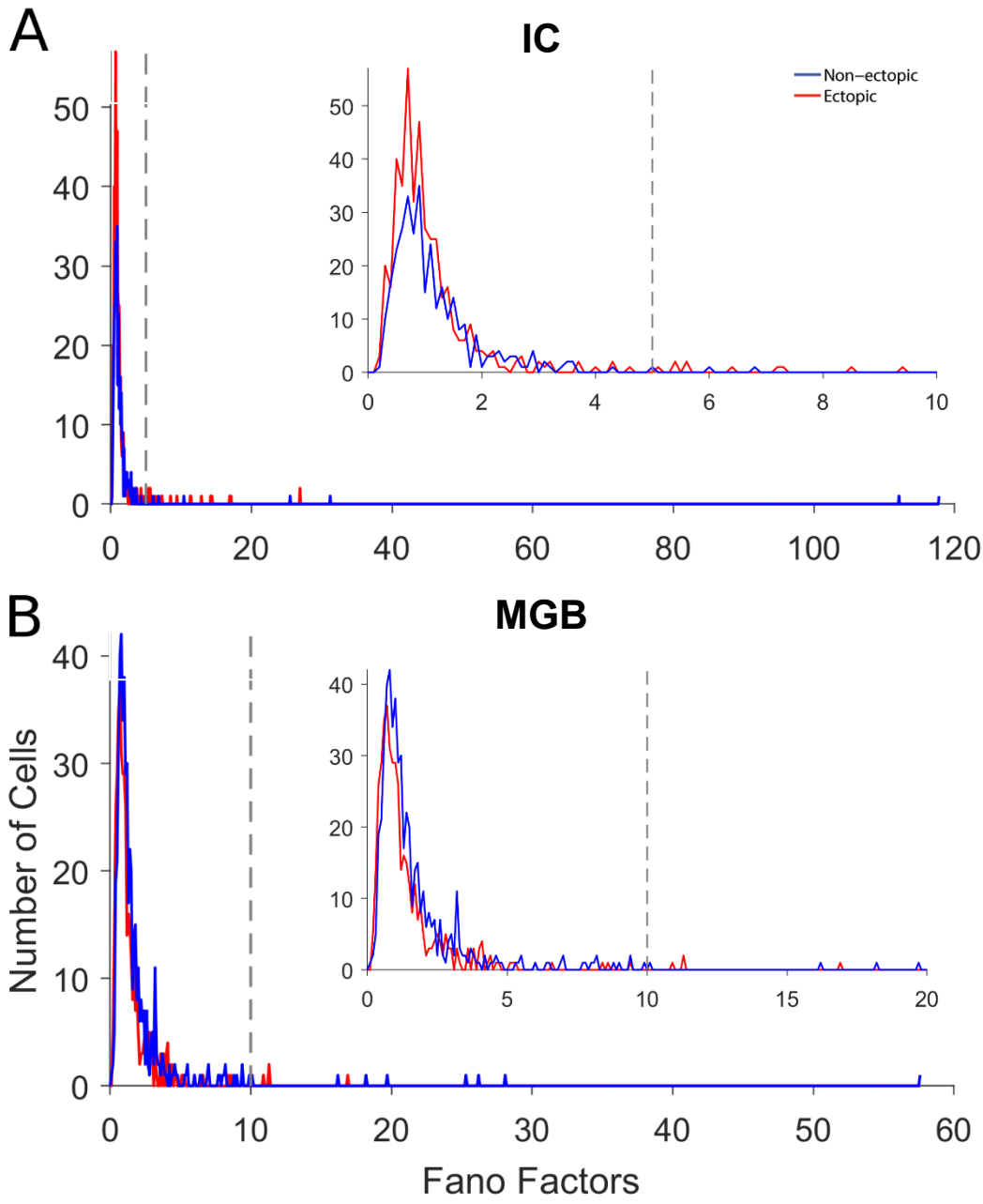

Figure 20: Trial by trial variability for MGB and IC recordings. Histograms showing for trial by trial variability in firing rate in extracellular recordings made in IC and MGB together with threshold used to reject the most unstable recordings. Fano factor analysis was performed on recordings to a 250ms white noise in both IC (A) and MGB (B). The histogram was used for analysis and placement of the threshold used to identify and reject the most unstable recordings (grey line). The threshold was set at 5 for IC (4.34% of ectopic and 2.12% non-ectopic cells rejected by this measure) and 10 for MGB recordings (0.94% ectopic and 1.53% non-ectopic cells rejected by this measure). Any recordings with a fano factor above the threshold were not used in any of the subsequent analysis.

For re-analysis of MGB recordings from Anderson and Linden 2016 (discussed later in this chapter), a threshold of 10 was chosen instead, since the distribution of Fano factors was shifted to higher values overall in the MGB data (figure 20B). Any cells

that were above this threshold value were deemed to be unstable recordings and were not included in subsequent analysis.

The neural gap-detection threshold is defined as the shortest gap evoking a change in firing rate. For the 60dB gap-in-noise stimuli thresholds were determined using both automated and manual methods. Manual detection of the thresholds was performed by the researcher blind to the ectopic status of the animal, using MatLab code to display the PSTHs for all gap lengths for each cell, in cells presented in random order. The MatLab script then asked for a threshold value to be entered and the researcher entered the relevant value after inspection of the display PSTHs. To aid the researcher, the display included indicator lines for 2 times the standard deviation for the last 50ms of the response in the 0ms gap condition. This threshold determination procedure was performed on 3 separate occasions and the final thresholds from manual detection were taken to be mean across these 3 separate attempts.

For the automated detection of neural gap-detection thresholds three tests were performed for each gap length: (1) the firing in the time of the gap was compared (using a ranksum test) to the same time period in the 0ms gap condition, (2) the first 10ms of the response to the second noise was compared (using a ranksum test) to the same period in the 0ms gap condition and (3) the mean firing rate over a 10ms period which was chosen as centring on the peak (maximum) response to the second noise response and was compared (using a ranksum test) to the mean firing rate over the same time intervals in the 0ms gap condition. The threshold was taken as the shortest gap at which one of these condition was significant using an alpha of 0.05. Reliability of this automated was assessed by comparing the results to manually obtained thresholds.

For analysis of responses to a white noise, the 0ms gap condition from the gap-in-noise stimuli was used. The onset response period was defined as the first 50ms of the response to the noise, as inspection of the population PSTH revealed this to be a suitable time period. The sustained response period was defined as the response to a noise minus the onset response period, that is, 50ms after noise onset for period of 200ms. CV_{isi} was calculated as the standard deviation of the inter-spike intervals divided by the mean inter-spike interval. The Fano factor was calculated as the square of the standard deviation of the spike count across trials, squared divided by the mean of the spike counts across trials. The median firing rate was taken as the median value across the given time period from the PSTH. The fall-off in the sustained response period was calculated as the mean firing rate between 150-200ms after noise onset minus the mean firing rate 200-250ms after noise onset (i.e. the last 50ms response to a noise).

Offset response status was determined by manual inspection. A MatLab script was used to randomly choose a cell and present the PSTH for the 0ms gap condition from the gap-in-noise stimuli, to the researcher, who was blind to the ectopic status of the animal. The response was then coded manually as either no offset, excitatory offset if the firing seemed to increase after the noise had gone off, or suppression/inhibitory offset if the firing seemed to decrease to below spontaneous rate firing after noise offset.

Click-train synchronisation thresholds were determined using a custom MatLab script to determine the vector strength and associated Rayleigh statistic. The click-train synchronisation thresholds was determined as the shortest inter-click interval for which the Rayleigh statistic was greater than 13.8 (i.e., test of uniformity, $p<0.01$). Note, this test was performed on the response 50ms after the click-train onset (until

click-train offset, that is a period of 150ms) in order to prevent the onset response from disrupting the calculation of the click-train synchronisation rate.

Frequency responses areas (FRAs) were analysed for characteristic frequency (CF) defined as the peak in the frequency-intensity map, i.e. the sound frequency for which responses could be evoked at threshold sound intensity. Estimation of CF was performed by manual inspection, blind to the ectopic status of the animal. A custom MatLab script displayed the FRA for a randomly chosen cell and the CF was chosen by clicking on the peak of the response. If the FRA was multi-peaked, the peak with lowest sound level threshold was chosen. During this analysis the shape of tuning curve was also recorded and used in addition to the depth of the recording to determine approximate IC subdivision.

Results

Neural gap-detection thresholds for primary IC cells are shorter in ectopic than non-ectopic mice

Anderson and Linden (2016) found fewer MGB cells with shorter neural gap-detection thresholds, in ectopic than non-ectopic mice and this abnormality was most evident in the ventral MGB subdivision. Since MGB is known to receive most of its input from IC, particularly the ventral MGB subdivision (Winer 1992), we investigated whether the neural gap-detection difference in ectopic mice was inherited from the IC. Multi-unit recording recordings were made from anaesthetised BXSB/MpJ-Yaa mice. Recordings were made from 533 locations in ectopic mice and 411 in non-ectopic mice. The final data set, after using the exclusion criteria described in Methods, included 419 recordings from 10 ectopic mice, and 323 recordings from 10 non-ectopic mice. Throughout the Results section, we refer to these recordings as

“cells” although the data were not spike-sorted; in the Discussion we briefly consider the possible implications of the multi-unit recording for interpretation of results.

In order to determine whether there were any differences in gap-detection thresholds within IC subdivisions the data was divided into primary, non-primary and untuned groups based upon the cells physiological properties. For reasons outlined in the methods section it was not possible to do this using histological techniques. ‘Primary cells’ (putative central IC cells) where defined as having a V-shaped tuning curve. Cells with clear frequency tuning but without a V-shaped tuning curve were defined as ‘non-primary cells’ (putative dorsal/external IC). Any cells which we found to be untuned but had a significant response to a noise (see methods for definition of significant response) were defined as ‘untuned cells’. See figure 21 for example PSTHs and FRAs from primary and non-primary cells.

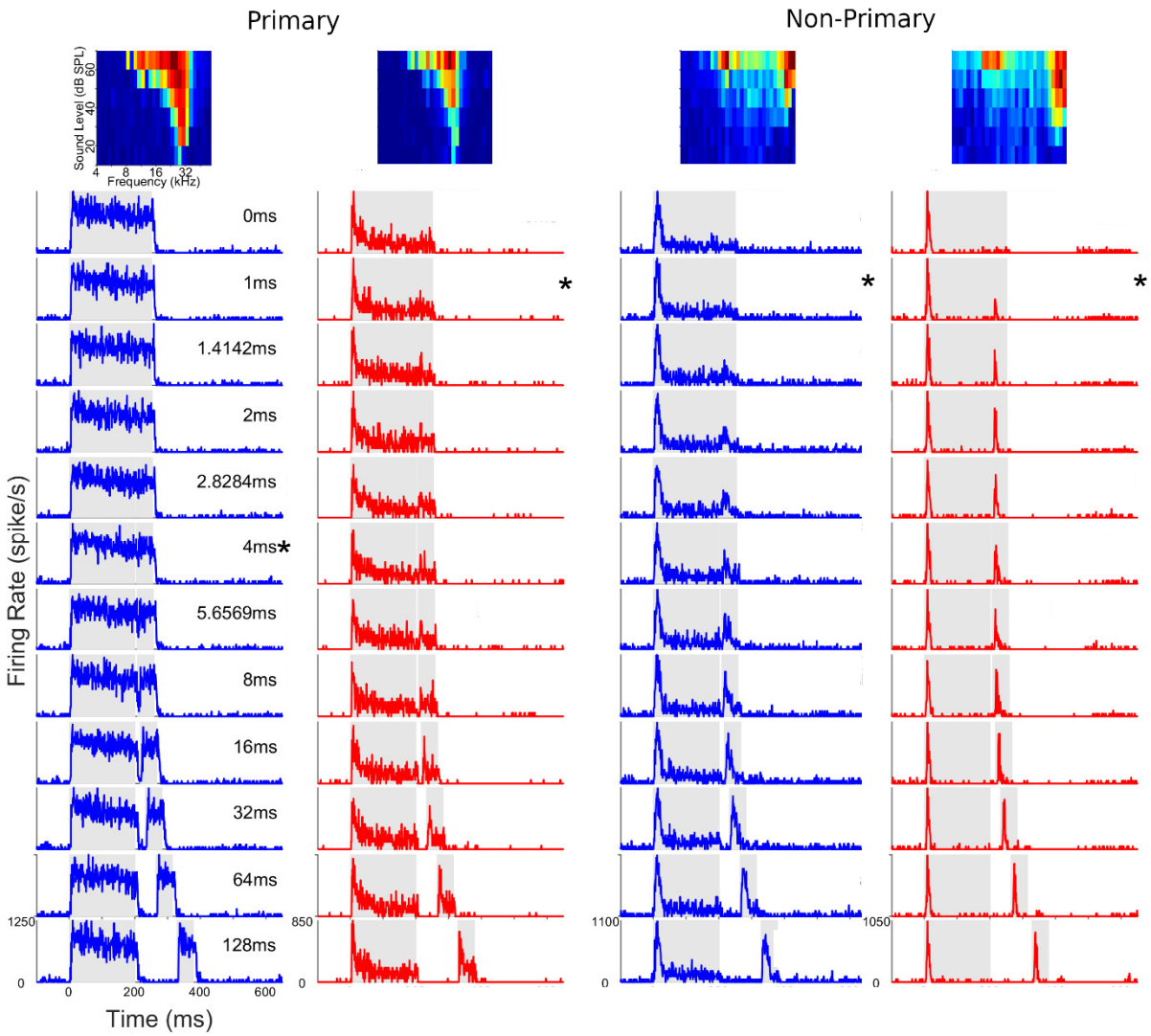

Figure 21: Example FRAs and corresponding PSTHs to gap-in-noise stimuli from four different cells. Examples are taken from ectopic (red) and non-ectopic (blue) mice and show examples of primary cells (as indicated by the sharp, well-tuned FRA) and non-primary cells (which are generally less well tuned and tend to have two peaks). Gap thresholds are indicated with a star and were identified by both computer script (analysising different aspects of the PSTH see methods for more details) and by eye by a research blind to the ectopic status. When thresholds were indentifed by-eye similar plots were used showing all of the PSTHs for the different gaps and the research identified threshold by starting at the longest gap, working towards the shortet gap and setting the threshold as the minimum gap a deflection in the PSTH can be seen for the gap location. Stars indicate chosen gap thresholds for examples.

There was no significant difference between ectopic and non-ectopic mice in neural gap-detection thresholds when data were pooled across all recorded cells with an auditory response. However, when comparing ectopic and non-ectopic neural gap-detection thresholds for primary cells, i.e. those with a V-shaped tuning curve, there was a significant difference (rmANOVA (groups~levels) $p<0.0001$; table A2) and post-hoc Tukey tests revealed a significant difference for 60dB SPL ($p<0.001$).

Figure 22 shows gap-detection thresholds from primary cells with V-shaped tuning curves and demonstrates that ectopic mice had *shorter* neural gap-detection thresholds compared to non-ectopic mice. This result is however, in contrast to the to the previous result from ventral MGB where the ectopic mice had *longer* neural gap-detection thresholds compared to the non-ectopic mice (Anderson & Linden 2016).

Note the neural gap-detection thresholds for gap-in-noise stimuli presented at 20 and 40 dB SPL were only obtained using automated methods whereas the thresholds for stimuli presented at 60 dB SPL were also confirmed by manual analysis (blind to the ectopic status of the animal; see methods for more details).

For the other cells (those with multi-peaked tuning curves likely from dorsal/external IC and cells which were untuned but had an auditory response) there was no difference in neural gap-detection thresholds between ectopic and non-ectopic mice (rmANOVA, all $p > 0.01$; table A2). Results are shown in figures 23 and 24, this result was also confirmed when untuned and non-primary cells were pooled (rmANOVA; all $p > 0.05$; table A2). These findings suggest there is no difference between ectopic and non-ectopic mice in neural gap-detection thresholds within non-primary (dorsal/external) IC cells, unlike in the primary (central) cells. Notably, the numbers of recordings with multi-peaked or untuned tuning curves were similar to or greater than the number of recordings with V-shaped tuning curves; thus statistical power to detect differences in presumed dorsal/external IC recordings should have been similar to or greater than that in presumed central IC recordings.

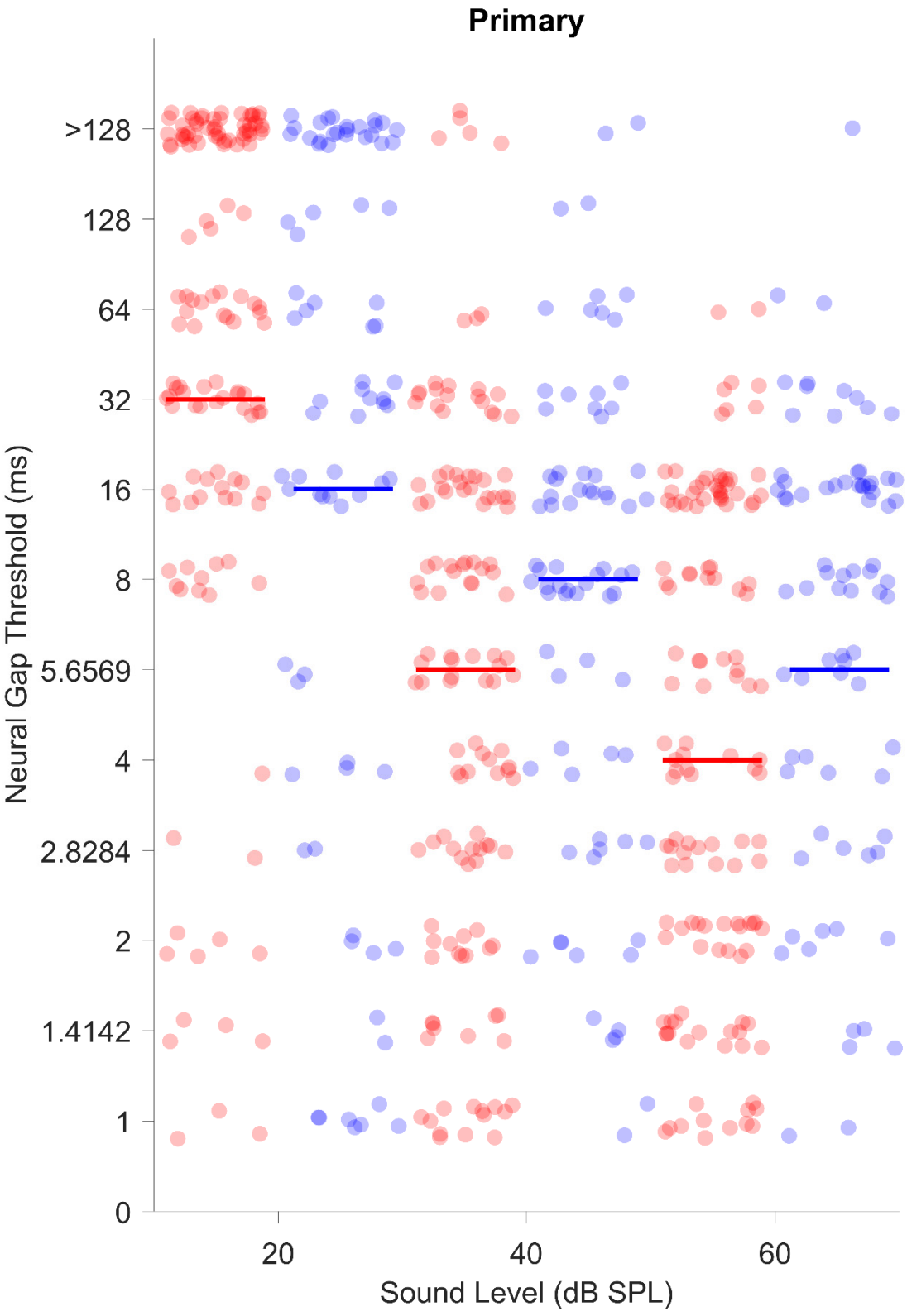

Figure 22: Ectopic mice have shorter gap detection thresholds than non-ectopic mice at 60dB SPL in primary IC cells. There is significant difference in gap-detection thresholds between ectopic and non-ectopic mice in primary IC cells (rmANOVA (groups~levels) $p<0.0001$). . There was a significant difference between ectopic and non-ectopic mice in post-hoc Tukey tests only at 60dB SPL only ($p<0.001$). Plot shows gap-detection thresholds for gap-in-noise stimuli at 20, 40 and 60 dB SPL. Thresholds from individual cells are indicated by dots (scattered for visualisation). Medians is are indicated by a horizontal line. Ectopic are indicated in red and non-ectopic in blue. Ectopic n=146, non-ectopic n=88.

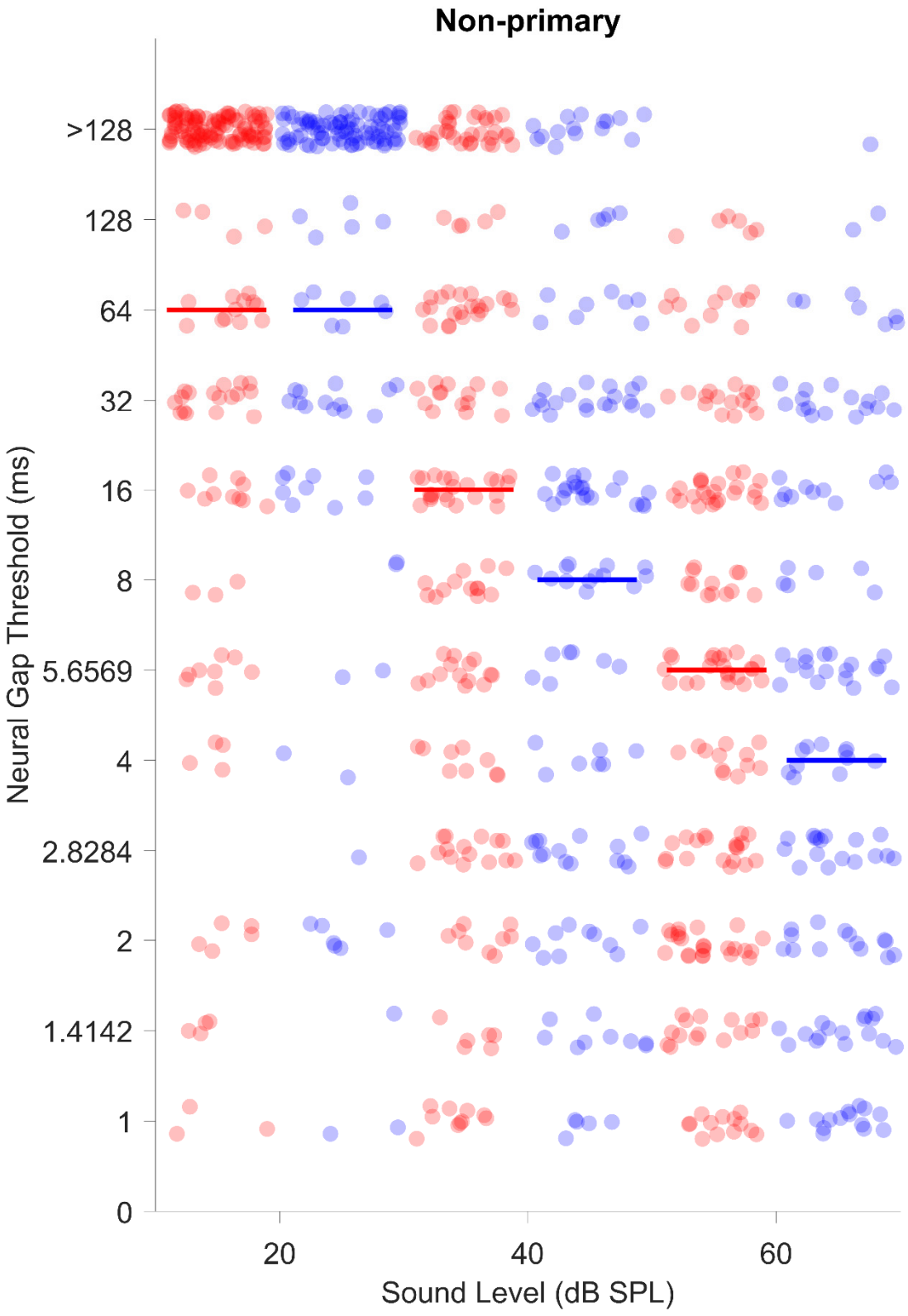

Figure 23: There is no significant difference in gap-detection thresholds between ectopic and non-ectopic mice in non-primary IC cells. Plot as in figure 24 but for non-primary cells. There is no significant difference between ectopic and non-ectopic mice at any sound level tested for non-primary cells (rmANOVA; p>0.01). Ectopic n=153, non-ectopic n=135.

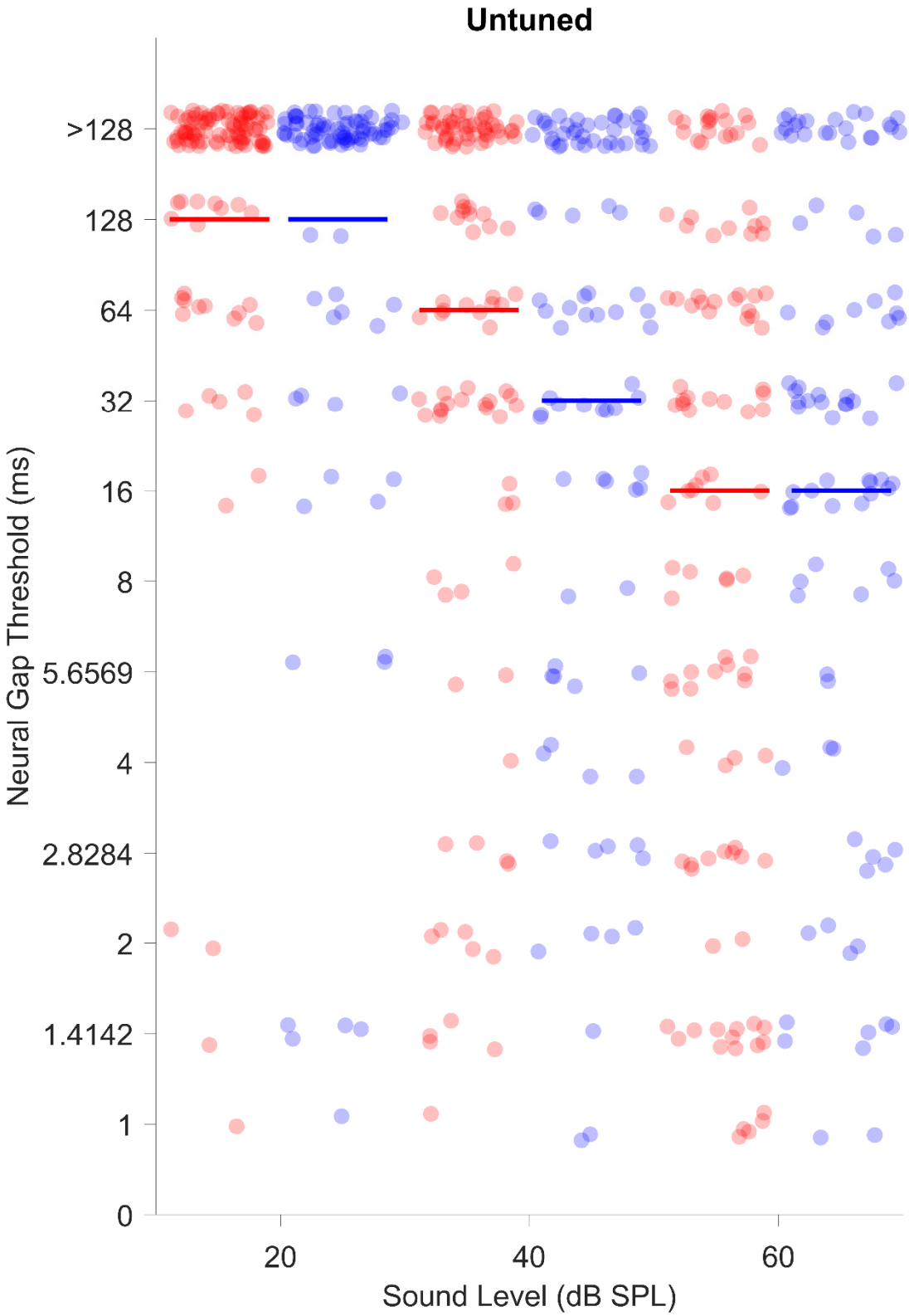

Figure 24: There is no significant difference in gap-detection thresholds between ectopic and non-ectopic mice in untuned IC cells. Plot as in figure 24 but for untuned cells. There is no significant difference between ectopic and non-ectopic mice at any sound level tested for untuned cells (rmANOVA; p>0.01). Ectopic n=145; non-ectopic n=135.

Differences in neural gap-detection thresholds in primary cells not due to differences in responses to noise between ectopic and non-ectopic mice

It is possible that the difference we observed in neural gap-detection thresholds between ectopic and non-ectopic mice for primary cells may arise from a difference in neural response to noise in these cells response to noise regardless of whether the noise is proceeded by noise or by silence. To determine whether this may be the case we examined responses to a 250ms 60dB SPL white noise. We analysed peak firing rates, peak response latencies, median firing rates, Fano factors (used here for to test for differences in trial-by-trial variability), coefficient of variance of inter-spike intervals (CV_{ISI}), the onset response to a noise (first 50ms of the response) and the sustained response to a noise (responses minus the first 50ms). Finally, we also considered the stability of the sustained response by analysing the fall-off of the sustained response.

When analysis was performed on the onset of the noise response, the primary cells were found to have similar amounts of firing and similar stability and regularity of firing over this period between ectopic and non-ectopic mice (ranksum; all $p>0.01$; figure 25). This means, the previously observed differences in gap-detection thresholds in the primary cells between ectopic and non-ectopic mice cannot be explained by a difference in onset responses to noise.

Analysis of the onset responses in the non-primary cells did, however, reveal a difference between ectopic and non-ectopic mice in the amount of firing (ranksum; $p<0.01$) but not in the stability or regularity of firing (ranksum; $p>0.01$; figure 27; table A3). The untuned cells had similar amounts of firing and stability or regularity of firing between ectopic and non-ectopic mice (all $p>0.01$; figure 27; table A3).

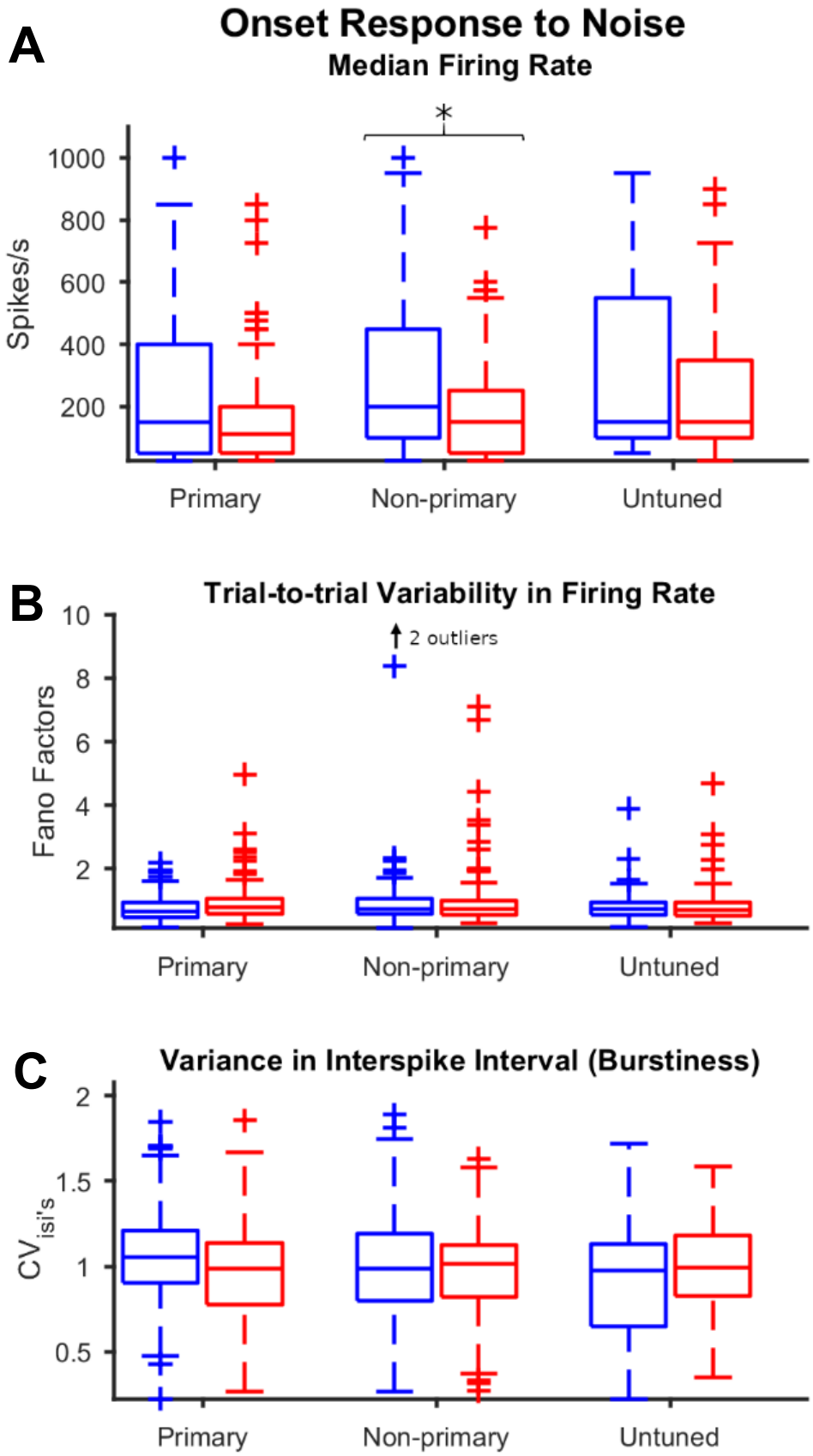

Figure 25: Noise onset responses similar between ectopic and non-ectopic mice in primary cells. Gap-detection threshold differences between ectopic and non-ectopic mice in primary cells cannot be explained by a difference in the onset response to a noise in isolation but there is a difference in the onset firing to a noise for non-primary cells. Analysis of the onset response (defined as the first 50ms of the response) to a 250ms white noise was performed for the median firing rate (A) and the stability of firing, measured using fano factors to look at the trial-to-trial variability (B) of the firing rate and the coefficient of variance of the interspike interval (CV_{ISI}) to assess the variance in the firing(C). There is no difference between ectopic and non-ectopic mice in the onset response to a noise for primary and untuned cells (ranksum; all $p>0.01$). However, there was a significant difference in the median firing rate between ectopic and non-ectopic mice for the non-primary cells ($p<0.01$). The stability of firing (fano factors and CV_{ISI}) and for the non-primary cells were not significantly different between ectopic and non-ectopic mice ($p>0.01$).

Similar to the results over the onset period there was no difference for primary cells in between ectopic and non-ectopic mice over the sustained period in amount of firing or stability or regularity of firing (ranksum; $p>0.01$; figure 26; table A3). Again consistent with the onset analysis is the result that non-primary cells have difference amounts of firing between ectopic and non-ectopic mice (ranksum; $p<0.01$; figure 26; table A3), although the stability or regularity of this firing is similar between ectopic and non-ectopic mice (ranksum; all $p>0.01$; table A3). The untuned cells again showed no difference between ectopic and non-ectopic mice over the sustained period for both amount of firing and stability or regularity of firing (ranksum; all $p>0.01$; figure 2t; table A3). In addition there was no difference in the fall-off rate of the sustained response between ectopic and non-ectopic mice for any group of cells (figure A3; all $p>0.01$).

Overall, any differences in responses to noise between ectopic and non-ectopic mice does not seem to be able to explain the gap-detection thresholds results we discuss in the previous section. For example, in the primary cells, which were found to have a significant difference in neural gap-detection thresholds between ectopic and non-ectopic mice we found higher peak firing rates to noise which would suggest for these mice there should be a higher firing rate to second noise and therefore more accurate neural gap-detection threshold. Furthermore, the differences in responses to noise between ectopic and non-ectopic mice seem to be most evident in the non-primary cells, in where we found no significant difference in neural gap-detection thresholds. The difference in median firing rate in the non-primary cells is interesting as there was found to be no significant difference in neural gap-detection thresholds in these cells suggesting a general reduction in the amount of firing to a noise does

not necessarily lead to a reduction in neural gap-detection ability. This all suggests the difference in neural gap-detection cannot be explained by an overall difference in a response to a noise.

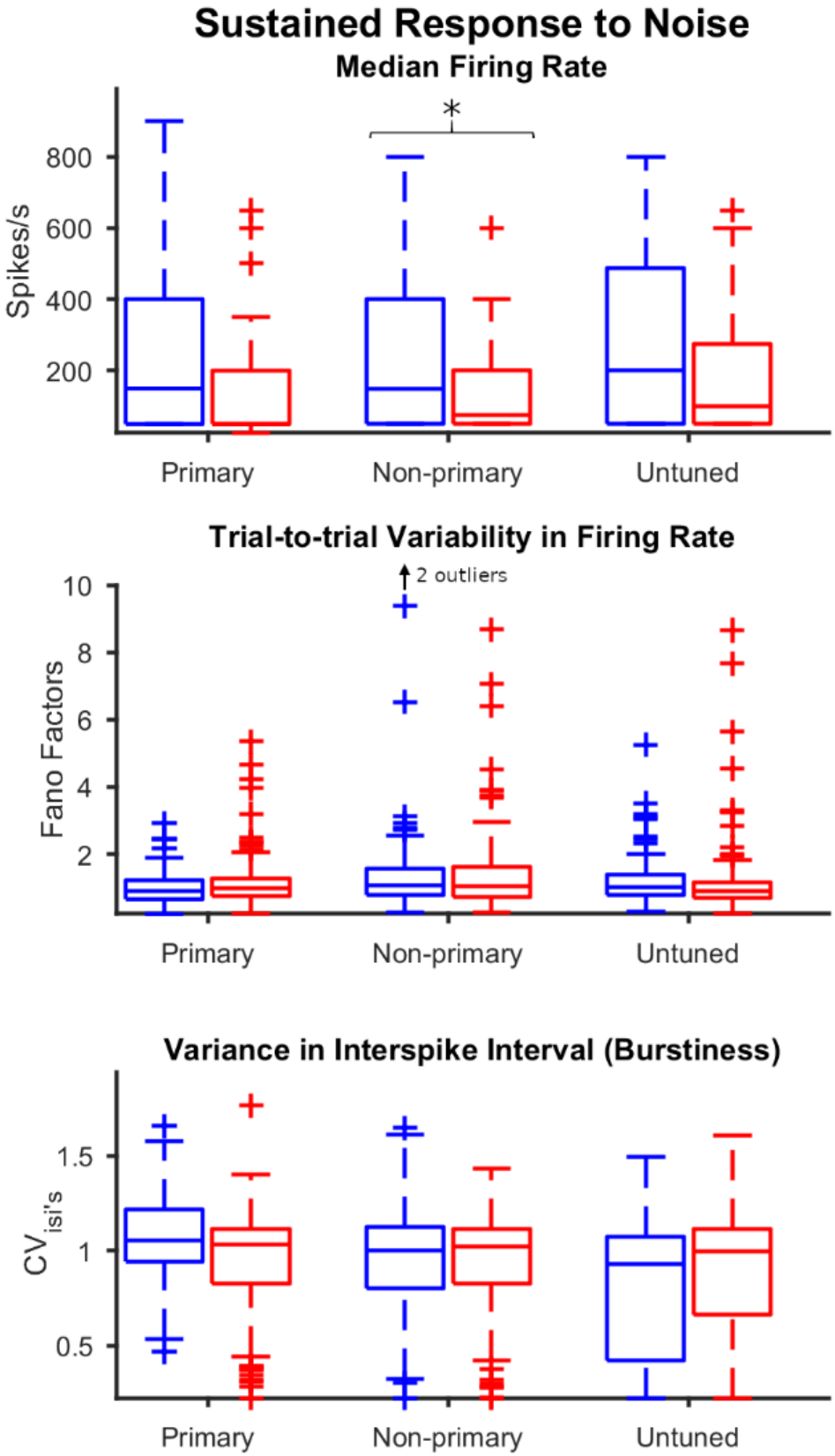

Figure 26: Sustained responses to noises are similar between ectopic and non-ectopic mice in primary cells. Gap-detection threshold differences between ectopic and non-ectopic mice in primary cells cannot be explained by a difference in the sustained response to a noise in isolation. Analysis of the sustained response (defined as the last 150ms of the response) to a 250ms white noise was performed as described in figure 27 but for the sustained response to a noise. This analysis revealed there no difference between ectopic and non-ectopic mice in the sustained response to a noise for the primary and untuned cells (ranksum; all $p>0.01$), as for the onset response. However as reveal in the onset response analysis there is a significant difference in the median firing rates of the sustained response for non-primary cells (ranksum; $p<0.001$) but the stability of firing in these cells is similar in ectopic and non-ectopic mice (ranksum; all $p>0.01$).

Cells with offset responses are reduced in frequency in IC

Previous studies into the longer neural gap-detection thresholds in ventral MGB of ectopic compared to non-ectopic mice found there were also a reduction in the number of cells with offset responses in ventral MGB in ectopic compared to non-ectopic mice (Anderson & Linden, 2016). We therefore investigated whether there was also a difference in offset responses in the IC recordings.

Offset responses were analysed using a 250ms 60dB SPL noise. There were found to be two types of offset responses within IC: those with an excitatory increase in firing following noise offset (see figure 27 for examples) and those with inhibition or suppression of firing below spontaneous rate as has been noted previously (Kasai et al. 2012).

Overall, the percentage of offset responses in IC recordings was smaller than the previously reported percentage of offset responses in MGB (Anderson & Linden, 2016) which is a finding consistent with other studies which suggest offset responses are less common in IC compared to MGB. There were 15% of cells with some form of offset response in ectopic mice in IC compared to 23% of non-ectopic mice, this difference between number of offset responsive cells is significant (Fisher exact test $p=0.006$).

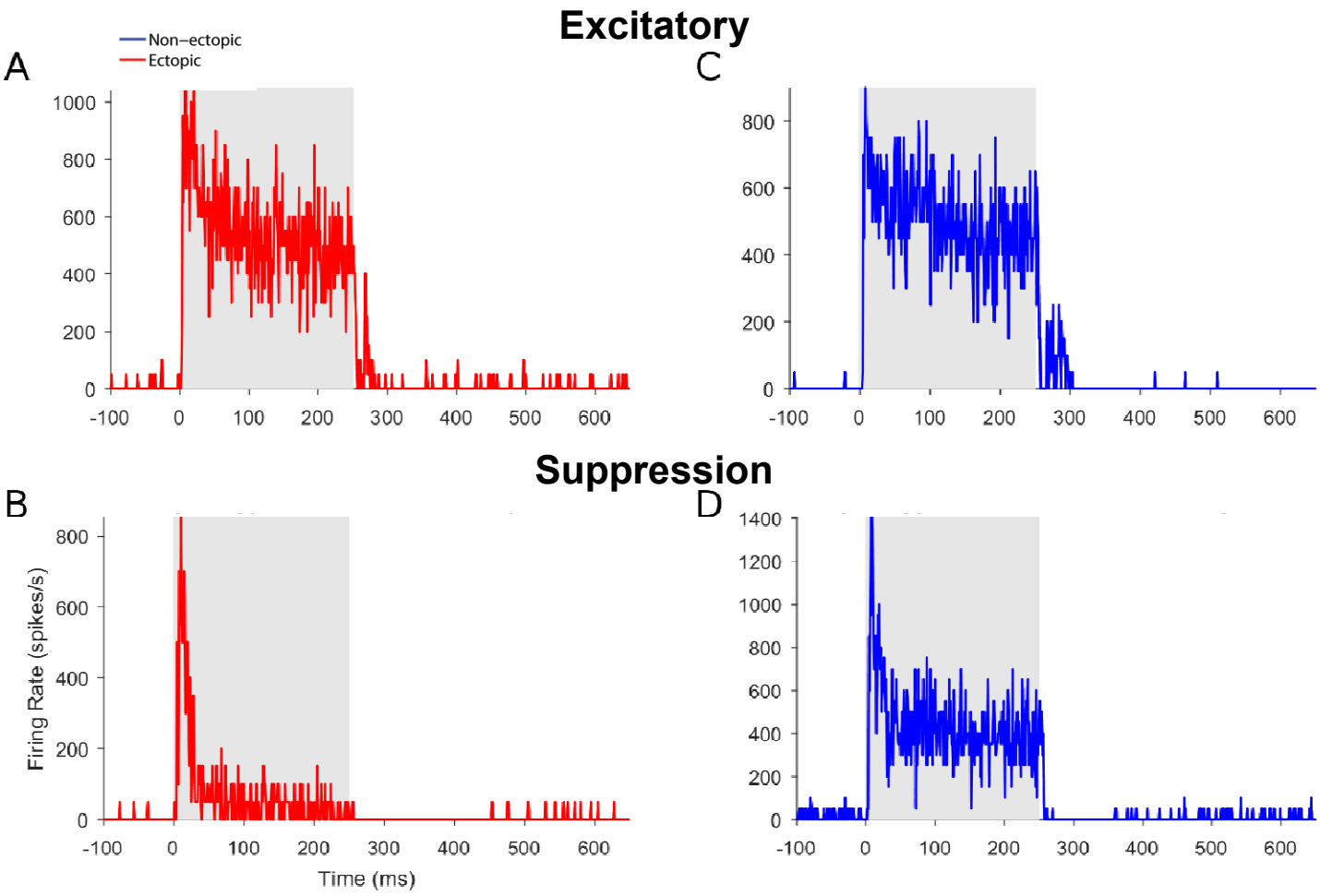

Figure 27: Single cell PSTH examples of offset responses recorded. Plots showing PSTHs for single cells response to a 250ms 60dB SPL noise showing sample excitatory from ectopic mouse (A), excitatory from non-ectopic mouse (B) and suppression/inhibitory offset responses from ectopic mouse (C) and non-ectopic mouse (D). Noise duration is indicated by grey shading. X-axis is relative to noise onset.

Of these cells with offset responses 9% had excitatory offset responses from ectopic mice compared to 15% of cells with excitatory offset responses in non-ectopic mice, which is trending towards a significant difference (Fisher exact test p=0.03; figure 30), indicating a trend towards fewer excitatory offset responses in ectopic than non-ectopic mice. Analysis of the peak firing rates and latencies for the excitatory offset revealed no significant difference between ectopic and non-ectopic mice for offset peak firing rates or latencies (figure A2). This is consistent with the MGB study which also did not find a significant difference in peak firing rate or latency between ectopic and non-ectopic mice, only a difference in the percentage of cells with

excitatory offset responses (Anderson and Linden, 2016). The fact that the percentage of excitatory offsets is only trending towards significance in IC may be due to the small number of cells with excitatory offset responses (ectopic n=41, non-ectopic n=48) and may in fact be significant with a larger number of cells.

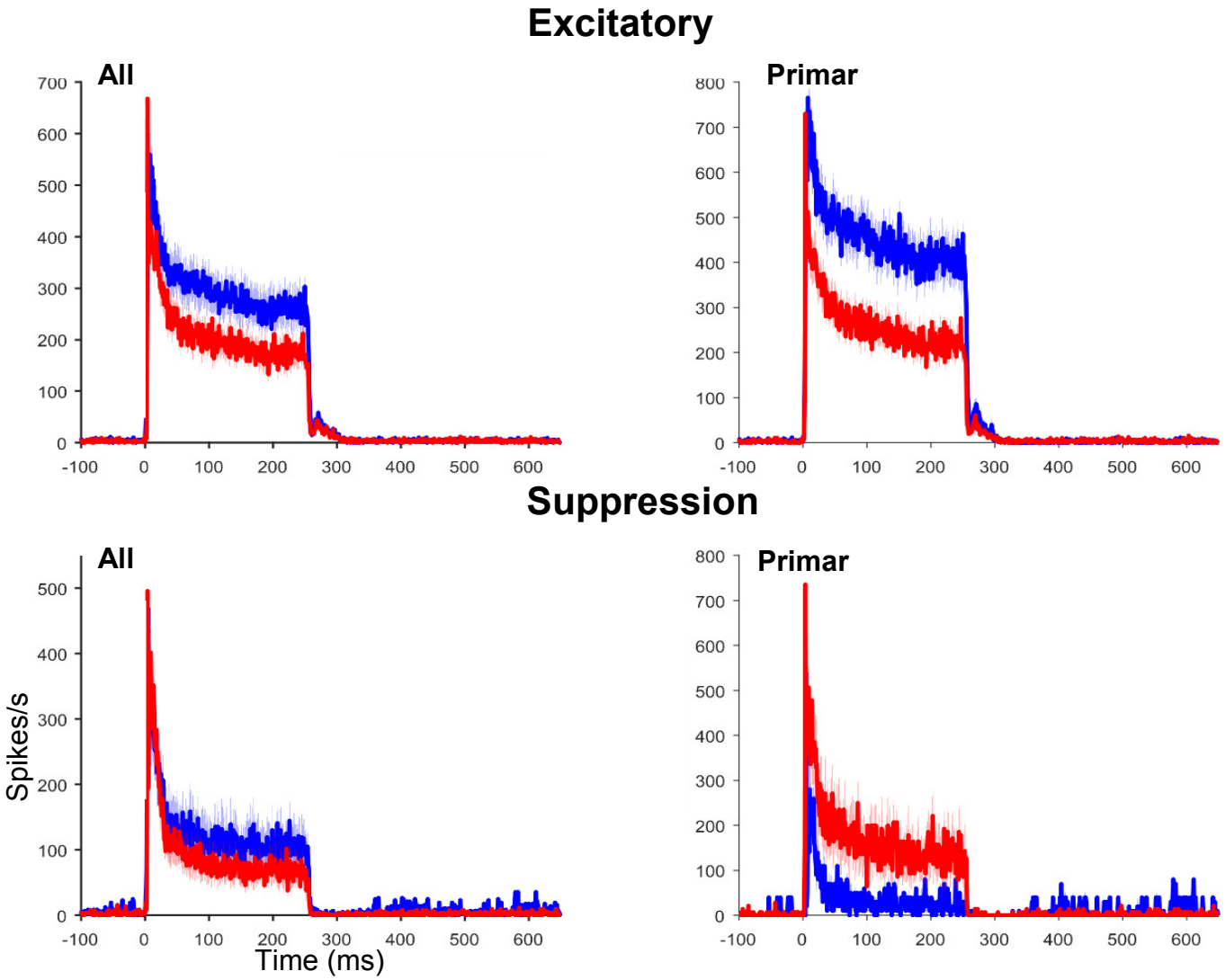

Figure 28: Population PSTHs for offset responsive IC cells. Population PSTH for cells across all IC subdivisions with excitatory offset responses for all cells and primary cells alone (top row). Also population PSTH for all cells and primary only cells with suppression/inhibitory offset responses (bottom row).Note time is relative to onset. Ectopic are shown in red and non-ectopic in blue with the bold line indicating the mean and shading either side of the mean indicating +/- SE.

As explained above in the IC we also found and analysed suppressive/inhibitory offset responses which were analysed in the previous MGB study (Anderson &

Linden, 2016). There were 6% of cells from ectopic mice with suppression offset responses and 8% of cells from non-ectopic mice, there was no significant difference between ectopic and non-ectopic mice for the suppression/inhibitory offset response (Fisher exact test p=0.151; figure 28). A population PSTH for cells identified with suppression offsets is shown in figure 28.

Overall, across all areas of IC, there was a significant reduction in the proportion of cells with offset responses in ectopic compared to non-ectopic mice. This reduction seems to arise from a reduction in the number of excitatory offset responses whereas the number of suppression/inhibitory offset responses appears similar between ectopic and non-ectopic mice. This result is consistent with the previous study from the MGB where they found a significant reduction in the number of excitatory offset responses in ventral MGB in ectopic compared to non-ectopic mice (Anderson & Linden, 2016). However, our observations also argue against the link between neural gap-detection thresholds and sound-offset responses hypothesised by Anderson & Linden (2016). Neural gap detection thresholds in the IC were shorter in ectopic than non-ectopic mice, even while the percentage of offset-responsive cells was reduced; therefore reductions in the percentage of offset-responsive cells do not necessary produce a lengthening of neural gap-detection thresholds, in the IC.

Since there was found to be a difference between ectopic and non-ectopic mice in neural gap-detection thresholds for primary cells in IC but not non-primary cells, further analysis was focused on primary IC cells with offset responses. In ectopic mice, 24% of primary cells had offset responses (either excitatory or suppression/inhibitory), while the percentage was 38% for primary cells in non-ectopic mice. This difference between ectopic and non-ectopic mice shows a trend

towards significance (Fisher exact test p=0.045). When analysing excitatory offset responses in primary cells alone, we found excitatory offset responses in 19% of cells from ectopic mice and 31% of cells from non-ectopic mice (Fisher exact test p=0.05). The proportion of offset-responsive cells among primary IC cells (likely recorded from central IC) is similar to the proportion of offset-responsive cells found in ventral MGB in the previous study (25% of cells in ectopic mice and 36% of cells in non-ectopic mice; Anderson & Linden, 2016) even though the difference in number of cells with excitatory offset responses was not significant in IC. There was a trend towards significance for the peak firing rate of the excitatory offset responses to be reduced in ectopic compared to non-ectopic mice (ranksum p=0.037; figure A2) but no significant difference or trend for peak latencies of the excitatory offset responses (ranksum p=0.721; figure A2). Consistent with there being no significant difference between ectopic and non-ectopic mice in numbers of suppression/inhibitory offset responses across all cells, there was also no significant difference for only the primary cells (Fisher exact test p=0.759; figure A2). The fact that there was only a trend toward significance for a reduction the number of all types of offset responses in primary cells in ectopic compared to non-ectopic mice may be due to the smaller number of cells with offset responses when only analysing the primary cells.

Similar synchronisation of firing to rapid click trains in ectopic and non-ectopic mice

Following Anderson and Linden 2016 and to further investigate temporal processing within IC, we also analysed synchronisation of firing to rapid click trains by calculating vector strength of responses to click trains with various inter-click-intervals (see Methods for details). Figure 29 shows example recordings of click trains.

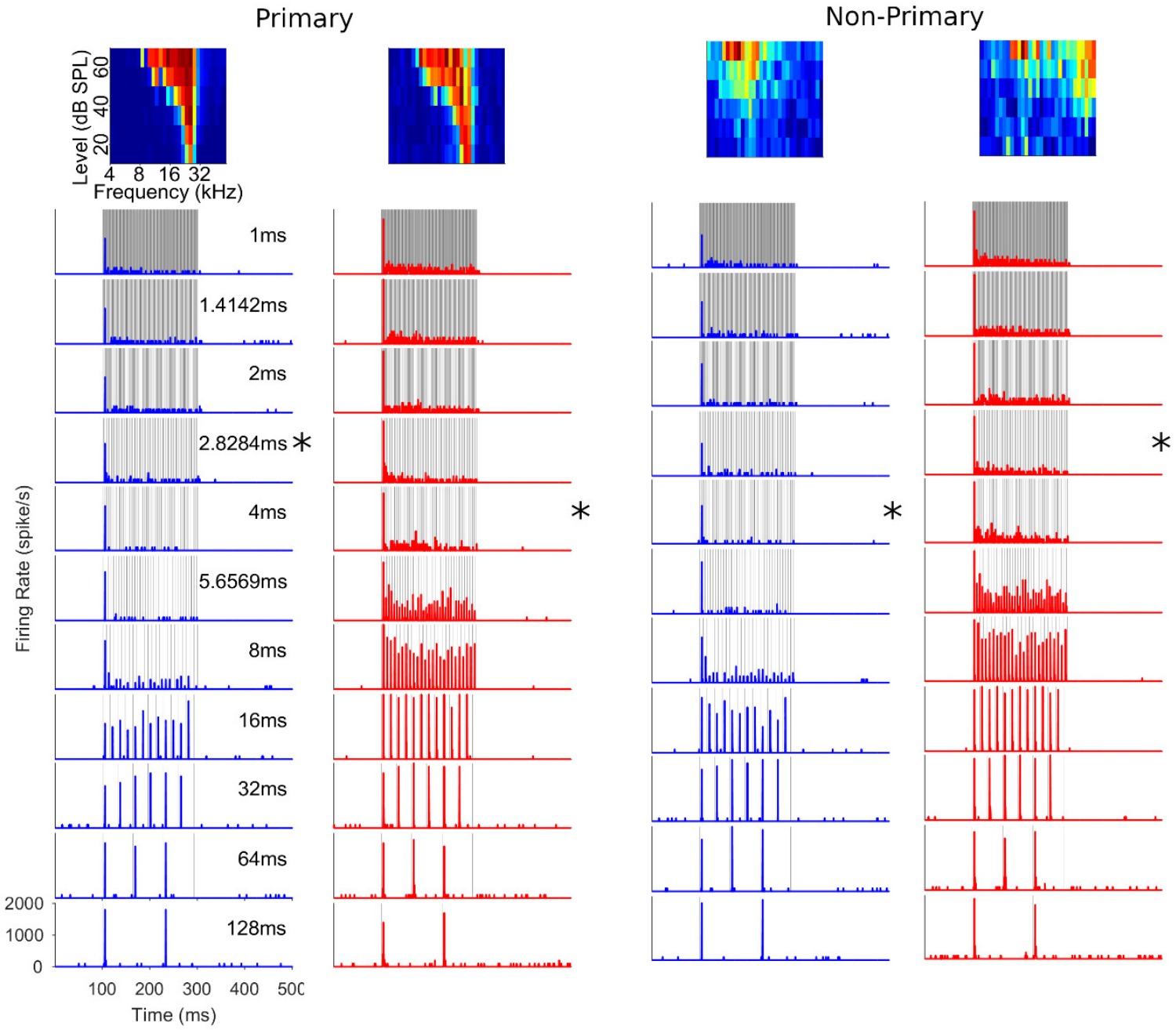

Figure 29: Example FRAs and PSTHs for clicktrains from primary and non-primary cells. Examples from both ectopic (red) and non-ectopic (blue) cells. Figure convension as in figure 23.

We defined the click train synchronisation threshold to be the minimum inter-click-interval for which the Rayleigh test statistic for vector strength exceeded 13.8 (i.e. test for uniformity, null hypothesis rejected at $p<0.01$). There was no significant difference in synchronisation thresholds between ectopic and non-ectopic mice for primary IC cells and non-primary IC cells (figure 30; all $p>0.01$).

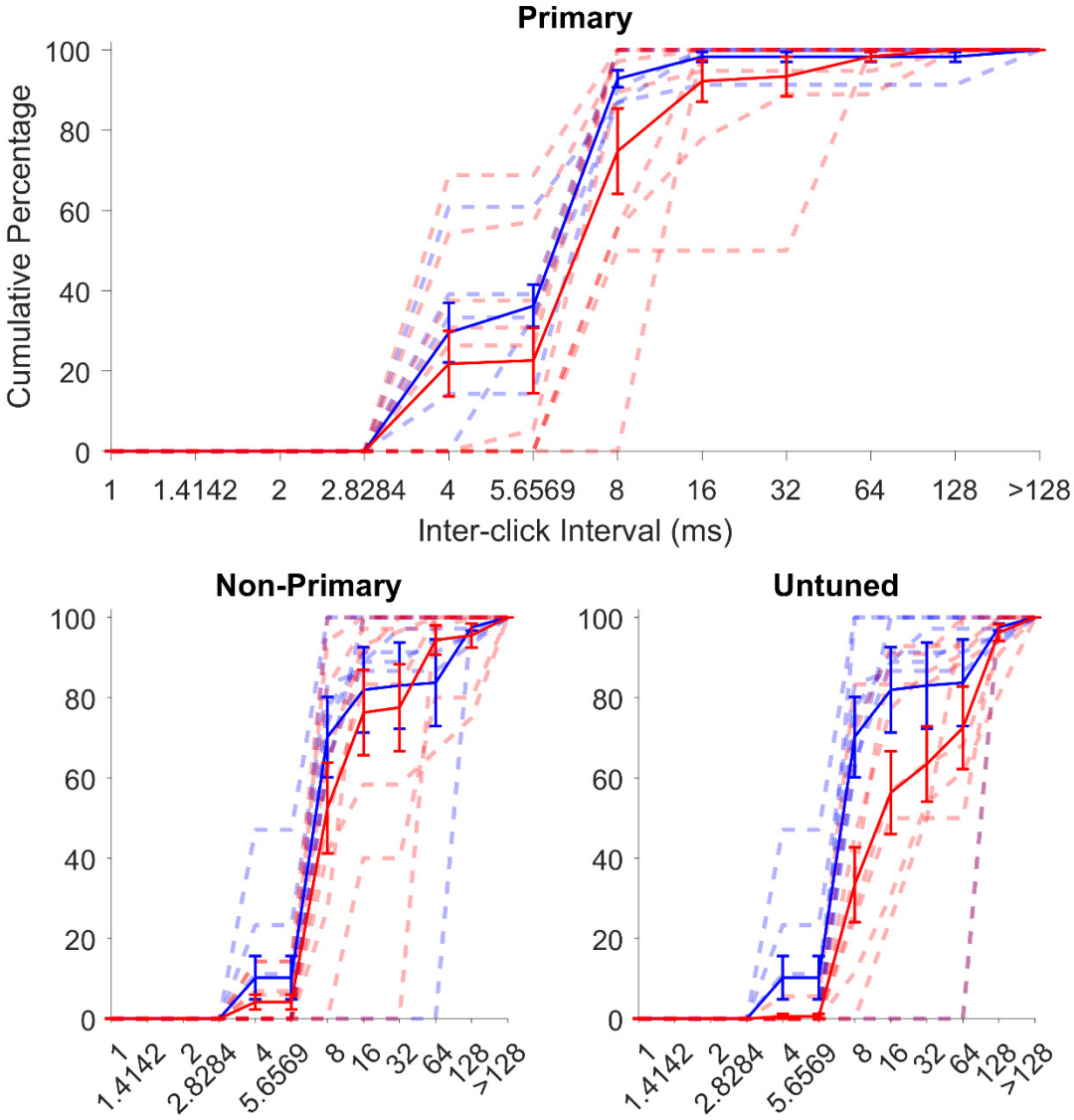

Figure 30: No difference in click-train synchronisation for primary cells between ectopic and non-ectopic mice. Click-train synchronisation thresholds across different IC subdivision groups. Dashed faded lines indicate individual animals, solid lines indicate means across animals +/- SE with ectopic in red and non-ectopic in blue. Top plot shows click-train synchronisation thresholds for primary (ranksum p>0.01). Bottom plots show click-train synchronisation thresholds for and non-primary IC cells (p>0.01) and untuned cells (p<0.01).

There was a significant difference between ectopic and non-ectopic mice for click train synchronisation thresholds for the untuned IC cells (ranksum p=3.18e-12; figure 30) with a reduction in the percentage of cells with shorter inter-click intervals in the ectopic compared to the non-ectopic mice. This is contrast to the previous study in MGB where they found no significant difference in click-train synchronisation thresholds between ectopic and non-ectopic mice for any of the MGB subdivisions.

This results is however, complicated by the fact that we do not have histological data to determine the location of the untuned cells.

No difference in frequency tuning of neurons in ectopic and non-ectopic mice

Among primary cells, there was also no significant difference in CFs between ectopic and non-ectopic mice although again there was a trend towards ectopic mice having significantly more highly tuned cells than non-ectopic mice (figure 31; rank-sum p=0.013).

Likewise, among non-primary cells there was no significant difference between ectopic and non-ectopic mice (rank-sum p=0.03; figure 31). For obvious reasons, we could not analyse the CF for untuned cells. Overall, these results indicated there is no significant difference in tuning between ectopic and non-ectopic mice.

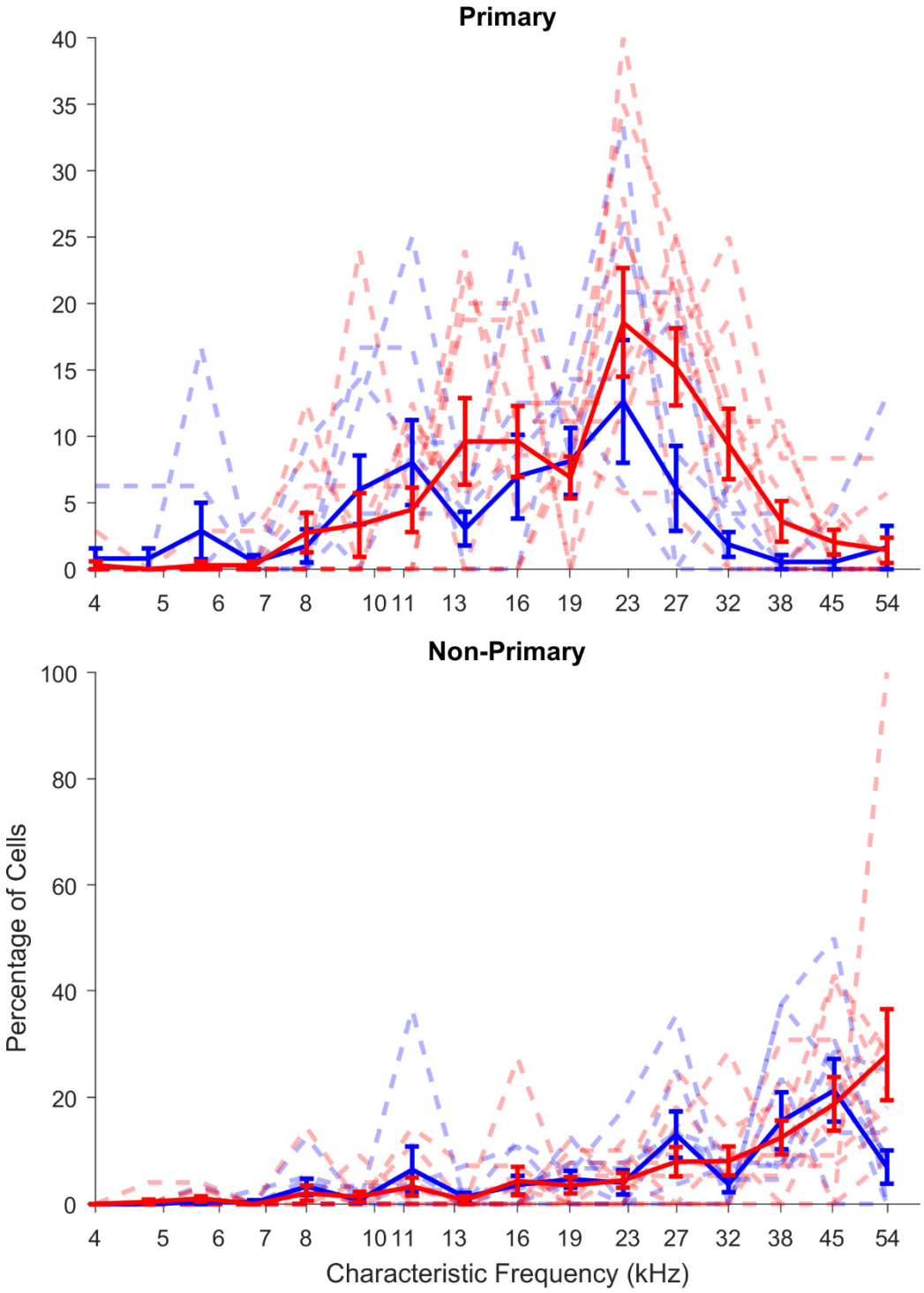

Figure 61: No difference between ectopic and non-ectopic mice in characteristic frequencies. Characteristic frequencies for primary (top plot; ectopic n=150; non-ectopic n=90; p>0.01) and non-primary IC cells (bottom plot; ectopic n=181; non-ectopic n=153; p>0.01). Figure conventions as in figure 30.

Spontaneous firing rates are lower in ectopic than in non-ectopic mice in non-primary IC cells.

In addition to examining differences in evoked activity recordings, we also analysed spontaneous rate over a 100ms period. There was found to be no difference between ectopic and non-ectopic mice for spontaneous rate in the primary IC cells on any of the measures used (see figure 32; ranksum all $p > 0.04$; table A3). So ectopic and non-ectopic mice have similar amounts of firing in the primary cells which are likely from central IC.

The non-primary cells where were significantly different between ectopic and non-ectopic mice for CV_{ISI} (ranksum p=2.8E-5, figure 32; table A3). Whereas the mean firing rate and fano factors over the spontaneous period in these cells was not significantly different between ectopic and non-ectopic mice (ranksum; all $p>0.01$; figure 32; table A3). This means the non-primary cells in the ectopic mice vary in the regularity of spontaneous firing between ectopic and non-ectopic mice but not in the amount of firing or the stability of firing across trials.

Similarly, in the untuned cells there was a difference between ectopic and non-ectopic mice in the CV_{ISI} (ranksum p=0.006; figure 32; table A3) but not in the amount of firing and stability of firing across trials over the spontaneous period (ranksum; all $p>0.01$; figure 32; table A3).

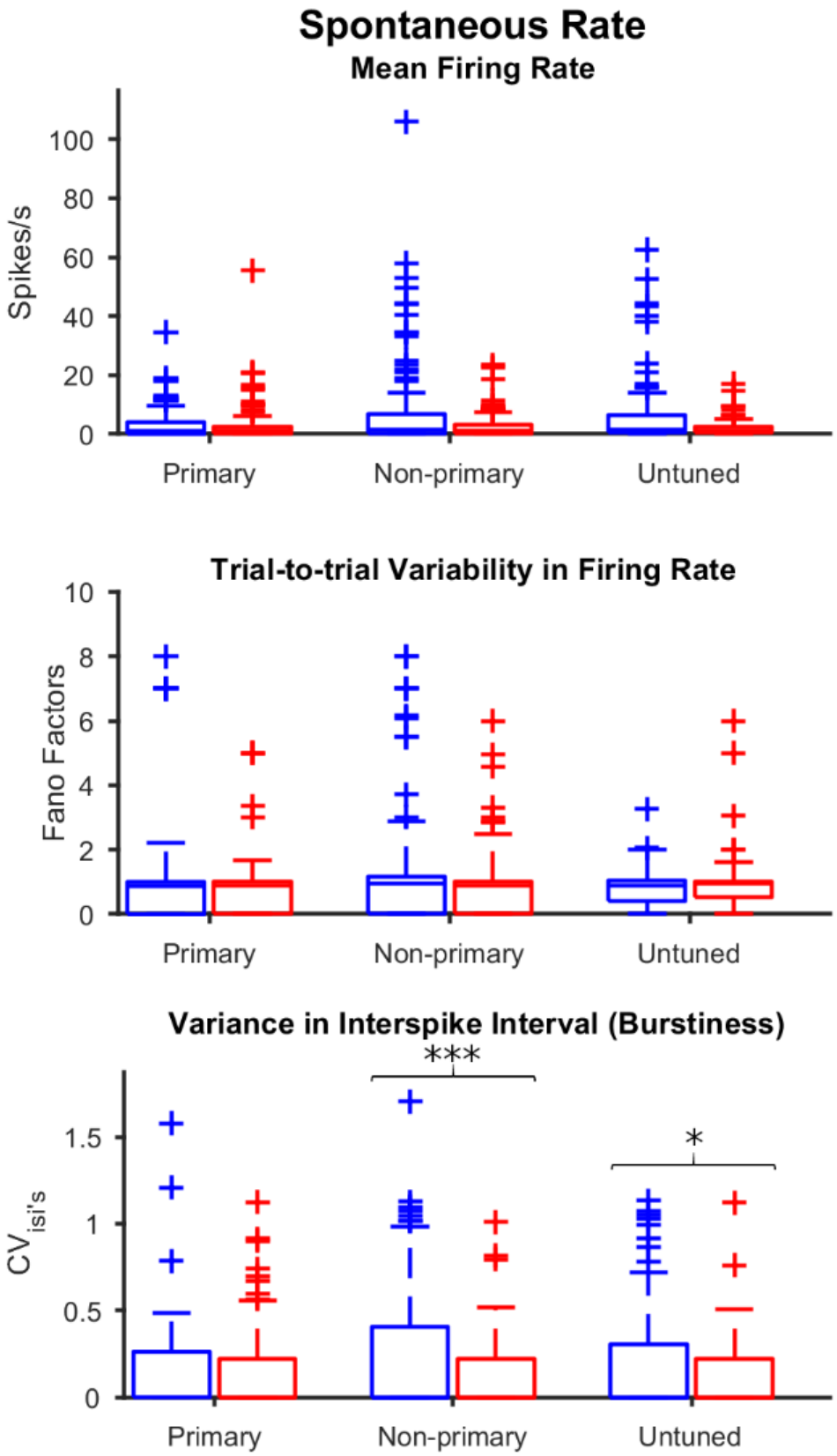

Figure 32: Non-primary and untuned cells but not primary cells differ in the variance of the interspike interval between ectopic and non-ectopic mice for spontaneous rate. Analysis performed on spontaneous rates: CV_{isi}, Fano factors and mean firing rates. Figure conventions as in figure 27. Non-primary cells were found have a significant difference between ectopic and non-ectopic mice for the variance in interspike interval (ranksum; $p<0.001$). Similarly untuned also showed a significant difference between ectopic and non-ectopic mice (ranksum; $p<0.01$). The variance in interspike intervals for primary cells was similar between ectopic and non-ectopic mice as was the trial-to-trial variability and mean firing rates (ranksum; all $p>0.01$).

Overall, these results indicate the difference found in the spontaneous rate between ectopic and non-ectopic mice arises primarily from the non-primary IC cells, i.e. from cells likely recording in dorsal/external IC. Furthermore, the spontaneous rate difference cannot account for the differences found in neural gap-detection thresholds between ectopic and non-ectopic mice where the difference was found only in the primary IC cells.

Ectopic mice have different rate of decline in MGB sustained response to a noise compared to non-ectopic mice

After analysing the IC recordings in this detailed way, we wondered if the same analysis on the MGB data from the previous study (Anderson & Linden 2016) might reveal further differences between ectopic and non-ectopic mice. For the MGB recordings some of the experimental parameters differ from the IC recordings (for example, electrode type, rise/fall gating of noise, some stimulus parameters such as duration of gaps in gap-in-noise stimuli); however, the recordings and stimulus conditions were similar enough to allow for general comparison of the results.

To allow comparison with the IC recordings, we applied a Fano factor restriction criteria, which was not applied in the original study. Using analysis of the histogram of Fano factor values across all recorded cells (see Methods) a Fano factor threshold of 10 was chosen. Any recordings above this threshold value were not used for the subsequent analysis. Before applying the Fano factor restriction criteria there were 427 ectopic cells and 522 non-ectopic cells, after the application of the Fano factor criteria 423 ectopic cells and 514 non-ectopic cells.

The previously published MGB study (Anderson & Linden, 2016) had investigate mean firing rates over the sustained responses to a noise but did not look directly at

the fall-off rate in the sustained response. A re-examination of populations PSTHs for the previous extracellular recordings in MGB suggested a possible difference between ectopic and non-ectopic animals in the fall-off of sustained responses to a noise. Figure 33 shows the population response to a 250ms white noise for both ectopic and non-ectopic mice and demonstrates an apparent different in fall-off of the sustained responses to a noise together with the previously noted differences in offset responses.

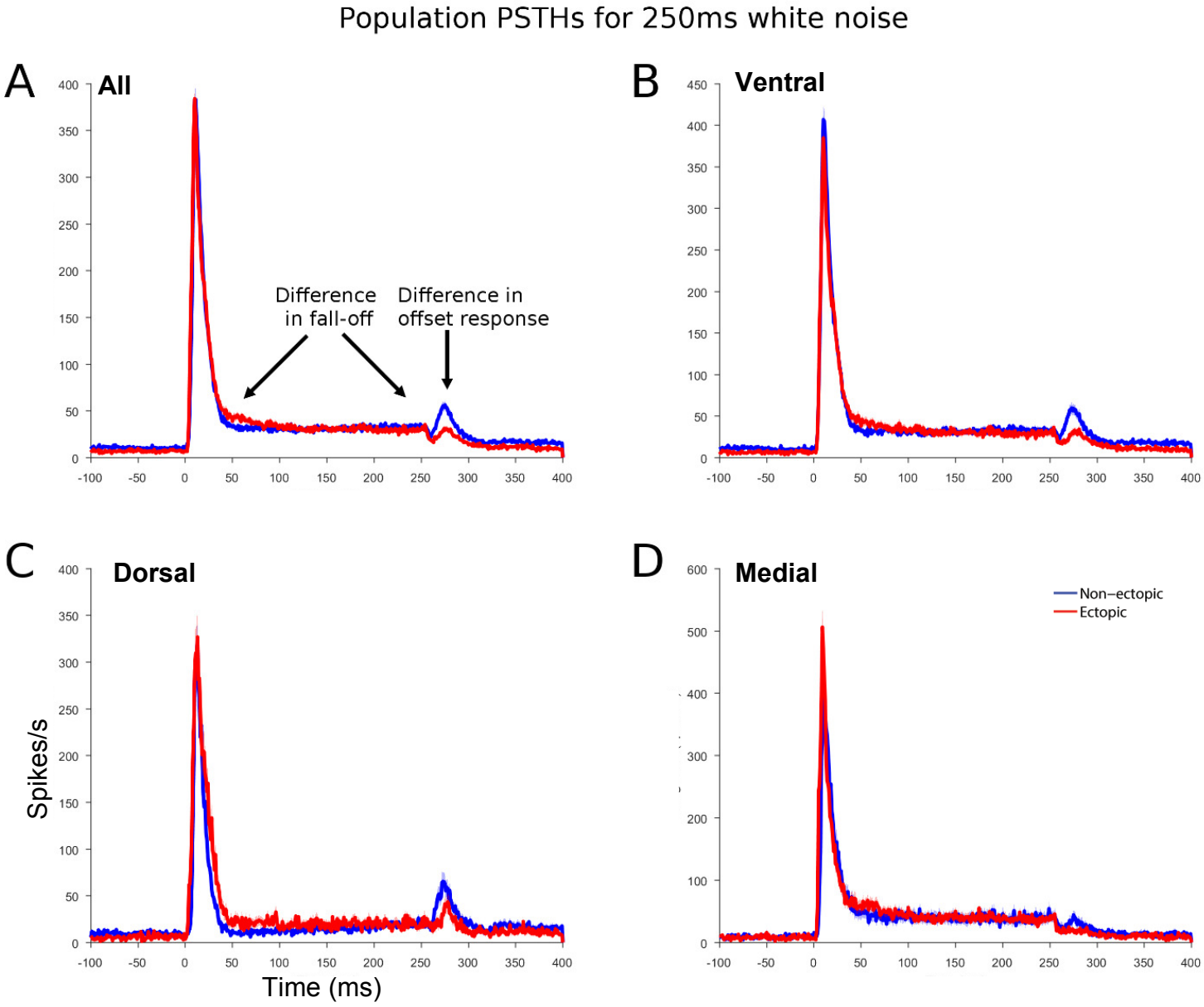

Figure 83: PSTHs of MGB recordings. Re-analysis of data from Anderson & Linden (2016), MGB population PSTHs to 250ms 60dB SPL white noise. Ectopic in red and non-ectopic in blue. Line thickness represents +/- SE. (A) Across all MGB recorded cells. (B) For cell recorded from ventral MGB. (C) For cells recorded from dorsal MGB. (D) For cells recorded form medial MGB.

A re-analysis of this data revealed that in addition to the previously reported reduction of offset response firing in the ectopic versus non-ectopic mice, there was also a significant difference in response rate fall-off in the later portion of the noise. The previous analysis had shown there to be no significant difference between ectopic and non-ectopic mice in mean firing rate for the first 50ms of the response to a noise and to the last 50ms of the response to a noise. However, our re-analysis revealed that while the amount of firing to the later portion of the noise is not different between ectopic and non-ectopic mice there is a difference in the rate of fall-off in the sustained response to the noise; in the non-ectopic mice cells seem to continue firing at a steady rate after the initial period of firing to the onset of the noise where as in the ectopic mice this sustained firing declines more rapidly. This difference in fall-off was analysed by subtracting, for each cell, the mean firing rate over the period of 150ms to 200ms after noise onset minus the mean firing rate of responses over the period of 200ms to 250ms after noise onset (from response to a 250ms white noise). Across all recorded MGB cells this measure of fall-off in sustained response was significantly different between ectopic and non-ectopic mice (ranksum p=1.726e-6; figure 34A). Moreover, the MGB subdivision specificity of this finding mirrored that of the previous findings and differences between ectopic and non-ectopic mice in neural gap-detection thresholds and number of cells with offset responses that was most evident in ventral MGB (p=1.062e-4; figure 34B), also present in dorsal MGB (p=1.796e-6; figure 34C) and not evident in medial MGB (p=0.226; figure 34D).

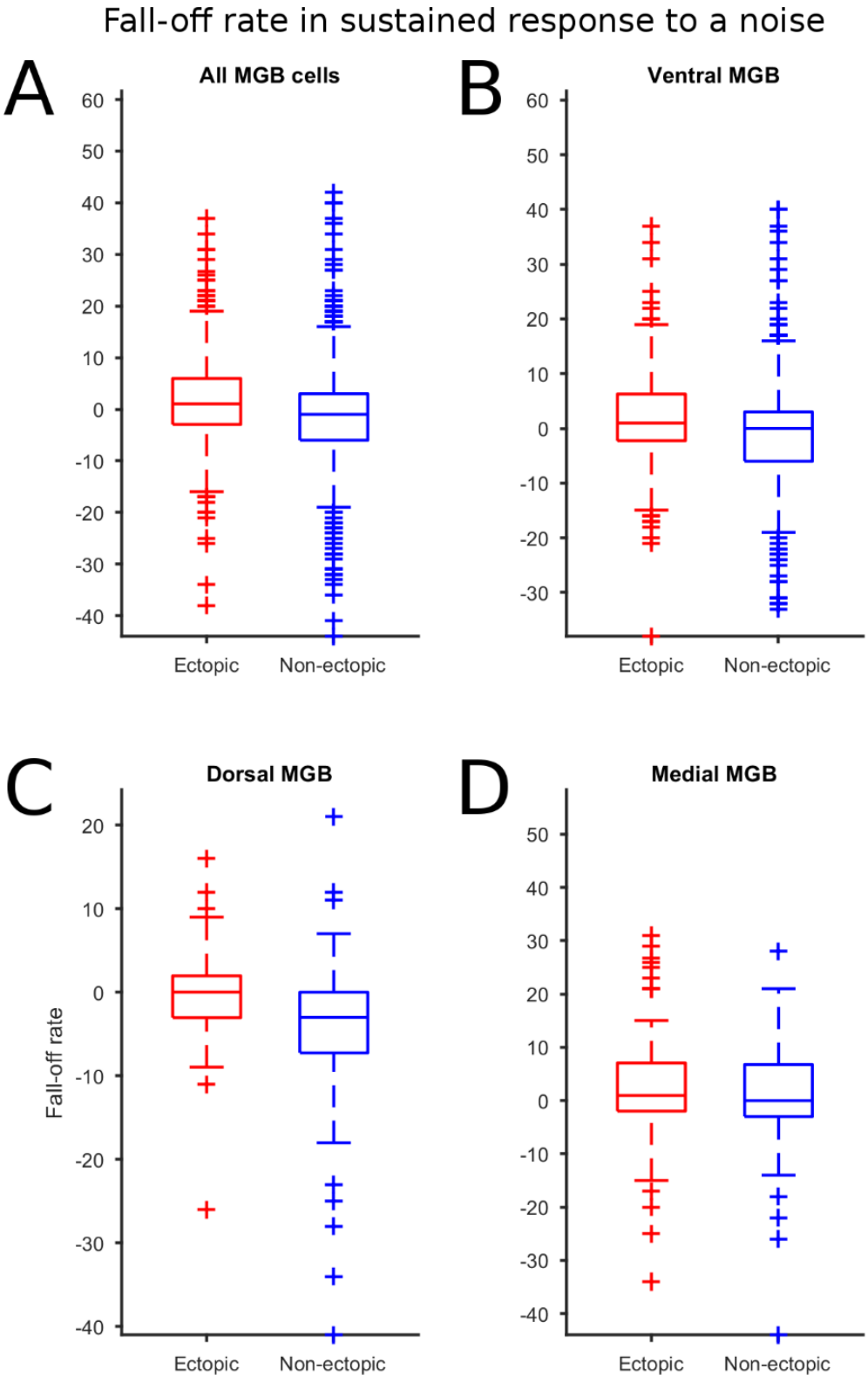

Figure 34: Fall-off rates for sustained portion of a response to noise differ between ectopic non-ectopic mice for ventral and dorsal MGB cells. Ectopic in red, non-ectopic in blue. (A) Across all MGB cells (ranksum; $p<0.01$). (B) For only ventral MGB cells ($p<0.01$). (C) For only dorsal MGB cells ($p<0.01$). (D) For only medial MGB cells ($p>0.01$).

These results suggest that ectopic mice may have a specific deficit in adaptation to noise where there is a failure to adapt to continuous sounds at the level of MGB. Note we did not observe any evidence of differences between ectopic and non-ectopic mice in fall-off of sustained responses to noise in IC (or any of its physiologically defined subdivisions), so this result points to a possible difference between MGB and IC in ectopic mice.

Next, we wondered whether this observed difference in the rate of decline in the sustained response to a noise might be coming from only the MGB cells with offset responses. We found a significant difference between ectopic and non-ectopic mice for fall-off rate for both offset only cells and onset only cells when analysed across all MGB cells (figure A4). This result was also found when analysing only cells recorded from ventral MGB (figure A4). There was no significant difference between ectopic and non-ectopic mice for either onset only cells or cells with an offset response recorded from medial MGB (figure A4). In the cells recorded from dorsal MGB, however, we found a significant difference in the rate of decline of the sustained response between ectopic and non-ectopic mice for cells with offset responses but not for cells with onset responses (figure A4). Thus we conclude in ventral MGB abnormally rapid fall-off in sustained responses to noise in MGB can affect cells without offset responses however in dorsal MGB this fall-off abnormality appears to only affect the offset responsive cells.

Ectopic mice have greater trial-to-trial variability in sustained response to noise in MGB compared to non-ectopic mice

We further investigated the sustained response to a noise in MGB by calculating median firing rate, CV_{isi}, and Fano factors over this period. Since this analysis was not performed in the original study we also calculated these for the onset responses.

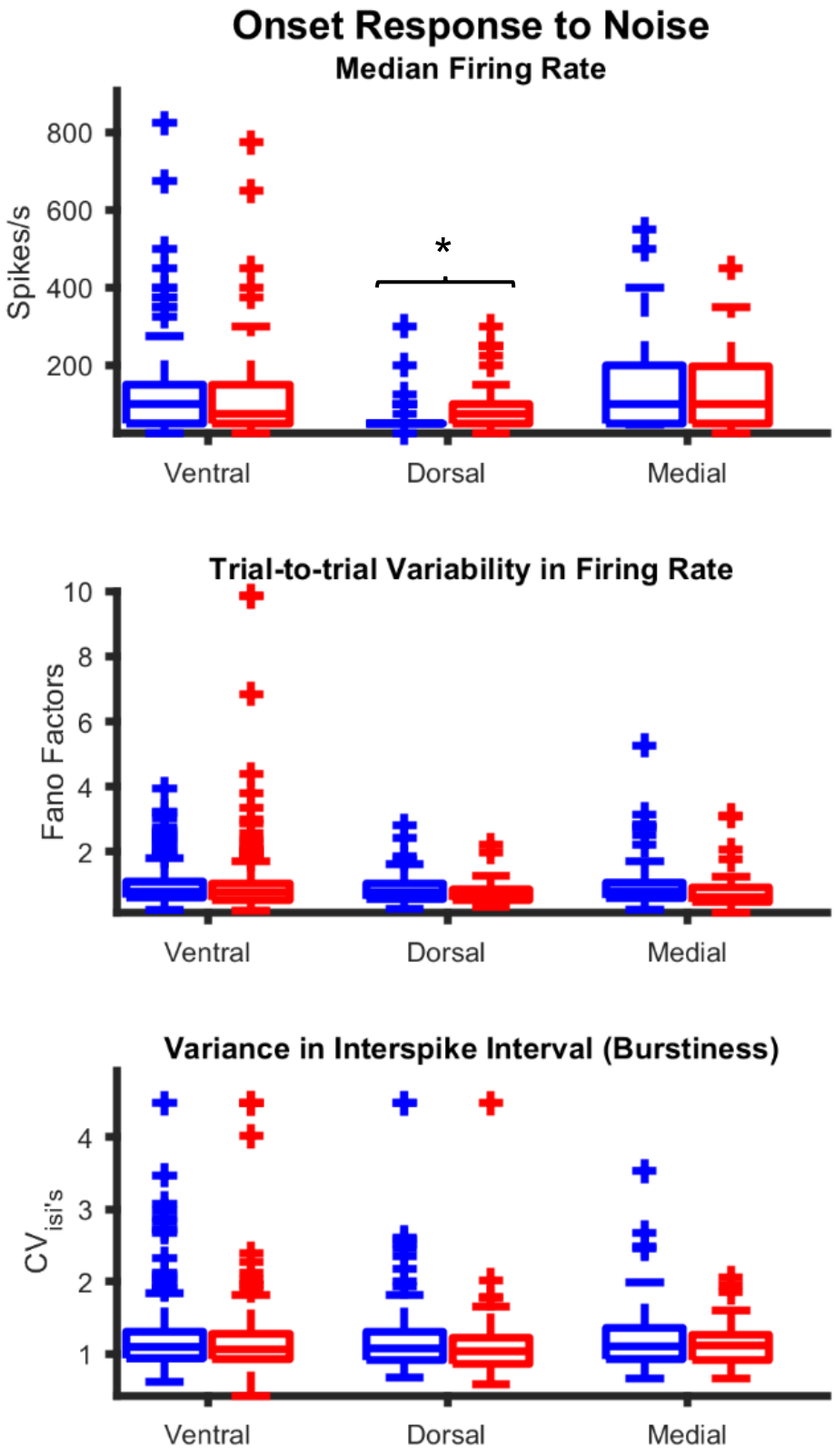

Figure 35: Onset responses to noise differ only in dorsal MGB between ectopic and non-ectopic in the amount of firing. Figure conventions as in figure 27 but for MGB recordings. Ventral and medial MGB were found to have a similar onset responses to a noise between ectopic and non-ectopic mice (ranksum; $p>0.01$). Dorsal MGB was found to have a significantly higher median firing rate in ectopic mice compared to non-ectopic mice ($p<0.01$) but the variability of firing between trials and in the interspike intervals did not differ from non-ectopic mice.

Over the onset period there was no difference between ectopic and non-ectopic mice in the recordings from ventral MGB and medial MGB in terms of amount of firing and regularity or stability of firing (ranksum; all $p>0.01$; figure 35; table A4). However for dorsal MGB the amount of firing over the onset period was found to differ between ectopic and non-ectopic mice (ranksum; $p<0.01$; figure 35; table A4). The ectopic mice have higher amounts of firing over the onset period than non-ectopic mice. The stability and regularity of firing in dorsal MGB was found to be similar, however, between ectopic and non-ectopic mice (ranksum; all $p>0.01$; figure 35; table A4).

Over the sustained period there is a significant difference between ectopic and non-ectopic mice in the trial-by-trial variability of the recordings from ventral MGB (ranksum; $p<0.0001$; figure 36). So, the consistency of firing across trials varies between ectopic and non-ectopic mice in ventral MGB over the sustained period. The amount of firing and regularity of firing in ventral MGB over the sustained period was found to be similar between ectopic and non-ectopic mice (ranksum; all $p>0.01$; figure 36; table A4). For dorsal and medial MGB there was no difference between ectopic and non-ectopic in firing over the sustained period for any of the measures used (ranksum; all $p>0.01$; figure 36; table A4).

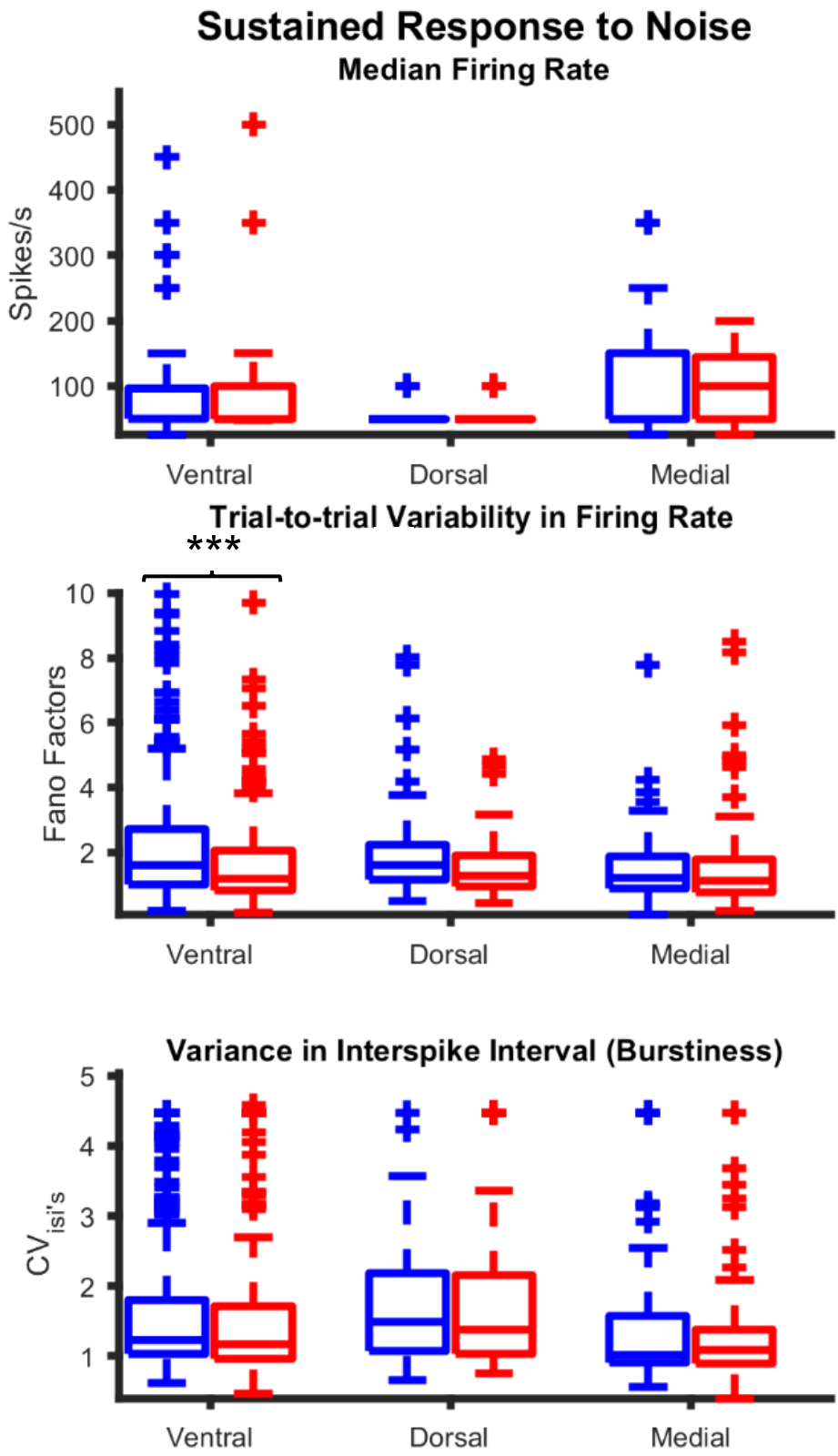

Figure 36: Sustained responses to noise differ between ectopic and non-ectopic mice only in ventral MGB trial-by-trial variability. Figure conventions as in figure 28 but for MGB recordings. The sustained portion of the noise response was found to have a significantly different variability in the trial-to-trial firing rate between ectopic and non-ectopic mice (ranksum; $p<0.0001$). The sustained portion of the noise was found to have similar responses in dorsal and medial MGB between ectopic and non-ectopic mice (all $p>0.01$).

These results suggest that in addition to the increased rate of fall-off in the sustained response to a noise in ectopic compared to non-ectopic mice there are additional differences in the trial-by-trial stability in the cells response to a noise over this period of the response. Given that the onset response does not show this instability, this demonstrates that the variability in sustained response for ectopic compared to non-ectopic mice is limited to the late, sustained response to a noise rather than a general instability in response to a noise as would be evidenced by a similar difference in the onset response. Although it is important to consider that the calculations for the peak response are over a much shorter time period (50ms) than for the sustained response (200ms).

Spontaneous firing rate in ventral and dorsal MGB differs between ectopic and non-ectopic mice

Since there was found to a difference between ectopic and non-ectopic mice for spontaneous rates in the IC recordings which seem to arise in the non-primary and untuned IC cells, the MGB recordings were also re-analysed for differences in spontaneous firing rates between ectopic and non-ectopic mice. Anderson and Linden (2016) found no significant differences between ectopic and non-ectopic mice as quantified over a very brief interval (4ms) but across 100 trials. Here, however, we re-analysed the MGB spontaneous firing rates in the same way as for the IC recordings, using a longer time period to obtain the mean firing rate (100ms) but using fewer trials than in the previous study (20 trials vs. 100 trials). In addition, we also performed CV_{isi} and Fano factor analysis over the spontaneous rate period, which was not performed in the previous study.

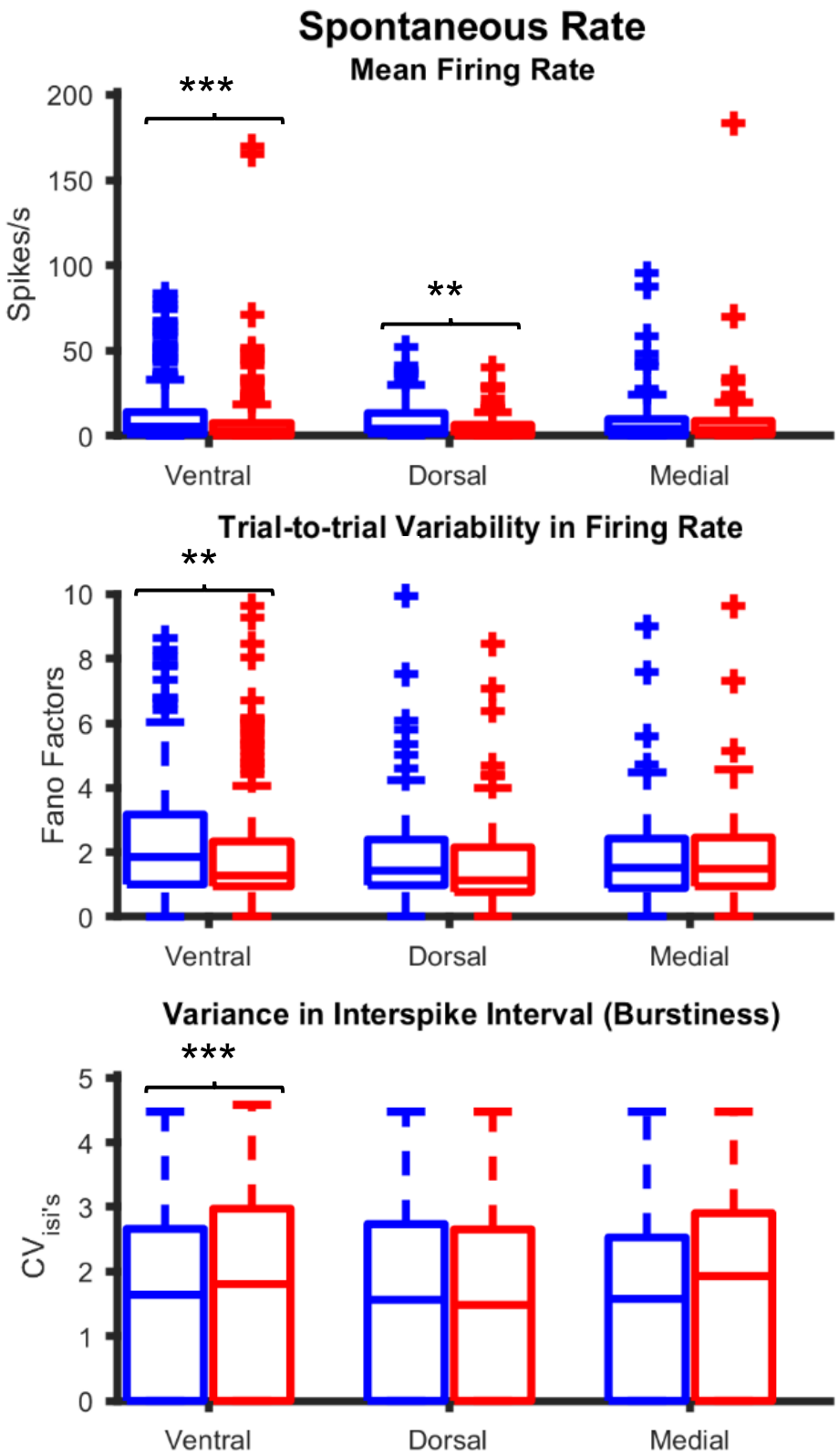

Figure 37: Ectopic mice have lower and less reliable spontaneous rates in ventral MGB. Figure conventions as in figure 34 but for MGB recordings. Analysis revealed differences in ventral between ectopic and non-ectopic mice for mean firing rate (ranksum; $p<0.0001$); variability of trial-to-trial firing rate ($p<0.0001$) and variance in interspike intervals ($p<0.0001$). This result demonstrates ventral MGB spontaneous rate are both lower and less reliable in ectopic compared to non-ectopic mice. Dorsal MGB was found to have lower spontaneous rates in ectopic compared to non-ectopic mice ($p<0.01$) but the variability in firing was found to be similar in ectopic and non-ectopic mice ($p>0.01$). The median firing rates were found to be similar between ectopic and non-ectopic mice in medial MGB ($p>0.01$).

This analysis revealed the differences in amount, stability and regularity of spontaneous firing in ventral MGB between ectopic and non-ectopic mice (ranksum; all $p<0.0001$; figure 37; table A4). For dorsal MGB, there was a significant difference between ectopic and non-ectopic mice for amount of firing (ranksum $p=0.003$; figure 37; table A4) but not for stability or regularity of firing (ranksum all $p>0.3$; figure 39; table A4). For medial MGB, there was no significant difference between ectopic and non-ectopic mice for any of the measures (ranksum; all $p>0.01$; figure 37; table A4).

These results, while consistent with the differences in neural gap-detection thresholds between ectopic and non-ectopic mice in MGB, appear to be surprising given the IC results. In the IC a difference between ectopic and non-ectopic mice in spontaneous rate was found only in the non-primary and untuned cells, not in the primary cells where a difference in gap-detection thresholds was found between ectopic and non-ectopic mice and which are thought to send most of the projections to ventral MGB.

Discussion

In this chapter, we set out to determine if the difference in gap-detection thresholds between ectopic and non-ectopic mice could be found electrophysiologically within IC. We did find a difference between ectopic and non-ectopic mice in the primary IC cells (which are likely from central IC) in gap-detection thresholds however in the MGB the ectopic mice have longer thresholds than non-ectopic mice and in the IC they have shorter thresholds so the difference seems to be contrasting in MGB and IC. We investigated whether the observe difference in gap-detection thresholds between ectopic and non-ectopic mice could be explained by differences in responses to noise. This does not seem to be the case as the only cells found to differ in noise responses were the non-primary cells where gap-detection were found

to be similar in ectopic and non-ectopic mice. The ectopic mice were found to have lower amounts of firing than non-ectopic mice over both the onset and sustained periods. In all cells recorded from the IC the stability and regularity of firing to a noise is similar between ectopic and non-ectopic mice. We offset responses in IC showed both excitatory and inhibitory responses and that there is a lower proportion of offset responses in ectopic compared to non-ectopic mice within IC mostly from a reduction in the number of excitatory offset responses. This response is consistent with the findings from MGB which also showed a lower proportion of offset responses between ectopic and non-ectopic mice in MGB. Also consistent with MGB is the result that there is no difference in click-train synchronisation between ectopic and non-ectopic mice in IC and so the difference gap-detection thresholds seems specific to a sounds following a noise and not rapid sounds per se. Also the gap-detection threshold difference cannot be explained by a difference in CFs between ectopic and non-ectopic mice as these were found to be similar.

We also found several new, interesting findings in both IC and a re-analysis of the previous MGB recordings. We found, spontaneous firing rates differ between ectopic and non-ectopic mice in both IC and MGB. In IC this was found to be in the non-primary cells where the regularity of firing was differed ectopic and non-ectopic mice. In the non-primary cells there was no gap-detection threshold difference between ectopic and non-ectopic mice and so is the spontaneous rate difference is unlikely to explain this result. The spontaneous rate difference in MGB between ectopic and non-ectopic mice was found to be more wide-spread in both ventral and dorsal subdivisions with ventral having differences in stability and regularity and dorsal having a different amounts of firing. Further investigation of the MGB recordings to a noise revealed a difference in the sustained portions of the noise

response between ectopic and non-ectopic mice in ventral and MGB. In ventral MGB we found differences between ectopic and non-ectopic mice in the trial-by-trial variability and in the rate of decline over the sustained period. In dorsal MGB, we found different amounts of firing and also a difference in the rate of decline over the sustained response period. Dorsal MGB was also found to have different amounts of firing over the onset period between ectopic and non-ectopic mice.

Overall, the most intriguing result from the IC recordings is in the neural gap-detection thresholds as this is in complete contrast to the previous study where they had found the ectopic mice had longer neural gap-detection thresholds than non-ectopic mice, primarily in ventral MGB but also in dorsal MGB, indicating the ectopic mice are impaired at detecting short gaps in noise compared to non-ectopic mice in these brain areas (Anderson & Linden, 2016). Here, however, we found in primary (putative central) IC cells, neural gap-detection thresholds were shorter in ectopic than non-ectopic mice, suggesting greater IC sensitivity to gap-in-noise stimuli in ectopic than non-ectopic mice. Analysis of the IC data showed that this difference in gap-detection differences, between ectopic and non-ectopic animals in this area, was not due to differences between responses to noise per se, but seems specific to the detection of the gap itself.

In addition, the MGB study found a reduction in the number of cells with offset responses to a noise in the ectopic mice which was thought, in part, to explain the neural gap-detection results in that study (Anderson & Linden, 2016). In the IC recordings, we also find a reduction in cells with offset responses to a noise in ectopic compared to non-ectopic mice or at least a trend towards it but in combination with shorter neural gap-detection thresholds in the ectopic mice.

Table 3: Differences in recording parameters between MGB and IC recordings.

MGB recordings	IC recordings
Custom made parylene-coated tungsten microelectrodes (WPI, TM33A20) in 8 horizontal linear array ~75μm apart with impedance of 1–2 MΩ at 1 kHz.	Neuronexus Technologies silicon linear array, single 5mm shank, 16 electrodes spaced 100μm, 177μm electrode site area (A1x16-5mm-100-177-A16) with impedance between 0.5-3 MΩ at 1 kHz.
5ms rise/fall time at the start of the first noise and end of the second noise (0 rise/fall on the end of the first noise and start of the second noise).	0ms rise/fall time.
500ms sweep length: 100ms delay, 200ms first noise, gap of varying length, 50ms second noise.	750ms sweep length: 100ms delay, 200ms first noise, gap of varying length, 50ms second noise.
Gap lengths: 0, 1, 2, 4, 6, 8, 10, 20, 50 and 100ms	Gap lengths: 0, 1, 1.4142, 2, 2.8284, 4, 5.6569, 8, 16, 32, 64 and 128ms

There were some small differences in recording parameters between the MGB and IC study which are summarised in table 3. It seems unlikely, however, that a difference in electrode type or sweep length could account for the ectopic mice having impaired neural gap-detection within MGB and enhanced neural gap-detection with IC although it is possible that these differences may have influenced the results. For example, the MGB study did not use a long sweep length and therefore on trials with a 100ms gap meant there was only 50ms at the end of trial whereas in the IC recordings, where a longer sweep length was chosen there was

300ms at the end of a the trial. If the neural gap-detection deficits in the MGB arose from the ectopic mice having sluggishness recovery from adaptation, compared to the non-ectopic mice, then it is possible that the shorter sweep length may have influenced the results. Such an effect would presumably also influence the response to the first noise on subsequent trials and indeed, on re-analysis of the data there were found to be differences in the response to the first noise, in the sustained response at least where there was a difference in trial-by-trial variability between the ectopic and non-ectopic mice. This explanation, does not however, explain why the ectopic mice seemed to have enhanced neural gap-detection compared to the non-ectopic mice in the primary cells of the IC.

Furthermore, the study of offset responses is limited, especially in mouse. Is it possible offset responses in MGB are doing something different than in IC or are generated by difference mechanisms? As noted the IC seems to have different types of offset response and are thought to be generated by different mechanisms through either rebound mechanisms or direct synaptic connections (Kasai et al., 2012). It seemed to be the excitatory offset responses that were affected in both MGB and IC and as Kasai et. al. discuss these are unlike to come from the most well-known area of the brain for generating offset responses, the superior paraolivary nucleus (SPON) since the connections from SPON are known to be GABAergic (Kulesza & Berrebi 2000; González-Hernández et al., 1996; Saldaña et al., 2009). Kasai et al. suggest there could be connections from dorsal cochlear nucleus which may be a source of ascending projections which could account for the IC excitatory offset responses (Kasai et al., 2012) and future studies in the BXSB/MpJ-Yaa mice may want to consider this as a candidate along with further studies into IC possibly using intracellular techniques.

Another candidate for future studies is the connections between MGB and IC. Do offset responses in MGB arise in the MGB itself or are they transferred from IC and if so, is it possible there is some disruption of this transfer of information in the ectopic mice? Ventral MGB, where the largest deficit in neural gap-detection was found in ectopic mice was found, is known to receive most of its connection from central IC (Calford & Aitkin, 1983; Kudo & Niimi, 1978; Weinberger, 2012) and the enhanced neural gap-detection ability in ectopic mice is in the primary cells, which are thought to be in central IC. Is it possible there is some disruption of the transfer of information from one area to next?

In addition to the neural gap-detection threshold differences we also found a difference in spontaneous rate which seemed to arise from the non-primary IC cells, which were likely recorded from dorsal/external IC. On re-analysis of the MGB recordings, using similar criteria as for the IC recordings we also found a difference in spontaneous rate in the MGB which seems to be most evident in ventral MGB. This again is a surprising result since a difference in dorsal/external IC would have been expected to produce a difference in medial MGB, but medial MGB is the one area of MGB which appears to be completely similar between ectopic and non-ectopic(Weinberger, 2012). Is it possible the changes in spontaneous rate are not related? This spontaneous rate difference does not seem to be related to the changes in neural gap-detection thresholds since the spontaneous rate difference is found in the non-primary cells and neural gap-detection threshold differences are found in the primary cells with IC but in MGB both of these changes are found in ventral MGB.

Our classification of recording location was not as accurate as if we had histology, although this would present its own problem since there are limited adequate

markers for the different IC subdivisions particularly in mouse. Regardless of whether the primary cells *are* all recorded from central IC the results do reveal a clear difference between ectopic and non-ectopic mice which is unlikely to have arisen purely by chance. Future experiments would be required to record IC and MGB either at same time or in same experiment and more behavioural data is needed to determine if the ectopic mice are actually impaired behaviourally in detection short gap in noise compared to the non-ectopic mice.

In summary, in this chapter we set out to determine if the difference in gap-detection thresholds found between ectopic and non-ectopic mice could be found within IC. We did find a difference IC gap-detection thresholds between ectopic and non-ectopic mice but in IC the thresholds were shorter in ectopic mice than non-ectopic mice and in MGB the ectopic mice thresholds were longer than non-ectopic mice. Future experiments will need to investigate this anomaly as it may lead to further understand of how gap-detection is performed within these brain nuclei. An ideal future experiment would use multi-electrode electrophysiologically from IC and MGB in the same animal to determine if the gap-detection thresholds in IC and MGB differ in the same animal and whether this is found only within the ectopic mice.

Chapter 4 – Auditory brainstem responses in BXSB/MpJ-*Yaa* mice

Abstract

In order to address an overlooked area of the previous study which suggested no difference in lower parts of the auditory pathway from click ABR results (Anderson and Linden, 2016). ABR measurements were performed for click, tone and masker-probe stimuli. There was found to be no difference between ectopic and non-ectopic mice for any of the stimuli that was used. The results suggest the auditory brainstem is functioning similarly in ectopic and non-ectopic mice and that the observed deficit to sounds following noise, in ectopic mice, is first found within the IC.

Introduction

The main study underlying this work is the previously discussed Anderson and Linden study which found a difference in gap-detection thresholds between ectopic and non-ectopic in extracellular MGB recordings (Anderson and Linden, 2016). Furthermore, they went on to show that which deficit is specific to a sound following a noise since they found similar deficits when a click followed a noise but there was no difference between ectopic and non-ectopic mice in click-train synchronisation. This study also look at ABRs within the same mice and found no difference in ABR thresholds, wave amplitudes or wave latencies between ectopic and non-ectopic mice. A possible failing in this study however, is that, the ABRs we only performed using multiple presentations of single clicks. Since the MGB revealed a deficit only when a sound follows a noise any possible deficit would not be expected to be detected using a click ABR.

In light of the problems in the previous study and in an attempt to probe whether the observed deficit in detecting sounds following a noise, exists in lower areas of the auditory pathway which are recording by the ABR, we performed ABR measurements using a masker-probe stimuli. This can be described as a click following a noise. In addition we repeated the click ABRs as in the previous study and also recorded tone ABRs to look for any frequency specific deficits in the auditory pathway. We found no difference between ectopic and non-ectopic animals in any of the measures tested in terms of threshold of suprathreshold features, suggesting the early part of the auditory pathway functions similarly between ectopic and non-ectopic mice.

Methods

Animals

We used 13. ectopic and 17 non-ectopic BXSB/MpJ-*Yaa* mice. Animals ranged in age from 2 to 4 months in age. Only male BXSB/MpJ-Yaa were used for ABR recordings.

Experimental procedure

The ABR recordings were made by placing subdermal electrodes at the vertex of the skull (+), behind the ear oriented toward the speaker (ipsilateral ear) (-) and behind the contralateral ear (ground). Mice were anaesthetised with urethane for these recordings, (with ringers solution and atropine as required) and were perfused following the procedure to extract brain tissue for histological analysis and identification of ectopias. The stimuli were presented free-field to the left ear. Acoustic stimuli were calibrated near to the opening of the left ear canal before the

start of each experiment to ensure a flat frequency response within +/- 2 dB from 2 to 80kHz.

All ABR data was analysed with bespoke MatLab software to determine wave peaks and troughs.

Click ABR

Click ABRs were recorded for clicks at 10-80dB intensity (increasing in 10dB steps). The inter-onset interval was 100ms and the click was monopolar square wave with duration of 50μs. The results were analysed with a repeated measures ANOVA (rmANOVA) with group as an independent measure and sound level as a repeated measure. Multiple testing issues were corrected for using a Bonferroni correction (α/n where n is the number of tests applied). In this data the number of tests was taken as the number of the waves and therefore statistical significance was considered to be achieved only for p-values<0.0125.

Tone ABR

Tone ABRs were recorded for sound levels between 10 and 80dB (increasing in 10 dB steps) for tone frequencies of 8Hz, 16Hz and 32Hz. Tones lasted for 5ms (with 1.5ms cosine-squared gating) and the inter-onset interval was 100ms. The results were again analysed with a repeated measures ANOVA (rmANOVA) with group as an independent measure and sound level as a repeated measure. Multiple testing issues were corrected for as in the click ABRs as described above.

Masker-probe ABR

The masker-probe stimulus was composed of a 200ms white noise burst, followed by 20ms silent gap and then a click (probe click), followed by a further 500ms silent gap and another click (reference click) at 60dB SPL. On a separate set of animals a

200ms white noise burst, followed by 8ms silent gap (probe click) and then a click, followed by a further 500ms silent gap (reference click) and another click. Figure 44 demonstrates this stimuli.

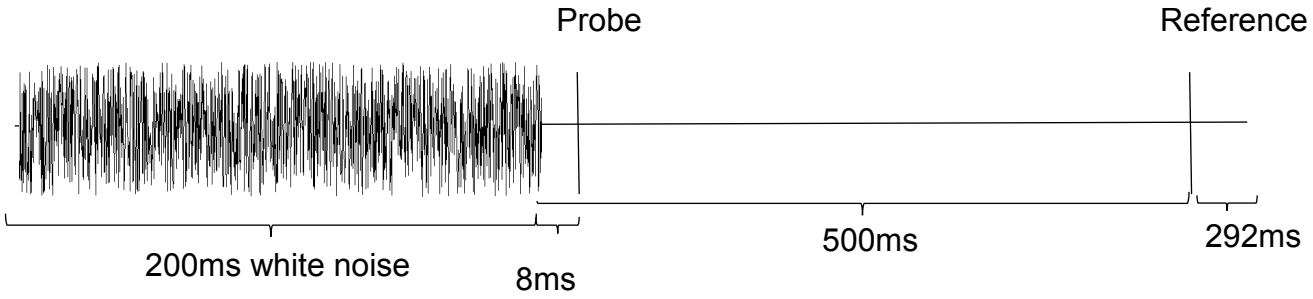

Figure 38: Masker-probe stimuli. Diagram of masker-probe stimuli used in ABR experiments. A 200ms white noise masker is followed shortly by a probe click (in this example 8ms after the end of masker noise). 500ms after the end of the masker noise is a second click, called the reference click. This means the probe click is preceded by noise whereas the reference click is preceded by silence. When the ABRs have been obtained the responses from the two clicks can be used to compare the effects of a preceding noise on a click response. This stimulus is analogous to the gap-in-noise stimuli used in the electrophysiological recordings (where the gap is represented by the 8ms silence after the end of the masker noise but before the probe click occurs) but is better suited to the ABR where a stronger response is recorded for a click versus a noise.

ABR measurements were collected for responses to the clicks, particularly the click presented immediately following the noise (the other click was used as a reference for control analyses). The results were analysed in two ways. Using a binomial analysis of the probe and reference clicks amplitudes or latencies where the number of ectopic points above the non-ectopic best fit line are counted and a binomial test is performed. Also analysis of the probe click amplitudes and latencies normalised by division with the reference click amplitudes and latencies was performed using a repeated measures ANOVA (rmANOVA) with group as an independent measure and wave as a repeated measure. Multiple testing issues were corrected for both sets of analysis as described for the click ABRs above.

Results

Previous study showed no difference between ectopic and non-ectopic mice for click ABR thresholds however the study also showed no difference between ectopic and non-ectopic mice for clicks within MGB recordings. What it did show was a significant difference for short gaps in noise in order to test this with ABRs to find if the deficit is evident in lower parts of the auditory pathway a masker-probe stimuli was used (see methods section for further description of masker-probe stimuli). A probe delays of 8 were used. Tone ABRs recording were made to look for any evidence of a frequency specific deficit not evident in the click ABRs.

Click ABR waveforms show no difference between ectopic and non-ectopic mice

Examples of the types of recordings taken from individual animals during this study in response to a click ABR stimulus is shown in figure 39. Generally a clearer ABR signal is obtained with a click ABR opposed to a tone ABR since the click ABR is across all frequencies which will activate neurons across frequency bands.

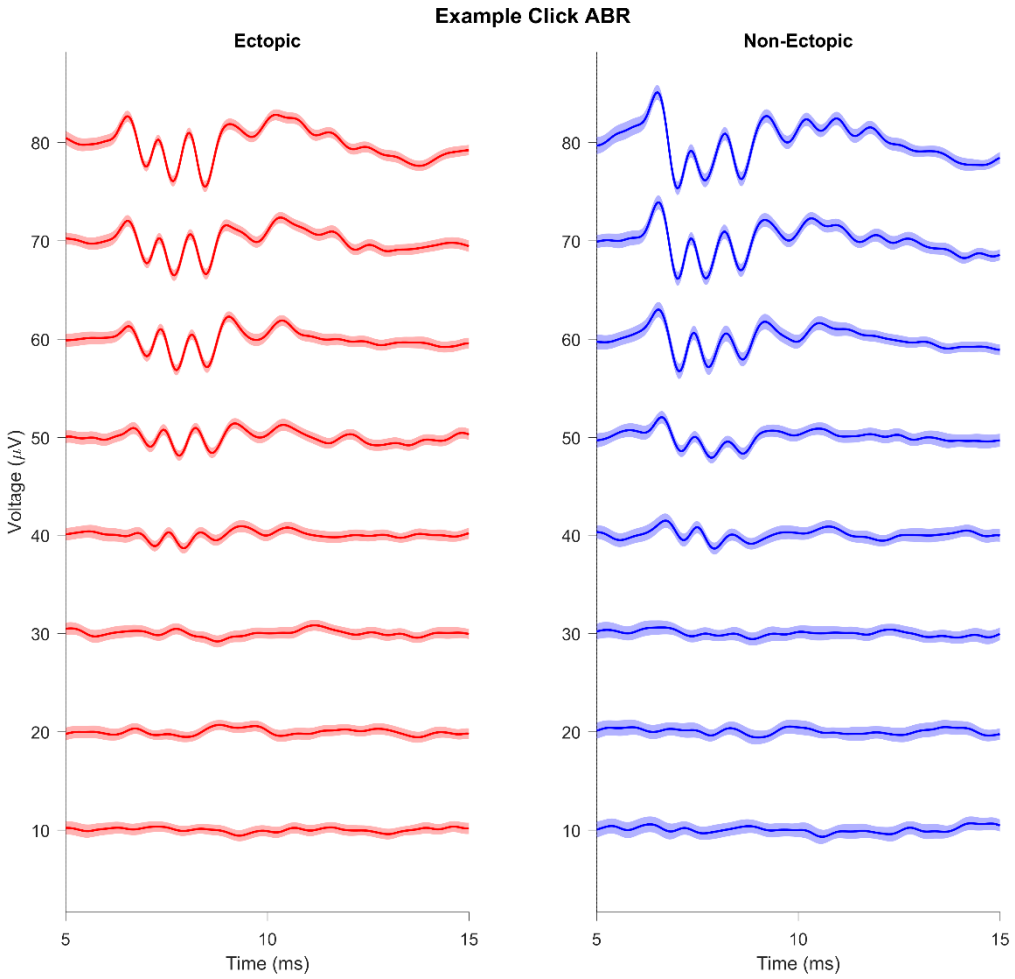

Figure 45: Examples of ABRs to a click. Plots show an example ABRs to clicks recorded from individual ectopic and non-ectopic mice. Click ABRs were obtained at different sound levels from 10-80dB SPL in 10dB steps. The ABRs at different sound levels are shown, stacked on the y-axis where the deflection in the y-axis for each sound level represents the change in voltage. Time is indicated on the x-axis. Note the time is relative to the trial onset (and therefore contains a 5ms onset delay i.e. the start of the x-axis is the time of the click). Time is relative to trial onset (with a 5ms delay). Each sound level is repeated 500 times, the mean across these repeats are indicated on the plots by the red/blue lines. +/-standard error is indicated by the red/blue shading either side of the mean lines.

The results from the click ABR recordings showed no difference between ectopic and non-ectopic for ABR threshold, wave amplitudes nor wave latencies as shown in figures 40 and 41 respectively. This confirms the finding of the previous study suggesting to clicks in isolation there is no difference between ectopic and non-ectopic mice in the lower parts of the auditory pathway (rmANOVA; all $p>0.05$; table A5).

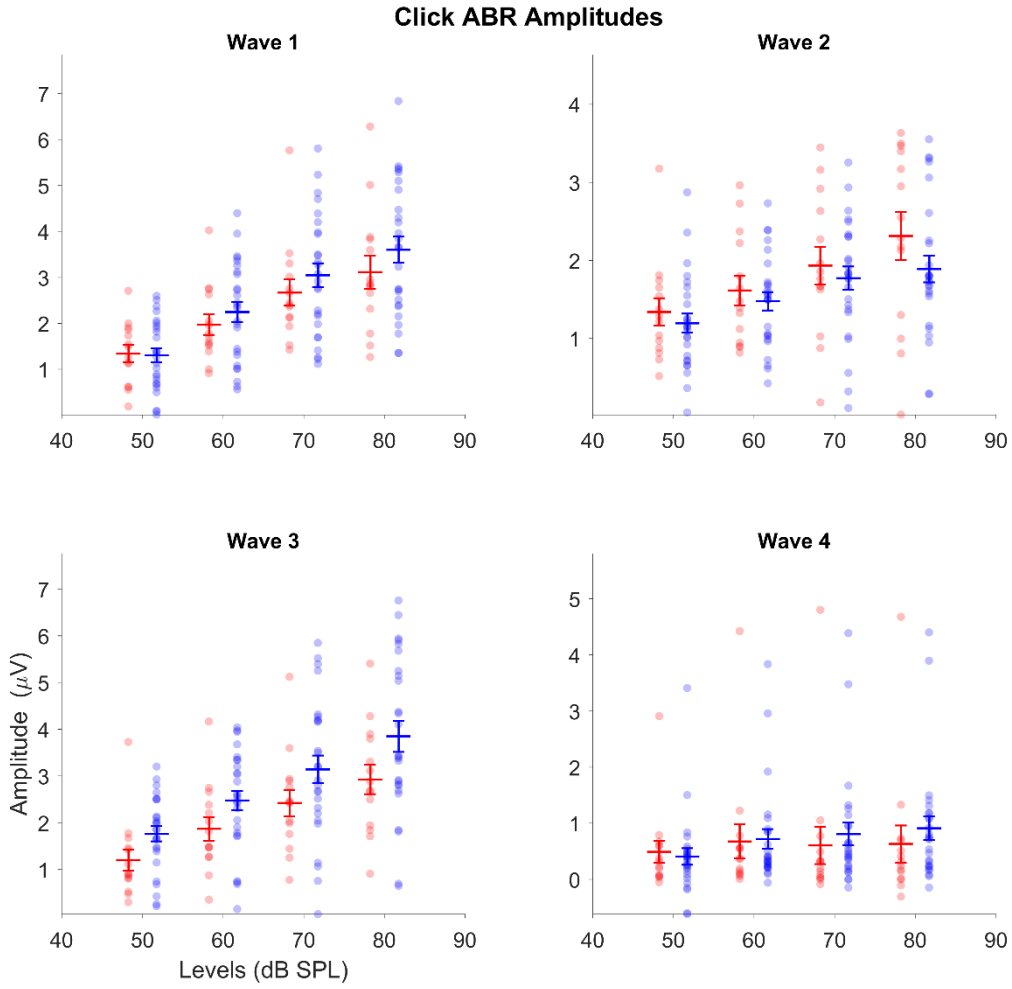

Figure 40: No significant difference between ectopic and non-ectopic mice in click ABR amplitudes. The responses to click ABRs were analysed to extract amplitudes of each wave (see text for methods). The results for waves 1-4 are shown in each figure for ectopic (red) and non-ectopic (blue) mice at different sound levels. Means are indicated by a horizontal line where the error bars indicate +/- 1 standard error. Individual animal data is represented by dots. There was no significant difference between ectopic and non-ectopic mice for any of the wave amplitudes (rmANOVA; all $p>0.05$).

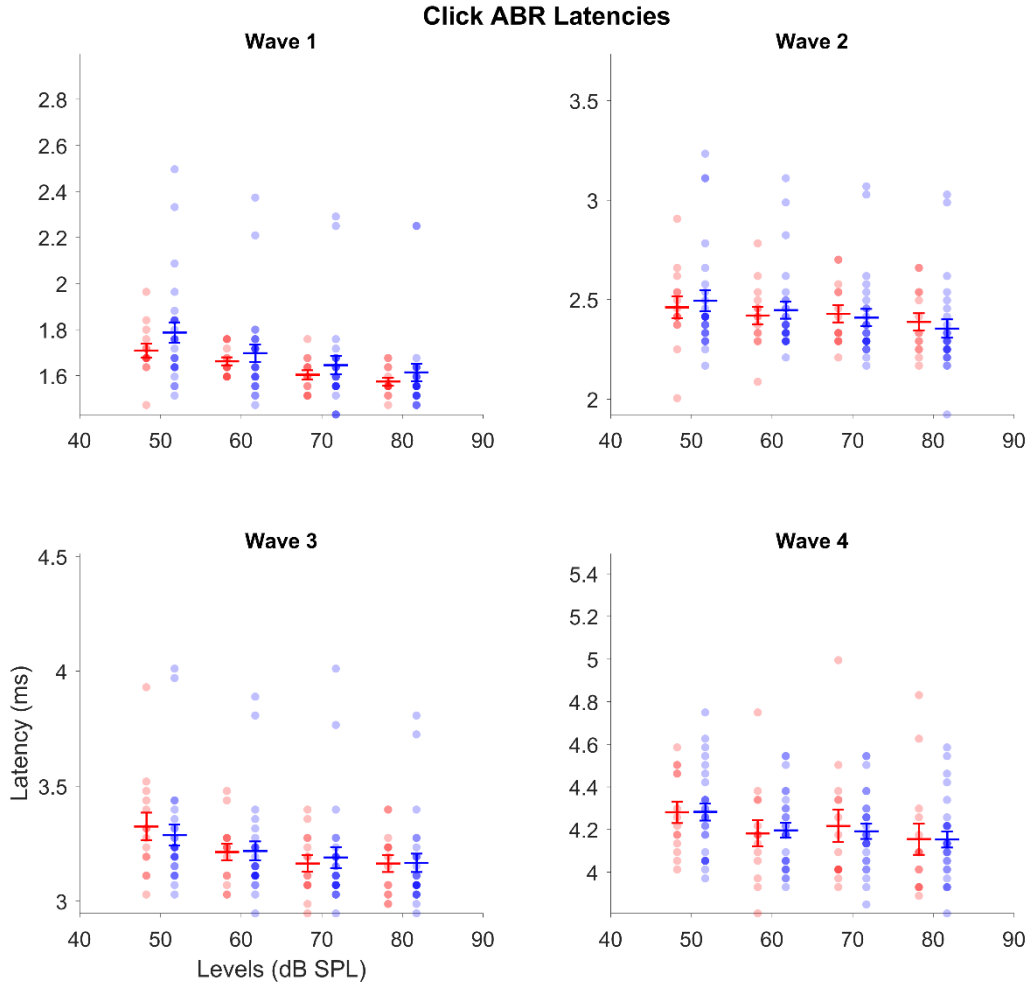

Figure 41: No significant difference between ectopic and non-ectopic mice in click ABR wave latencies. As in figure 46 but for click ABR wave latencies. There was no significant difference between ectopic and non-ectopic mice for any of the click ABR wave latencies (rmANOVA; all $p>0.05$).

Tone ABRs at 8,16 and 32kHz show no difference between ectopic and non-ectopic mice

Tone ABRs for tones at 8, 16 and 32kHz were recorded. Examples of tone ABRs from individual animals can be found in figure 42. Note, generally for mice, 16kHz tone gives a clearer signal than the 8kHz or 32kHz tone ABRs.

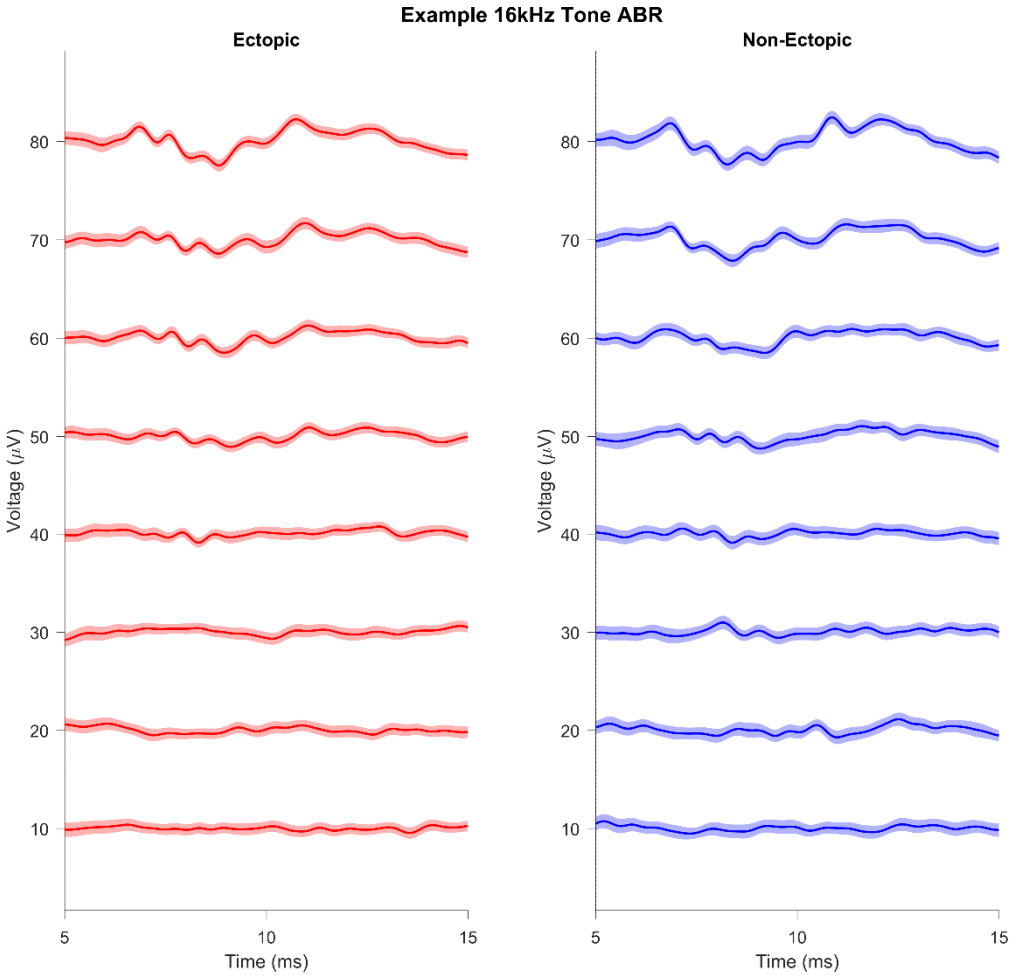

Figure 42: Examples of 16kHz Tone ABR. As in figure 45 but for a 16kHz tone rather than a click. Note 8kHz and 32kHz tones were also used. The tone duration was 5ms. Tones are known to evoked a weaker ABR than clicks as only a single frequency is being played (as opposed to a click which contains all frequencies) and therefore a smaller number of neurons will be activated by the tone.

Similar to the click ABRs, tone ABR recordings for 8, 16 and 32hz showed no difference for wave amplitude or wave latency as shown in figure 43-48 respectively. This results shows that there is no frequency specific difference between ectopic and non-ectopic mice in responses to different frequencies as might be expected from the findings of the previous study (Anderson and Linden, 2016).

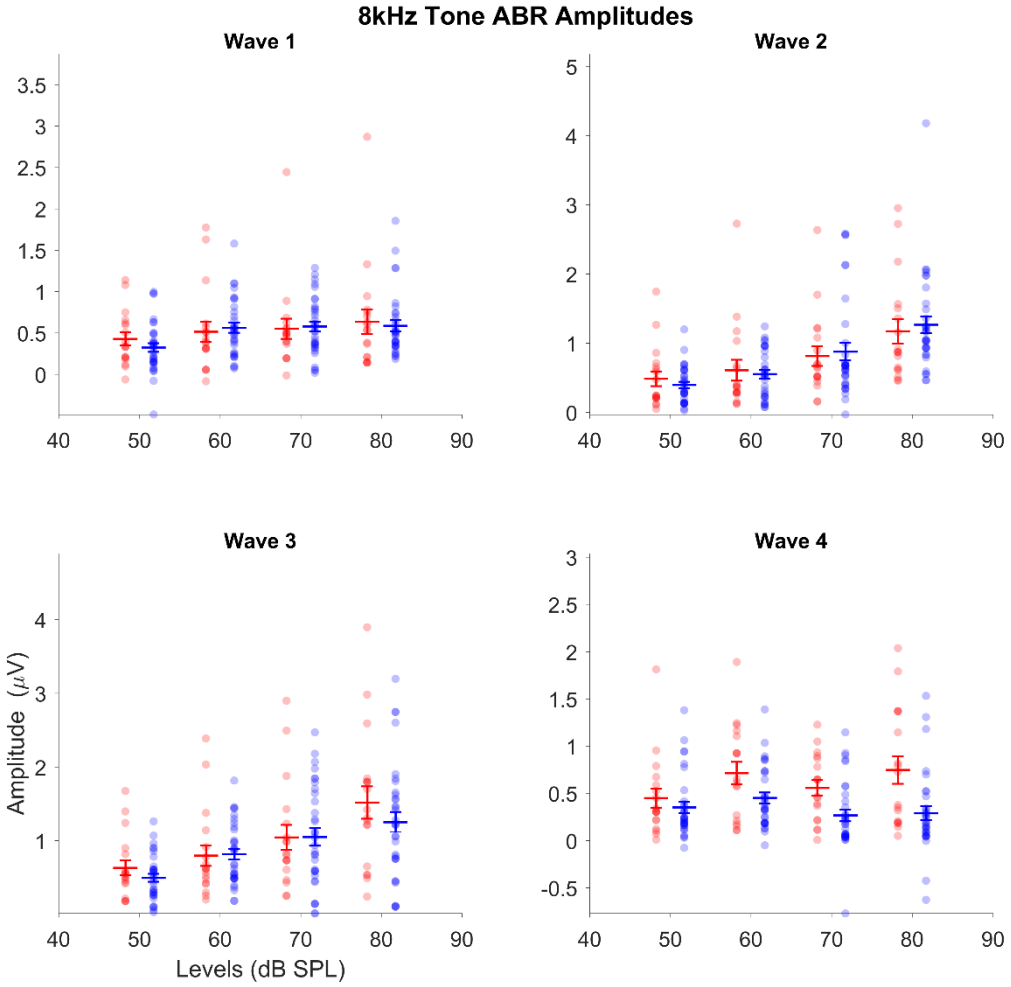

Figure 43: No significant difference between ectopic and non-ectopic mice in ABR wave amplitudes to an 8kHz tone. As in figure 46 but for 8kHz tone ABR wave amplitudes.

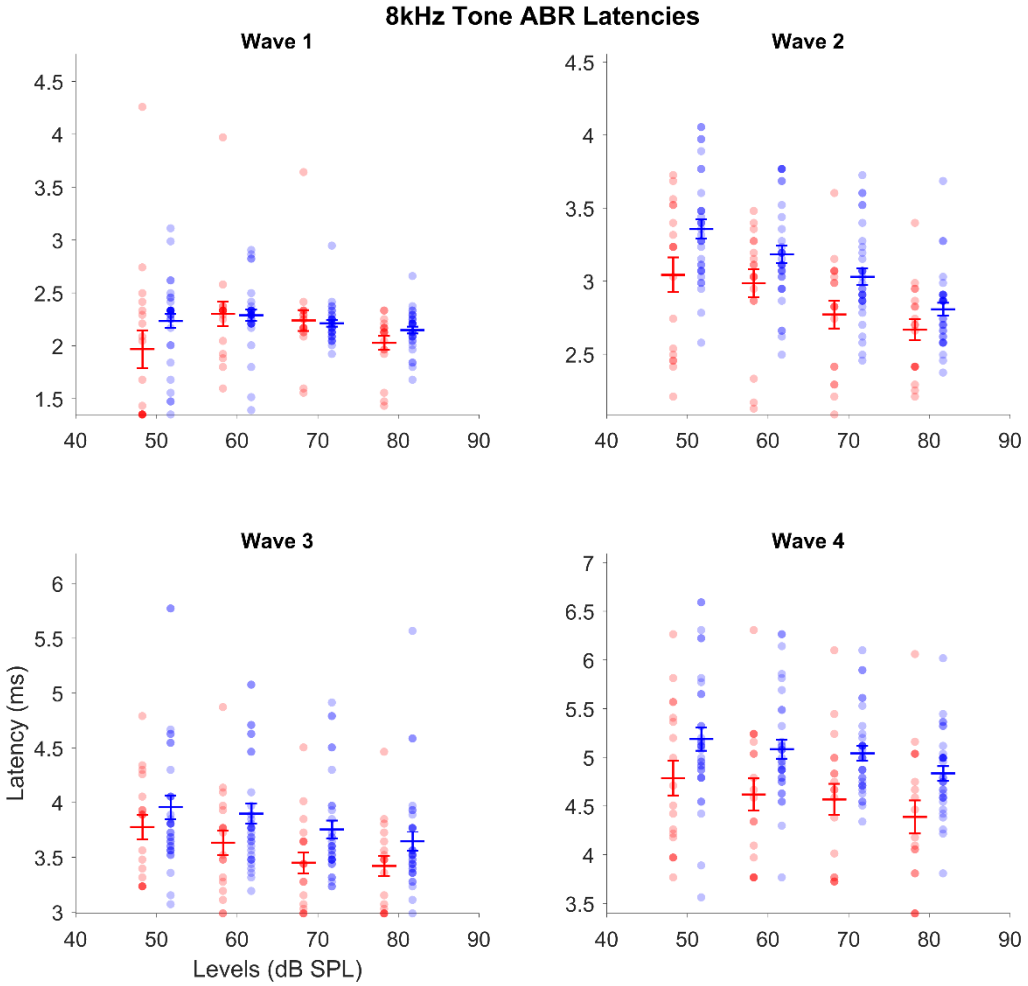

Figure 44: No significant difference between ectopic and non-ectopic mice in ABR wave latencies for a 8kHz tone. As in figure 46 but for 8kHz tone ABR wave latencies.

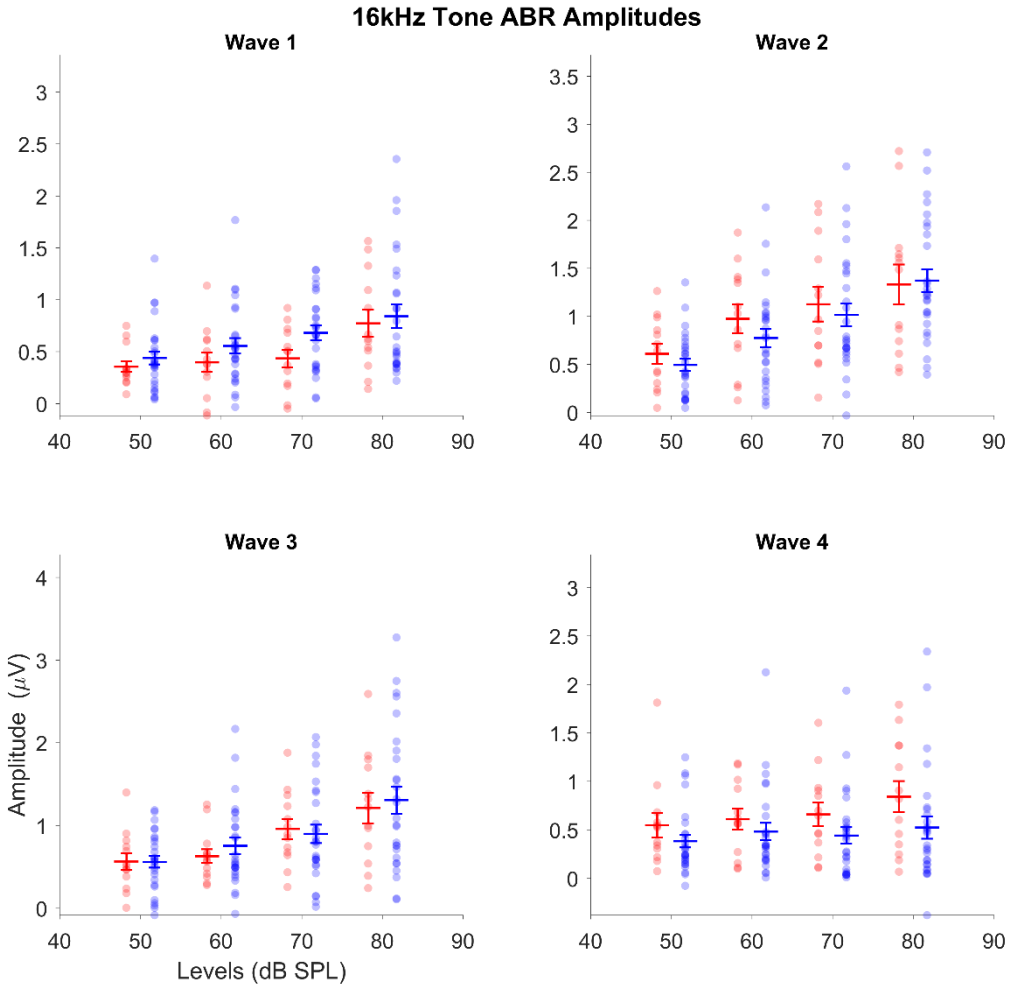

Figure 45: No significant difference between ectopic and non-ectopic mice in ABR wave amplitudes for a 16kHz tone. As in figure 46 but for 16kHz tone ABR wave amplitudes.

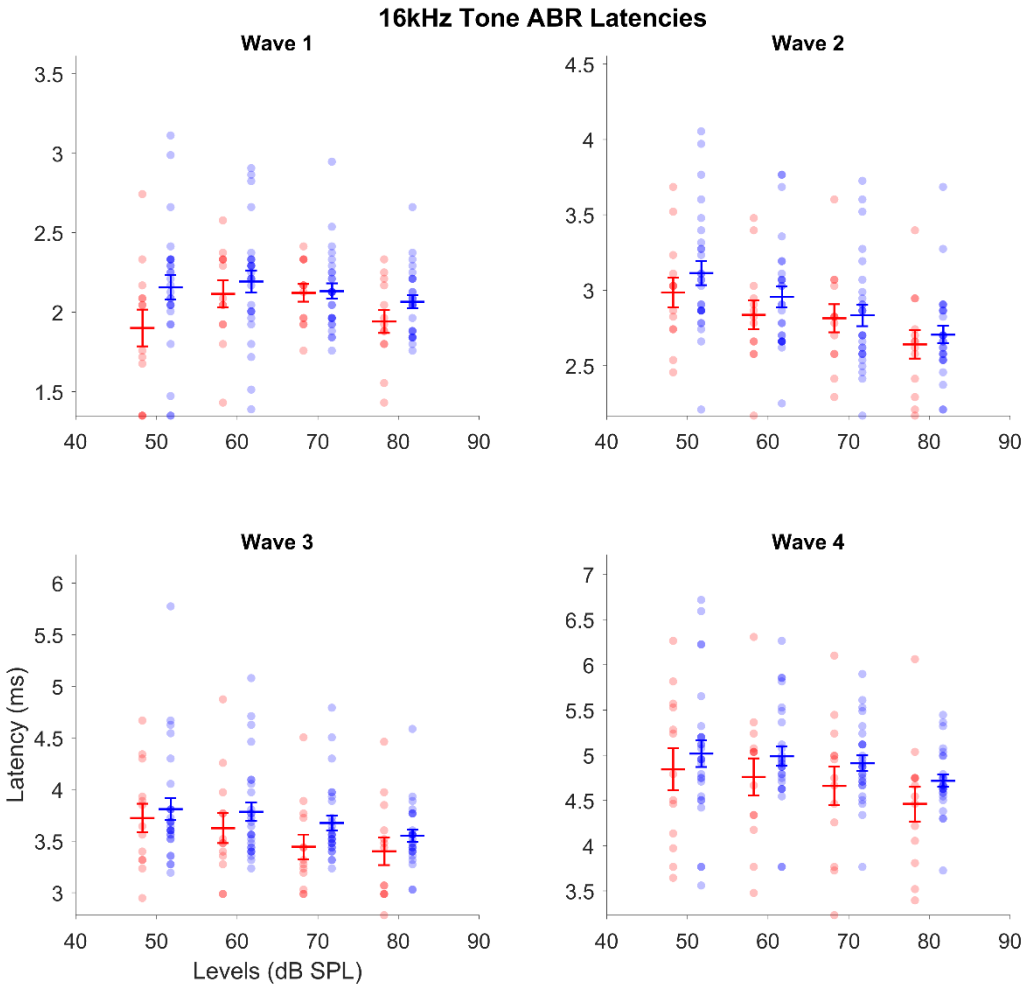

Figure 46: No significant difference between ectopic and non-ectopic mice in ABR wave latencies for a 16kHz tone. As in figure 46 but for 16kHz tone ABR wave latencies.

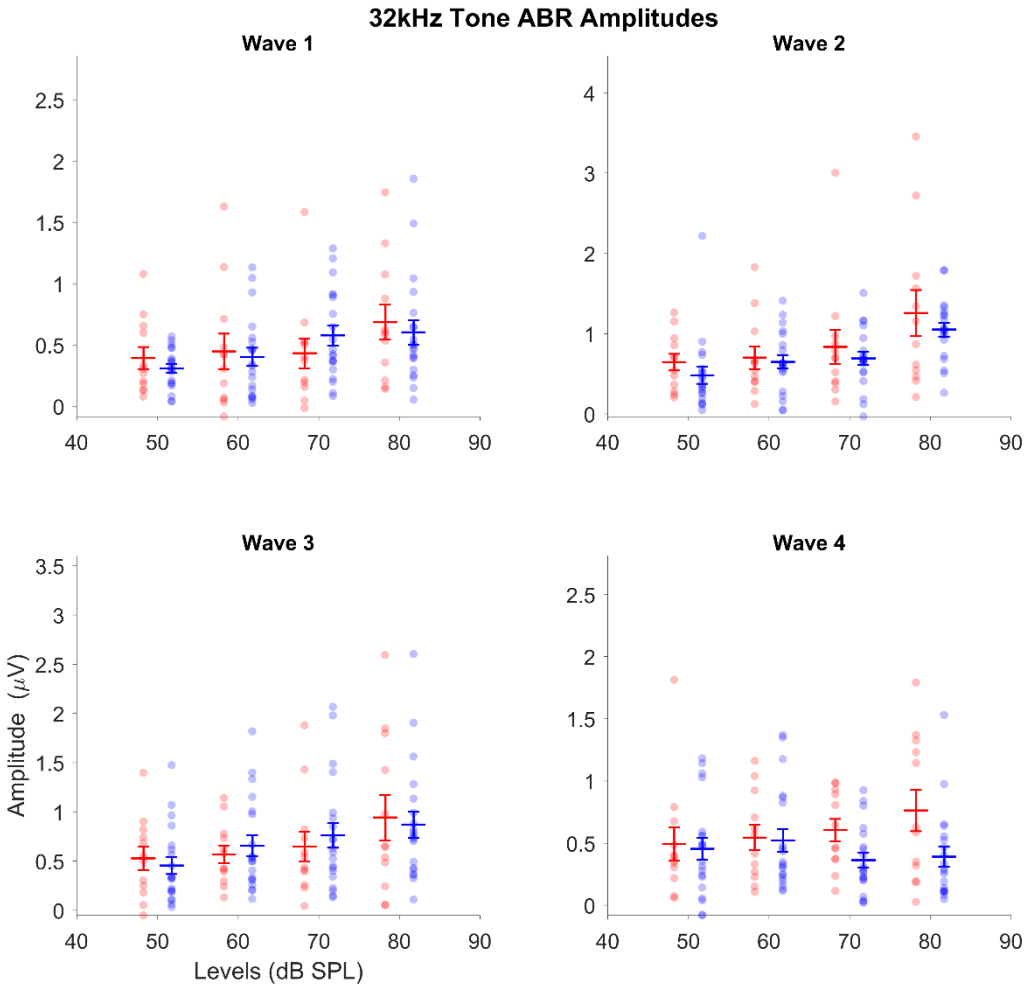

Figure 47: No significant difference between ectopic and non-ectopic mice in ABR wave amplitudes for a 32kHz tone. As in figure 46 but for 32kHz tone ABR wave amplitudes.

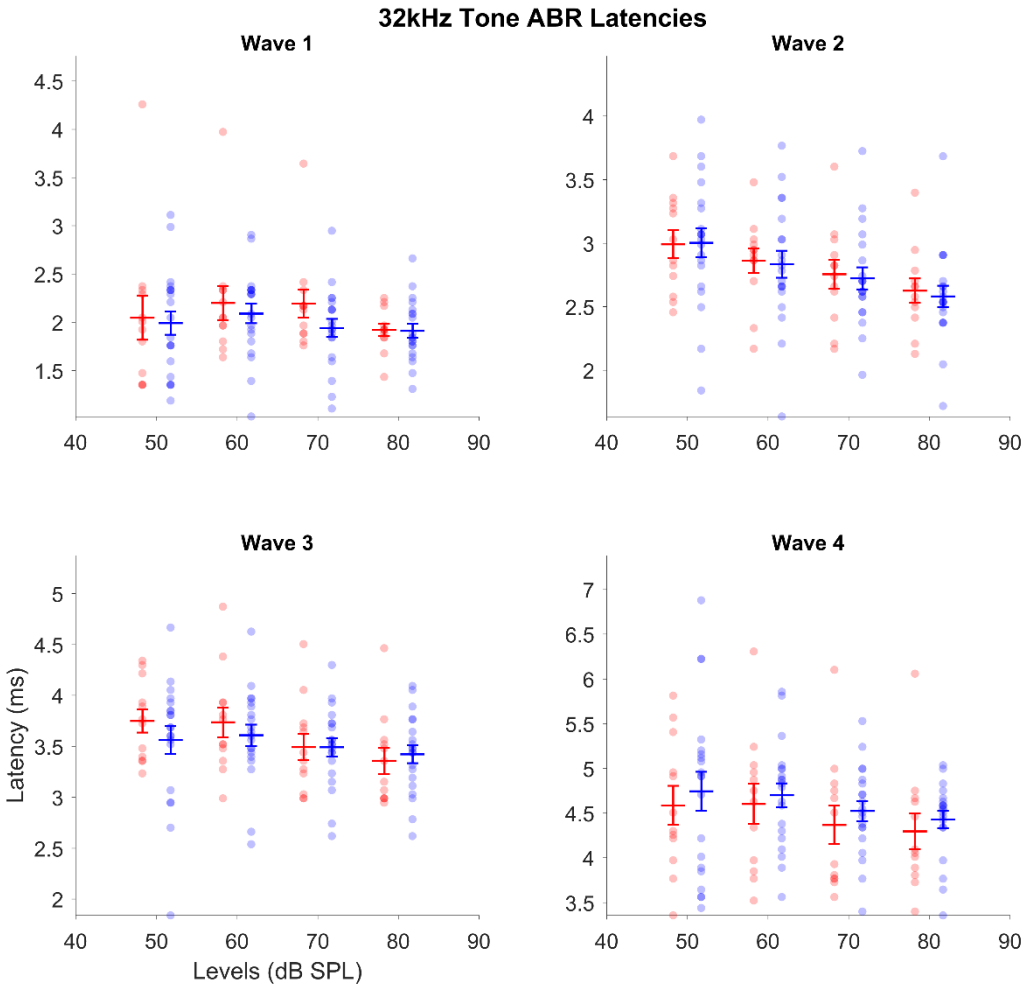

Figure 48: No significant difference between ectopic and non-ectopic mice in ABR wave latencies for a 32kHz tone. As in figure 46 but for 32kHz tone ABR wave latencies.

Ectopic and non-ectopic do not differ in the response to a click following a noise

If any difference between ectopic and non-ectopic was to be found it could be expected to be revealed in the masker-probe stimuli ABR as this tests the response to a click that follows a noise. Masker probe ABRs were recorded with 8ms probe delay. 8ms probe delay was originally used as the previous MGB recordings indicated the deficit in gap in noise response was restricted to short gaps. Example reference and probe clicks from the masker-probe ABRs from individual mice are shown in figure 49.

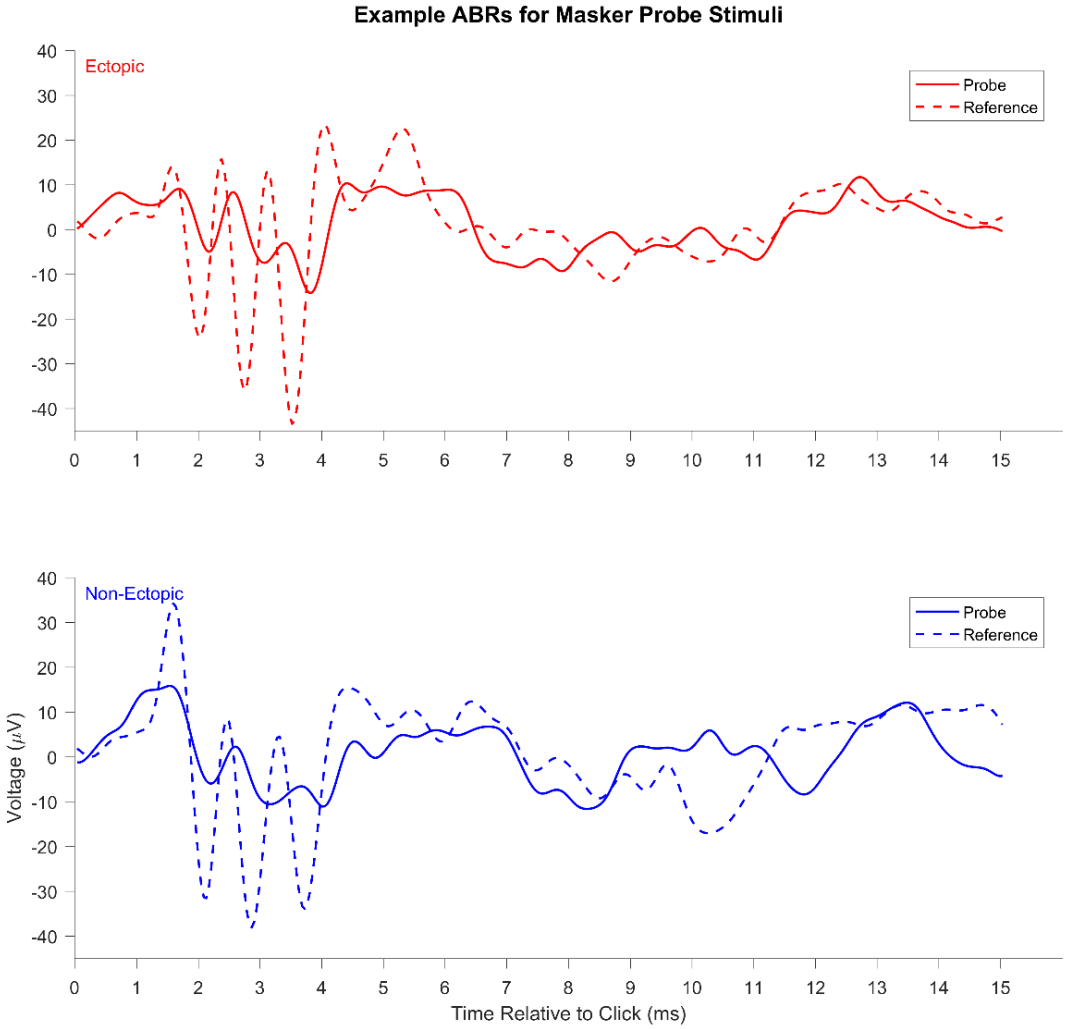

Figure 49: Example ABRs to masker-probe stimuli. Example responses to the probe and reference clicks of the masker-probe stimuli (see figure 44) from individual ectopic and non-ectopic mice. The probe click response is indicated by a solid red/blue line and the reference click response is represented by a dashed red/blue line. The x-axis represents the time relative to the reference/probe click onset.

ABRs analysis of waves and latencies for 8ms probe delay showed no difference between ectopic and non-ectopic mice when using either a binomial analysis (Binomial test; all p>0.05; figures 50 and 51; table A6) or analysis of the ratio of probe/reference click amplitudes or latencies (rmANOVA; all p>0.0125; figures 52 and 53; table A6). The lack of a difference however, may be due to the small signal response for 8ms probe delay.

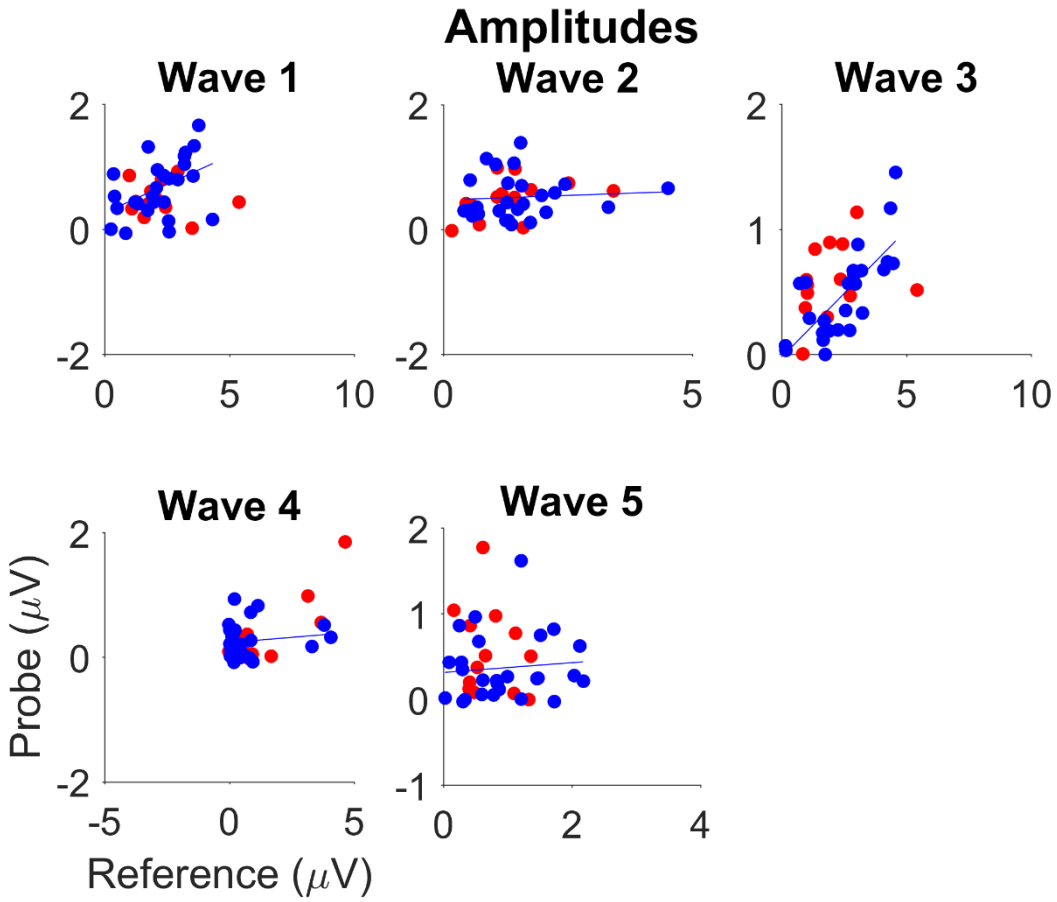

Figure 50: No significant difference between ectopic and non-ectopic mice in the impact of preceding a noise on the ABR to a click on wave amplitudes. The masker-probe stimulus (see figure 44) was used to test the effects of a preceded by noise on the ABR to a click. Binomial analysis (see text for details) was performed on the reference and probe click ABR wave amplitudes. There was no significant difference between ectopic and non-ectopic in the effect of a preceding noise of the ABR to a click (binomial; all p>0.05). In other words the relationship between the amplitudes of the probe and reference clicks is similar for ectopic and non-ectopic mice.

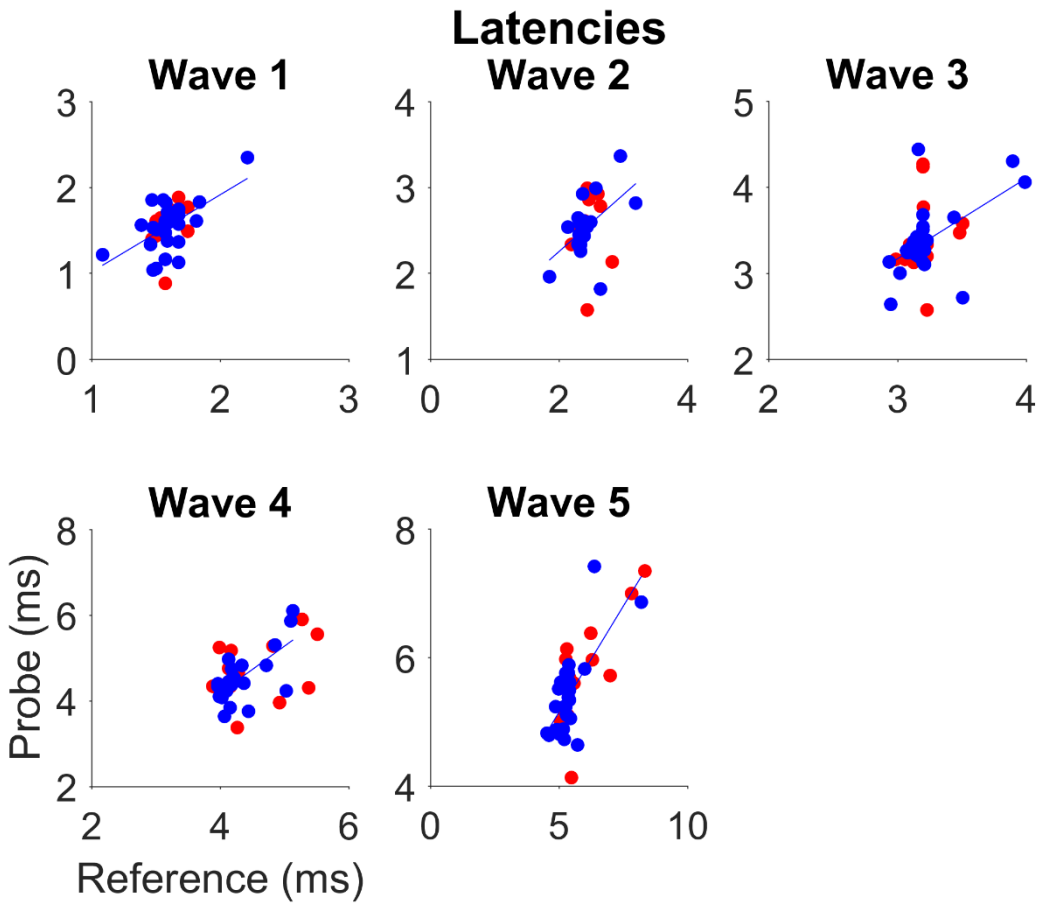

Figure 51: No significant difference between ectopic and non-ectopic mice in wave latencies in the impact of a preceding noise on the ABR to a click. As in figure 56 but for ABR wave latencies. There was no significant difference between ectopic and non-ectopic mice in the relationship between probe and reference click wave latencies (binomial; all $p>0.05$).

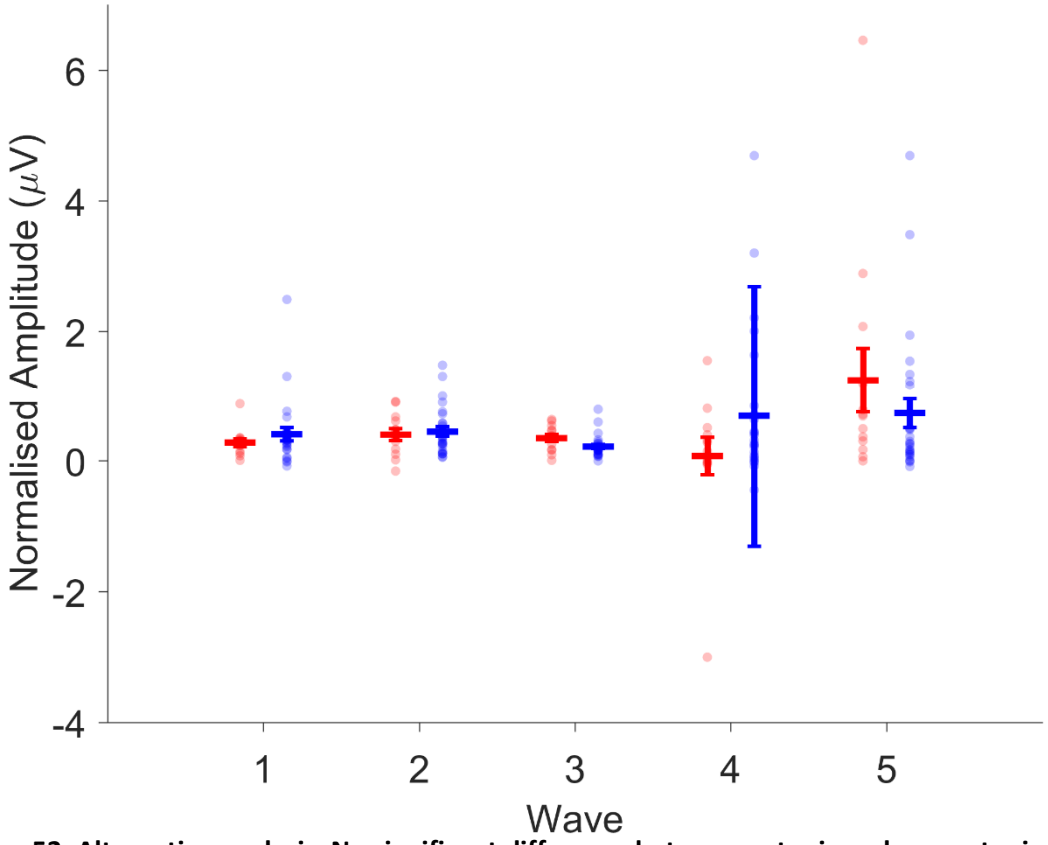

Figure 52: Alternative analysis: No significant difference between ectopic and non-ectopic mice in the impact of preceding a noise on the ABR to a click on wave amplitudes. Results for the masker-probe ABR were analysed using normalisation. When the probe click response was normalised by the reference click response for each animal there was still no difference between ectopic and non-ectopic mice for ABR wave amplitudes (ANOVA; all p>0.05).

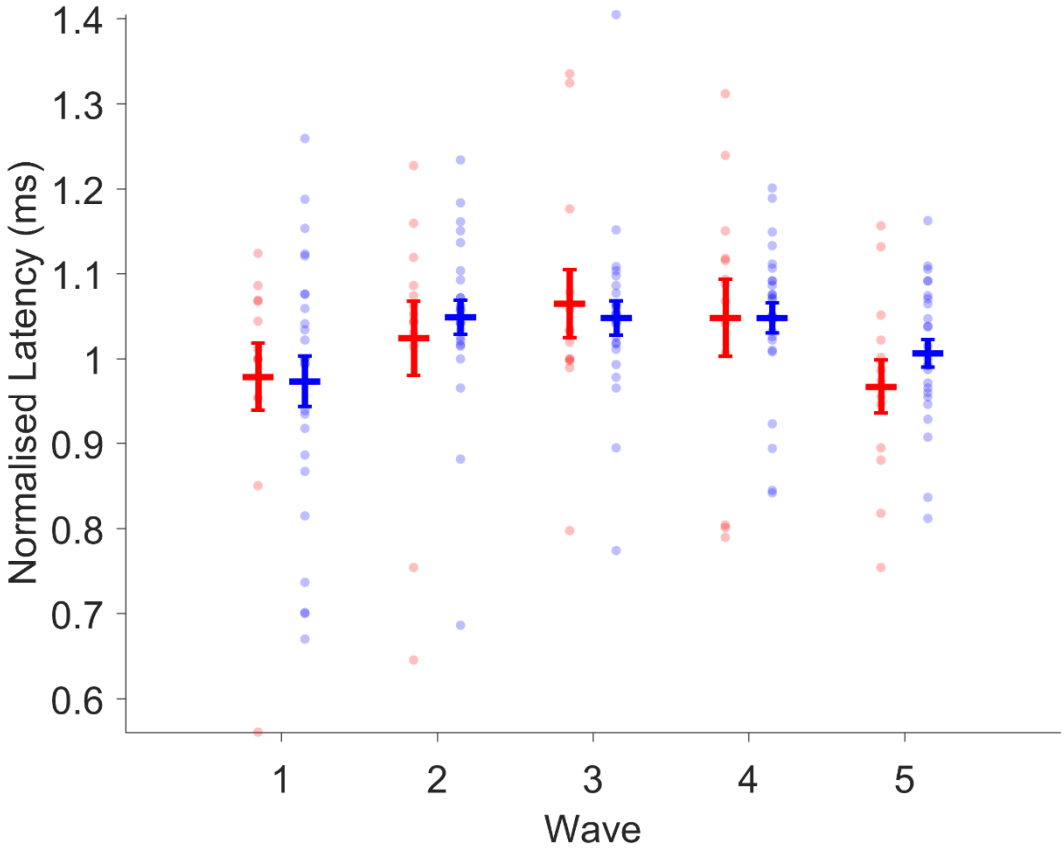

Figure 53: Alternative analysis: No significant difference between ectopic and non-ectopic mice in wave latencies in the impact of a preceding noise on the ABR to a click. As in figure 58 but for ABR wave latencies.

Discussion

The work in this chapter is a follow-up to published work from the Linden Lab in which they showed there was no difference in click ABRs between ectopic and non-ectopic mice (Anderson and Linden, 2016). The electrophysiological results of the previous study in the BXSB mice suggest the difference would not be found with a click-train stimulus but only to a click following noise furthermore it did not investigate whether there were any frequency specific differences in the ABRs. The aim of this chapter therefore was to address these questions: 1, can differences be detected in the ABR signal to a click following noise versus a click following silence; 2, can any frequency specific difference be identified between ectopic and non-ectopic mice in the lower parts of the auditory pathway using the ABR. Further click ABRs were recorded in order to reproduce the findings of the original study. The results discussed in this chapter demonstrate there are no differences in the ABR signals between ectopic and non-ectopic mice for any of the recorded stimuli. The results both confirm the previous results of the click ABRs being similar between ectopic and non-ectopic mice and reveal response to clicks following noise are similar in lower part of the auditory pathway between ectopic and non-ectopic. Furthermore, the results indicated there were no frequency specific differences between ectopic and non-ectopic mice in the lower parts of the auditory pathway. Taken together these results indicate the lower parts of the auditory pathway seems to be working similarly between ectopic and non-ectopic mice using ABRs.

The ABR measurement results extend the previous findings of Anderson and Linden (2016) by showing ectopic and non-ectopic mice have similar ABR thresholds, wave amplitudes and latencies even when using stimuli used in the previous MGB study. The results also confirm the previous findings for click ABRs and reveal no

differences in frequency responses in the early part of the auditory. This all suggests that early part of the auditory pathway is function similarly between ectopic and non-ectopic mice and therefore the noted differences arise later in the auditory pathway, possibly starting in the IC.

The original aims were to investigate the lower parts of the auditory system using stimuli more which would be expected to show a difference as indicated by the results of the MGB study. This aim was met and there was found to be no difference between ectopic and non-ectopic mice in the early part of the auditory pathway as measured by the ABR. Although there are some limitations of using the ABR which is an indirect measurement and therefore may not be able to reveal subtle differences between ectopic and non-ectopic mice. Furthermore, the response to the probe click 8ms after the end of the noise is almost entirely masked by the response to the noise which makes it more difficult to identify any differences. Using a longer probe delay or multiple probe delays in a similar study may be worth future investigation.

Chapter 5 – ABRs in genetic models of neurodevelopmental disorders

Abstract

Dyslexia, a common reading disability, is a highly heritable neurodevelopmental disorder. Genetic linkage and association studies have repeatedly identified *KIAA0319* and subsequently *KIAA0319-Like* as candidate susceptibility genes in humans. Downregulation of either *Kiaa0319* or *Kiaa0319-Like* expression in rats, using RNA-interference techniques, has been shown to produce cortical migration abnormalities and (in some cases) deficits in auditory processing. However, no cortical migration abnormalities have been found in recently developed *Kiaa0319* and *Kiaa0319-Like* knockout mice, nor in mice with double-knockout of both *Kiaa0319* and *Kiaa0319-Like* (Martinez-Garay et al., 2016 and unpublished observations). Here we investigated auditory processing in mice with knockouts of *Kiaa0319*, *Kiaa0319-Like*, or both *Kiaa0319* and *Kiaa0319-Like* by measuring auditory brainstem responses (ABRs) to clicks and to clicks following noise.

ABR thresholds did not differ between any of the groups, and there were no significant differences between *Kiaa0319* knockout and wildtype animals in amplitudes or latencies of ABR waves I-IV after correction for multiple testing. However, in *Kiaa0319-Like* knockout mice, amplitude of the late ABR wave III (but not wave I) was significantly reduced and latency increased. In the double-knockout animals, amplitudes of early ABR wave was significantly reduced. These results suggest that knockout of *Kiaa0319-Like* disrupts the strength or synchrony of neural activity in the auditory brainstem, while double-knockout of both *Kiaa0319* and *Kiaa0319-Like* produces more profound deficits in early auditory processing.

Introduction

The work conducted in this chapter arises from a collaboration with the University of Oxford with Luiz Guidi, Isabel Martinez-Garay, Antony Monaco, Antonio Velayos-Baeza and Zoltan Molnar who generated the knock-out (KO) mice models and performed immunological examination of these models together with a number of behavioural tests which are detailed below (Guidi et al., 2017). All ABR recordings and analysis of these recordings were performed by Jane Mattley. The work discussed in this chapter has been published in Cerebral Cortex (Guidi et al. 2017).

Dyslexia is one of the most prevalent neurodevelopment disorders affecting about 5-12% of the population(Schumacher et al., 2007). It has also be shown to be highly heritable (DeFries et al., 1978; Fisher & Francks, 2006; Wadsworth et al., 2007). Therefore, not surprisingly, there have been a number of genes identified as being associated with dyslexia. The key genes identified include DCDC2, DYX1X1, ROBO1 and KIAA0319 (Schumacher et al., 2007). The focus of this chapter will be on the KIAA0319 (KIAA) gene and another analogous gene which has also been associated with dyslexia called KIAA0319-Like or the mouse homolog AU040320 (KIAA-Like).

Initial manipulation of the identified dyslexia candidate genes was performed using RNA interference in rats in order to disrupt the creation of the proteins encoded by the genes. These studies showed disrupting the protein creation led to a disruption in neuronal migration (Paracchini et al., 2007). Further studies using the RNAi technique also showed altered auditory processing in the rats particularly for the KIAA and KIAA-Like genes (Szalkowski et al., 2013; Centanni et al., 2013). However the RNAi manipulation has been shown produce a number of off-target

effects which are thought to arise from functionally overlapping paralogous genes (Edelman & Gally, 2001; Kitano et al., 2008; Su et al. 2014).

One way to avoid the limitations of the RNAi technique is to use knockout mouse models of particular gene. Our colleagues at the University of Oxford recently demonstrated that manipulation of either or both of the KIAA and KIAA-Like genes in knock-out (KO) mice do not lead to the neuronal migration abnormalities which were reported in the rat RNAi studies (figure 54; Guidi et al., 2017; Martinez-Garay et al., 2016). However, they did find in the mice with a KO for both KIAA and KIAA-Like genes (double KOs) were impaired on behavioural gap-in-noise experiments compared to wild-type mice (Guidi et al., 2017). In order to investigate this finding further we performed ABR recordings on the mice to look for any abnormalities in auditory processing within the brainstem in these mice. We used three sets of KO mice, two sets of single KO mice for either KIAA or KIAA-Like genes and one set of double KO mice for both KIAA and KIAA-Like.

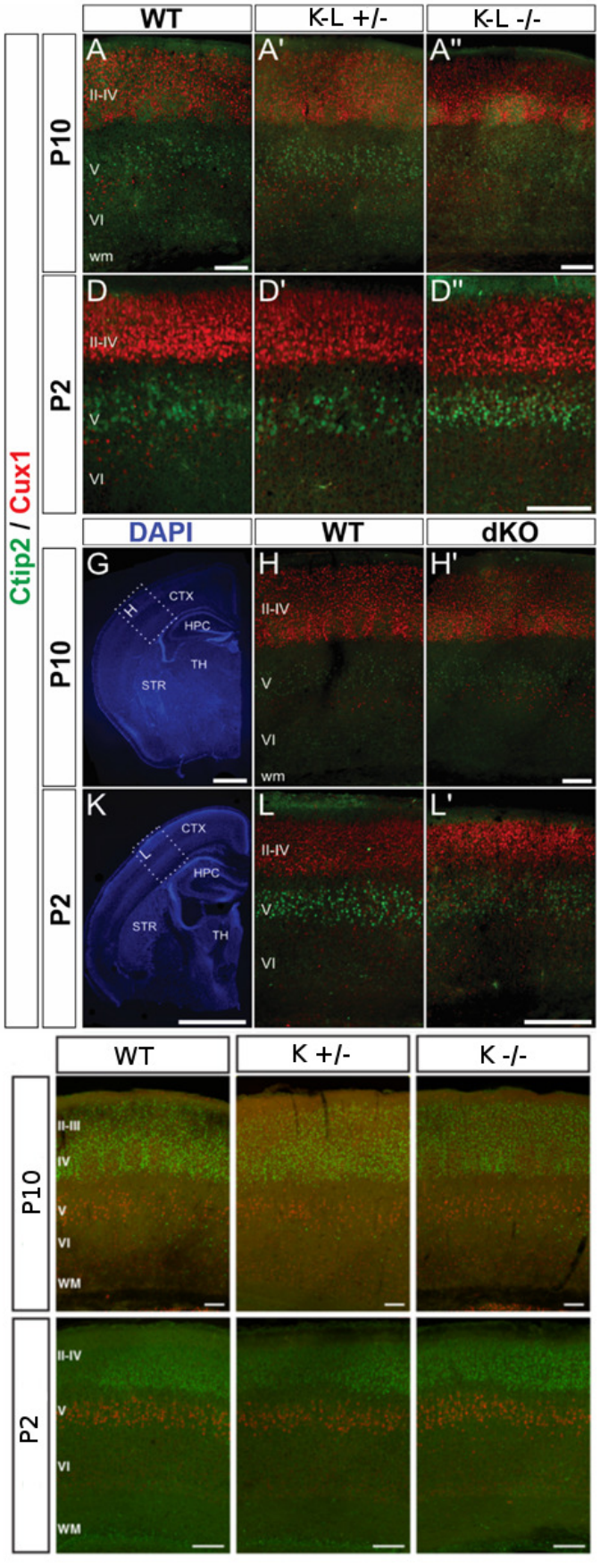

Figure 54: There is no abnormalities cortical lamination in KIAA and KIAA-Like mice. Modified from Guidi et al. 2017 and Martinez-Garay et al. 2016 comparing cortical lamination in brains from KIAA, KIAA-Like and double KO mice. Immunohistochemistry showing Ctip2 (green; lower layer pyramidal cells, layers V-VI) and Cux1 (red; upper cortical layer pyramidal cells, layers II-IV) in KIAA heterozygotes and knock-outs (K+/- and K-/-), KIAA-Like heterozygotes and knock-outs (K-L+/- and K-L-/-) and double knock-out mice (dKO) together with their respective wild-type (WT) animals for both P2 and P10 aged mice**.** No apparent differences in cortical lamination were observed.

Methods

Recording procedures

All ABR recordings were made in an isolated sound booth (Industrial Acoustics Company, Inc.). Subdermal electrodes at the vertex of the skull (+), behind the ear oriented toward the speaker (ipsilateral ear) (-) and behind the contralateral ear (ground). The stimuli were presented free-field to the left ear via a Tucker-Davis Technologies speaker (FF1). Acoustic stimuli were calibrated, using a G.R.A.S. 40BF ¼" microphone placed near to the opening of the left ear canal before the start of each experiment to ensure a flat frequency response within +/- 2 dB from 2 to 80 kHz. Stimuli were generated and data was recorded using Tucker Davis Technologies RX6 and RX5 signal processes, PA5-attenuator, SA1 speaker amplifier, RA4Li-low-impedence headsage (20X gain) and RA16SD signal amplifier with bandpass filtering from 2.2 Hz to 7.5 kHz (and 20-sample, 800 μs group delay). The recording were made with a sampling rate of 24.414kHz and a software bandpass filter of 100 – 3000 Hz (5^{th} order Butterworth filter) was applied. All stimuli were generated using a custom MatLab script.

Animals

All animals used in experiments were imported from University of Oxford to UCL for recordings. When at UCL animals were house in ventilated cages for around 2-8 weeks before being transferred to standard mouse housing at the Ear Institute at least 3 days before experiments. Recordings were made on 11 KIAA KO (83-117 days; 6 males; 5 females), 12 KIAA-Like mice KO (97-127 days; 4 male, 8 female) and 13 double KO mice (69-72 days; 6 male, 7 female), together with 14 wild-type (WT) mice age-matched to single KO mice (83-117 days; 9 male, 5 female) and 11 WT mice age-matched to double KO mice (65-74 days; 6 male; 5 female). There

were no significant differences in age between any of the knock-out mice groups and their corresponding wild-type comparison group (Wilcoxon rank-sum; all $p>0.1$).

ABRs recordings on double KO mice were not performed blind, single KO mice recordings were performed blinded. All analysis was performed blind to the genetic status of the animal.

Surgical procedures

Mice were anaesthetised with a mixture of ketamine (100 mg/kg) and medetomidine (0.83 mg/kg) administered intraperitoneally. Supplementary doses of ketamine were given as required. Anaesthesia level was evaluated every 30-60 minutes. Atropine (up to 0.2mg/kg) subcutaneously (s.c.) as required to decrease any bronchial secretions. Ringers solution was given every hour to maintain hydration (0.1ml per hour, s.c.). Breathing rate and temperature were monitored throughout the experiment. Temperature was maintained at 37.5±0.5℃ using a homeothermic blanket (Harvard Apparatus).

Auditory Stimuli

Click ABR

Click ABRs were recorded for clicks at 10-80dB intensity (increasing in 10dB steps in single KO mice and increasing in 5dB steps for double KO mice). The inter-onset-interval used was 100ms for double and single KO recordings. For the single KO recordings an additional set of click ABRs were made with a 500ms inter-onset-interval at sound intensity levels of 50-80dB SPL (increasing in 10dB steps). The click used in all experiments was monopolar square wave with duration of 50μs.

Tone ABR

Tone-evoked ABR recordings were made for tones at 8, 16, and 32 kHz in double KO and corresponding wild-type mice only. The inter-onset-interval used 100ms and tones were of 5ms duration with 5ms rise/fall time. Recordings were made at 10-80dB SPL in 10dB steps.

Masker-probe ABR

See chapter 4 ABR methods for more detailed explanation of the masker-probe stimuli. For the single KO mice: the masker-probe stimulus was composed of a 200ms white noise burst (masker), followed by 20ms silent gap and then a click (probe click) and followed by another click which occurred 500ms after the end of the noise (reference click). All stimuli were at 60dB SPL.

For the double KO mice a 200ms masker was used followed by a probe click 8, 20 or 50 ms after the end of the noise; the reference click occurred 500 ms after the end of the noise regardless of the probe delay length.

Data Analysis

All ABR analysis was performed blinded to genetic status of the animal and analysed with bespoke MatLab software to manually determine the ABR wave peaks and troughs in response to a click/tone. This identification of the peaks and troughs was performed on 3 independent occasions for all mice and all stimuli. For the masker-probe stimuli both the probe and reference click recordings were analysed for peaks and troughs of the ABR waveforms. The wave amplitudes and latencies were then calculated from the identified peaks and troughs. The final amplitudes and latencies used were taken as a mean across the 3 measurements. ABR waves I-IV only were used for analysis as there were the waves which were most reliably observed.

ABR threshold determined using custom MatLab software. ABR threshold was defined as the lowest sound intensity at which at least two clear wave deflections exceeding background variability (±SEM across repeated trials) could be identified by-an observer blind to animal genotype.

For statistical testing, we used data from ABRs evoked by 50-80 dB SPL clicks, to ensure the amplitudes/latencies tested were above click-evoked ABR threshold level for all animals. As noted above double KO click ABRs were recorded at 5dB interval and single KO mice were recorded at 10dB intervals. All statistical tests were performed on data from 10dB intervals in both single and double KO mice in order to give equal statistical power for all groups to facilitate comparison between groups.

Unless otherwise indicated the statistical tests used were repeated measures ANOVAs followed by *post-hoc* Tukey tests. Alpha value of 0.05 and therefore any p-value found to be below this value is described as being significant. However, it should be noted that analysis of the ABR wave amplitudes and latencies involves performing significance testing on four different ABR waves including multiple stimulus conditions (for example different click rates) which introduces issues of multiple testing. Multiple testing correction is applied using the Bonferroni correction (α/n, where n is the number of tests) throughout. Example when analysing wave amplitudes/latencies for 4 ABR waves then the correction used is 0.05/4=0.0125. Any results to be considered significant must therefore have a p-value of less than 0.0125.

Results

No abnormalities in click ABR thresholds in either double or single KO mice

Analysis of click ABR thresholds showed no difference for ABR thresholds for any group. Figure 55 shows percentage of mice for each threshold value with thresholds for all mice (wild-types and mutants) for comparison between the two sets of differently aged mice (i.e. double KOs and age-matched wild-types and single KOs with age-matched wild-types). The thresholds for most mice were around 30-40dB SPL and there was no significant difference either within or between groups (rank-sum; all p-values > 0.05). This indicates that there are no differences in overall hearing sensitivity between the mice. Also, there is no indication of an effect of age on ABR thresholds as the single WTs have a higher percentage than the younger double WTs at 30dB SPL. Note that ABRs were recorded using 5 dB click intensity steps in double KO mice but 10 dB steps in single KO mice.

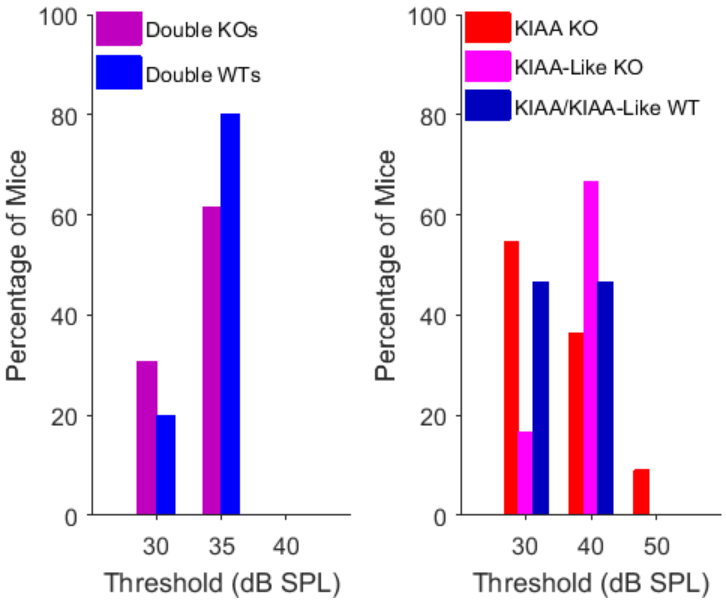

Figure 55: No difference between mutant and wild-type mice in ABR click thresholds. Bar charts showing ABR click thresholds. Left, data for double KO mice (purple) and age-matched WT mice (light blue). Right, data for KIAA single KO mice (red), KIAA-Like single KO mice (magenta) and age-matched WT animals (dark blue). The ABR click thresholds (see text for how threshold is determined) were not significantly different between wild-types and mutants for any of the groups of mice (ranksum; all p>0.05).

Reduced ABR wave 1 amplitudes in double KO mice

Double KO mice were found have a significantly lower amplitude for wave 1 (see figure 62 and table 4; table A7) compared to age-matched wild-types. Wave 1 was significantly different between double KO and wild-type mice across sound levels indicating for the early ABR wave there is a reduction in ABR wave amplitude in the double KO mice compared to wild-types which is dependent on sound level. This indicates there is some reduction in auditory processing early in the double KO mice despite similar click ABR thresholds.

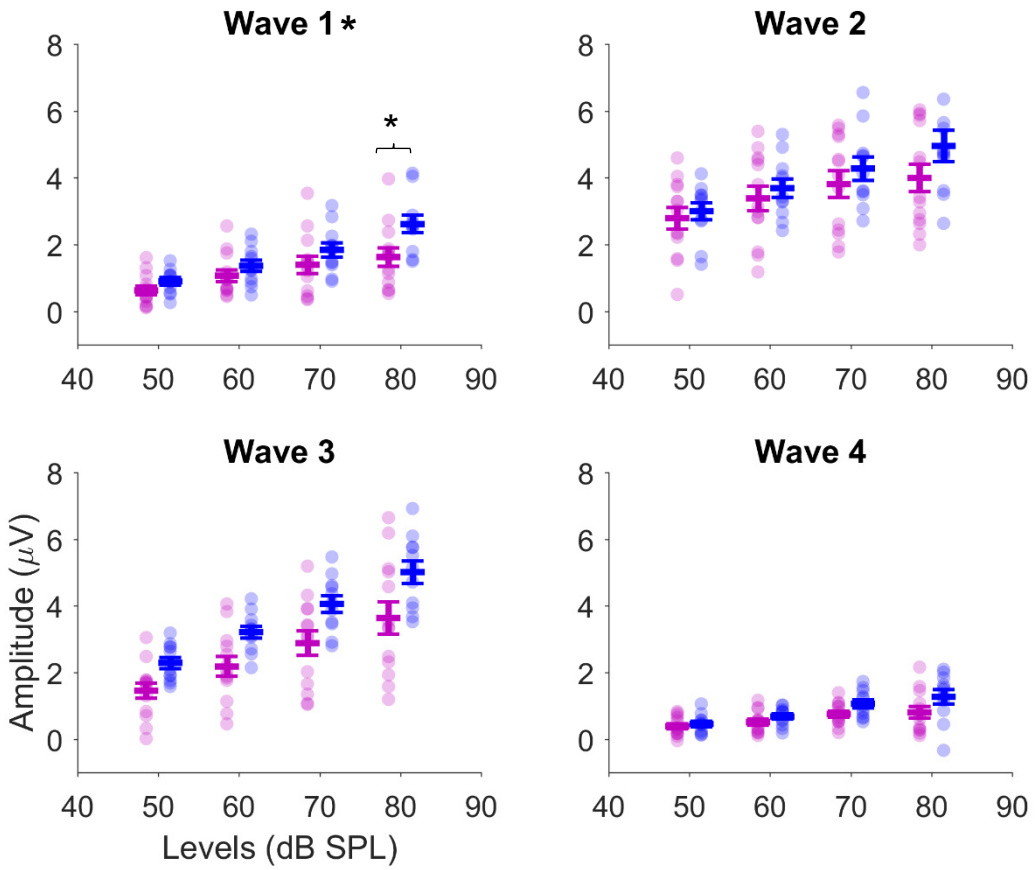

Figure 56: Click ABR wave I amplitudes are reduced in double KOs compared to WTs. Plots showing click ABR wave I-IV amplitudes for double KO and WT mice (double KO n=13, wild-type n=11). Plot symbols indicate data for individual animals and straight line indicates mean for that group (+/- 1 standard error). Purple for double KO animals, blue for age-matched wild-type animals. Wave I is significantly different between double KO and wild-types across all sound levels using a repeated measures ANOVA ($p<0.01$). Stars in titles indicate significant results in an rmANOVA with correction for multiple testing across the four waves. Only wave I at 80dB SPL has a significant post-hoc Tukey test ($p<0.05$). Individual sound levels with significance (using post-hoc Tukey tests) are marked with stars.

Table 4: P-values RM-ANOVAs and Tukey tests for double KO mice compared to age-matched wild-type for click ABR amplitudes

Double KO Amplitudes	RM-ANOVA (sound level x Group)	RM-ANOVA (Group)	*Post*-hoc Tukey test			
			50dB SPL	60dB SPL	70dB SPL	80dB SPL
Wave I	**p=0.002; F=5.536**	p=0.079; F=3.401	0.132	0.251	0.208	**0.016**
Wave II	p=0.044; F=2.855	p=0.336; F=0.968	NA	NA	NA	NA
Wave III	p=0.317; F=1.200	p=0.014; F=7.132	NA	NA	NA	NA
Wave IV	p=0.258; F=1.375	p=0.053; F=4.190	NA	NA	NA	NA

Reduction in wave 3 amplitude in KIAA-Like but not KIAA KOs for slower click rate

For the single KO mice and their respective WTs two click speeds were used during for the ABRs (see methods). The results from the faster click rate show Wave III of KIAA-Like KO mice was significantly different from wild-type mice before correction for multiple testing but not afterwards(see table 5 and figure 57; table A8). KIAA KO mice were not significantly different from wild-type mice (see table 5 and figure 57; table A8).

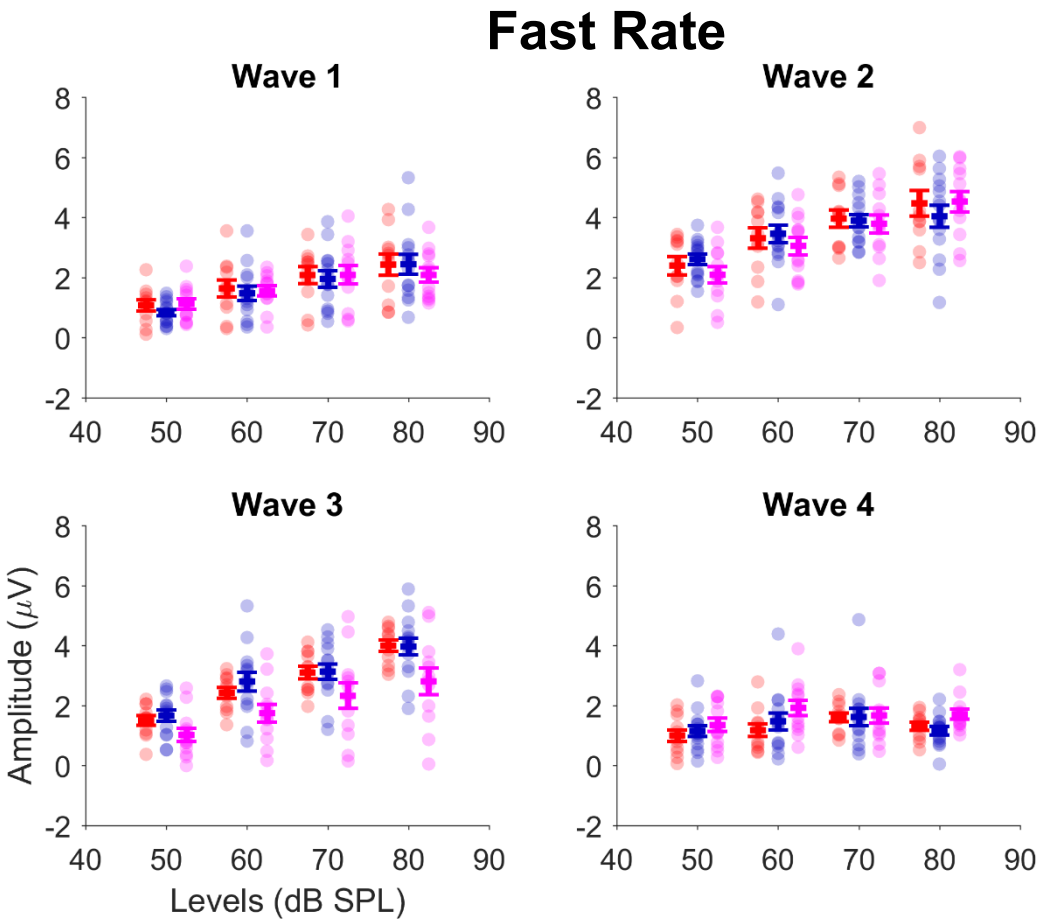

Figure 57: Fast click ABR wave amplitudes are not significantly different between wild-types and KIAA-Like or KIAA mice. Plots showing wave I-IV amplitudes for clicks with 100ms in between clicks for KIAA and KIAA-Like single KO mice together with age-matched WT mice (KIAA n = 11; KIAA-Like n = 12, WT n=14). Figure convention as in figure 62. No significant difference between KIAA-Like KO mice and WT mice amplitudes after correction for multiple testing (rmANOVA; all p>0.0125). KIAA KO mice were also not significantly different from wild-type mice for any statistical tests used (rmANOVA; all p>0.05).

KIAA-Like KO **Amplitudes (fast click)**	RM-ANOVA (sound level x Group)	RM-ANOVA (Group)
Wave I	p=0.209; F=1.550	p=0.896; F=0.018
Wave II	p=0.061; F=2.563	p=0.679; F=0.176
Wave III	p=0.339; F=1.141	p=0.029; F=5.405
Wave IV	p=0.426; F=0.940	p=0.240; F=1.451

Table 5: P-values from RM-ANOVAs and Tukey tests for KIAA-Like KO compared to age-matched wild-types click ABR amplitudes

The results for the slow-click click ABR, however, demonstrate there is a significant difference between KIAA-Like KOs and wild-type mice for click ABR amplitude of wave III which isn't dependent on sound level (see table 6 and figure 58; table A8).

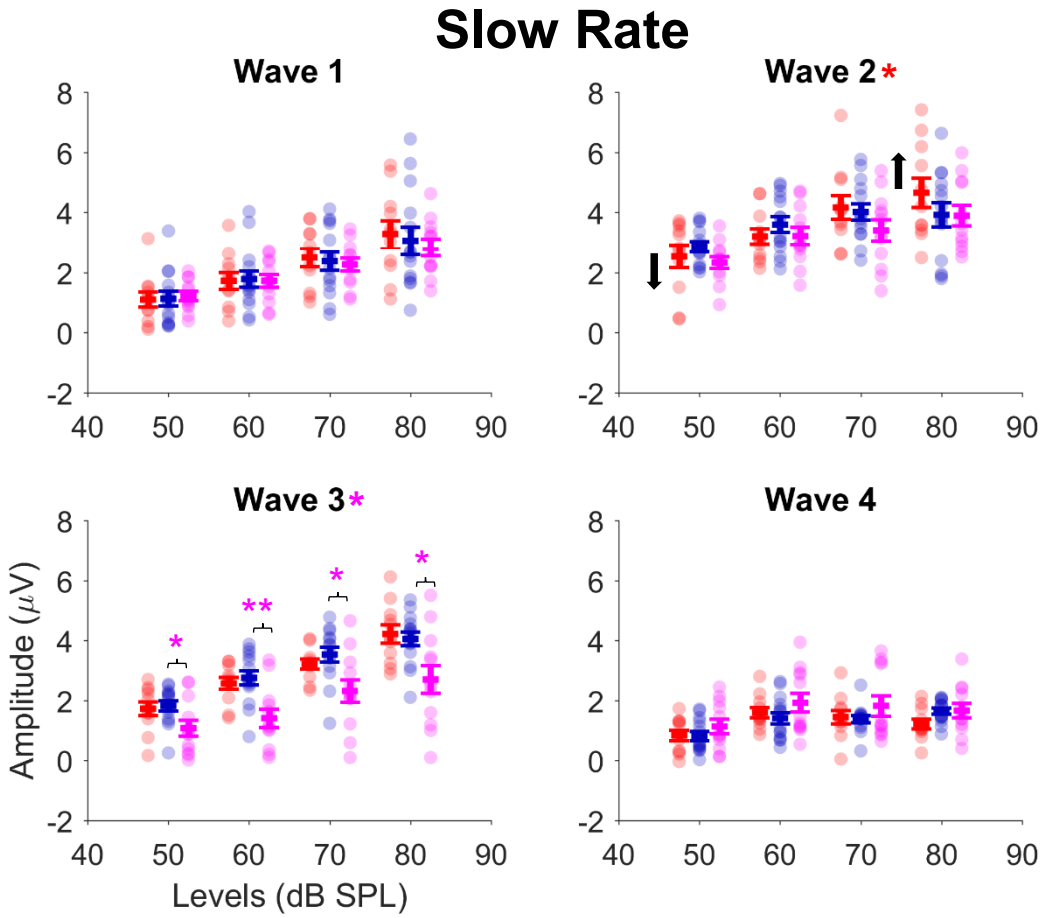

Figure 58: At slower click rate ABR wave III amplitudes for KIAA-Like mice for a slower click rate and wave II amplitudes are significantly different KAA mice from WT. Plots showing wave I-IV amplitudes at slower click rate (500ms between clicks) for KIAA and KIAA-Like single KO mice together with age-matched WT animals. Figure conventions as in figure 62. Significant differences across sound levels for wave III amplitudes between KIAA-Like and WT mice using repeated measures ANOVA with correction for multiple testing ($p<0.01$). Individual sound levels that were found to be significant using post-hoc Tukey tests are indicated by stars. Significant differences across sound levels for wave II amplitudes between KIAA and WT mice using repeated measures ANOVA with correction for multiple testing ($p<0.01$). Black arrows indicate direction of mean for KIAA relative to the wild-type mean demonstrating that although the KIAA mean is significantly different from the wild-type it deviates in different directions at different sound levels. The differences observed in the slow versus fast click conditions could arise from a clearer or less variable ABR signal in the slow click condition where the neurons have more time to recover in between clicks.

These results are also confirmed by the post-hoc Tukey tests which were found to be significant for each sound level tested. No other wave amplitudes were significantly difference from wild-type mice. These results implicate a deficit in wave III amplitudes in the KIAA-Like mice compared to WTs suggesting some disruption to auditory processing in the trapezoid body/superior olive (Henry, 1979).

KIAA-Like KO Amplitudes (Sow click)	RM-ANOVA (sound level x Group)	RM-ANOVA (Group)	*Post*-hoc Tukey test			
			50dB SPL	60dB SPL	70dB SPL	80dB SPL
Wave I	p=0.704; F=0.470	p=0.849; F=0.037				
Wave II	p=0.301; F=1.242	p=0.297; F=1.137				
Wave III	p=0.056; F=2.640	**p=0.005; F=9.347**	**0.024**	**0.002**	**0.010**	**0.012**
Wave IV	p=0.204; F=1.569	p=0.233; F=1.496				

Table 6: Table showing results of statistical tests for KIAA-Like KO mice compared to the wild-type mice for click ABR amplitudes with a 500ms inter-click-interval. The statistical tests used were repeated measures ANOVAs and post-hoc Tukey tests.

In contrast to the results obtained for the fast-click condition the KIAA KO mice were significantly different from WTs for wave II amplitude across sound levels using a repeated measures ANOVA (see table 7 and figure 58; table A8). However, the

ANOVA wave II amplitude result was not confirmed by post-hoc Tukey tests at any sound level and analysis of the mean shows some sound levels to be above (70 and 80dB) wild-types and others sound levels below (50 and 60dB) wild-types (indicated by the black arrow in figure 58; table A8). This all indicates, together with the fact that the difference was not found in the fast-click condition, that the wave II result may be due to chance rather than any real difference however it is possible that there is some subtle difference in the wave II amplitude in the KIAA KO mice, the direction of which differs with sound intensity. Taken together these results suggest no real difference in slow-click click ABR amplitudes for KIAA KO mice compared to wild-type mice as in the fast-click ABR recordings.

KIAA KO Amplitudes (slow click)	RM-ANOVA (sound level x Group)	RM-ANOVA (Group)	*Post*-hoc Tukey test			
			50dB SPL	60dB SPL	70dB SPL	80dB SPL
Wave I	P=0.677 F0.510	P=0.879 F=0.024				
Wave II	**P=0.009** **F=4.186**	P=0.918 F=0.011	0.401	0.303	0.754	0.247
Wave III	P=0.394 F=1.009	P=0.692 F=0.161				
Wave IV	P=0.127 F=1.968	P=0.824 F=0.051				

Table 7: Table showing results of statistical tests for KIAA KO mice compared to wild-types for click ABR amplitudes with a 500ms inter-click-interval.

No abnormalities in ABR wave latencies in any KO mice

Despite differences in ABR wave amplitudes in double KO mice compared to wild-types the latencies of all waves were not significantly different from wild-type animals. The double KO mice did not show significant latency difference across sound levels nor at any individual sound level (see figure 59; table A7) nor for genotype alone; thus repeated tests failed to provide strong evidence for a lack of difference in wave latency. Similarly the KIAA single KO mice did not show any differences in wave latencies across sound levels or at individual sound levels nor genotype alone indicating these mice also do not have a difference in wave latency for either click rate (see figures 60 and 61; table A8).

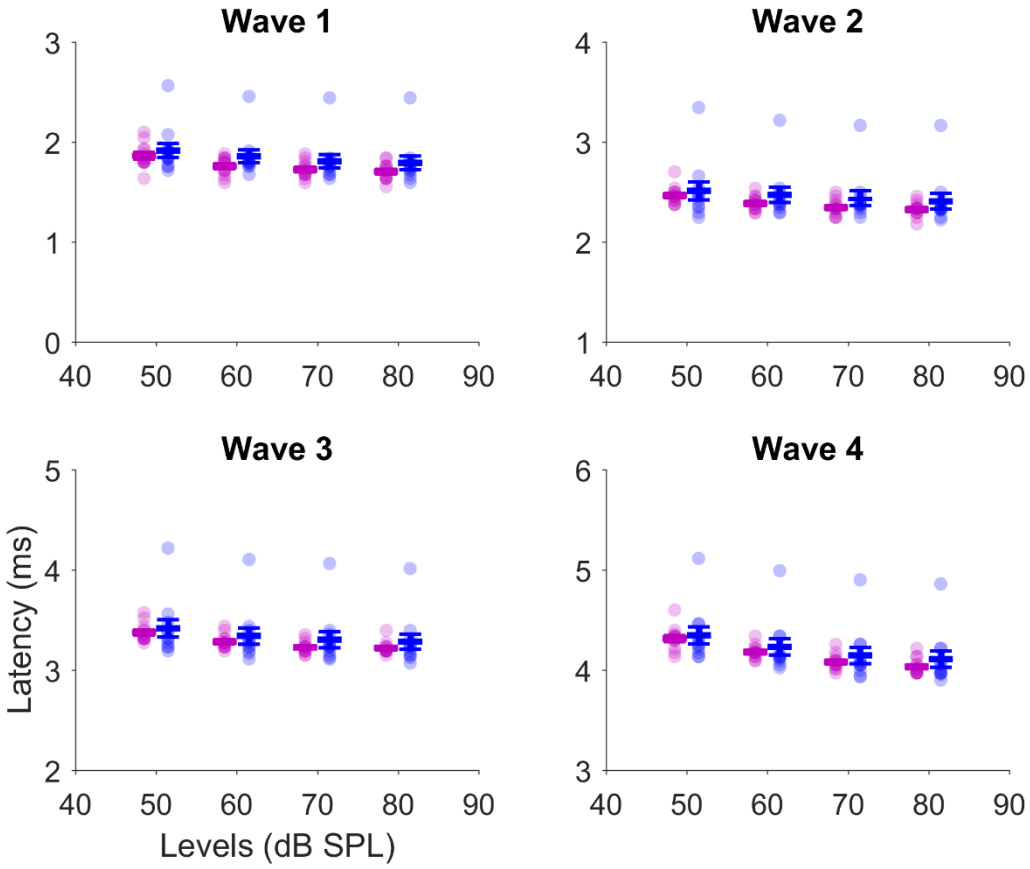

Figure 59: No significant differences between double KO and WT mice in click ABR wave latencies. Figure conventions as in figure 63.

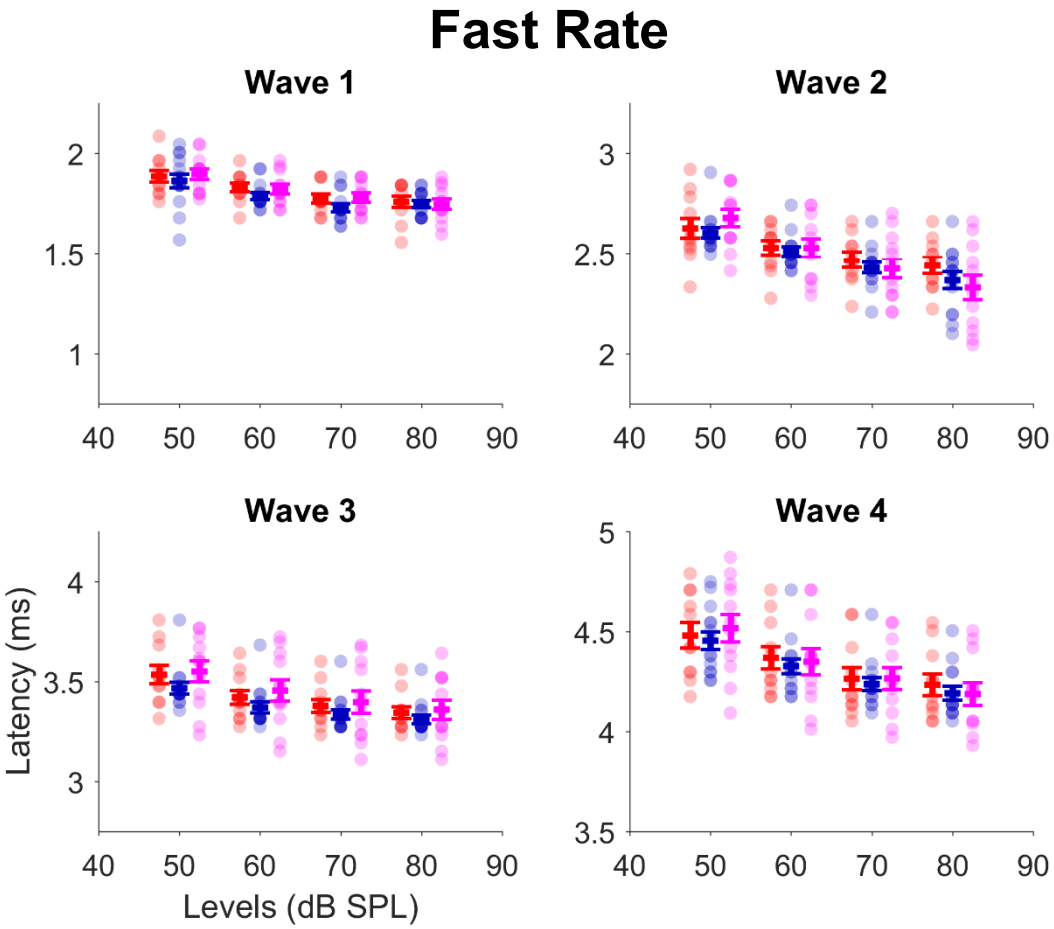

Figure 60: No significant difference in WT and KIAA or KIAA-Like mice for ABR click wave latencies for fast clicks. Plots showing wave I-IV latencies for fast click condition (100ms between clicks) for KIAA and KIAA-Like single KO mice together with age-matched WT animals. Figure conventions as in figure 62.

There was a significant difference between KIAA-Like KO and wild-type animals for wave II click ABR latency using a repeated measures ANOVA for group and sound levels however, this did was not significant after correction for multiple testing indicating there was no significant difference between KIAA-Like and WT mice for click ABR latencies for either click rate (tables 8 and 9; figures 66 and 67; table A8).

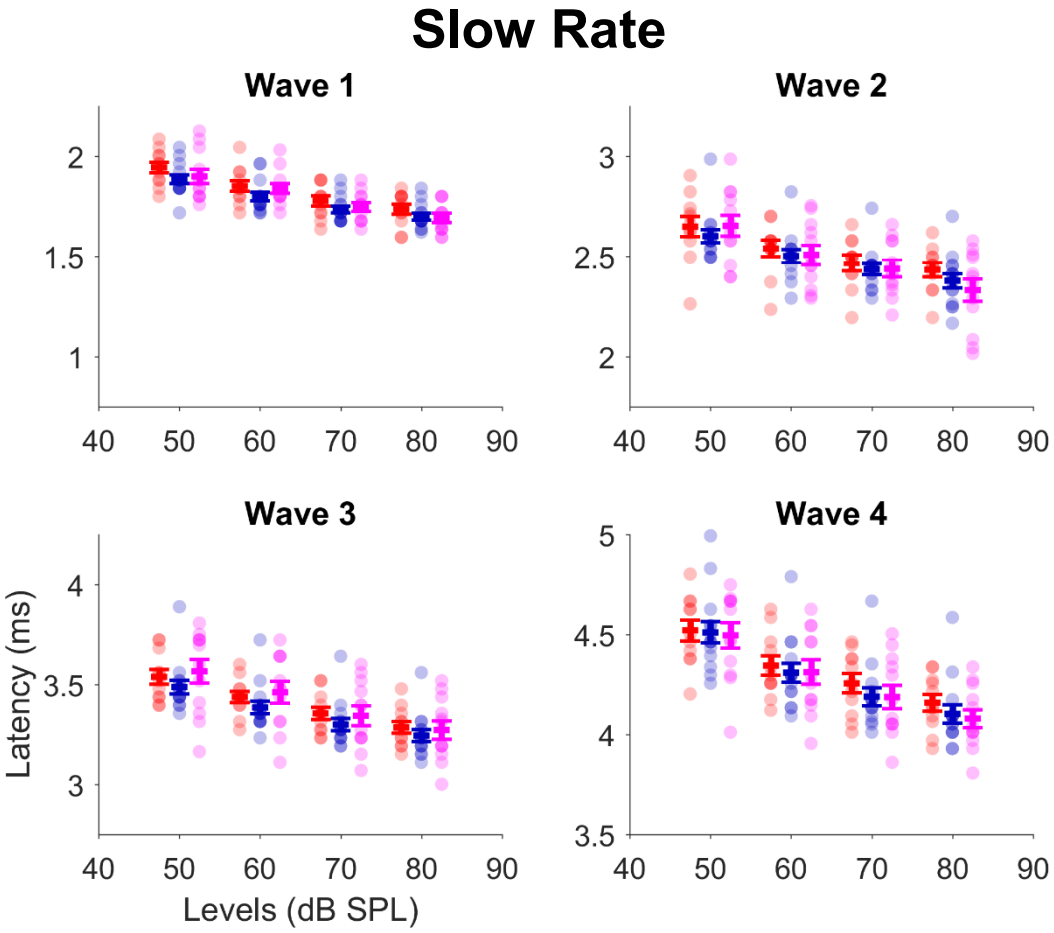

Figure 61: At slower click rates, no significant difference from WTs in ABR click wave latencies. Plots showing wave I-IV latencies for slow click condition (500ms between clicks) for KIAA and KIAA-Like single KO mice together with age-matched WT animals. Figure conventions as in figure 62.

KIAA-Like KO **Latencies (fast click)**	RM-ANOVA (sound level x Group)	RM-ANOVA (Group)
Wave I	P=0.537; F=0.732	P=0.288; F=1.183
Wave II	P=0.027; F=3.241	P=0.804; F=0.063
Wave III	P=0.239; F=1.438	P=0.216; F=1.613
Wave IV	P=0.251; F=1.398	P=0.681; F=0.173

Table 8: Results of statistical tests for click ABR latencies of KIAA-Like KO mice compared to wild-types.

KIAA-Like KO **Latencies (slow click)**	RM-ANOVA (sound level x Group)	RM-ANOVA (Group)
Wave I	P=0.335; F=1.149	P=0.578; F=0.317
Wave II	P=0.048; F=2.759	P=0.951; F=0.004
Wave III	P=0.048; F=2.759	P=0.336; F=0.965
Wave IV	P=0.818 F=0.310	P=0.898; F=0.017

Table 9: Results of statistical tests for slow-click click ABR latencies for KIAA-Like KO compared to wild-type mice. Repeated measures and post-hoc Tukey tests were used as before.

Suprathreshold ABR wave amplitude abnormalities in double KO mice are not explained by gender differences

The previous results were further analysed taking into account differences in age and gender in to determine whether the noted results could be explained by differences in age or gender rather than as a result of genotype. Previous studies have found differences in ABR wave amplitudes due to differences in gender (Henry, 2004). So a confounding factor in the ABR results could occur from differences in the gender of the animals since both male and female animals were used in the experiments. The percentages of males to females in each group of mice are shown in figure 62. When interpreting the following results it should be noted that for some groups (for example KIAA-Like single KOs) there is a disproportion of males to females which may affect the results.

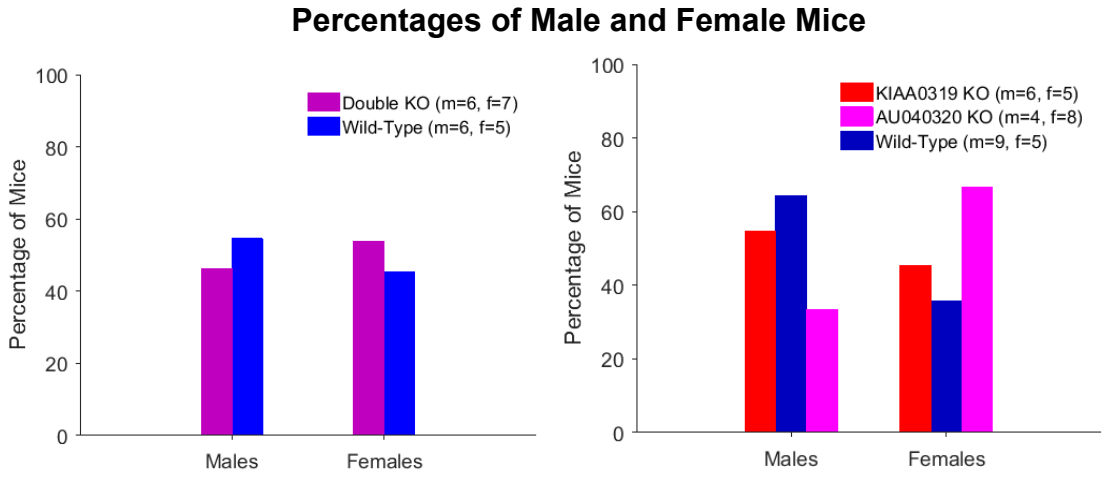

Figure 62: There is no significant difference in percentages of male to female mice between WT and mutant mice. Plots showing gender assignment for each group. Left-hand plot shows percentage of male and female mice for double KOs and age-matched WT mice. Right-hand plot shows percentage of male and female mice for each single KO group and age-matched WT mice. Legends on plots indicate total number of mice for each group together with actual number of males and females for each group. There was no significant difference in the proportions of male and females between WT and mutants (fishers exact test; $p>0.05$).

In order to look for differences in click ABR recordings due to differences in gender the click results were reanalysed with gender as an additional factor in the repeated-measures ANOVA. For display purposes the click ABR amplitudes and latencies for the 80dB SPL only condition are shown by gender.

When the click ABR amplitudes were reanalysed using gender as an additional factor the results showed no major effects of gender (see table 10 and figure 63). For double KO mice the wave I amplitude was still significantly different from wild-types and there was found to be no significant effect of gender when considering gender with group only or group by sound level and therefore gender differences cannot explain the observe difference in click ABR amplitudes between double KO and WT mice.

Double KO Amplitudes	RM-ANOVA (sound level x group)	RM-ANOVA (sound level x group x gender)	RM-ANOVA (group)	RM-ANOVA (gender)	RM-ANOVA (group x gender)	*Post*-hoc Tukey test (group x gender)	
						Females	Males
Wave I	**P=0.003 F=5.345**	P=0.597 F=0.633	P=0.100 F=2.970	P=0.171 F=2.021	P=0.883 F=0.022	P=0.204	P=0.276
Wave II	P=0.020 F=3.538	P=0.463 F=0.867	P=0.284 F=1.213	P=0.188 F=1.858	P=0.547 F=0.376		
Wave III	P=0.309 F=1.223	P=0.977 F=0.067	P=0.019 F=6.544	P=0.947 F=0.005	P=0.565 F=0.343		
Wave IV	P=0.221 F=1.509	P=0.568 F=0.679	P=0.058 F=4.031	P=0.906 F=0.014	P=0.282 F=1.221		

Table 10: Double KO p-values for repeated measures ANOVAs of click ABR amplitudes from double KO versus wild-type mice together with p-values from post-hoc Tukey tests. The results confirm an effect of genotype on wave I, II and III amplitudes even when considering variance due to differences in gender. Post-hoc Tukey tests indicate there may be some small differences in amplitudes between males and females for waves III and IV.

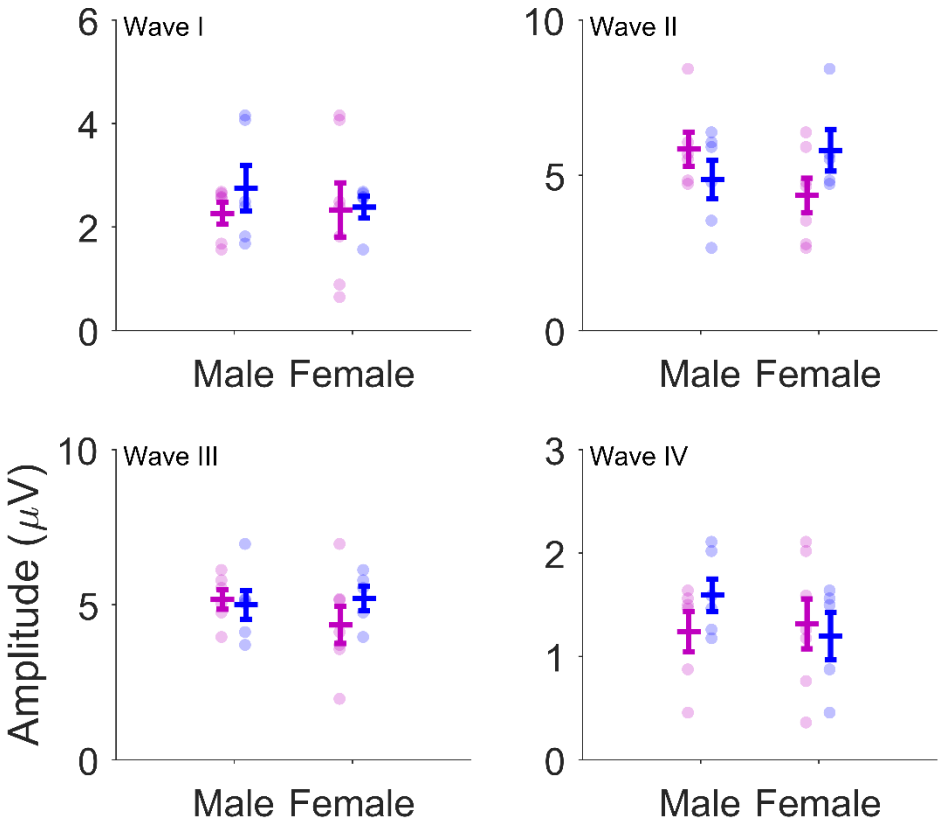

Figure 63: Wave I click amplitude difference between double KO and WT mice cannot be explained by gender. Plots show amplitudes versus gender for each wave for double KO mice and age-matched WT mice at 80dB SPL. Plots symbols show data for individual animals, error bars indicate +/- standard error, vertical line indicates the mean. Repeated measures ANOVA across multiple sound levels with gender additional factor revealed no significant The wave I click amplitude difference between double KO and WT mice is similar between male and female mice (rmANOVA all p>0.0125).

Similarly, there appears to be no major effect of gender for double KO versus wild-type mice on click ABR wave latencies (see table 11 and figure 64). For wave III latencies there was found to be a significant difference between double KOs and wild-types when considering group by sound level by gender (p=0.0001) however since this results is not confirmed by the *post-hoc* Tukey tests and is not significant for group only or group by sound level alone the effect appears to be minimal or due to chance rather than any consistent difference.

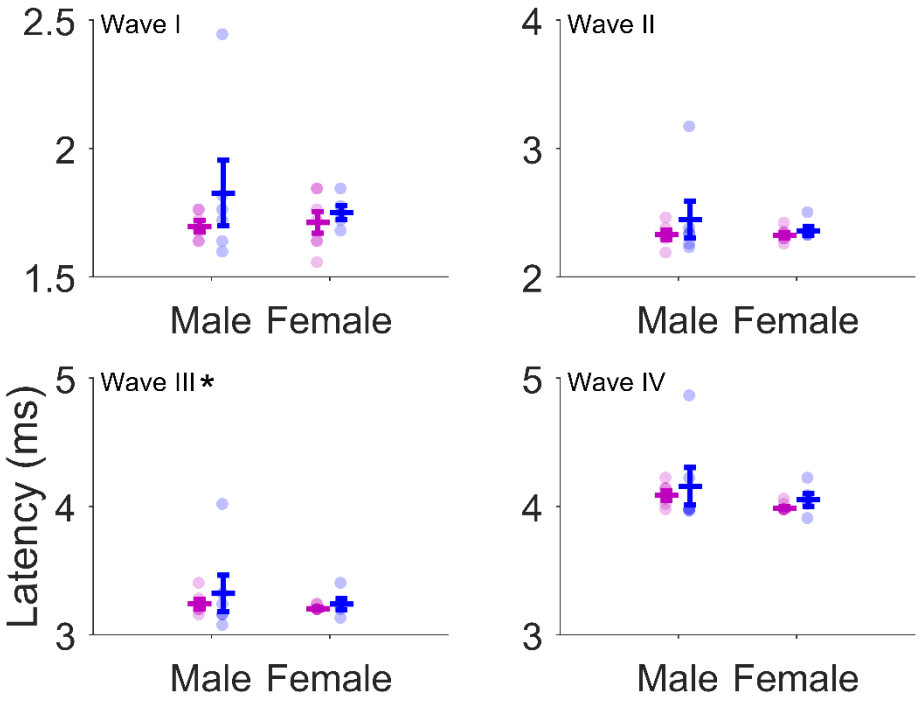

Figure 64: Significant effect of gender on click ABR wave III latencies for double KO compared to WT mice. Plots showing wave latencies 80dB SPL versus gender for double KO mice and age-matched wild-types. Figure conventions as in figure 69. There is a significant effect of gender on wave latencies between double KO and WT mice after correction for multiple testing (rmANOVA groupxgenderxsound level; all $p<0.001$) as indicated in the plot title with a star. Post-hoc Tukey tests for wave III were not significantly different between double KO and WT mice (all $p>0.05$).

Double KO Latencies	RM-ANOVA (sound level x group)	RM-ANOVA (sound level x group x gender)	RM-ANOVA (group)	RM-ANOVA (gender)	RM-ANOVA (group x gender)	*Post*-hoc Tukey test (group x gender)	
						Females	Males
Wave I	P=0.555 F=0.702	P=0.837 F=0.284	P=0.266 F=1.309	P=0.576 F=0.324	P=0.679 F=0.176		
Wave II	P=0.254	P=0.186 F=1.656	P=0.355	P=0.639 F=0.227	P=0.396		

	F=1.393		F=0.898		F=0.752		
Wave III	P=0.13 1 F=1.949	**P=0.000 1 F=7.971**	P=0.50 2 F=0.467	P=0.455 F=0.579	P=0.51 5 F=0.439	P=0.989	P=0.34 9
Wave IV	P=0.21 0 F=1.554	P=0.438 F=0.917	P=0.55 7 F=0.358	P=0.228 F=1.550	P=0.78 2 F=0.079		

Table 11: P-values from repeated measures ANOVAs for click ABR latencies for double KO vs. wild-type mice with gender as an additional factor together with p-values for post-hoc Tukey tests. Results show no signficiant difference between double KO and wild-type latencies except for wave III when considering group by sound level by gender.

Weak gender differences in click ABR wave amplitudes and latencies do not explain results for single KOs

No major effects of gender on KIAA KO wave amplitudes (see table 12 and figure 65). KIAA KOs wave amplitudes were found not to be significant different to wild-types for the fast-click or slow-click condition when considering gender as an additional factor after correction for multiple testing. Similarly, for KIAA KO wave latencies there were no significant effects of gender on wave latencies (see figure 66).

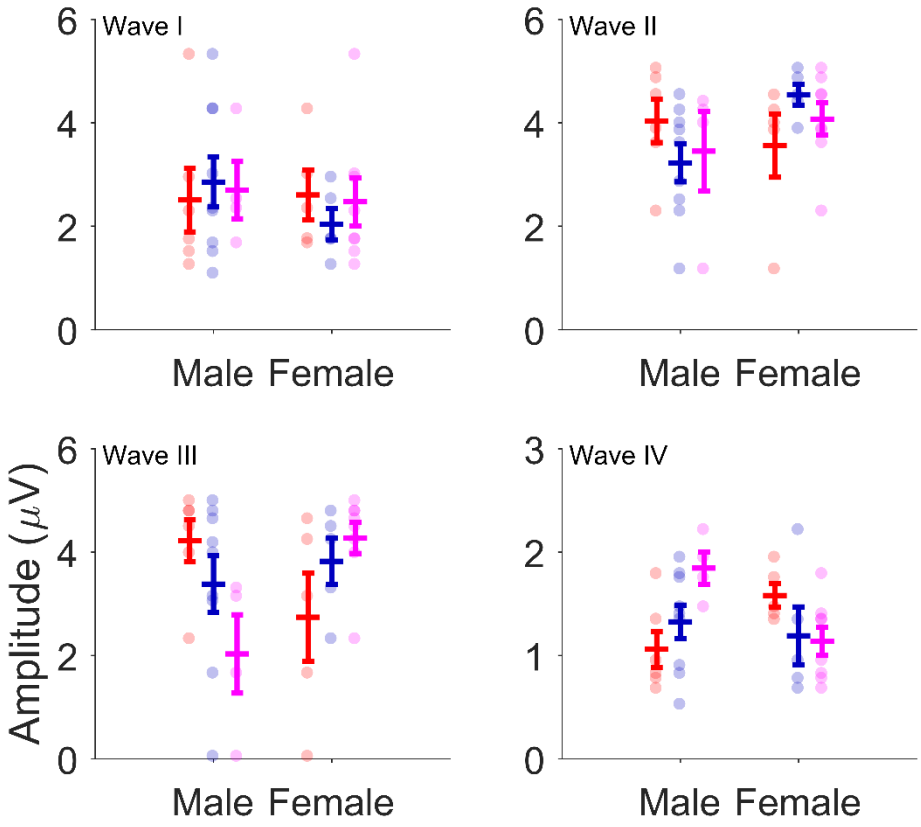

Figure 65: No significant effect of gender on ABR click wave amplitudes for KIAA-Like, KIAA and WT mice. Plots showing wave amplitudes versus gender for each click ABR (fast click rate) wave for KIAA and KIAA-Like single KO mice and age-matched wild-types at 80dB SPL. Figure conventions as in figure 69. No significant effect of gender on wave amplitude within each group (rmANOVA; all p>0.05).

KIAA0319 KO Amplitudes Slow click	RM-ANOVA (sound level x group)	RM-ANOVA (sound level x group x gender)	RM-ANOVA (group)	RM-ANOVA (gender)	RM-ANOVA (group x gender)
Wave I	P=0.556 F=0.700	P=0.051 F=2.733	P=0.914 F=0.012	P=0.280 F=1.228	P=0.720 F=0.132
Wave II	P=0.030 F=3.190	P=0.557 F=0.698	P=0.897 F=0.017	P=0.709 F=0.143	P=0.713 F=0.139

Wave III	P=0.500 F=0.798	P=0.853 F=0.261	P=0.908 F=0.014	P=0.561 F=0.348	P=0.015 F=7.021
Wave IV	P=0.125 F=1.988	P=0.429 F=0.936	P=0.897 F=0.017	P=0.215 F=1.634	P=0.848 F=0.038

Table 12: P-values for repeated measures ANOVAs for click ABR amplitudes (slow-click condition) together with post-hoc Tukey tests. Results show no significant difference between KIAA single KO and wild-types for repeated measures ANOVA when considering gender as an additional factor.

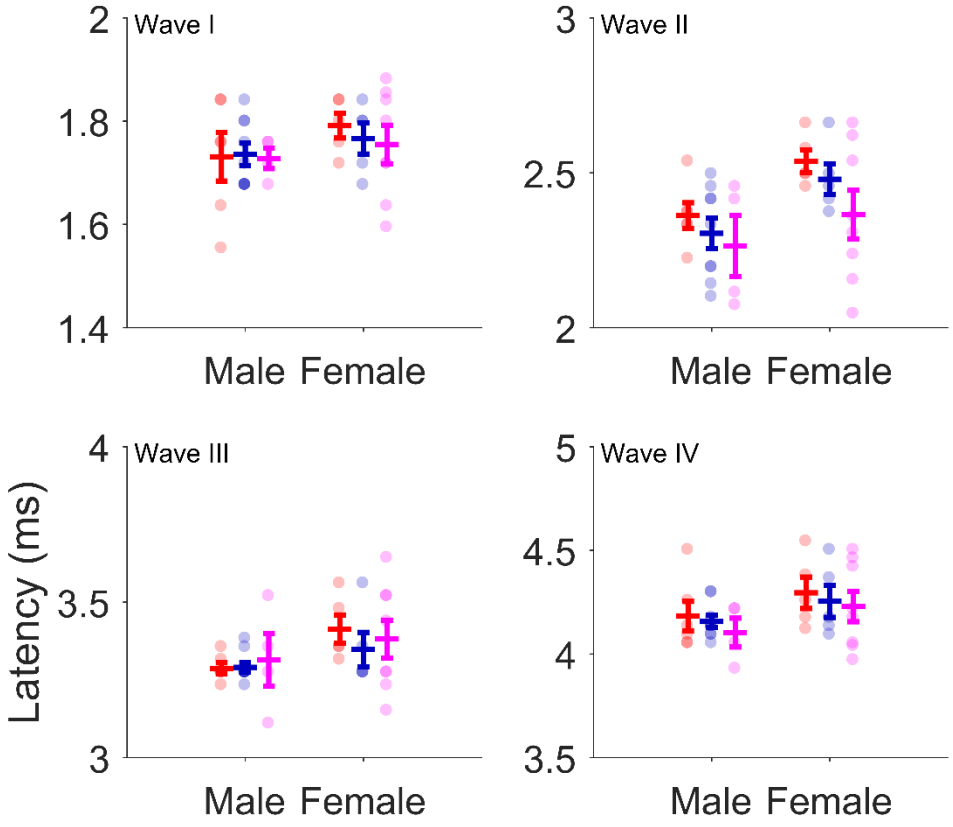

Figure 66: No significant effect of gender on ABR click wave latencies for KIAA-Like, KIAA and WT mice. Plots showing wave latencies versus gender for each click ABR (fast click rate) wave for KIAA and KIAA-Like single KO mice and age-matched wild-types at 80dB SPL. Figure conventions as in figure 69. No significant effect of gender on wave latencies within each group (rmANOVA; all p>0.05).

KIAA-Like KO wave III amplitudes were significantly different from wild-types even when considering gender as an additional factor for both the slow click conditions using a repeated measures ANOVA for group alone (see tables 13, 14 and figure 66) confirming the previously noted results. This suggests that the wave III amplitude result cannot be explained by differences in gender.

KIAA-Like KO Amplitudes Fast click	RM-ANOVA (sound level x group)	RM-ANOVA (sound level x group x gender)	RM-ANOVA (group)	RM-ANOVA (gender)	RM-ANOVA (group x gender)
Wave I	P=0.175 F=1.702	P=0.199 F=1.594	P=0.847 F=0.038	P=0.794 F=0.070	P=0.776 F=0.083
Wave II	P=0.185 F=1.656	P=0.422 F=0.950	P=0.711 F=0.141	P=0.939 F=0.006	P=0.541 F=0.385
Wave III	P=0.158 F=1.791	P=0.630 F=0.581	P=0.043 F=4.615	P=0.888 F=0.021	P=0.312 F=1.072
Wave IV	P=0.305 F=1.233	P=0.569 F=0.677	P=0.278 F=1.236	P=0.955 F=0.003	P=0.446 F=0.603

Table 13: P-values for repeated measures ANOVAs for KIAA-Like vs. wild-type mice click ABR amplitudes (fast-click condition) together with post-hoc Tukey tests. Results show significant difference in wave III amplitude for group. Post-hoc tests indicate males wave III amplitudes may be more affected.

KIAA-Like KO Amplitudes Slow click	RM-ANOVA (sound level x group)	RM-ANOVA (sound level x group x gender)	RM-ANOVA (group)	RM-ANOVA (gender)	RM-ANOVA (group x gender)
Wave I	P=0.450 F=0.892	P=0.612 F=0.608	P=0.730 F=0.122	P=0.569 F=0.335	P=0.797 F=0.068
Wave II	P=0.500 F=0.797	P=0.727 F=0.437	P=0.253 F=1.380	P=0.571 F=0331	P=0.574 F=0.325
Wave III	P=0.092 F=2.241	P=0.818 F=0.310	**P=0.011 F=7.714**	P=0.542 F=0.384	P=0.175 F=1.963
Wave IV	P=0.071 F=2.452	P=0.301 F=1.245	P=0.187 F=1.852	P=0.463 F=0.558	P=0.897 F=0.017

Table 14: As in figure 10 but for slow-click condition. Results confirm fast-click condition results indicating a significant difference between KIAA-Like and wild-types for wave III amplitudes which the post-hoc Tukey tests indicate is mostly from the males.

For KIAA-Like analysis, the repeated measures ANOVA was significant for gender alone but not for group by gender in wave II latencies of the fast-click condition and waves II, III and IV of the slow-click condition indicating there may be some overall effect of gender on the wave latencies (as also found in the KIAA mice) but this is not dependent on group. The wave III latency in the slow-click condition was significant

for group by sound level even with gender as an additional factor indicating this result cannot be explained by differences in gender.

KIAA-Like KO Latencies Slow click	RM-ANOVA (sound level x group)	RM-ANOVA (sound level x group x gender)	RM-ANOVA (group)	RM-ANOVA (gender)	RM-ANOVA (group x gender)
Wave I	P=0.394 F=1.011	P=0.948 F=0.120	P=0.918 F=0.011	P=0.047 F=4.440	P=0.528 F=0.411
Wave II	P=0.072 F=2.438	P=0.534 F=0.736	P=0.335 F=0.973	**P=0.003** **F=11.272**	P=0.483 F=0.510
Wave III	P=0.031 F=3.152	P=0.402 F=0.993	P=0.733 F=0.120	P=0.057 F=4.037	P=0.862 F=0.031
Wave IV	P=0.983 F=0.054	P=0.761 F=0.390	P=0.314 F=1.062	**P=0.010** **F=7.941**	P=0.412 F=0.699

Table 15: P-values for repeated measures ANOVAs for click ABR latencies for KIAA-Like KO mice for slow-click condition together with post-hoc Tukey. Results show significant effect of gender for waves I,II and IV but not for group by gender but not confirmed by post-hoc Tukey tests. Wave III latencies significant for group across sound levels even with gender as an additional factor.

Observed click ABR wave abnormalities in KO mice cannot be explained by age-related factors

Since the KO mice are on a C57/Blk6 background age may be a factor in the click ABR results (Hunter & Willott 1987). The single KO mice had the largest age range with the KIAA KO and single WT animals both having a maximum difference in age of 34 days whereas the double KO mice only differed by 3 days (see table 16). There are no significant differences between each KO group and their WTs (rank-

sum all p-values > 0.05). The click ABR amplitudes and latencies were investigate further for any correlations with age by using regression analysis on the 80dB SPL condition only.

Group	Min age (days)	Max age (days)	Medium age (days)
KIAA KO	83	117 (34)	89
KIAA-Like KO	97	124 (27)	105
Single WT	83	117 (34)	104
Double KO	69	72 (3)	71
Double WT	65	74 (9)	67

Table 66: Table showing age range (minimum and maximum ages) together with median age for each mouse group. Note figures in brackets in max age column indicate the maximum difference in age (in days).

There were no significant effect of age on double KO mice. A regression analysis of age versus click ABR wave amplitudes and latencies for each wave at 80dB SPL reveal no significant p-values for either double KOs, wild-types or double KOs and wild-types grouped together (data not shown).

There were no major correlation with age on click ABR wave amplitudes for single KO mice and WTs (figures 67 and 68). A regression analysis on click ABR wave amplitudes for 80dB SPL click against age for the single WT mice and for all the mice (single KO and WTs grouped together) produced no significant correlation with age for either the fast or slow click rate. For KIAA-Like KO mice there was found to be a significant correlation with age for wave I amplitudes of the fast-click condition ($p=0.004$) however this was not found in the slow-click condition which indicates this result may be due to chance rather than a consistent correlation of age and wave I

amplitudes. There were no other significant correlations with age and wave amplitudes for the KIAA-Like KO mice for either the fast or slow click conditions. KIAA KO mice had no significant correlation with age and wave amplitudes for either cli

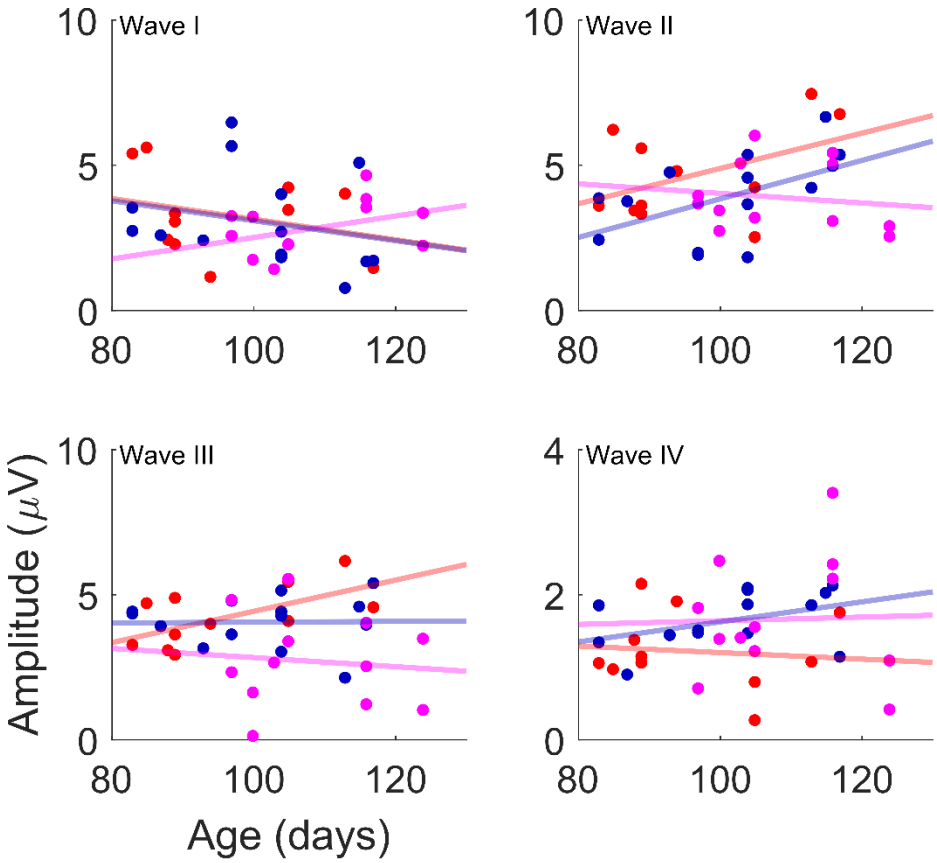

Figure 67: Significant effect of age on wave I amplitudes for KIAA-Like mice. Plots showing wave amplitudes versus age for 80dB SPL click ABR wave (at fast click rate) for KIAA, KIAA-Like single KO mice and age-matched WT. Scatter plots represent individual animals (magenta for KIAA-Like KO, red for KIAA KO, blue for WT). Age is in days with a (maximum range 41 days). Lines indicate regression lines. Wave I amplitude showed a significant dependence on age for wave I amplitude for KIAA-Like single KO mice after correction for multiple testing ($p<0.01$). This suggests there may be some effect of age on wave I amplitudes for KIAA-Like mice although only a single sound level is tested in this instance.

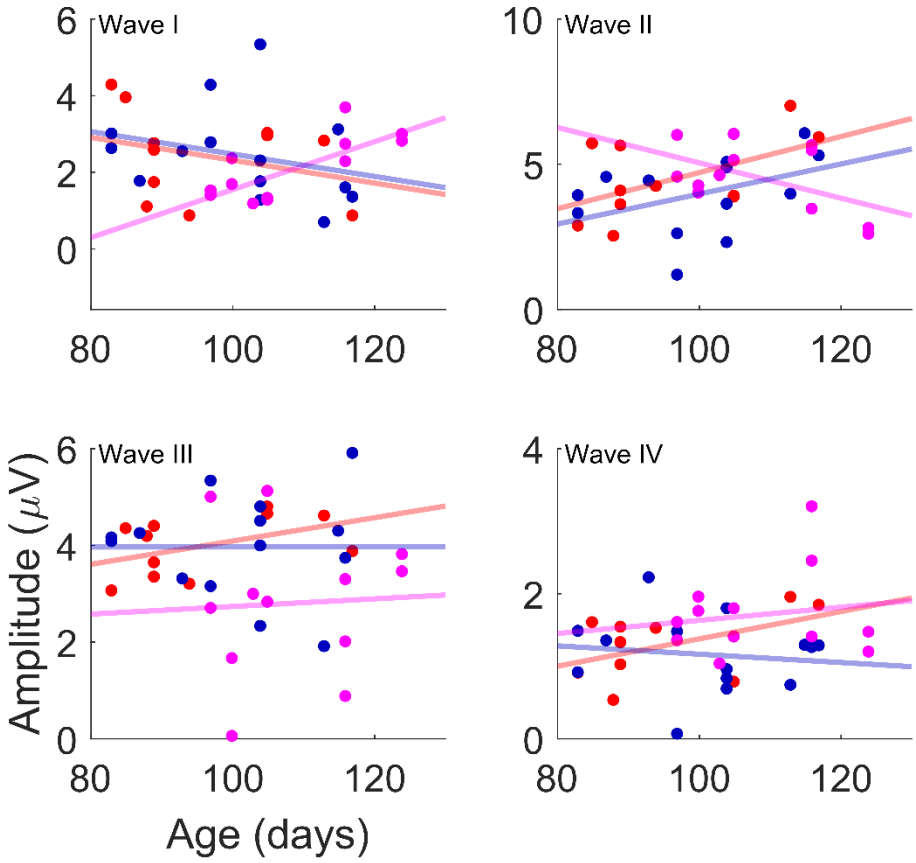

Figure 68: No significant effect of age on slow-click ABR wave amplitudes for KIAA-Like, KIAA or WT mice. Plots showing wave amplitude versus age for 80dB SPL click ABR waves (at the slow click rate) for KIAA, KIAA-Like single KO mice and age-matched WTs. Figure convention as in figure 75. No significant dependence of wave amplitudes on age for either group or all mice together (regression line for all mice not shown; all p>0.05).

There were no significant correlations with age and click ABR wave latencies for KIAA KO or single WT mice (see figures 69 and 70). For both the slow and fast there were no significant correlation with age for any wave in both the KIAA KO, KIAA-Like KO and single WT groups after correction for multiple testing. Overall, whilst there may be some correlations with age the waves affected do not seem to be the same as the waves which were found to have a group difference and therefore differences in age cannot explain the observed group effects.

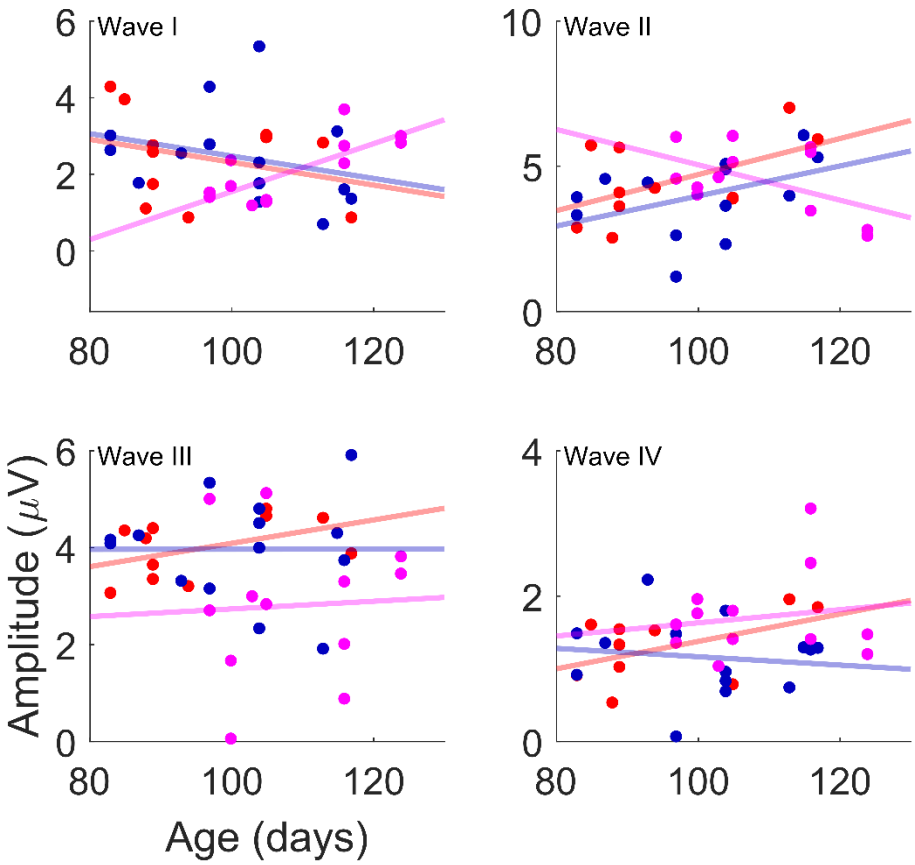

Figure 69: No significant effect of age on slow-click ABR wave amplitudes for KIAA-Like, KIAA or WT mice. Plots showing wave amplitude versus age for 80dB SPL click ABR waves (at the slow click rate) for KIAA, KIAA-Like single KO mice and age-matched WTs. Figure convention as in figure 75. No significant dependence of wave amplitudes on age for either group or all mice together (regression line for all mice not shown; all p>0.05).

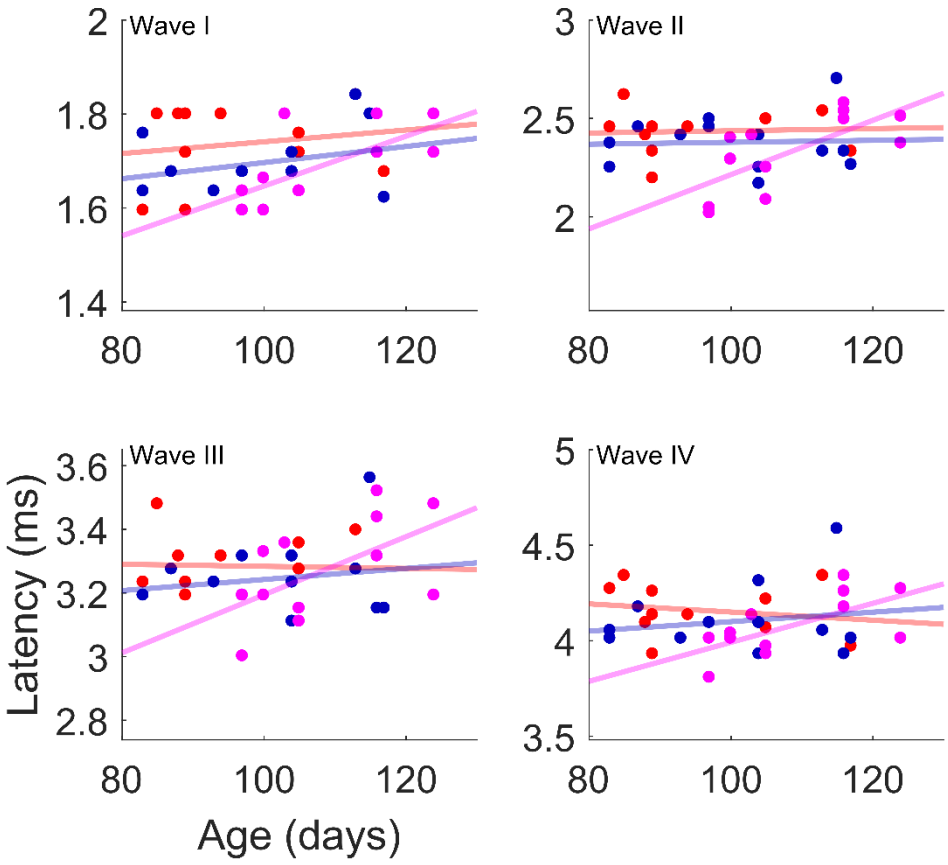

Figure 70: No significant effect of age on ABR slow-click wave latencies for KIAA-Like, KIAA or WT mice. Plots showing wave latencies versus age for 80dB SPL slow-click ABR (slow click rate) wave for KIAA, KIAA-Like single KO mice and age-matched wild-types at 80dB SPL. Figure conventions as in figure 75. No significant dependence of wave latencies the slow click condition for any group or all mice together after correction for multi-testing (regression line for all mice not shown; all p>0.0125).

Frequency specific deficit at or around 16kHz latencies for double KO mice

In order to investigate if the deficits in the double KO mice click ABRs were across frequencies or only at specific frequencies tone ABRs were recorded at 8, 16 and 32 kHz. Note, these stimuli were not recorded for single KO mice. There was a significant difference between double KO and wild-type at 16 kHz tone ABR for wave III amplitude and latency (figures 71 and 72; wave III amplitude: RM-ANOVA (group) p=0.031, F=5.342; table A7) but this was not significant after correction for multiple

testing. Indicating at 16 kHz there is no evidence of a deficit wave amplitudes in the double KO mice.

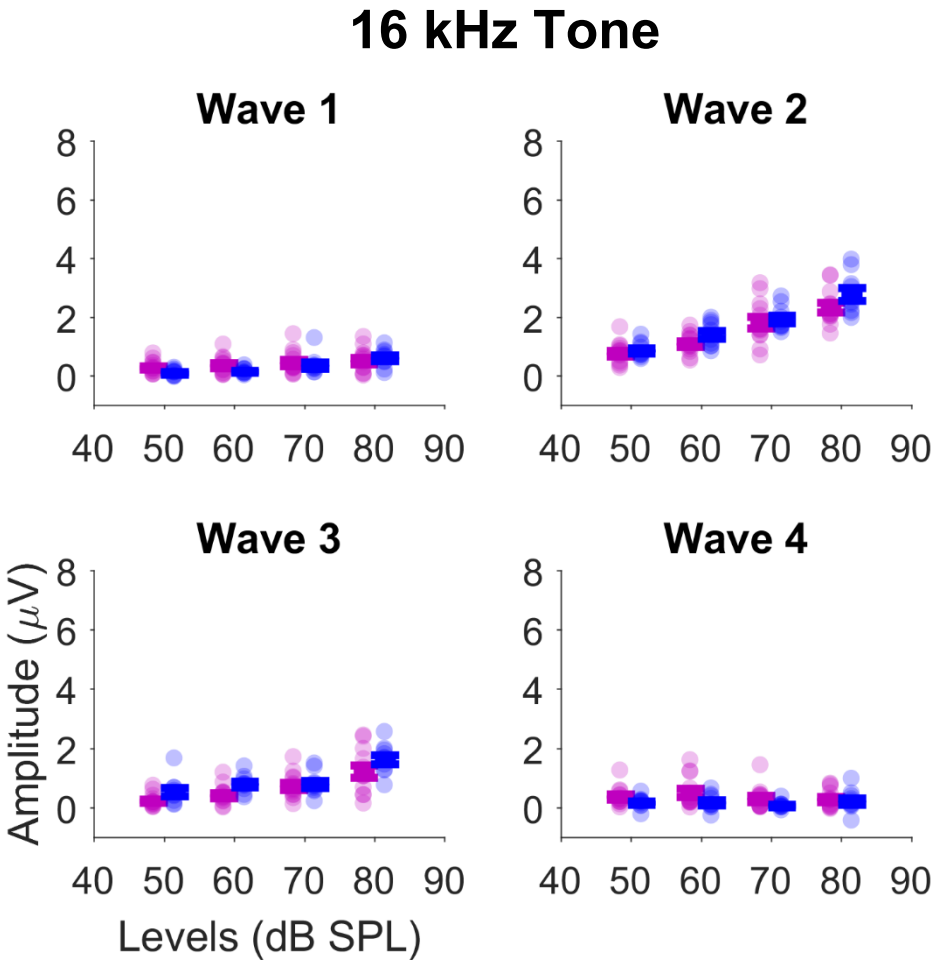

Figure 71: No significant difference between Double KO and WT for 16kHz tone ABR amplitudes. Conventions as in figure .. After correction for multiple testing there were no significant differences between double KO and WT (rmANOVA; all p>0.0125).

For wave latencies, however, there was a significant difference between double KO and WT for a 16kHz tone which is significant even after correction for multiple testing (figure 80; RM-ANOVA (group x level) p=0.0004, F=7.015; table A7) suggesting there may be a specific deficit at this done frequency in the double KO mice.

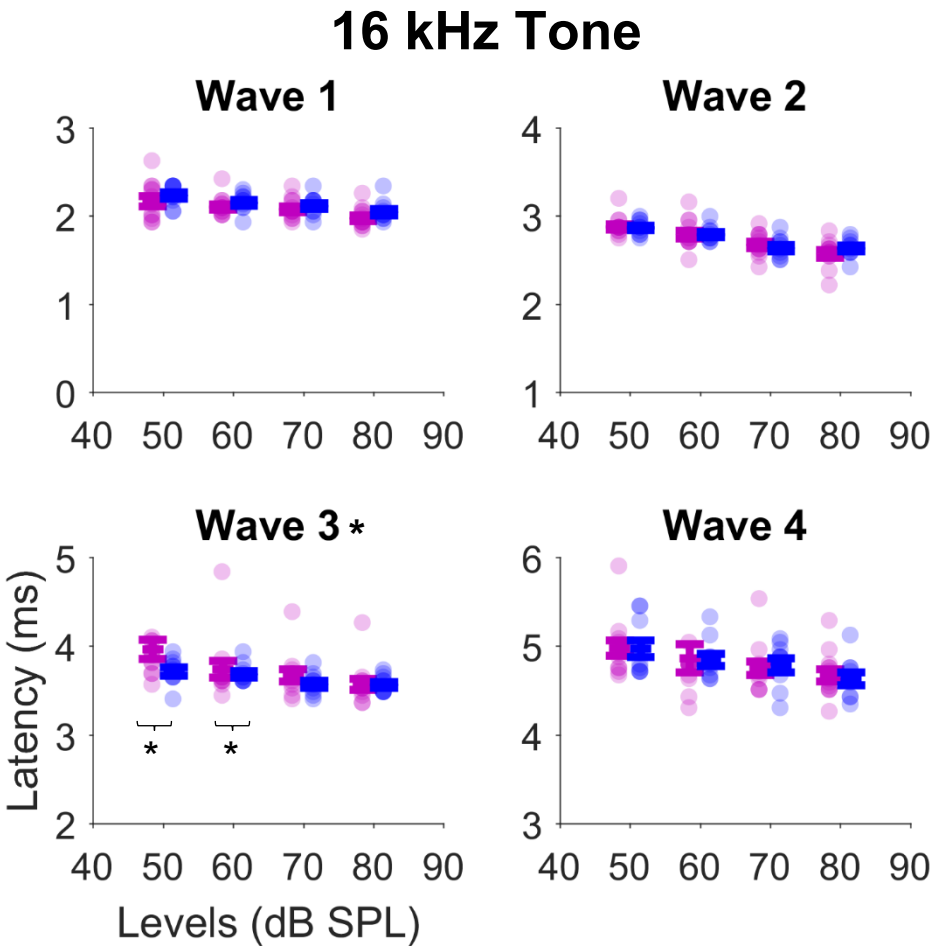

Figure 72: Double KO mice have significantly longer wave III latencies for 16kHz tones compared to WT mice. Repeated measure ANOVA significance after correction for multiple testing is indicated by star in the title (rmANOVA $p<0.001$). Significant post-hoc Tukey tests are indicated by stars and brackets on plots.

There was some weak evidence for a small change in wave IV latency at 8 kHz (figure 72; RM-ANOVA (group x level) $p=0.041$, $F=2.91$; table A7) although this is not significant after correction for multiple testing. There were no significant differences between double KO and wild-type mice for amplitudes or latencies of any wave for the 32 kHz tone ABR (RM-ANOVAs all p-values >0.05; table A7). These results indicate that there is some evidence for the a frequency specific component to the

wave III latency differences found in the double KO mice which arises at around 16 kHz but not 8 or 32 kHz.

No evidence from click ABR recordings for increased trials-by-trial variability in any of the KO mice.

It is possible that one explanation for the reduction wave amplitudes found in the double KO and single KIAA-Like KO mice may be a due to inconsistent firing in the

KO mice compared to WTs. One way to test for inconsistent firing is look at the standard deviation across trials. When we did this we found no differences in SD for any group. Indicating consistent firing across trials.

No evidence for asynchronous firing in any of the KO mice

To investigate whether the reduction in wave amplitudes found in the KIAA-Like single KO and double KO mice were due to a reduction in synchrony rather than a reduction in amount of firing we looked at the width of the waves since asynchronous firing may be evident in a broader, flatter wave that would lead to a reduction in wave amplitude. The wave widths were calculated as the distance from the wave peak to the following trough in order to avoid any potential bias in that may result due to the wave troughs being uneven on the y-axis. There were no significant differences for any KO group from wild-type animals on the half-widths of any waves (RM-ANOVA all $p > 0.05$) nor for any sound level on any of the *Post-hoc* Tukey tests. This may indicate the reduction in wave amplitudes arises from a reduction in the amount of firing rather than a reduction in the synchrony of firing.

One of the problems with the half-width analysis is that it relies on the assumption that the wave peak is symmetrically located therefore any change in the wave width would be seen in a change in the width of the last half of the wave however this may

not necessary be the case. It could be that a particular wave is wider but the peak of the wave is shifted over to the second half of the wave and so by only looking at the width of the second half of the wave any differences could be missed. In order to address this issue, we looked at the width of wave III which was where there was found to be the largest difference in wave amplitudes. To test this the half-width of the first part of wave III was calculated (i.e. distance from preceding trough to peak) and added to the half-width of the second portion of wave III (i.e. distance from the peak to the following trough). Again the results were not significant for any KO group compared to their corresponding wild-type animals (RM-ANOVA $p > 0.05$). This again indicates the reduction in wave III amplitude may arise from a reduction in amount of firing rather than a reduction in synchronous firing.

Double KO mice have increased ABR waves II and III latencies when click is preceded by noise compared to a click preceded by silence

In order to examine if there was any differences in the response to a click following a noise, which may indicate a similar temporal processing disorder as that seen in the BXSB/MpJ-*Yaa* mice described earlier, the responses to a 200ms noise followed by a click 20ms later and a further click 500ms after the end of the noise. The response of the click which is 500ms after the end of the noise i.e. proceeded by silence is then compared to the response of the click which is 20ms after the end of the noise ('probe delay'). If there were temporal processing or sound offset abnormalities which would affect this forward masking style task in the mutant mice compared to wild-type the ratio of probe to reference click would be disrupted.

In order to determine whether the effect of a click being preceded by noise ('probe click') has more of a deficit than a click preceded by silence ('reference click') the amplitude/latency of probe click versus the reference click was plotted for each

wave. A best fit line for the wild-type mice was then calculated and plotted. The number of KO amplitudes above the best fit line was calculated and a binomial cumulative distribution function calculated in order to determine any significant deviations.

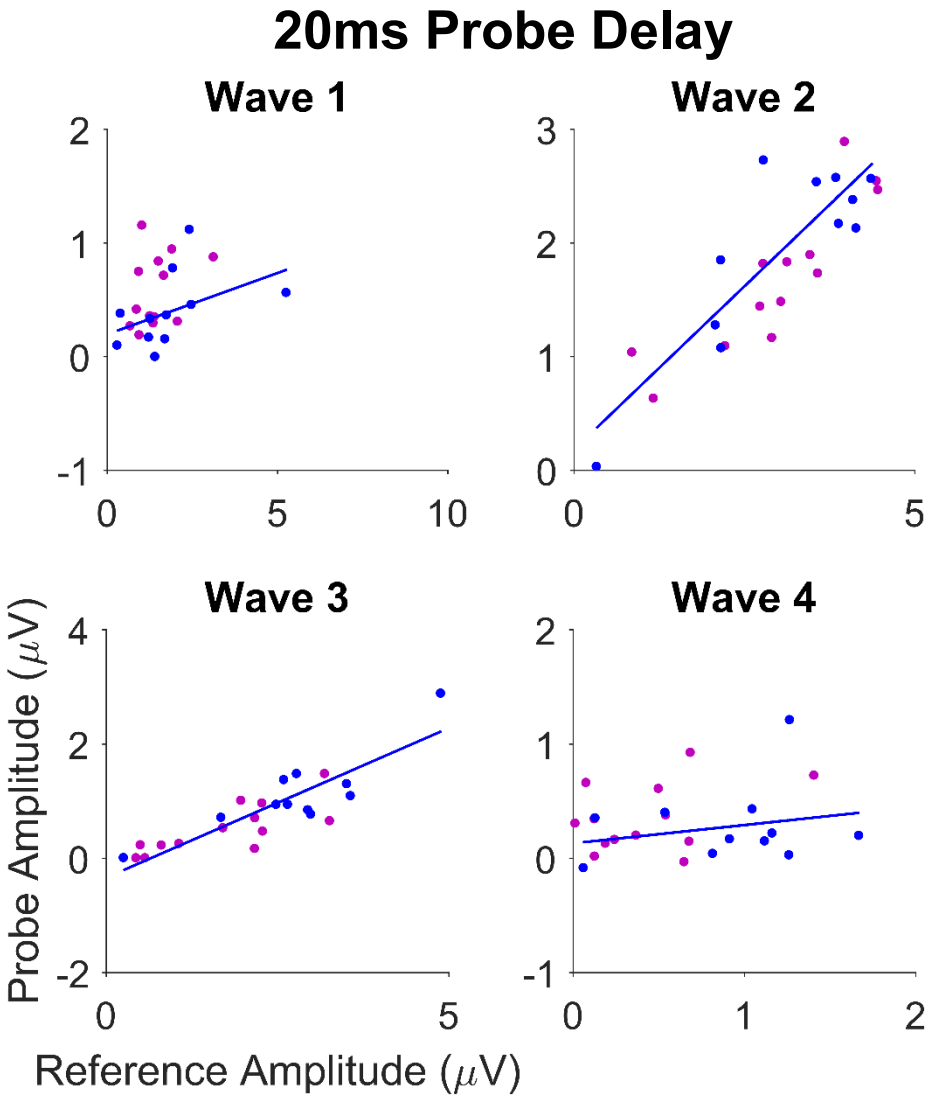

Figure 73: No significant difference between double KO and WT mice in the impact of a preceding noise on click wave amplitudes. The masker-probe stimulus (see figure 44) was used to test the effects of a preceding by noise on the ABR to a click. Binomial analysis (see text for details) was performed on the reference and probe click ABR wave amplitudes. There was no significant difference between double KO and WT mice in the effect of a preceding noise on the ABR to a click (binomial; all $p>0.05$). In other words the relationship between the amplitudes of the probe and reference clicks was similar for double KO and WT mice.

The double KO had no significant differences from wild-type mice for any wave amplitude (binomial test, all p>0.05; figure 73; table A9). This demonstrates that the double KO mice have no additional abnormalities in ABR wave amplitudes when a click is preceded by noise rather than a click preceded by silence compared to WTs.

The latency of waves II and III was found to have a significantly different number of double KO points below the WT line of best fit (p<0.01; figure 74; table A9). Analysis of the plots reveal most of the data points for the double KO mice are above the best fit line indicating a longer wave III latency compared to WTs.

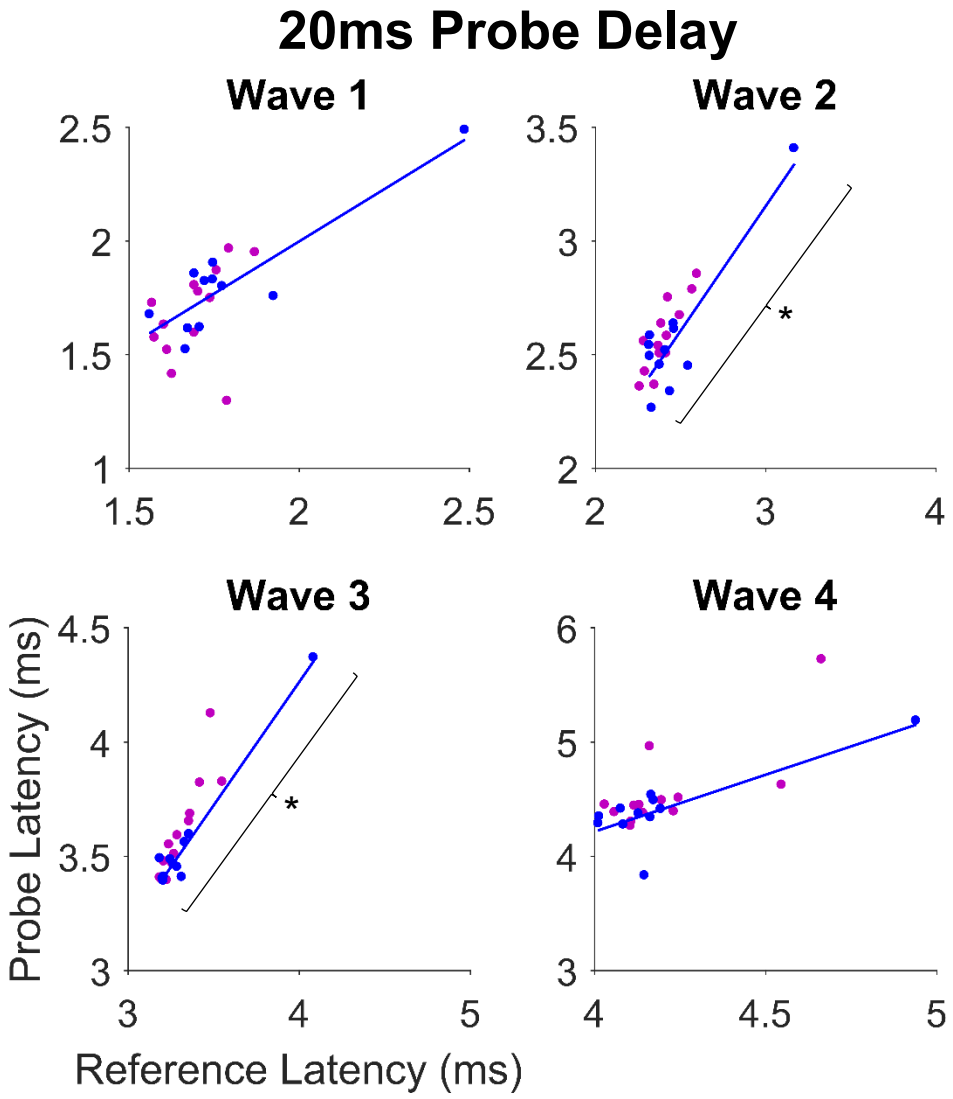

Figure 74: Significant difference between double KO and WT mice in the impact of a preceding noise on click ABR on wave II and III latencies (probe delay of 20ms). Figure conventions as in figure 82. There was a significant difference between double KO and WT mice in the effect of a preceding noise on the ABR to a click even after correction for multiple testing (binomial test; p<0.01).

These results indicate the double KO mice are more affected by a sound preceded by noise than wild-type mice in wave III of the ABR waveform where there appears to be a slow wave response in or around the cochlear nucleus and superior olivary complex.

KIAA-Like but not KIAA single KO mice have reduction in ABR wave II amplitude for clicks preceded by noise compared to clicks preceded by silence

KIAA-Like have a significant reduction in wave II amplitude to a click following noise compared to wild-types. KIAA-Like mice have a significantly different number of data points below the line of best fit (binomial test; p=0.006) for wave II amplitudes. Analysis of the plot (figure 75; table A10) reveals a larger number of points below the line of best fit for wild-types indicating a reduction in wave II amplitudes to a click following noise. No other wave amplitudes were found to be significantly different from wild-types.

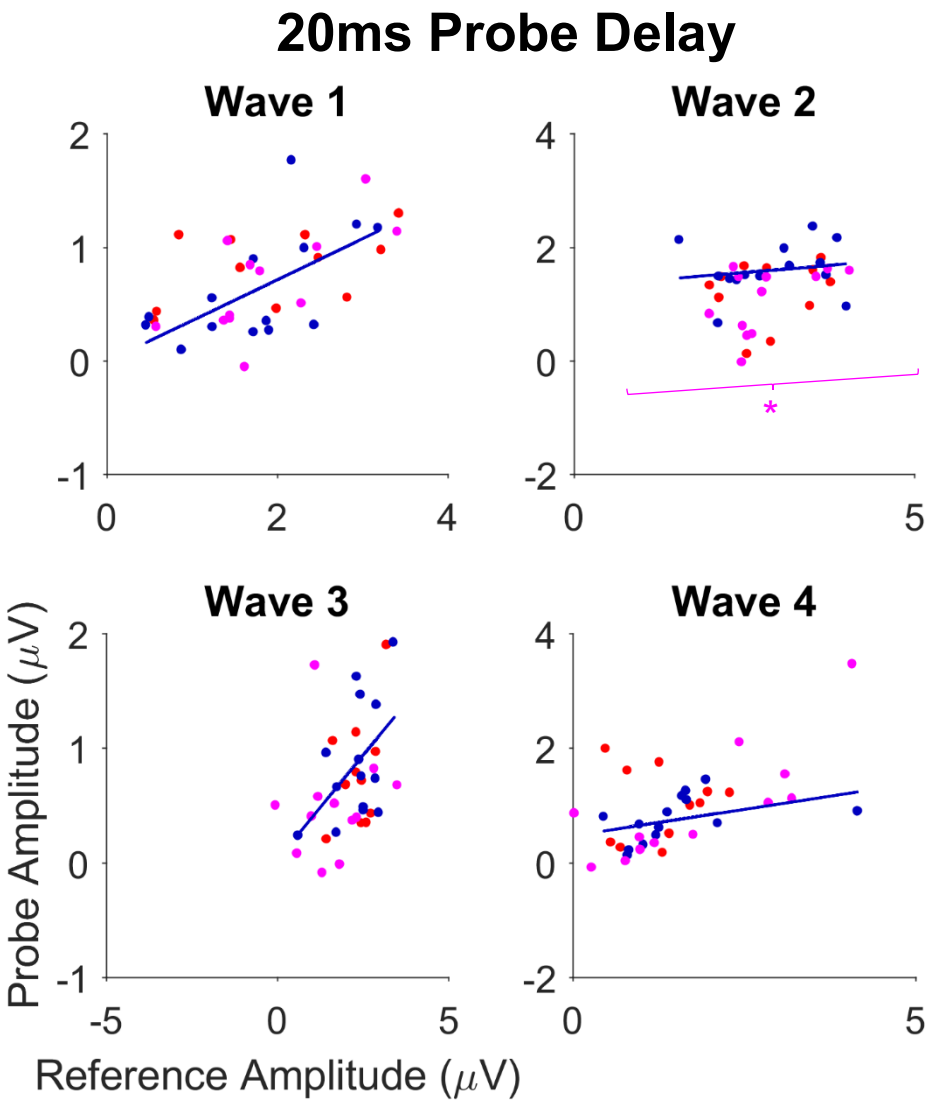

Figure 75: Significant difference between KIAA-Like KO and WT mice in the impact of a preceding noise on click ABR wave II amplitudes. Figure conventions as in figure 82 but for single KO mice. There was a significant difference between KIAA-Like KO and WT mice in the effect of a preceding noise on the ABR to a click even after correction for multiple testing (binomial test; $p<0.01$).

Furthermore, wave latencies were also found to not be significantly different from WTs (figure 76; table A10). These results suggest a specific deficit in wave II amplitude to a click following noise in KIAA-Like KO mice compared to wild-type mice.

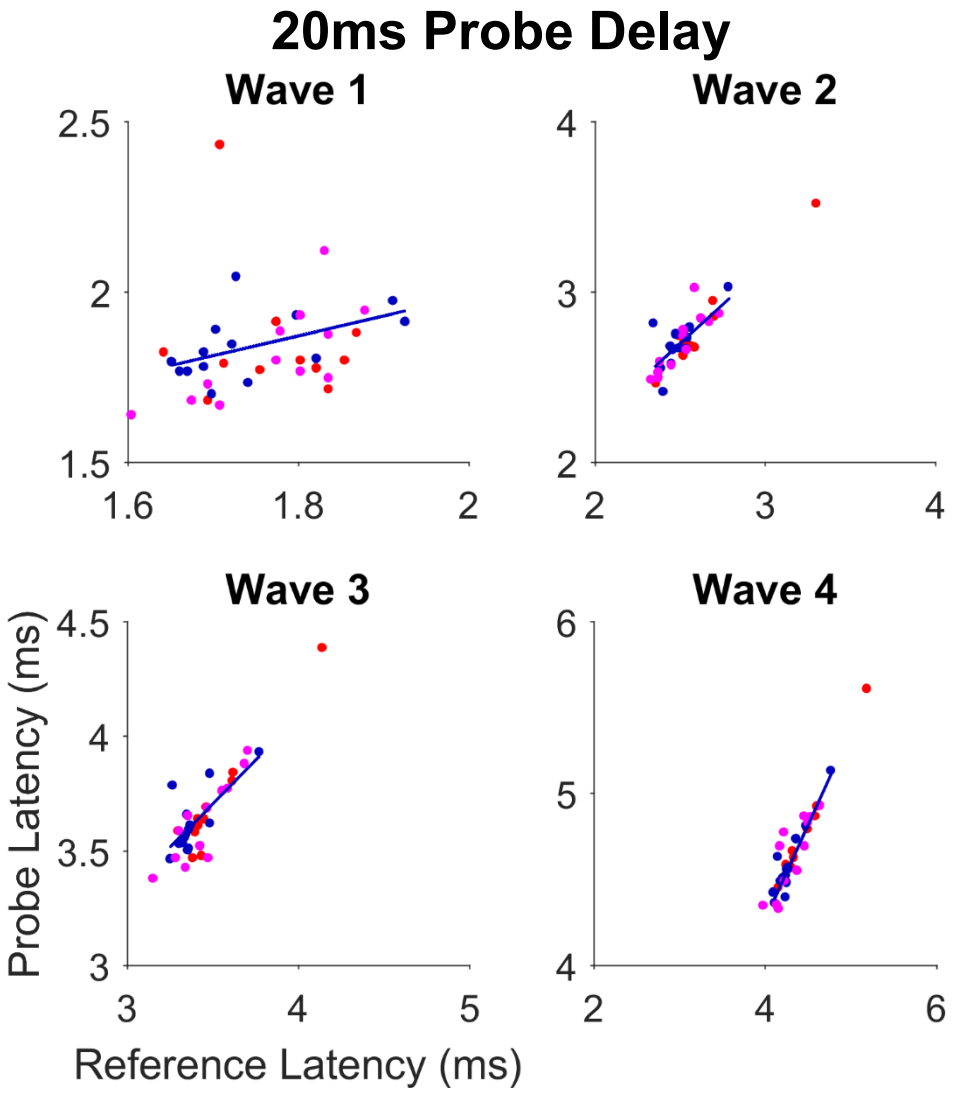

Figure 76: No significant difference between KIAA-Like, KIAA KO and WT mice in the impact of a preceding noise on click ABR wave latencies. Figure conventions as in figure 82 but for single KO mice. There was no significant difference between KIAA-Like, KIAA KO and WT mice in the effect of a preceding noise of the ABR to a click even after correction for multiple testing (binomial test; $p>0.05$).

The ABR response to a click following noise in the KIAA KO mice is similar to wild-type mice. For all wave amplitudes and latencies there were found to be no significant deviations in the number of KIAA KO data points from the wild-type line of the best fit (figures 75 and 76; table A10). These results indicate the KIAA KO have a similar ability to process a click following noise as wild-type animals.

ABR wave III abnormalities of click following noise in double KO mice confirmed for clicks 50ms but not 8ms following the end of the noise

For the double KO mice only the masker-probe stimuli was recorded with different probe delays. Note that responses to these stimuli were not recorded for either of the single KO mice. In the data described above a 20ms probe delay was used (i.e. the probe click occurs 20ms after the end of the noise). The additional probe delays used were 8ms and 50ms. The reference click all cases occurs 500ms after the end of the noise. This stimuli can be used to determine if the mice are more or less sensitive to gap length than wild-type animals. Analysis was performed with a binomial test on the number of points above the wild-type regression line was calculated for each probe delay as described in the previous section.

As for the 20ms probe delay condition, double KOs have impaired wave III amplitude and latency with a 50ms probe delay (figures 77 and 78; table A9). Using the 50ms probe delay there was found to a significant difference in the number of data points below the wild-type best fit line for both wave III amplitude and latency (binomial test; wave III amplitude $p = 0.003$ and wave III latency $p < 0.0002$). For the amplitude difference the plot indicates a larger number of data points below the best fit line suggesting a reduction in wave III amplitudes (figure 77; table A9) whereas for wave III latency the plot shows a larger number of points above the best fit line indicating a longer latency for the double KO mice compared to wild-types (figure 78; table A9). This is consistent with the 20ms probe delay described in the previous section where the double KOs had a longer wave III latency compared to wild-types.

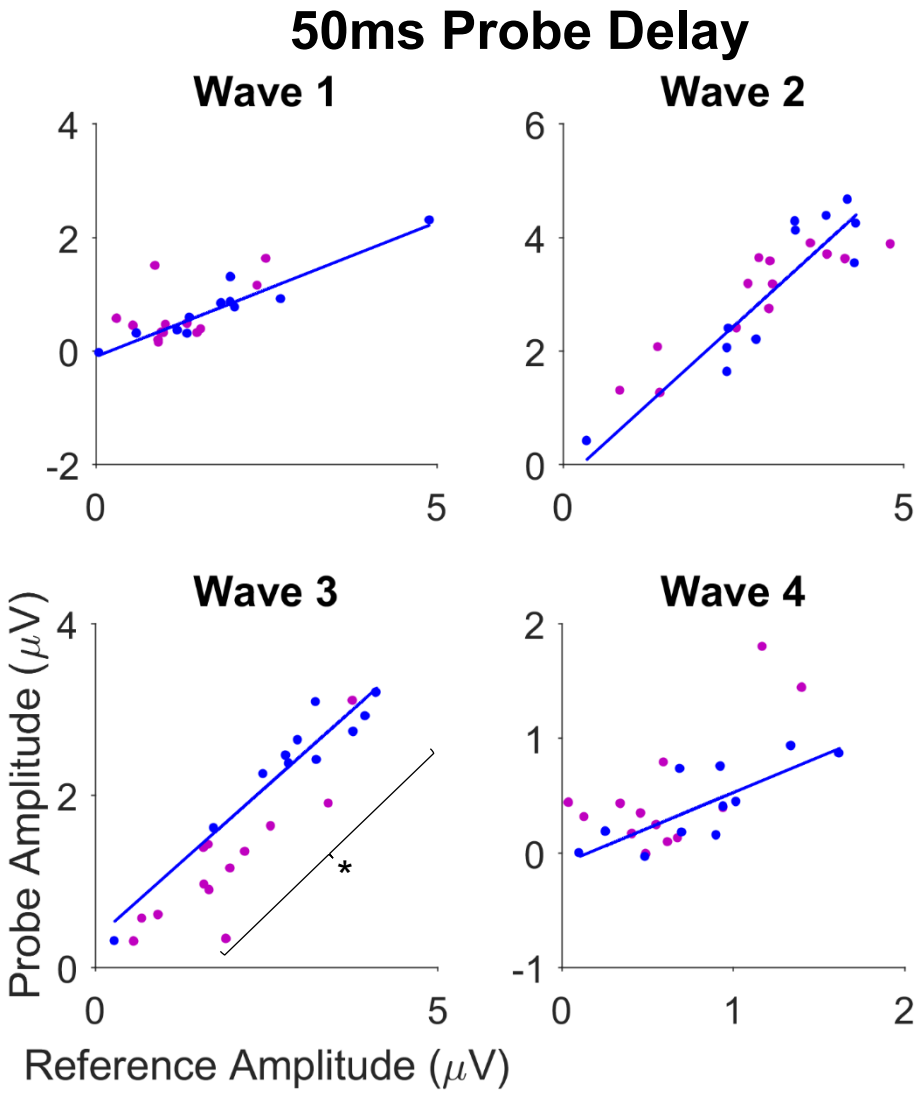

Figure 77: Significant difference between Double KO and WT mice in wave III amplitude for a click preceded by noise (50ms probe delay). Figure conventions as in figure 82. There was a significant difference in wave III ampltidues between double KO and WT mice in the effect of a preceding noise on the ABR to a click even for the longer probe delay, even after correction for multiple testing (binomial test; $p<0.01$).

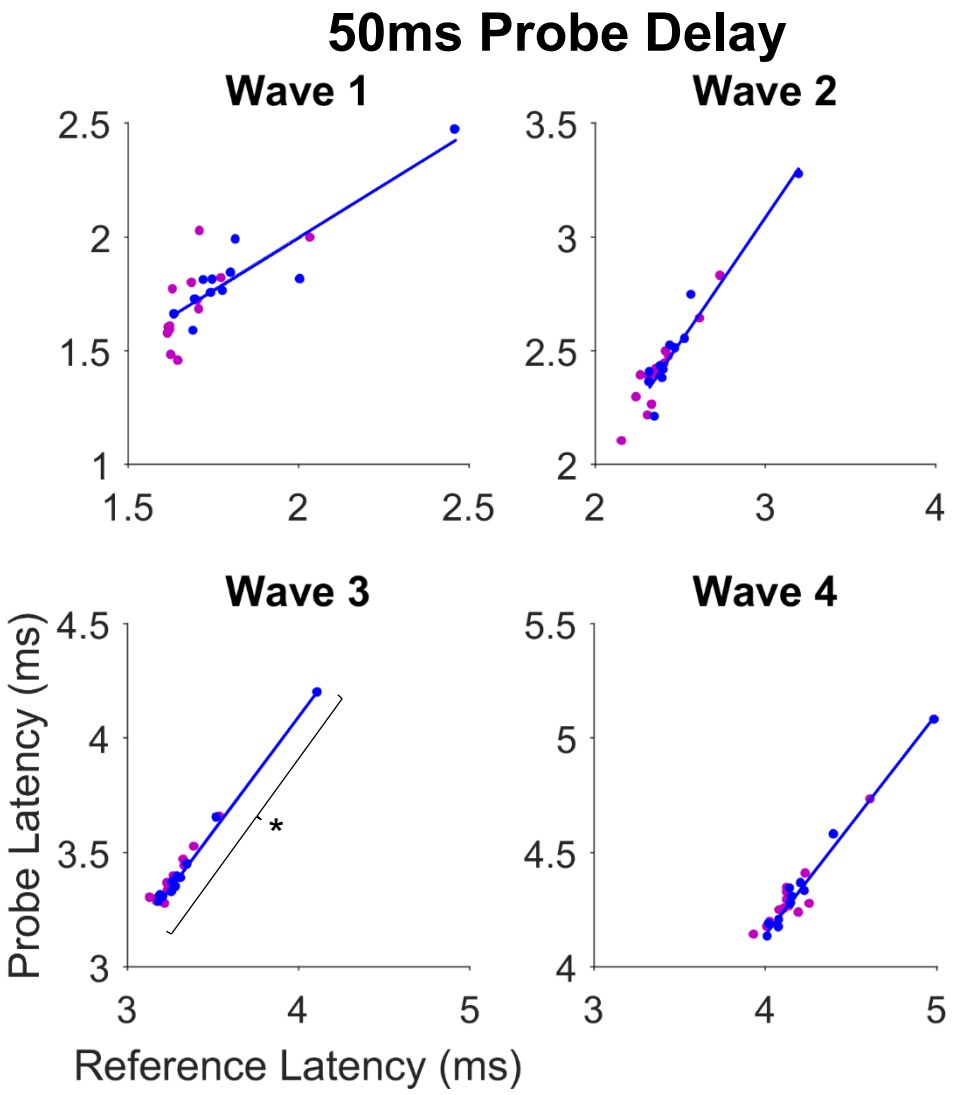

Figure 78: Significant difference between double KO and WT mice in the impact of a preceding noise on click ABR wave II latencies (probe delay of 50ms). Figure convention as in figure 82. There was a significant difference between double KO and WT mice in the effect of a preceding noise on the ABR to a click at the longer probe delay, after correction for multiple testing (binomial test; $p<0.01$).

With a 8ms probe click delay there was no significant difference for either wave amplitude or latency for any wave (data not shown). Therefore with a 8ms probe click delay the double KO animals appear to similar to wild-type animals but this may be due to the small amplitudes in the 8ms condition.

Alternative analysis of click following noise ABR recordings reveals no difference in ABR waveform for any KO mice group compared to WT for a click preceded by noise

The above analysis suggests a difference in the probe click in addition to any differences that exist in the reference click between mutants and controls however the analysis used relies on deviations from the line of best fit for the wild-type animals which means the analysis is based on an estimate rather than direct comparison between KO and wild-type animals. In order to try to address this issue, a further set of analysis was performed by normalising the probe click amplitudes/latencies by dividing by the reference click amplitudes/latencies. This then allows direct statistical tests to be used (in this case a rank-sum test for each wave) between KO and wild-type data.

Figure 79 shows the normalised probe click amplitudes for wave I-IV for the single KO mice. Similar to the results from the binomial tests for the KIAA single KO mice there were no significant differences for the normalised probe click amplitudes for any wave tested. For the KIAA-Like mice in the binomial tests wave II amplitudes were significantly different from wild-types and when testing the normalised probe click amplitudes for wave II were significantly different from wild-type mice (Wilcoxon rank-sum p= 0.029; table A10), however this is not significant after correction for multiple testing. This suggests that in KIAA-Like mice ABR wave II amplitudes are not affected by the precedence of noise than wild-types mice.

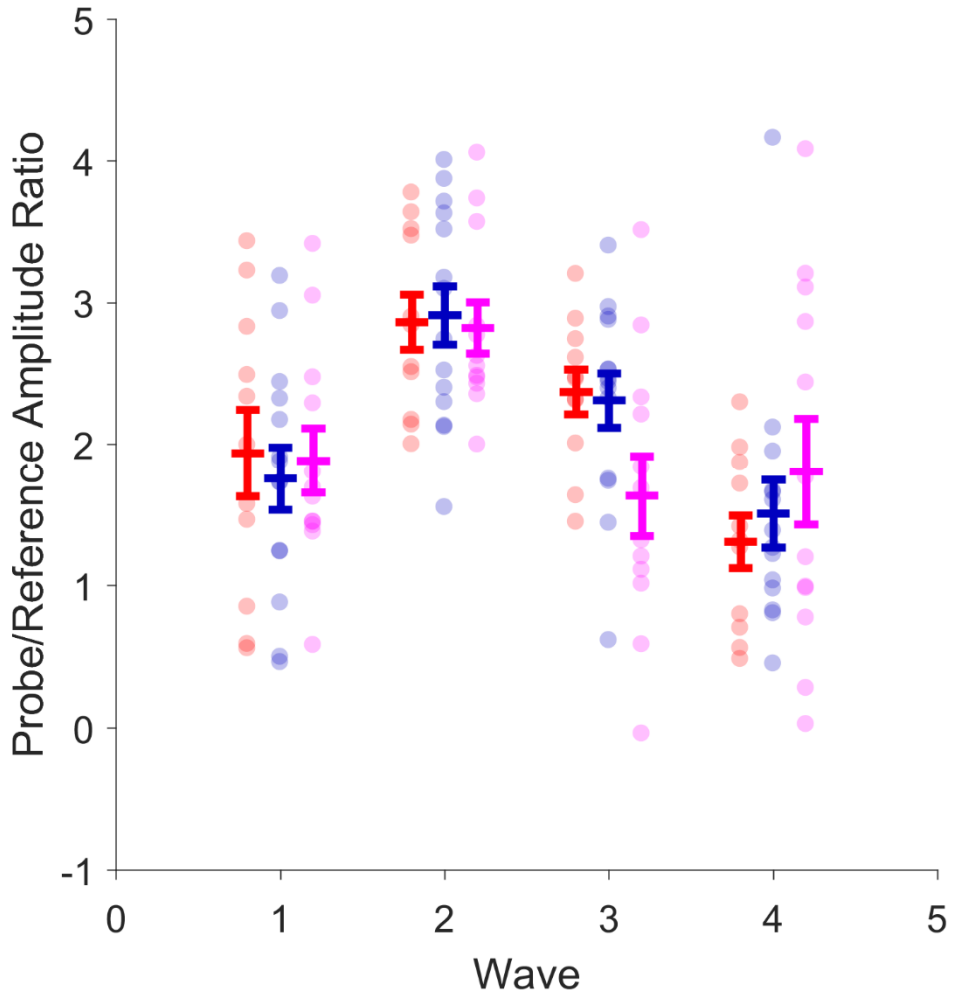

Figure 79: No significant difference between mutant and WT mice in the impact of a preceding noise on click ABR wave amplitudes for a 20ms probe delay. Horizontal lines and error bars indicate normalised mean +/- SE probe click amplitudes obtained from masker-probe stimuli for 20ms probe delay for KIAA and KIAA-Like single KO mice together with age-matched WTs as indicated on plot, by. KIAA KO mice displayed in red, KIAA-Like in magenta and WT in dark blue. Individual animal means are represented by dots. There was no significant difference between mutant and WT mice in the effect of a preceding noise of the ABR wave amplitudes to a click with a 20ms probe delay, after correction for multiple testing (ranksum; p>0.0125).

For both the KIAA KO and KIAA-Like KO mice there were no significant differences from wild-type mice for waves I-IV latencies when the click was preceded by noise (figure 80; table A10). These findings are consistent with the binomial tests in the previous section indicating the latency of the ABR waves does not seem to be affect by the precedence of noise in the single KO mice.

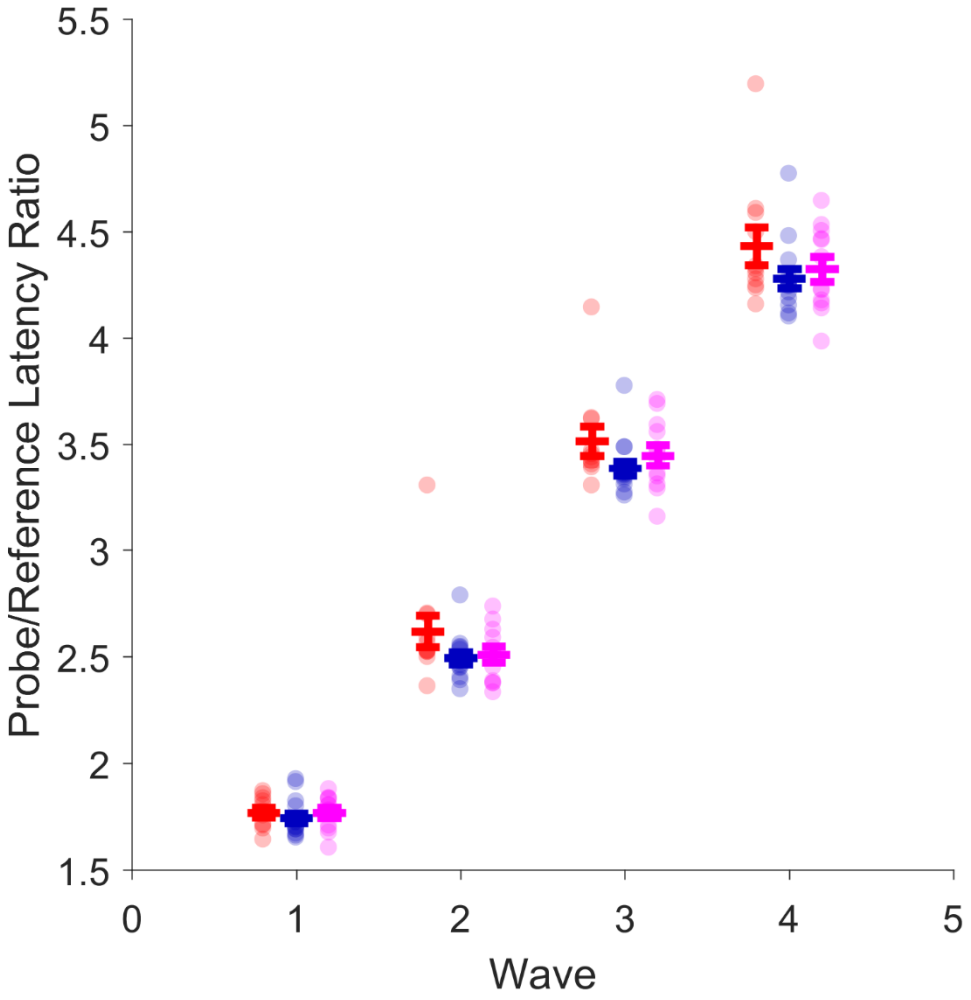

Figure 80: No significant difference between mutant and WT mice in the impact of a preceding noise on click ABR wave latencies for a 20ms probe delay. Figure conventions as in figure 90. There was no significant difference between mutant and WT mice in the effect of a preceding noise on ABR wave latencies to a click with a probe delay of 20ms, even before correction for multiple testing (ranksum; $p>0.05$).

For the double KO mice, normalised wave amplitudes for all probe delay were not significantly different between double KO and wild-type mice (rmANOVA p>0.05; figure 81; table A9).

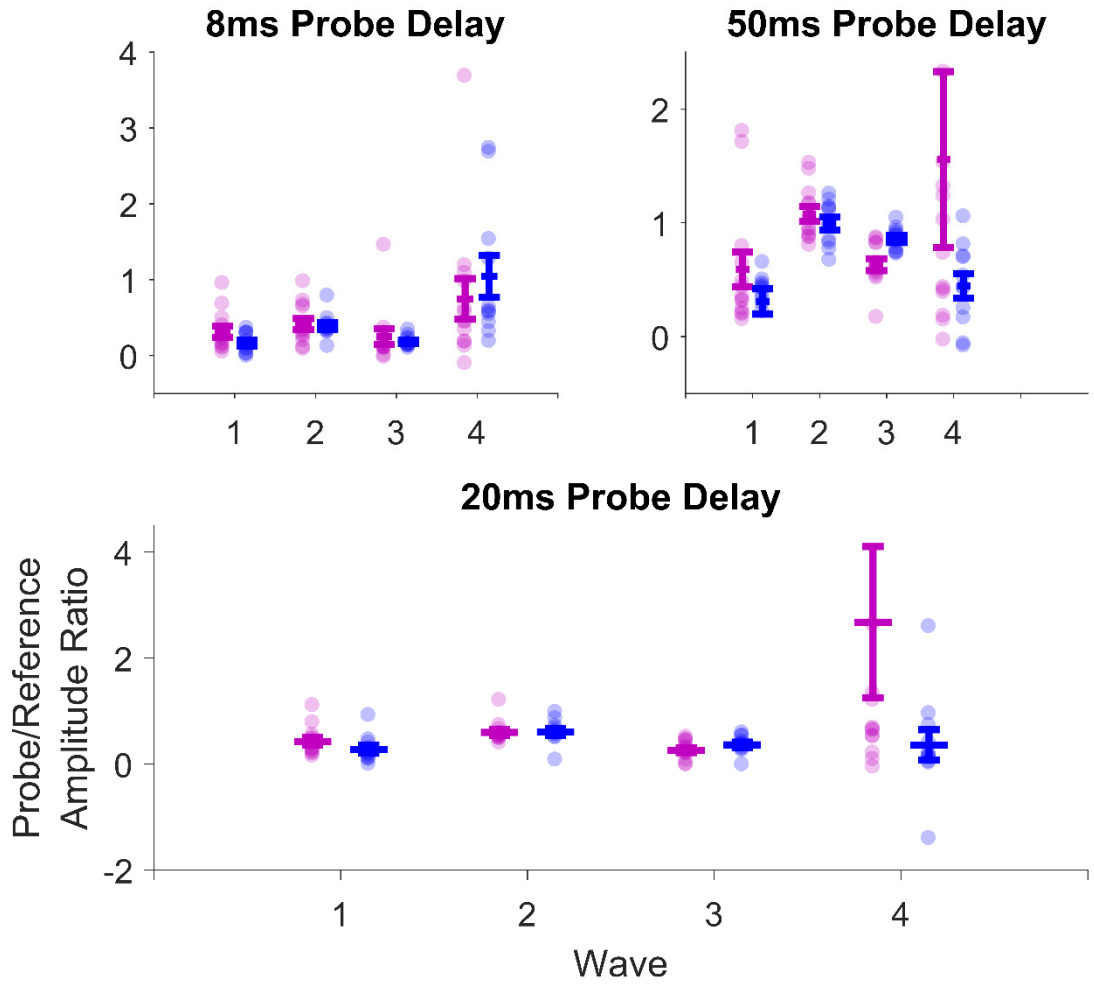

Figure 81: No significant difference between double KO and WT mice in the impact of a preceding noise click ABR wave amplitudes for either a 8ms, 20ms or 50ms probe delay. Figure conventions as in figure 90 but for double KO (purple) and their age-matched WTs (blue). There was no significant difference between mutant and WT mice in the effect of a preceding noise on ABR wave amplitudes to a click at any probe delay, even before correction for multiple testing (rmANOVA; p>0.05).

For wave latencies the binomial tests revealed a significant difference for waves II and III for 20ms probe delay (waves II and IV with outlier removed) and wave III for the 50ms probe delay. For the normalised probe latencies the statistical tests revealed no significant difference between double KO and wild-type mice for wave

latencies for any probe delay (rmANOVA; all p>0.0125; see figure 82; table A9). These results indicate there is no difference in the response to a click following noise compared to a click following silence between double KOs and WTs.

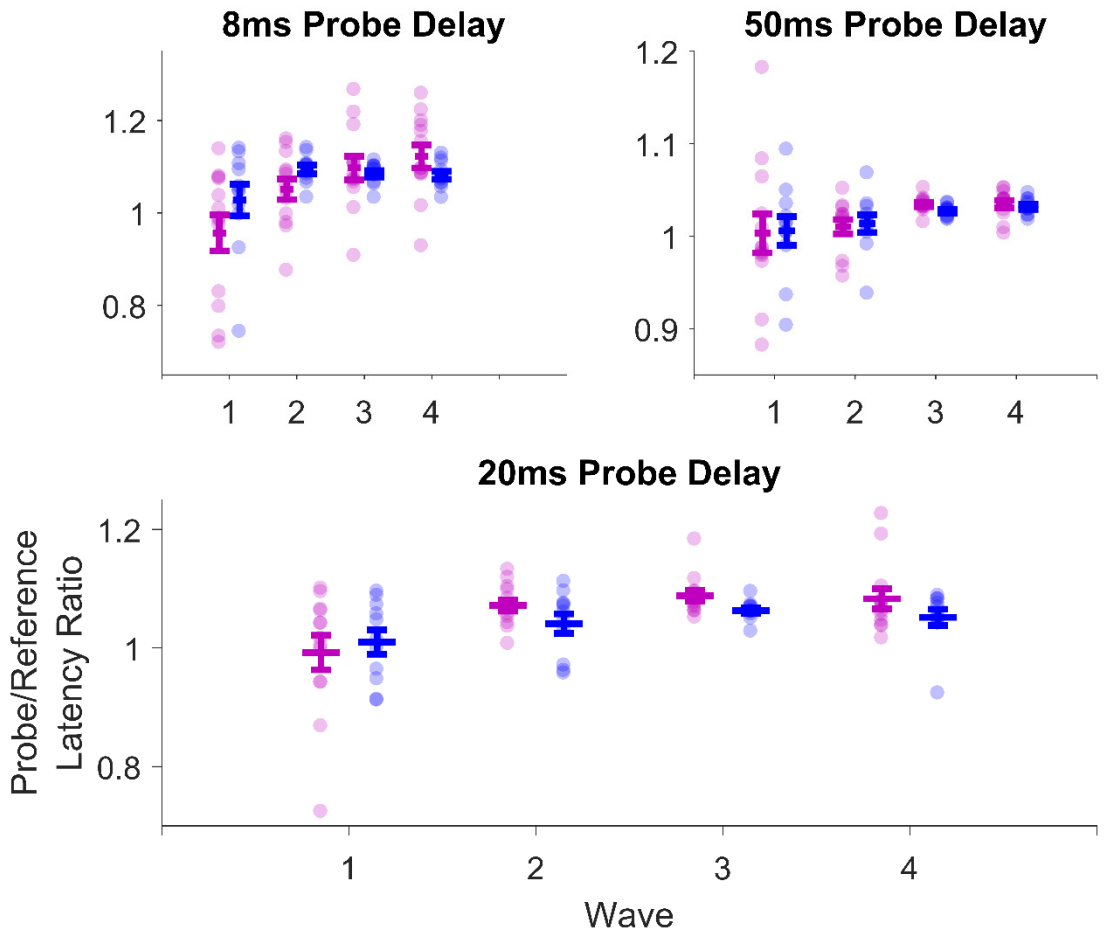

Figure 82: No significant difference between double KO and WT mice in the impact of a preceding noise on click ABR wave latencies for either a 8ms, 20ms or 50ms probe delay. Figure conventions as in figure 90 but for double KO mice and their age-matched WTs. There was no significant difference between mutant and WT mice in the effect of a preceding noise on ABR wave latencies to a click at any of the probe delays, after correction for multiple testing (rmANOVA; p>0.0125).

Discussion

The original aim of the data presenting in this chapter was to identify if the KO of genes, which have been associated with dyslexia, KIAA and KIAA-Like, has any impact on auditory processing. The results contained in this chapter demonstrate the KO of either KIAA and/or KIAA-Like genes does not affected hearing per se, as the ABR click thresholds were similar in all KO models to WT thresholds. The results did show, however, there were suprathreshold changes in both double KO and KIAA-Like KO mice for click ABRs. Moreover, double KO mice had frequency specific changes around 16kHz but tone ABRs were not recorded for the single KO mice. The single KO mice results suggest there is no temporal processing problems in these mice as the difference in click ABR amplitudes was found only in the slow-click (not the fast-click) condition. A masker-probe initially reveal some possible additional differences in the double KO (waves 2 and 3 latencies for 20ms probe delay and wave 3 latency for 50ms probe delay) and KIAA-Like KO mice (wave 2 amplitudes) compared to WTs but these results were not confirmed when a stricter analysis was performed using ratios of the reference and probe click amplitudes/latencies. So the results currently indicate there is no additional differences to a click preceded by noise versus a click preceded by silence.

The double KO mice were found to have reduced wave 1 amplitudes compared to WT mice on click ABRs was as the KIAA-Like KO mice were found to have reduced wave 3 amplitudes but this was only significant when using a longer interval between clicks. So the double KO mice seem to have abnormality arising from the auditory nerve whereas the KAA-Like mice have a more subtle abnormality around the superior olivary complex/trapezoid body (Henry, 1979). This suggests the KO of both KIAA and KIAA-Like genes leads to a more severe phenotype so although the

KIAA KO mice did not show abnormalities the results of the double KO mice indicate there may be some compensatory mechanism of the *Kiaa0319* protein in the KIAA-Like mice.

For the KIAA KO mice a wave 2 amplitude difference was found but since the mean was found to vary in direction across sound levels and as there were no significant results for the post-hoc Tukey tests, this suggests this results may not be reliable. Further study is required to confirm this, for example using a larger number of mice in order to increase statistical power.

The click ABR wave latencies were unaffected by the KO of the KIAA and KIAA-Like genes so KO of these genes does not produce or a slower or more sluggish auditory response. Furthermore, the fast-click condition did not produce more significant deficits than on the slow-click condition suggesting there is no temporal processing deficits in the single KO mice. Although this is complicated by the fact that the ABR signal is likely to be more reliable in the slow-click condition where the auditory system has had more time recover in-between clicks. Also the slow-click condition was not recorded for the double KO so it is unknown if these mice would have shown a temporal deficit problem and this a further reason to record this data in any future experiments. When analysing factors which may have confounded the ABR results it was found that any differences in gender or age cannot explain the differences identified in the click-ABR results.

For the double KO mice tone ABRs were recorded and reveal a specific deficit in 16kHz tone ABR wave 3 latency but not for 8kHz or 32kHz tone ABRs. This result suggests a frequency specific deficit at or around 16kHz however it should be noted that the 16kHz tone is known to produce a stronger ABR signal in mice so it is

possible that other tone frequencies are affected but cannot be identified in the current data set given the limitations of the ABR measurement. However, the click latencies were found to be similar to WT in the double KO mice and as a click is across all frequencies, this indicates that there is a frequency specific deficit in the latencies even though it might not be entirely restricted to 16kHz. This result indicates for some frequencies there is a more delayed ABR wave i.e. the neurons do not have a reduced response but have a slower response for certain frequencies. If this is the case then it may explain the click ABR amplitude changes in the double KO mice as a delayed response at certain frequencies would be expected to produce a wider ABR wave and therefore a lower amplitude. An attempt to investigate this possibility was performed using the half-width of the ABR waves. This analysis did not produce any significant results but also does not fully rule out the possibility as the half-width measurement relies on various assumptions such as the peak of the ABR wave is symmetrically located and the location of the trough of the ABR wave. Future studies should investigate this intriguing finding further, ideally using a more direct measure such as collecting FRAs using extracellular recordings around the level of the brainstem.

The masker-probe stimuli was used to determine whether any further differences in the KO mice occurred when a click was preceded by noise versus a click preceded by silence such as that found in the BXSB mice discussed in early chapters. Initial analysis of this data using a Binomial analysis based on the number of KO point above the WT best-fit line indicated there may be some differences in wave 2 and 3 latencies for double KO mice and wave 2 amplitudes for KIAA-Like KO mice when using a 20ms probe delay. These results however were not confirmed when using analysis of the probe click/reference click ratios. The lack of statistical significant

results for the ratio analysis may be due to a lack of power when dealing with such small changes and this hinted of by the consistency of having a wave 3 latency change for both 20ms and 50ms probe delays. Different probe delay were not recorded for the single KO mice and therefore it is unknown if the KIAA-Like result is also consistent across probe delays. Future studies should investigate these initial results further using a more direct measure such as extracellular recordings which would be more likely to identify small differences than the ABR.

A recent paper has linking KIAA gene to problem in auditory brainstem processing in humans confirms the finding in this chapter (Neef et al., 2017). Likewise in humans speech in noise performance has been correlated with auditory brainstem responses (Anderson et al., 2013). And in turn speech-in-noise performance has been linked with ability on phonological task (White-Schwoch et al., 2016). So the link to humans seems strong. It will be important in future experiments to look at the brainstem with more direct measures such as intracellular and extra cellular recordings in order to start look for the specific locations and mechanisms underlying the observed deficits.

Overall, the work presented in this chapter has identified some initial differences in auditory processing in the lower part of the auditory pathway in both double KO and KIAA-Like KO mice with KIAA KO mice either not affected or so minimally affected it cannot be detected by indirect measurement like the ABR. This not only fulfils the original aim of these experiments but offers potential interesting areas of future study such as whether there is any compensatory mechanism of the *Kiaa0319* protein in addition to a more direct electrophysiological method such as extracellular recordings. An alternative would be intracellular recording however these would be more useful after an extracellular electrophysiological study has refined the exact

brainstem nuclei affected as can be achieve with multi-electrode extracellular recordings.

Overall conclusions and suggestions for future work

The mechanisms of how the brain detections of very short gaps between sounds, such as those between phonemes in speech, are not well understood. Furthermore a number of studies have indicated people with neurodevelopmental disorders may have deficits in gap detection (Bhatara et al. 2013; Van Ingelghem et al. 2001; Phillips, Comeau, and Andrus 2010) however the results of these studies controversial (Rosen, 2003). Most of this controversy comes from the limitations of experiments in humans which leads to the use of animal models. The principal aim of the work presented in this thesis was therefore to investigate auditory processing, specifically gap detection, in mouse models of neurodevelopmental disorders.

Firstly we investigated the BXSB/MpJ-Yaa mouse model which had previously been shown to have differences in gap-detection thresholds for behavioural statle responses to this stimuli (Clark, et al., 2000) and neurally in auditory thalamus (Anderson & Linden, 2016; Frenkel et al., 2000) between mice with ectopias and mice within the same strain without ectopias. We set out to determine the histological details of ectopias, looked for histological analogies of the observed neural differences in MGB and investigated whether there are any further electrophysiological abnormalities between ectopic and non-ectopic mice in lower areas of the auditory pathway. These are all areas of study which have not, to date, been studied in the BXSB mice but have been demonstrated in other animal model of neurodevelopmental disorders.

Secondly, we made principle studies into auditory processing in the lower parts of the auditory pathway in knock-out mouse models of KIAA and KIAA-Like genes

which have been identified as key genes involved in dyslexia in humans. As for the experiments in the BXSB this is an area of study that has not been investigated in this mouse model. We performed an initial screen of auditory processing electrophysiolgically using ABRs to look for differences in these mice.

In Chapter 1, we demonstrate approximately half the male mice develop cortical abnormalities referred to as ectopia in 50% of male mice and are located in or around motor cortex. From immunohistochemical experiments on the ectopic they contain and mix of neurons and glia and seem to form from a bursting up of cells into the upper layers of the cortex as has previously been suggested in other animal models.

In Chapter 2 we found no difference between ectopic and non-ectopic in MGB cell density or volume size together with no difference in auditory cortex layer thickness. These two negative results argue against of the electrophysiological gap-detection difference in MGB arises from MGB or auditory cortex although there could be other more subtle histological differences in these areas between ectopic and non-ectopic mice such as in synapse numbers.

Recordings from IC (Chapter 3) revealed differences in gap detection between ectopic and non-ectopic mice are found in primary IC cells (which are likely from central IC) as was found in MGB. However, the difference in IC is the ectopic mice to have shorter gap-detection thresholds compared to the non-ectopic mice whereas in MGB the ectopic mice had longer gap-detection thresholds than non-ectopic mice. Whilst this might initially seem to be a contradictory finding, it does demonstrate the ectopic mice to have abnormal processing of short gaps in noise in both IC and MGB. The difference in results may arise, for example, from a difference inhibitory

connections between the IC and MGB but further work is need to investigate this theory.

Consistent with the idea of the difference arising between IC and MGB are the results from chapter 3 which showed no difference between ectopic and non-ectopic mice in ABR measurements for either threshold or suprathreshold measurements even when using the masker-probe stimuli which has been shown reveal similar differences in MGB extracellular recordings to the gap-in-noise stimuli. This suggests at the level of the auditory pathway below IC function similarly in ectopic and non-ectopic mice. Although it should be noted that ABR measurements are an indirect measure of auditory processing and therefore it is likely that any subtle differences in firing such as from a single, small nuclei, would not be detected by this method of recording.

Together these results suggest a possible origin for the gap-detection differences between ectopic and non-ectopic to arise either in the IC itself. Consistent with this idea is the finding that the difference in gap detection is found in central IC which feeds into ventral MGB which is where the largest difference in gap detection in MGB was found. One limitation of linking the results of these two studies is that they were performed in different animals by different researchers and using different electrodes and stimuli parameters (see chapter 3 discussion for more detailed explanation). Future experiments should therefore address this issue for example by extracellular multi-unit recording from IC and MGB in the same animal to determine if the gap-detection thresholds differ in these two areas in the same animal.

A further problem with the interpretation of the results for BXSB mice is the issue that there is only currently one study, from 20 years ago, which has looked for behavioural differences between ectopic and non-ectopic for gap-in-noise stimuli (Clark, et al., 2000). It is therefore of necessity to replicate the findings of this study. If the experiment suggest above for recording in both IC and MGB were performed in awake animals then potential behaviour data could also be obtained from the same animals which would allow more direct linking of the bhaviour and electrophyioslogy results than is currently able.

In terms of future histology experiments since a large number of the histology work presented here has produced negative results the primary focus of future experiments should be on understanding the differences between ectopic and non-ectopic using electrophysiology. However if the differences in gap-detect thresholds in IC and MGB were confirmed in the same animal future histological experiments could investigate the connections between IC and MGB, possibly using immunohistochemistry to look at inhibitory connections.

Future experiments could also consider single cell, intracellular recordings since the currently results are limited by fact that the neural recordings were extracellular recordings and therefore actually each recording may be from a number of cells rather than single cells. This may also reveal extra information on the relevance of the result that offset responses appear reduced in the ectopic animals in both IC and MGB. The original hypothesis in the MGB study (Anderson and Linden, 2016) had been that the reduction in offset responses could explain the gap-detection deficit in this area but the findings from IC suggest this may be more complicated that original thought but may reveal further understanding of the role of offset responses in the brain which is currently limited.

Whilst the results from BXSB/MpJ-Yaa mice do not suggest any deficit in auditory processing in area of the early auditory pathway, the results from Chapter 5 on KO mice for dyslexia candidate genes KIAA and KIAA-Like suggest in other animal models of neurodevelopmental disorders, disruption to auditory processing in early parts of the auditory pathway is possible. In particular the results showed the most reliable suprathreshold wave differences can be found in double KO mice for both candidate genes, suggesting both genes may play a role in auditory processing in the early parts of the auditory pathway even though we found deficiencies only in the KIAA-Like single KO mice. Furthermore, since the ABR revealed all mice to have similar ABR thresholds this suggests that hearing level is similar in both the KO and WT mice. More work is needed to investigate these initial insights into disrupted auditory processing in these mice models, perhaps using extracellular recordings within the auditory brainstem. A good candidate for an initial electrophysiolgical study would be multi-unit recordings around the super olivary nucleus/trapezoid body (which produced differences in both double KO and single KIAA-Like KO mice compared to their respective WTs) to determine if the ABR results can be replicated using a more direct method of neural activity.

Overall, the work covered in this thesis provides a contrast between a mouse models of spontaneously occurring cortical anatomical abnormalities in neurodevelopmental disorders. Which show disrupted auditory processing in higher areas of the auditory pathway. Whereas, genetic KO of neurodevelopmental revealed disrupted auditory processing in lower parts of the auditory pathway. Together this work may suggest that in humans neurodevelopmental disorders can have multiple origins for auditory processing dysfunction which may explain some of the controversies and conflicting results in studies in this area.

References

Aghakhani, Y, Kinay, D, Gotman, J, Soualmi, L, Andermann, F, Olivier, A, and Dubeau, F. 2005. “The Role of Periventricular Nodular Heterotopia in Epileptogenesis.” Brain : A Journal of Neurology 128 (Pt 3): 641–51. doi:10.1093/brain/awh388.

Akil O, Oursler AE, Fan K, Lustig LR. 2016. “Mouse Auditory Brainstem Response Testing.” Bio Protoc. 2016 Mar 20;6(6). pii: e1768. doi: 10.21769/BioProtoc.1768.

Anderson, LA, Wallace, MN, and Palmer, AR. 2007. “Identification of Subdivisions in the Medial Geniculate Body of the Guinea Pig.” Hearing Research 228 (1–2): 156–67. doi:10.1016/j.heares.2007.02.005.

Anderson, LA & Linden, JF, 2016. Mind the Gap: Two Dissociable Mechanisms of Temporal Processing in the Auditory System. The Journal of neuroscience : the official journal of the Society for Neuroscience, 36(6), pp.1977–95. Available at: http://www.ncbi.nlm.nih.gov/pubmed/26865621%5Cnhttp://www.pubmedcentral.nih.gov/articlerender.fcgi?artid=PMC4748080.

Anderson, LA, and Linden, JF. 2011. “Physiological Differences between Histologically Defined Subdivisions in the Mouse Auditory Thalamus.” Hearing Research 274 (1–2). Elsevier B.V.: 48–60. doi:10.1016/j.heares.2010.12.016.

Anderson, LA, Christianson, GB, and Linden, JF. 2009. “Mouse Auditory Cortex Differs from Visual and Somatosensory Cortices in the Laminar Distribution of Cytochrome Oxidase and Acetylcholinesterase.” Brain Research 1252 (February). Elsevier B.V.: 130–42. doi:10.1016/j.brainres.2008.11.037.

Anderson, S, Parbery-Clark A, White-Schwoch T, Kraus N, 2013. Auditory Brainstem Response to Complex Sounds Predicts Self-Reported Speech-in-Noise Performance. Journal of speech and hearing research, Feb:56(1):31-43. doi: 10.1044/1092-4388(2012/12-0043).

Barsz, K, Ison, JR, Snell, KB, and Walton, JP. 2002. “Behavioral and Neural Measures of Auditory Temporal Acuity in Aging Humans and Mice.” Neurobiology of Aging 23 (4): 565–78. http://www.ncbi.nlm.nih.gov/pubmed/12009506.

Bhatara, A, Babikian, T, Laugeson, E, Tachdjian, R, and Sininger, YS. 2013. “Impaired Timing and Frequency Discrimination in High-Functioning Autism Spectrum Disorders.” Journal of Autism and Developmental Disorders, February. doi:10.1007/s10803-013-1778-y.

Boehm, G W, Sherman GF, Hoplight BJ, Hyde, LA, Waters, NS, Bradway, DM, Galaburda, AM, and Denenberg, VH. 1996. “Learning and Memory in the Autoimmune BXSB Mouse: Effects of Neocortical Ectopias and Environmental Enrichment.” Brain Research 726 (1–2): 11–22. http://www.ncbi.nlm.nih.gov/pubmed/8836540.

Bowen, GP, Lin, D, Taylor, MK, and Ison, JR. 2003. “Auditory Cortex Lesions in the Rat Impair Both Temporal Acuity and Noise Increment Thresholds, Revealing a Common Neural Substrate.” Cerebral Cortex (New York, N.Y. : 1991) 13 (8): 815–22. http://www.ncbi.nlm.nih.gov/pubmed/12853367.

Calford, MB & Aitkin, LM, 1983. Ascending projections to the medial geniculate body of the cat: evidence for multiple, parallel auditory pathways through thalamus. J Neurosci, 3(11), pp.2365–2380.

Centanni, TM, Booker AB, Sloan AM, Chen F, Maher BJ, Carraway RS, Khodaparast N, Rennaker R, LoTurco JJ, Kilgard MP. 2013. Knockdown of the Dyslexia-Associated Gene Kiaa0319 Impairs Temporal Responses to Speech Stimuli in Rat Primary Auditory Cortex. Cerebral cortex. Available at: http://www.ncbi.nlm.nih.gov/pubmed/23395846.

Clark, MG, Rosen, GD, Tallal, P, and Fitch, RH. 2000. “Impaired Two-Tone Processing at Rapid Rates in Male Rats with Induced Microgyria.” Brain Research 871 (1): 94–97. http://www.ncbi.nlm.nih.gov/pubmed/10882787.

Clark, MG, Sherman, GF, Bimonte, HA, and Fitch, RH. 2000. “Perceptual Auditory Gap Detection Deficits in Male BXSB Mice with Cerebrocortical Ectopias.” Neuroreport 11 (4): 693–96. http://www.ncbi.nlm.nih.gov/pubmed/10757502.

DeFries, JC, Singer SM, Foch TT, Lewitter FI. 1978. Familial nature of reading disability. British Journal of Psychiatry, 132(4), pp.361–367.

Deng, A, Lu, J, and Sun, W. 2010. “Temporal Processing in Inferior Colliculus and Auditory Cortex Affected by High Doses of Salicylate.” Brain Research 1344 (July). Elsevier B.V.: 96–103. doi:10.1016/j.brainres.2010.04.077.

Duque D, Ayala YA, Malmierca MS. 2015. “Deviance detection in auditory subcortical structures: what can we learn from neurochemistry and neural connectivity?” Cell Tissue Res. Jul;361(1):215-32. doi: 10.1007/s00441-015-2134-7.

Edelman, GM & Gally, JA, 2001. Degeneracy and complexity in biological systems. Proceedings of the National Academy of Sciences, 98(24), pp.13763–13768. Available at: http://www.pnas.org/cgi/doi/10.1073/pnas.231499798.

Escabí, MA, Higgins, NC, Galaburda, AM, Rosen, GD, and Read, HL. 2007. “Early Cortical Damage in Rat Somatosensory Cortex Alters Acoustic Feature Representation in Primary Auditory Cortex.” Neuroscience 150 (4): 970–83. doi:10.1016/j.neuroscience.2007.07.054.

Fisher, SE & Francks, C, 2006. Genes, cognition and dyslexia: learning to read the genome. Trends in cognitive sciences, 10(6), pp.250–7. Available at: http://www.ncbi.nlm.nih.gov/pubmed/16675285 [Accessed October 8, 2012].

Fitch, RH, Brown, CP, Tallal, P, and Rosen, GD. 1997. “Effects of Sex and MK-801 on Auditory-Processing Deficits Associated with Developmental Microgyric Lesions in Rats.” Behavioral Neuroscience 111 (2): 404–12. http://www.ncbi.nlm.nih.gov/pubmed/9106679.

Fitch, RH, Tallal, P, Brown, CP, Galaburda, AM, and Rosen, GD. 1980. “Induced Microgyria and Auditory Temporal Processing in Rats: A Model for Language Impairment?” Cerebral Cortex (New York, N.Y. : 1991) 4 (3): 260–70. http://www.ncbi.nlm.nih.gov/pubmed/8075531.

Frenkel, M, Sherman, GF, Bashan, KA, Galaburda, AM and LoTurco, JJ. 2000. “Neocortical Ectopias Are Associated with Attenuated Neurophysiological Responses to Rapidly Changing Auditory Stimuli.” Neuroreport 11 (3): 575–79. http://www.ncbi.nlm.nih.gov/pubmed/10718317.

Friedman, JT, Peiffer, AM, Clark, MG, Benasich, AA, and Fitch, RH. 2004. “Age and Experience-Related Improvements in Gap Detection in the Rat.” Brain Research. Developmental Brain Research 152 (2): 83–91. doi:10.1016/j.devbrainres.2004.06.007.

Gabel, LA. 2011. “Layer I Neocortical Ectopia: Cellular Organization and Local Cortical Circuitry.” Brain Research 1381 (March). Elsevier B.V.: 148–58. doi:10.1016/j.brainres.2011.01.040.

Galaburda, AM, and Kemper, TL. 1979. “Cytoarchitectonic Abnormalities in Developmental Dyslexia: A Case Study.” Annals of Neurology 6 (2): 94–100. doi:10.1002/ana.410060203.

Galaburda, AM, Sherman, GF, Rosen, GD, Aboitiz, F, and Geschwind, N. 1985. “Developmental Dyslexia: Four Consecutive Patients with Cortical Anomalies.” Annals of Neurology 18 (2): 222–33. doi:10.1002/ana.410180210.

Galaburda, AM, Menard, MT and Rosen, GD. 1994. “Evidence for Aberrant Auditory Anatomy in Developmental Dyslexia.” Proceedings of the National Academy of Sciences of the United States of America 91 (17): 8010–13. http://www.pubmedcentral.nih.gov/articlerender.fcgi?artid=44534&tool=pmcentrez&rendertype=abstract.

Gleich, O, and Strutz, J. 2011. “The Effect of Gabapentin on Gap Detection and Forward Masking in Young and Old Gerbils.” Ear and Hearing 32 (6): 741–49. doi:10.1097/AUD.0b013e318222289f.

Gleich, O, Hamann, I, Klump, GM, Kittel, M, and Strutz, J. 2003. “Boosting GABA Improves Impaired Auditory Temporal Resolution in the Gerbil.” Neuroreport 14 (14): 1877–80. doi:10.1097/01.wnr.0000089569.45990.74.

González-Hernández, T, Mantolán-Sarmiento B, González-González B, Pérez-González H. 1996. Sources of GABAergic input to the inferior colliculus of the rat. Journal of Comparative Neurology, 372(2), pp.309–326.

Guerrini, R, and Barba, C. 2010. “Malformations of Cortical Development and Aberrant Cortical Networks: Epileptogenesis and Functional Organization.” Journal of Clinical Neurophysiology : Official Publication of the American Electroencephalographic Society 27 (6): 372–79. doi:10.1097/WNP.0b013e3181fe0585.

Guidi LG, Mattley J, Martinez-Garay I, Monaco AP, Linden JF, Velayos-Baeza A, Molnár Z. 2017. Knockout Mice for Dyslexia Susceptibility Gene Homologs KIAA0319 and KIAA0319L have Unaffected Neuronal Migration but Display Abnormal Auditory Processing. Cerebral Cortex, Dec 1;27(12):5831-5845. doi: 10.1093/cercor/bhx269.

Hämäläinen, JA, Salminen, HK, and Leppänen, PHT. 2012. “Basic Auditory Processing Deficits in Dyslexia: Systematic Review of the Behavioral and Event-Related Potential/ Field Evidence.” Journal of Learning Disabilities 46 (5): 413–27. doi:10.1177/0022219411436213.

Hamann, I, Gleich, O, Klump, GM, Kittel, MC, and Strutz, J. 2004. “Age-Dependent Changes of Gap Detection in the Mongolian Gerbil (Meriones Unguiculatus).” Journal of the Association for Research in Otolaryngology : JARO 5 (1): 49–57. doi:10.1007/s10162-003-3041-2.

Henry, KR, 1979. Auditory brainstem volume-conducted responses: origins in the laboratory mouse. Journal of the American Auditory Society, 4(5), pp.173–178.

Henry, KR, 2004. Males lose hearing earlier in mouse models of late-onset age-related hearing loss; females lose hearing earlier in mouse models of early-onset hearing loss. Hearing Research, 190(1–2), pp.141–148.

Herman, AE, Galaburda, AM, Fitch, RH, Carter, AR, and Rosen, GD. 1997. “Cerebral Microgyria, Thalamic Cell Size and Auditory Temporal Processing in Male and Female Rats.” Cerebral Cortex, 7 (5): 453–64. http://www.ncbi.nlm.nih.gov/pubmed/9261574.

Hiroaki, K & Matsuno, F, 2008. Biological robustness. 2008 SICE Annual Conference, 5(November), pp.9–9. Available at: http://ieeexplore.ieee.org/document/4654600/.

Humphreys, P, Rosen GD, Sherman, GF, and Galaburda, AM. 1991. “Freezing Lesions of the Developing Rat Brain: A Model for Cerebrocortical Microgyria.”

Humphreys, P, Kaufmann, WE, and Galaburda, AM. 1990. “Developmental Dyslexia in Women: Neuropathological Findings in Three Patients.” Annals of Neurology 28 (6): 727–38. doi:10.1002/ana.410280602.

Hunter, KP & Willott, JF, 1987. Aging and the auditory brainstem response in mice with severe or minimal presbycusis. Hearing research, 30(2–3), pp.207–218.

Hyde, LA, Hoplight, BJ, Harding, S, Sherman, GF, Mobraaten, LE, and Denenberg, VH. 2001. “Effects of Ectopias and Their Cortical Location on Several Measures of Learning in BXSB Mice.” Developmental Psychobiology 39 (4): 286–300. http://www.ncbi.nlm.nih.gov/pubmed/11745324.

Hyde, LA, Jo, A, Bimonte, HA, Sherman, GF, and Denenberg, VH. 2002. “Spatial and Nonspatial Morris Maze Learning : Impaired Behavioral Flexibility in Mice with Ectopias Located in the Prefrontal Cortex.” Behavioural Brain Research 133: 247–59.

Jenner, AR, Galaburda, AM, and Sherman, GF. 2000. “Connectivity of Ectopic Neurons in the Molecular Layer of the Somatosensory Cortex in Autoimmune Mice.” Cerebral Cortex (New York, N.Y. : 1991) 10 (10): 1005–13. http://www.ncbi.nlm.nih.gov/pubmed/11007551.

Kasai, M, Ono, M & Ohmori, H, 2012. Distinct neural firing mechanisms to tonal stimuli offset in the inferior colliculus of mice in vivo. Neuroscience research, 73(3), pp.224–37. Available at: http://www.ncbi.nlm.nih.gov/pubmed/22579573.

King, AJ, Teki, S and Willmore, BDB. 2018. “Recent advances in understanding the auditory cortex”. Version 1. F1000 Res. 2018; 7: F1000 Faculty Rev-1555. Published online 2018 Sep 26. doi: 10.12688/f1000research.15580.1

Kudo, M & Niimi, K, 1978. Ascending projections of the inferior colliculus onto the medial geniculate body in the cat studied by anterograde and retrograde tracing techniques. Brain Research, 155(1), pp.113–117.

Kulesza, RJ & Berrebi, AS, 2000. The Superior Paraolivary Nucleus of the Rat Is a GABAergic Nucleus. JARO - Journal of the Association for Research in Otolaryngology, 1(4), pp.255–269. Available at: http://link.springer.com/10.1007/s101620010054 [Accessed May 7, 2014].

Hardisty-Hughes RE, Parker A and Brown SD. 2010. “A hearing and vestibular phenotyping pipeline to identify mouse mutants with hearing impairment.” Nat Protoc. 2010 Jan;5(1):177-90. doi: 10.1038/nprot.2009.204.

Humes LE, Busey TA, Craig JC, Kewley-Port D. 2009. “The Effects of Age on Sensory Thresholds and Temporal Gap Detection in Hearing , Vision , and Touch.” Attention, Perception and Psychophysics 71 (4): 860–71. doi:10.3758/APP.

Li S, Kalappa BI, Tzounopoulos T. 2015. “Noise-induced plasticity of KCNQ2/3 and HCN channels underlies vulnerability and resilience to tinnitus.” Elife. 2015 Aug 27;4. doi: 10.7554/eLife.07242.

Lipoff, Danielle M, Ankur Bhambri, Georgia J Fokas, Sanjeev Sharma, Lisa A Gabel, Joshua C Brumberg, Eric K Richfield, and Raddy L Ramos. 2011. “Neocortical Molecular Layer Heterotopia in Substrains of C57BL/6 and C57BL/10 Mice.” Brain Research 1391 (May): 36–43. doi:10.1016/j.brainres.2011.03.026.

Lipoff, DM, Bhambri, A, Fokas, GJ, Sharma, S, Gabel, LA, Brumberg, JC, Richfield, EK, and Ramos, RL. 2011. “Neocortical Molecular Layer Heterotopia in Substrains of C57BL/6 and C57BL/10 Mice.” Brain Research 1391 (May): 36–43. doi:10.1016/j.brainres.2011.03.026.

Livingstone, MS, Rosen, GD, Drislane, FW, and Galaburda, AM. 1991. “Physiological and Anatomical Evidence for a Magnocellular Defect in Developmental Dyslexia.” Proceedings of the National Academy of Sciences of the United States of America 88 (18): 7943–47.

Loftus WC, Malmierca MS, Bishop DC, Oliver DL. 2008. “The cytoarchitecture of the inferior colliculus revisited: a common organization of the lateral cortex in rat and cat.” Neuroscience. Jun 12;154(1):196-205. doi: 10.1016/j.neuroscience.2008.01.019.

Martinez-Garay I, Guidi LG, Holloway ZG, Bailey MA, Lyngholm D, Schneider T, Donnison T, Butt SJ, Monaco AP, Molnár Z, Velayos-Baeza A. 2016. Normal radial migration and lamination are maintained in dyslexia-susceptibility candidate gene homolog Kiaa0319 knockout mice. Brain Structure and Function, pp.1–18.

Neef NE, Müller B, Liebig J, Schaadt G, Grigutsch M, Gunter TC, Wilcke A, Kirsten H, Skeide MA, Kraft I, Kraus N, Emmrich F, Brauer J, Boltze J, Friederici AD. 2017. Dyslexia risk gene relates to representation of sound in the auditory brainstem. Dev Cogn Neurosci. Apr;24:63-71. doi: 10.1016/j.dcn.2017.01.008.

Paracchini, S, Scerri, T & Monaco, AP, 2007. The Genetic Lexicon of Dyslexia. Annual review of genomics and human genetics, 8, pp.57–79.

Peiffer, AM, Dunleavy, CK, Frenkel, M, Gabel, LA, LoTurco, JJ, Rosen, GD, and Fitch, RH. 2001. “Impaired Detection of Variable Duration Embedded Tones in Ectopic NZB/BINJ Mice.” Neuroreport 12 (13): 2875–79. http://www.ncbi.nlm.nih.gov/pubmed/11588594.

Peiffer, AM, Fitch, RH, Thomas, JJ, Yurkovic, AN, and Rosen, GD. 2003. “Brain Weight Differences Associated with Induced Focal Microgyria.” BMC Neuroscience 4 (June): 12. doi:10.1186/1471-2202-4-12.

Phillips, DP, Comeau, M, and Andrus, JN. 2010. “Auditory Temporal Gap Detection in Children with and without Auditory Processing Disorder.” Journal of the American Academy of Audiology 21 (6): 404–8. doi:10.3766/jaaa.21.6.5.

Poth, EA, Boettcher, FA, Mills, JH, and Dubno, JR. 2001. “Auditory Brainstem Responses in Younger and Older Adults for Broadband Noises Separated by a Silent Gap.” Hearing Research 161 (1–2): 81–86. http://www.ncbi.nlm.nih.gov/pubmed/11744284.

Radziwon, KE, June, KM, Stolzberg, DJ, Xu-Friedman, MA, Salvi, RJ, and Dent, ML. 2009. “Behaviorally Measured Audiograms and Gap Detection Thresholds in CBA/CaJ Mice.” Journal of Comparative Physiology. A, Neuroethology, Sensory,

Neural, and Behavioral Physiology 195 (10): 961–69. doi:10.1007/s00359-009-0472-1.

Ramus, F. 2003. “Theories of Developmental Dyslexia: Insights from a Multiple Case Study of Dyslexic Adults.” Brain 126 (4): 841–65. doi:10.1093/brain/awg076.

Ramus, F. 2004. “Neurobiology of Dyslexia: A Reinterpretation of the Data.” Trends in Neurosciences 27 (12): 720–26. doi:10.1016/j.tins.2004.10.004.

Rosen, GD, Herman, AE, and Galaburda, AM. 1999. “Sex Differences in the Effects of Early Neocortical Injury on Neuronal Size Distribution of the Medial Geniculate Nucleus in the Rat Are Mediated by Perinatal Gonadal Steroids.” Cerebral Cortex (New York, N.Y. : 1991) 9 (1): 27–34. http://www.ncbi.nlm.nih.gov/pubmed/10022493.

Rosen, GD, Mesples, B, Hendriks, M, and Galaburda, AM. 2006. “Histometric Changes and Cell Death in the Thalamus after Neonatal Neocortical Injury in the Rat.” Neuroscience 141 (2): 875–88. doi:10.1016/j.neuroscience.2006.04.035.

Rosen, GD, Sherman, GF, and Galaburda, AM. 1993. “Neuronal Subtypes and Anatomic Asymmetry: Changes in Neuronal Number and Cell-Packing Density.” Neuroscience 56 (4): 833–39. http://www.ncbi.nlm.nih.gov/pubmed/8284037.

Rosen, GD, Waters, NS, Galaburda, AM, and Denenberg, VH. 1995. “Behavioral Consequences of Neonatal Injury of the Neocortex.” Brain Research 681 (1–2): 177–89. http://www.ncbi.nlm.nih.gov/pubmed/7552277.

Rosen, GD, and Harry, JD. 1990. “Brain Volume Estimation from Serial Section Measurements: A Comparison of Methodologies.” Journal of Neuroscience Methods 35 (2): 115–24. http://www.ncbi.nlm.nih.gov/pubmed/2283883.

Rosen, GD, and Galaburda, AM. 2000. “Single Cause, Polymorphic Neuronal Migration Disorders: An Animal Model.” Developmental Medicine and Child Neurology 42 (10): 652–62. http://www.ncbi.nlm.nih.gov/pubmed/11085292.

Rosen, GD, Sherman, GF, Richman, JM, Stone, LV, and Galaburda, AM. 1992. “Induction of Molecular Layer Ectopias by Puncture Wounds in Newborn Rats and Mice.” Developmental Brain Research 67 (2): 285–91. doi:10.1016/0165-3806(92)90229-P.

Rosen, S. 2003. Auditory processing in dyslexia and specific language impairment: is there a deficit? What is its nature? Does it explain anything? Journal of Phonetics, Volume 31, Issues 3–4, 509-527, https://doi.org/10.1016/S0095-4470(03)00046-9.

Sakata, S. and Harris, KD. 2009. “Laminar Structure of Spontaneous and Sensory-Evoked Population Activity in Auditory Cortex” Neuron Volume 64, Issue 3, Pages 404-418

Saldaña E, Aparicio MA, Fuentes-Santamaría V and Berrebi AS. 2009. Connections of the superior paraolivary nucleus of the rat: projections to the inferior colliculus. Neuroscience, 163(1), pp.372–87. Available at: http://www.pubmedcentral.nih.gov/articlerender.fcgi?artid=2778228&tool=pmcentrez&rendertype=abstract [Accessed May 7, 2014].

Schrott, LM, Waters, NS, Boehm, GW, Sherman, GF, Morrison, L, Rosen, GD, Behan, PO, Galaburda, AM, and Denenberg, VH. 1993. “Behavior, Cortical Ectopias, and Autoimmunity in BXSB-Yaa and BXSB-Yaa+ Mice.” Brain, Behavior, and Immunity. doi:10.1006/brbi.1993.1022.

Schrott, LM, Denenberg, VH, Sherman, GF, Rosen, GD, and Galaburda, AM. 1992. “Lashley Maze Learning Deficits in NZB Mice.” Physiology & Behavior 52 (6): 1085–89. http://www.ncbi.nlm.nih.gov/pubmed/1484864.

Schrott, LM, Denenberg, VH, Sherman, GF, Waters, NS, Rosen, GD, and Galaburda, AM. 1992. “Environmental Enrichment, Neocortical Ectopias, and Behavior in the Autoimmune NZB Mouse.” Brain Research. Developmental Brain Research 67 (1): 85–93. http://www.ncbi.nlm.nih.gov/pubmed/1638744.

Schumacher J, Hoffmann P, Schmäl C, Schulte-Körne G, Nöthen MM. 2007. Genetics of dyslexia: the evolving landscape. Journal of medical genetics, 44(5), pp.289–97. Available at: http://www.pubmedcentral.nih.gov/articlerender.fcgi?artid=2597981&tool=pmcentrez&rendertype=abstract.

Sherman, G F, Galaburda, AM, and Geschwind, N. 1985. “Cortical Anomalies in Brains of New Zealand Mice: A Neuropathologic Model of Dyslexia?” Proceedings of the National Academy of Sciences of the United States of America 82 (23): 8072–74. http://www.pubmedcentral.nih.gov/articlerender.fcgi?artid=391444&tool=pmcentrez&rendertype=abstract.

Sherman, GF, and Holmes, LB. 1999. “Cebrebrocortical Microdysgenesis Is Enhanced in C57BL / 6J Mice Exposed In Utero to Acetazolamide.” Teratology 142 (July 1998): 137–42.

Sherman, GF, Galaburda, AM, Behan, PO, and Rosen, GD. 1987. “Neuroanatomical Anomalies in Autoimmune Mice” Acta Neuropathologica 74: 239–42.

Sherman, GF, Rosen, GD, Stone, LV, Press, DM, and Galaburda, AM. 1992. “The Organization of Radial Glial Fibers in Spontaneous Neocortical Ectopias of Newborn New Zealand Black Mice” 67: 279–83.

Sherman, GF, Rosen, GD, Stone, LV, Press, DM, and Galaburda, AM. 1992. “The Organization of Radial Glial Fibers in Spontaneous Neocortical Ectopias of Newborn New Zealand Black Mice” 67: 279–83.

Stein, J. 2001. “The Magnocellular Theory of Developmental Dyslexia.” Dyslexia (Chichester, England) 7 (1): 12–36. doi:10.1002/dys.186.

Su, Z, Wang, J & Gu, X, 2014. Effect of duplicate genes on mouse genetic robustness: An update. BioMed Research International, 2014(ii).

Syka, J, Rybalko, N, Mazelová, J, and Druga, R. 2002. “Gap Detection Threshold in the Rat before and after Auditory Cortex Ablation.” Hearing Research 172 (1–2): 151–59. http://www.ncbi.nlm.nih.gov/pubmed/12361878.

Szalkowski CE, Fiondella CF, Truong DT, Rosen GD, LoTurco JJ and Fitch RH. 2013. The effects of Kiaa0319 knockdown on cortical and subcortical anatomy in male rats. International journal of developmental neuroscience, 31(2), pp.116–22. Available at: http://www.ncbi.nlm.nih.gov/pubmed/23220223 [Accessed March 4, 2013].

Tallal, P. 1980. “Auditory temporal perception, phonics and reading disabilities in children.” Brain and Language, Vol:9:Issue 2, pgs 182-198.

Threlkeld, SW, Hill, CA, Szalkowski, CE, Truong, DT, Rosen, GD, and Fitch, RH. 2012. “Effects of Test Experience and Neocortical Microgyria on Spatial and Non-

Spatial Learning in Rats." Behavioural Brain Research 235 (2). Elsevier B.V.: 130–35. doi:10.1016/j.bbr.2012.07.031.

Threlkeld, SW, Rosen, GD, and Fitch, RH. 2007. "Age at Developmental Cortical Injury Differentially Alters Corpus Callosum Volume in the Rat." BMC Neuroscience 8 (January): 94. doi:10.1186/1471-2202-8-94.

Threlkeld, SW, McClure, MM, Rosen, GD, and Fitch, RH. 2006. "Developmental Timeframes for Induction of Microgyria and Rapid Auditory Processing Deficits in the Rat." Brain Research 1109 (1): 22–31. doi:10.1016/j.brainres.2006.06.022.

Van Ingelghem, M, Van Wieringen, A, Wouters, J, Vandenbussche, E, Onghena, P, and Ghesquière, P. 2001. "Psychophysical Evidence for a General Temporal Processing Deficit in Children with Dyslexia." Neuroreport 12 (16): 3603–7. http://www.ncbi.nlm.nih.gov/pubmed/11733720.

Wadsworth SJ, DeFries JC, Olson RK and Willcutt EG. 2007. Colorado longitudinal twin study of reading disability. Annals of Dyslexia, 57(2), pp.139–160.

Weinberger, NM, 2012. The Medial Geniculate, Not the Amygdala, as the Root of Auditory Fear Conditioning. Hearing Research, 274(949), pp.61–74.

White-Schwoch T, Nicol T, Warrier CM, Abrams DA, Kraus N, 2016. Individual Differences in Human Auditory Processing: Insights From Single-Trial Auditory Midbrain Activity in an Animal Model. Cerebral Cortex, (Ic), pp.1–21. Available at: http://www.cercor.oxfordjournals.org/lookup/doi/10.1093/cercor/bhw293.

Winer, J.A., 1992. The Functional Architecture of the Medial Geniculate Body and the Primary Auditory Cortex. In: Webster D.B., Popper A.N., Fay R.R. (eds) The

Mammalian Auditory Pathway: Neuroanatomy. Springer Handbook of Auditory Research, vol 1. Springer, New York, NY,

Zhou, X, Jen, PHS, Seburn, KL, Frankel, WN and Zheng, QY. 2006. “Auditory brainstem responses in 10 inbred strains of mice” Brain Res. 2006 May 26; 1091(1): 16–26.

Appendix

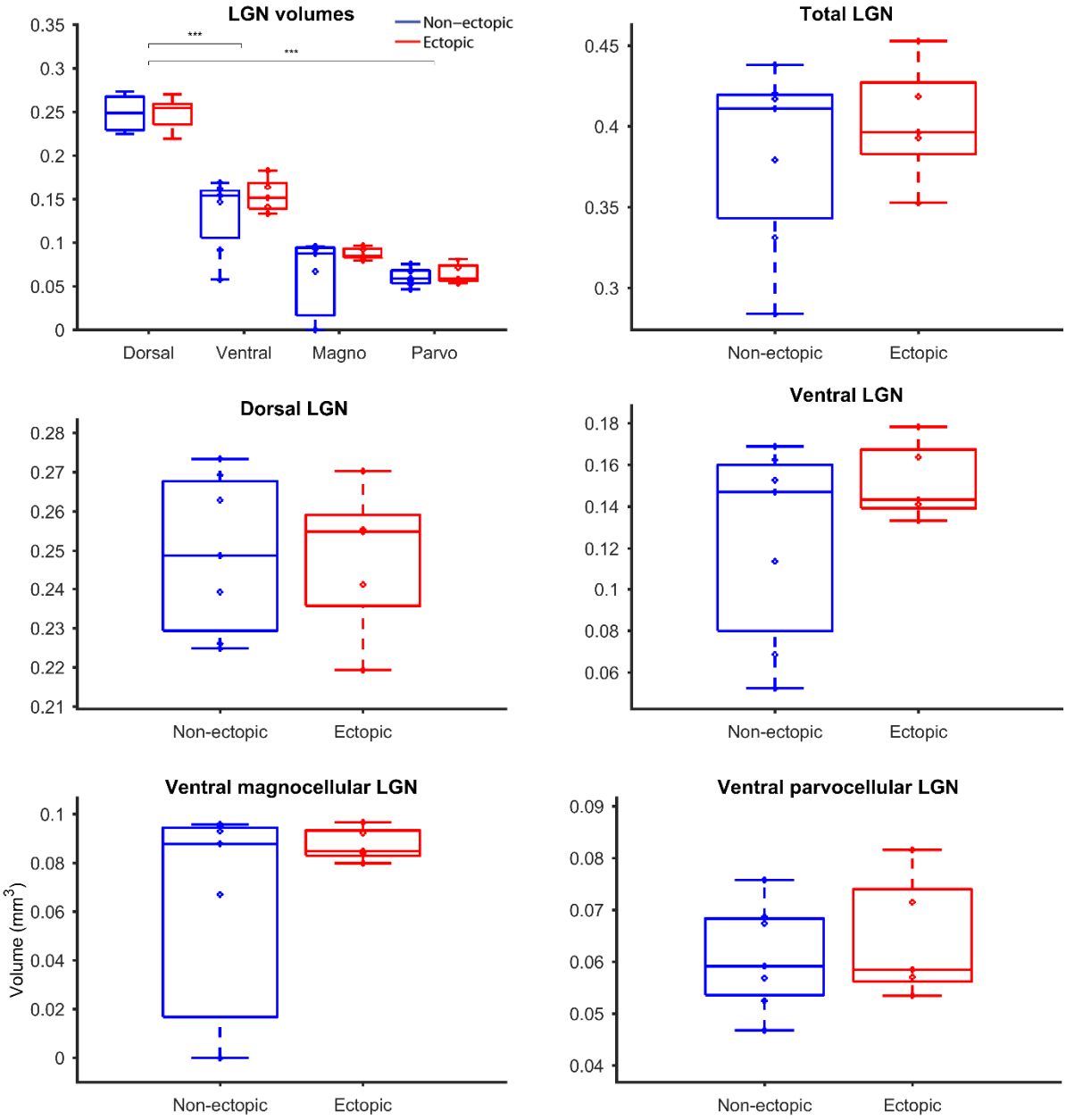

Figure A1: No significant difference between ectopic and non-ectopic in LGN size. There is no significant difference between ectopic and non-ectopic mice in the different LGN subdivisions (ranksum; all p>0.05). Figure conventions as in figure 17 but for LGN.

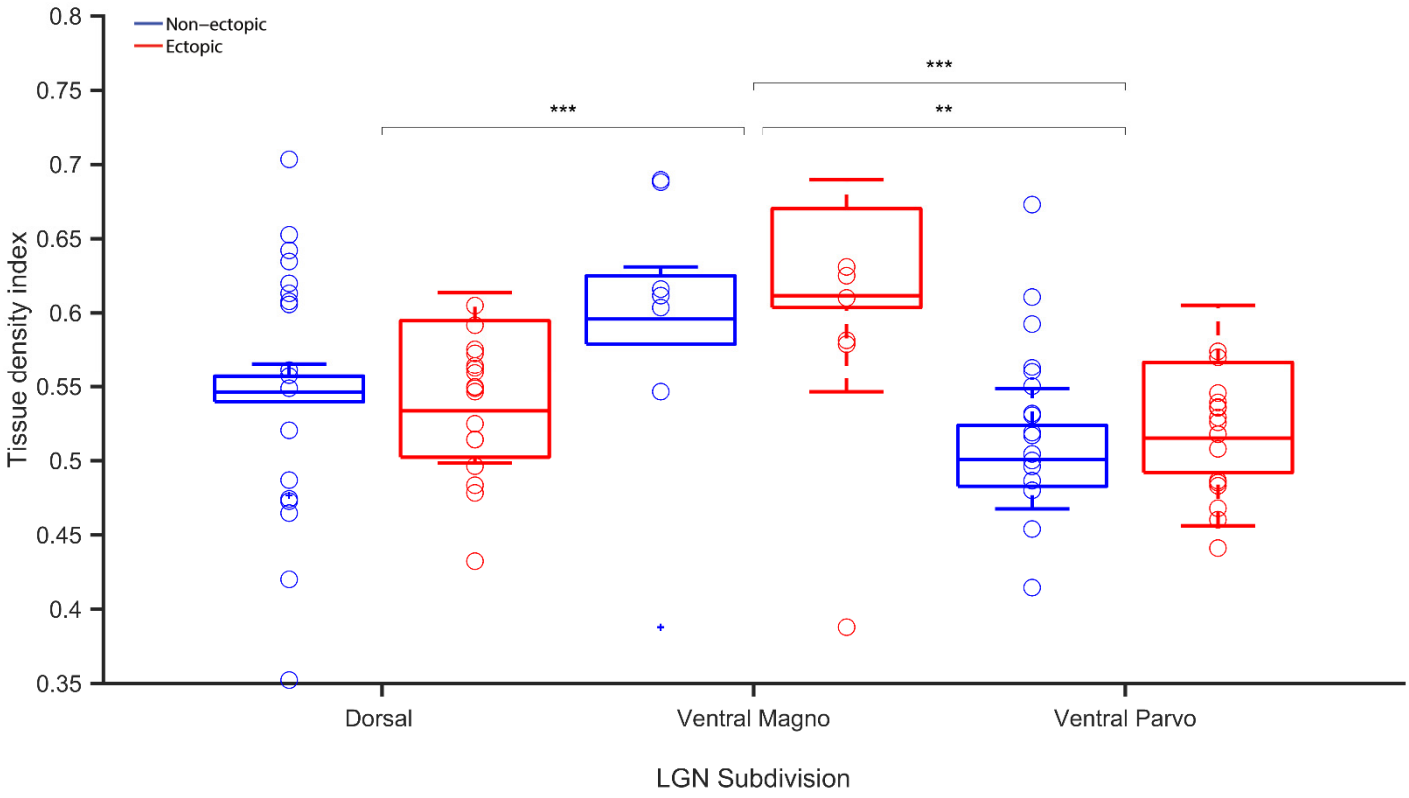

Figure A2: No significant difference in LGN cell density between ectopic and non-ectopic mice. There is no significant difference between ectopic and non-ectopic mice for cell density in LGN or any of its subdivisions (ranksum; all $p>0.05$). Figure conventions as in figure 17 but for LGN. Analysis of pixel depth showed no significant difference between ectopic and non-ectopic mice but a significant difference was found between the LGN subdivisions indicating a difference can be detected with this measure.

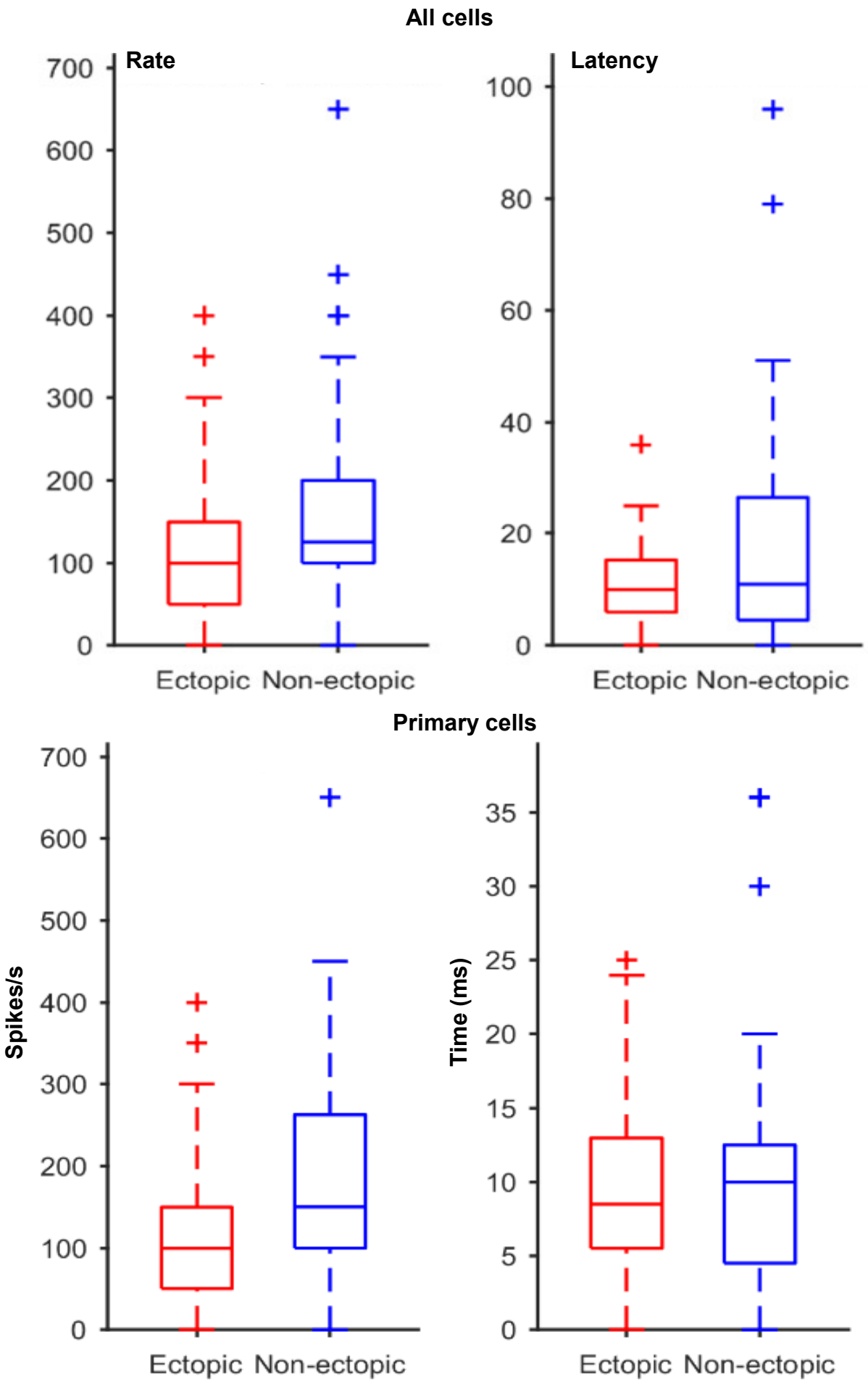

Figure Appendx A3: Similar peak rate and latency in ectopic and non-ectopic mice excitatory offset responses. Analysis of peak rate and latencies for excitatory offset responses showing no difference in either measure between ectopic and non-ectopic mice (ranksum; all p>0.01). Boxplots for peak rates of excitatory offset responses for all IC subdivisions and only for primary IC cells (left column). Boxplots for peak latencies of excitatory offset responses for all IC subdivisions and only for primary IC cells (left column)

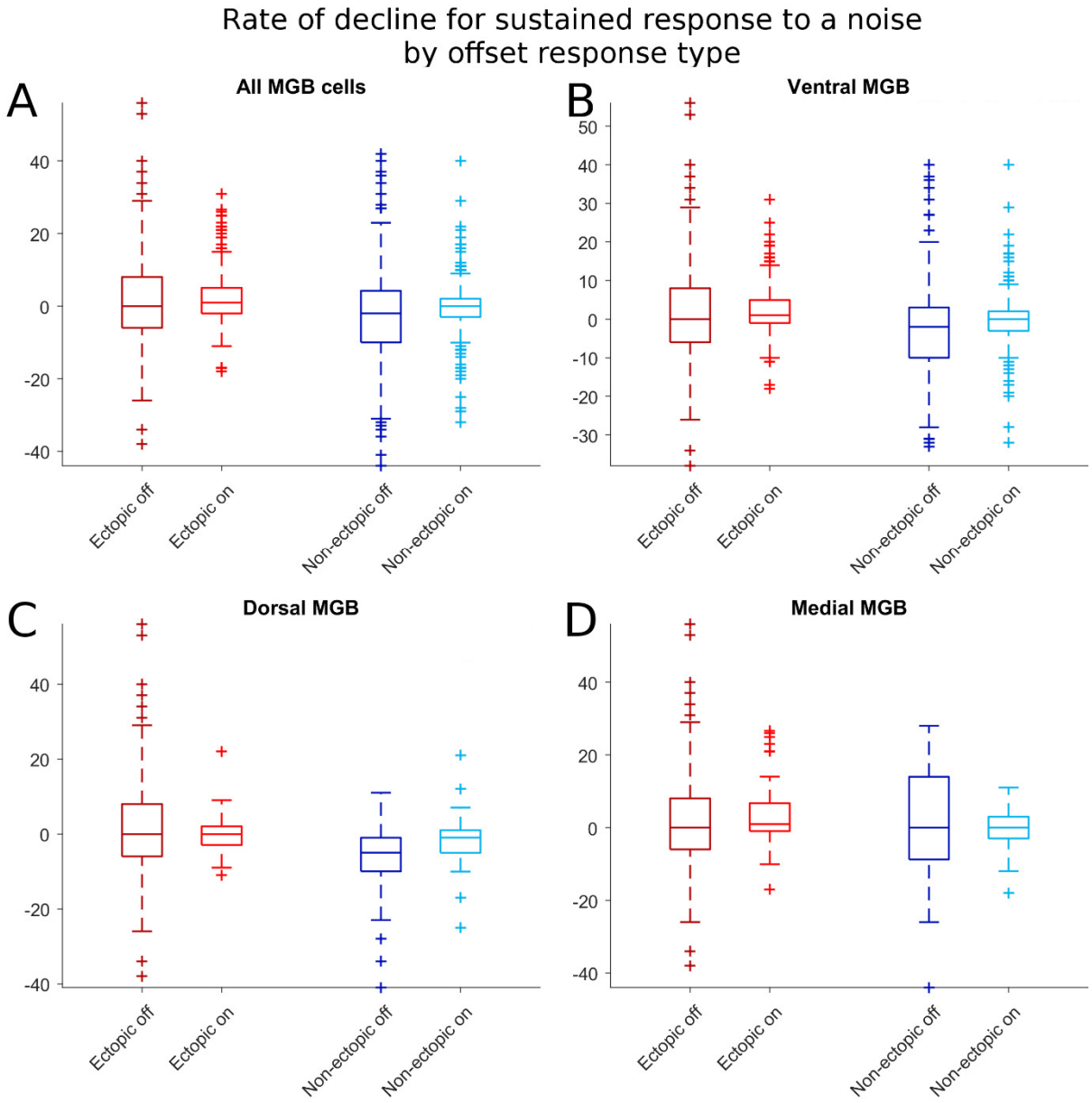

Figure A4: Fall-off rates in sustained response to a 250ms 60dB SPL noise for cells with and without offset responses. Dark colours for cells with offset responses, light colours for cells without offset responses. (A) Across all MGB cells (ranksum all $p<0.01$). (B) For ventral MGB (ranksum all $p<0.01$). (C) For dorsal MGB (ranksum; offset cells $p<0.01$; onset cells $p>0.01$). (D) For medial MGB (ranksum all $p>0.01$).

Medians	Ectopic	Non-ectopic
Volumes:		
MGB	0.40	0.42
MGB ventral	0.25	0.26
MGB dorsal	0.13	0.13
MGB medial	0.03	0.02
LGN dorsal	0.25	0.25
LGN ventral	0.15	0.15
LGN ventral magnocellular	0.08	0.09
LGN ventral parvocellular	0.06	0.06
Pixel (cell) densitites:		
MGB ventral	0.69	0.64
MGB dorsal (lateral)	0.67	0.64
MGB dorsal (medial)	0.76	0.73
LGN dorsal	0.54	0.53
LGN ventral magnocellular	0.49	0.52
LGN ventral parvocellular	0.08	0.09
Cortical layer thickness:		
Layer 1	11.02	11.54
Layers 2/3	23.18	23.68
Layer 4	11.02	11.47
Layer 5	34.50	33.74
Layer 5B	9.79	10.26
Layer 6	20.13	20.21

Table A1: Medians for data presented in Chapter 2

Gap threshold medians IC	Ectopic			Non-ectopic		
Sound level:	20	40	60	20	40	60
Primary cells	32	5.6569	4	16	8	5.6569
Non-primary cells	64	16	5.6569	64	8	4
Untuned cells	128	64	16	128	32	16

Table A2: Gap detection thresholds medians from IC as presented in Chapter 3.

IC	Ectopic			Non-ectopic		
Median	Firing rate	Fano factors	CVisi	Firing rate	Fano factors	CVisi
Onset response to noise:						
Primary cells	112.5	0.7957	0.985	150	0.6548	1.0534
Non-primary cells	150	0.7362	1.0117	200	0.7368	0.9851
Untuned cells	150	0.7044	0.9941	150	0.7368	0.9763
Sustained response to noise:						
Primary cells	50	0.9817	1.0335	150	0.9034	1.0531
Non-primary cells	75	1.0388	1.0237	150	1.0802	1.0005
Untuned cells	100	0.897	0.9978	200	1.0075	0.9296
Sponteous rates:						
Primary cells	50	0.9817	0.3186	150	0.9034	0.343
Non-primary cells	75	1.0388	0.3062	150	1.0802	0.4486
Untuned cells	100	0.897	0.2236	200	1.0075	0.4037

Table A3: Medians for analysis of responses to noise in IC as presented in Chapter 3.

MGB	Ectopic			Non-ectopic		
Median	Firing rate	Fano factors	CVisi	Firing rate	Fano factors	CVisi
Onset response to noise:						
Primary cells	75	0.7512	1.0655	100	0.7754	1.0945
Non-primary cells	75	0.6565	1.0332	50	0.7578	1.0748
Untuned cells	100	0.6084	1.1149	100	0.7943	1.0972
Sustained response to noise:						
Primary cells	50	1.1687	1.1743	50	1.5973	1.2288
Non-primary cells	50	1.2783	1.3821	50	1.61	1.4829
Untuned cells	100	1.1316	1.0844	50	1.2105	1.0206
Sponteous rates:						
Primary cells	20.1517	1.1687	2.6468	24.9583	1.5973	2.0942
Non-primary cells	10.1449	1.2783	2.5928	5.9406	1.61	2.1961
Untuned cells	29.7502	1.1316	2.3732	34.2299	1.2105	2.2063

Table A4: Median for analysis of responses to noise in MGB as presented in Chapter 3.

Mean (SE)	Ectopic (n=13)				Non-ectopic (n=17)			
Sound Level (dB SPL):	50	60	70	80	50	60	70	80
Click Amplitudes:								
Wave I	1.3 (0.15)	2.24 (0.21)	3.04 (0.26)	3.6 (0.29)	1.34 (0.18)	1.97 (0.22)	2.67 (0.29)	3.11 (0.36)
Wave II	1.19 (0.12)	1.48 (0.12)	1.77 (0.15)	1.89 (0.17)	1.34 (0.18)	1.61 (0.19)	1.93 (0.24)	2.31 (0.31)
Wave III	1.76 (0.16)	2.47 (0.21)	3.14 (0.3)	3.85 (0.33)	1.2 (0.23)	1.87 (0.25)	2.42 (0.29)	2.92 (0.31)
Wave IV	0.41 (0.15)	0.72 (0.18)	0.81 (0.2)	0.91 (0.21)	0.49 (0.2)	0.67 (0.3)	0.61 (0.33)	0.63 (0.33)
Click Latencies:								
Wave I	1.79 (0.04)	1.7 (0.04)	1.64 (0.04)	1.61 (0.04)	1.71 (0.03)	1.66 (0.02)	1.6 (0.02)	1.57 (0.02)
Wave II	2.49 (0.05)	2.45 (0.04)	2.41 (0.04)	2.35 (0.05)	2.46 (0.05)	2.42 (0.04)	2.43 (0.04)	2.39 (0.04)
Wave III	3.29 (0.05)	3.22 (0.04)	3.19 (0.05)	3.17 (0.04)	3.32 (0.06)	3.21 (0.04)	3.16 (0.04)	3.16 (0.04)
Wave IV	4.28 (0.04)	4.2 (0.04)	4.19 (0.04)	4.15 (0.04)	4.28 (0.05)	4.18 (0.06)	4.22 (0.08)	4.15 (0.07)
8kHz Tone Amplitudes:								
Wave I	0.32 (0.05)	0.56 (0.06)	0.58 (0.06)	0.58 (0.07)	0.43 (0.08)	0.51 (0.12)	0.55 (0.12)	0.63 (0.15)
Wave II	0.39 (0.05)	0.55 (0.06)	0.88 (0.13)	1.26 (0.12)	0.48 (0.11)	0.61 (0.15)	0.81 (0.14)	1.17 (0.18)
Wave III	0.5 (0.05)	0.82 (0.07)	1.05 (0.12)	1.25 (0.14)	0.63 (0.1)	0.8 (0.14)	1.04 (0.17)	1.52 (0.22)
Wave IV	0.35 (0.06)	0.45 (0.06)	0.27 (0.06)	0.29 (0.07)	0.45 (0.1)	0.71 (0.12)	0.56 (0.08)	0.75 (0.15)
8kHz Tone Latencies:								
Wave I	2.23 (0.07)	2.29 (0.05)	2.21 (0.03)	2.15 (0.03)	1.97 (0.18)	2.3 (0.11)	2.24 (0.1)	2.03 (0.06)
Wave II	3.36 (0.06)	3.18 (0.06)	3.03 (0.06)	2.81 (0.04)	3.04 (0.12)	2.98 (0.09)	2.77 (0.1)	2.67 (0.07)
Wave III	3.96 (0.11)	3.9 (0.09)	3.75 (0.08)	3.65 (0.09)	3.77 (0.11)	3.63 (0.11)	3.45 (0.1)	3.42 (0.09)
Wave IV	5.19 (0.12)	5.08 (0.1)	5.04 (0.07)	4.83 (0.07)	4.78 (0.18)	4.62 (0.17)	4.57 (0.16)	4.39 (0.17)
16kHz Tone Amplitudes:								

Wave I	0.44 (0.06)	0.55 (0.08)	0.68 (0.07)	0.84 (0.11)	0.36 (0.05)	0.4 (0.09)	0.44 (0.08)	0.77 (0.13)
Wave II	0.49 (0.06)	0.77 (0.1)	1.02 (0.12)	1.37 (0.12)	0.61 (0.1)	0.97 (0.15)	1.13 (0.18)	1.33 (0.21)
Wave III	0.56 (0.07)	0.75 (0.1)	0.9 (0.11)	1.31 (0.17)	0.56 (0.1)	0.63 (0.08)	0.96 (0.12)	1.21 (0.18)
Wave IV	0.38 (0.07)	0.48 (0.09)	0.44 (0.09)	0.52 (0.12)	0.55 (0.12)	0.61 (0.11)	0.66 (0.12)	0.84 (0.16)
16kHz Tone Latencies:								
Wave I	2.16 (0.08)	2.19 (0.07)	2.13 (0.05)	2.06 (0.04)	1.9 (0.12)	2.11 (0.08)	2.12 (0.06)	1.94 (0.07)
Wave II	3.11 (0.08)	2.96 (0.07)	2.83 (0.07)	2.71 (0.06)	2.98 (0.1)	2.84 (0.1)	2.81 (0.09)	2.64 (0.09)
Wave III	3.81 (0.11)	3.78 (0.09)	3.67 (0.07)	3.55 (0.06)	3.72 (0.14)	3.62 (0.14)	3.44 (0.12)	3.4 (0.13)
Wave IV	5.02 (0.15)	4.99 (0.11)	4.91 (0.08)	4.72 (0.07)	4.84 (0.23)	4.76 (0.21)	4.66 (0.22)	4.46 (0.19)
32kHz Tone Amplitudes:								
Wave I	0.31 (0.04)	0.4 (0.07)	0.58 (0.08)	0.6 (0.1)	0.39 (0.09)	0.45 (0.15)	0.43 (0.12)	0.68 (0.14)
Wave II	0.48 (0.1)	0.65 (0.09)	0.69 (0.08)	1.05 (0.09)	0.64 (0.1)	0.7 (0.14)	0.83 (0.22)	1.26 (0.29)
Wave III	0.45 (0.09)	0.65 (0.11)	0.76 (0.13)	0.87 (0.13)	0.53 (0.12)	0.57 (0.09)	0.65 (0.15)	0.94 (0.23)
Wave IV	0.45 (0.09)	0.52 (0.09)	0.36 (0.06)	0.39 (0.08)	0.49 (0.13)	0.54 (0.1)	0.6 (0.09)	0.76 (0.17)
32kHz Tone Latencies:								
Wave I	1.99 (0.12)	2.09 (0.1)	1.94 (0.09)	1.91 (0.07)	2.05 (0.23)	2.2 (0.18)	2.19 (0.14)	1.92 (0.07)
Wave II	3 (0.11)	2.83 (0.11)	2.72 (0.09)	2.58 (0.09)	2.99 (0.11)	2.86 (0.1)	2.76 (0.11)	2.63 (0.1)
Wave III	3.56 (0.14)	3.61 (0.1)	3.49 (0.09)	3.42 (0.09)	3.75 (0.11)	3.73 (0.15)	3.49 (0.13)	3.36 (0.13)
Wave IV	4.74 (0.22)	4.7 (0.13)	4.52 (0.11)	4.43 (0.1)	4.58 (0.22)	4.6 (0.22)	4.37 (0.22)	4.29 (0.2)

Table A5: Means (and SEs) for click and tone ABR data from BXSB mice presented in Chapter 4.

Mean (SE)	20ms probe delay	
	Ectopic	Non-ectopic
Probe Click:		
Amplitudes		
Wave I	0.49 (0.07)	0.66 (0.09)
Wave II	0.49 (0.09)	0.51 (0.07)
Wave III	0.59 (0.08)	0.47 (0.07)
Wave IV	0.34 (0.15)	0.26 (0.05)
Wave V	0.56 (0.14)	0.37 (0.08)
Latencies		
Wave I	1.56 (0.07)	1.55 (0.06)
Wave II	2.49 (0.1)	2.53 (0.06)
Wave III	3.41 (0.13)	3.38 (0.08)
Wave IV	4.71 (0.19)	4.51 (0.11)
Wave V	5.78 (0.24)	5.41 (0.12)
Reference click:		
Amplitudes		
Wave I	2.24 (0.33)	2.19 (0.22)
Wave II	1.34 (0.24)	1.5 (0.18)
Wave III	1.99 (0.35)	2.45 (0.25)
Wave IV	1.33 (0.42)	0.76 (0.22)
Wave V	0.72 (0.11)	0.95 (0.13)
Latencies		
Wave I	1.59 (0.03)	1.59 (0.04)
Wave II	2.44 (0.05)	2.42 (0.05)

Wave III	3.21 (0.04)	3.22 (0.05)
Wave IV	4.53 (0.16)	4.3 (0.07)
Wave V	6.03 (0.3)	5.39 (0.13)

Table A6: Means (and SEs) for masker-probe ABRs probe and reference clicks for BXSB mice as presented in Chapter 4.

	Double KO (n=13)				WT (n=11)			
Sound Level (dB SPL):	50	60	70	80	50	60	70	80
Click Amplitudes:								
Wave I	0.63 (0.13)	1.07 (0.17)	1.4 (0.26)	1.63 (0.27)	0.9 (0.11)	1.36 (0.17)	1.84 (0.21)	2.61 (0.26)
Wave II	2.79 (0.32)	3.39 (0.37)	3.81 (0.39)	4 (0.42)	3 (0.25)	3.69 (0.27)	4.28 (0.35)	4.95 (0.47)
Wave III	1.46 (0.23)	2.18 (0.3)	2.88 (0.37)	3.64 (0.49)	2.29 (0.17)	3.21 (0.18)	4.06 (0.25)	5.01 (0.33)
Wave IV	0.39 (0.08)	0.51 (0.09)	0.76 (0.09)	0.8 (0.17)	0.46 (0.09)	0.68 (0.08)	1.06 (0.12)	1.27 (0.22)
Click Latencies:								
Wave I	1.86 (0.03)	1.76 (0.02)	1.72 (0.02)	1.7 (0.02)	1.91 (0.07)	1.86 (0.06)	1.81 (0.07)	1.79 (0.07)
Wave II	2.46 (0.02)	2.39 (0.02)	2.34 (0.02)	2.32 (0.02)	2.51 (0.09)	2.47 (0.08)	2.44 (0.08)	2.41 (0.08)
Wave III	3.38 (0.02)	3.28 (0.02)	3.23 (0.02)	3.22 (0.02)	3.42 (0.09)	3.34 (0.08)	3.3 (0.08)	3.28 (0.08)
Wave IV	4.31 (0.03)	4.18 (0.02)	4.08 (0.02)	4.03 (0.02)	4.35 (0.08)	4.23 (0.08)	4.15 (0.08)	4.11 (0.08)
8kHz Tone Amplitudes:								
Wave I	0.16 (0.05)	0.25 (0.05)	0.3 (0.08)	0.52 (0.09)	0.31 (0.09)	0.42 (0.09)	0.54 (0.12)	0.56 (0.1)
Wave II	0.42 (0.08)	0.7 (0.11)	1.04 (0.13)	1.49 (0.14)	0.42 (0.08)	0.72 (0.09)	1.03 (0.12)	1.58 (0.13)
Wave III	0.46 (0.09)	0.55 (0.1)	0.91 (0.13)	1.11 (0.18)	0.53 (0.11)	0.91 (0.12)	1.25 (0.13)	1.55 (0.1)
Wave IV	0.41 (0.08)	0.32 (0.08)	0.27 (0.05)	0.25 (0.07)	0.48 (0.09)	0.42 (0.1)	0.24 (0.06)	0.06 (0.09)
8kHz Tone Latencies:								
Wave I	2.61 (0.04)	2.45 (0.04)	2.37 (0.02)	2.26 (0.02)	2.59 (0.1)	2.49 (0.08)	2.41 (0.07)	2.34 (0.07)
Wave II	3.26 (0.06)	3.12 (0.04)	2.98 (0.03)	2.86 (0.04)	3.31 (0.11)	3.2 (0.08)	3.08 (0.08)	2.94 (0.08)
Wave III	4 (0.08)	3.95 (0.07)	3.83 (0.03)	3.7 (0.04)	4.06 (0.07)	3.94 (0.09)	3.87 (0.08)	3.74 (0.08)
Wave IV	5.17	5.06	5.06	4.97	5.35	5.13	4.96	4.83

	(0.04)	(0.06)	(0.07)	(0.06)	(0.22)	(0.18)	(0.1)	(0.08)
16kHz Tone Amplitudes:								
Wave I	0.28 (0.06)	0.35 (0.08)	0.44 (0.11)	0.52 (0.11)	0.09 (0.03)	0.14 (0.03)	0.36 (0.11)	0.6 (0.1)
Wave II	0.77 (0.1)	1.09 (0.1)	1.81 (0.2)	2.32 (0.16)	0.86 (0.08)	1.4 (0.13)	1.93 (0.13)	2.77 (0.21)
Wave III	0.23 (0.06)	0.42 (0.09)	0.73 (0.12)	1.22 (0.2)	0.53 (0.14)	0.78 (0.09)	0.79 (0.12)	1.63 (0.16)
Wave IV	0.36 (0.09)	0.51 (0.14)	0.3 (0.11)	0.28 (0.09)	0.16 (0.06)	0.17 (0.08)	0.07 (0.04)	0.22 (0.12)
16kHz Tone Latencies:								
Wave I	2.17 (0.06)	2.1 (0.03)	2.08 (0.03)	1.98 (0.03)	2.23 (0.04)	2.15 (0.03)	2.11 (0.04)	2.05 (0.04)
Wave II	2.88 (0.03)	2.79 (0.04)	2.67 (0.04)	2.57 (0.04)	2.86 (0.03)	2.79 (0.03)	2.64 (0.04)	2.63 (0.03)
Wave III	3.97 (0.11)	3.74 (0.1)	3.67 (0.07)	3.57 (0.06)	3.72 (0.05)	3.68 (0.03)	3.57 (0.04)	3.56 (0.03)
Wave IV	4.98 (0.09)	4.87 (0.16)	4.75 (0.07)	4.67 (0.07)	4.97 (0.1)	4.85 (0.07)	4.79 (0.08)	4.63 (0.07)
32kHz Tone Amplitudes:								
Wave I	0.19 (0.04)	0.25 (0.05)	0.28 (0.06)	0.37 (0.13)	0.09 (0.04)	0.23 (0.09)	0.3 (0.08)	0.46 (0.11)
Wave II	0.27 (0.04)	0.41 (0.09)	0.45 (0.12)	0.56 (0.18)	0.41 (0.1)	0.51 (0.12)	0.71 (0.15)	0.93 (0.13)
Wave III	0.31 (0.1)	0.2 (0.05)	0.32 (0.08)	0.44 (0.09)	0.23 (0.04)	0.43 (0.09)	0.44 (0.14)	0.76 (0.16)
Wave IV	0.25 (0.07)	0.47 (0.15)	0.2 (0.04)	0.26 (0.07)	0.14 (0.03)	0.21 (0.05)	0.26 (0.07)	0.19 (0.07)
32kHz Tone Latencies:								
Wave I	2.45 (0.12)	2.5 (0.11)	2.28 (0.12)	2.16 (0.11)	2.42 (0.18)	2.28 (0.13)	2.29 (0.13)	2.05 (0.08)
Wave II	3.25 (0.15)	3.1 (0.09)	3.05 (0.11)	2.83 (0.13)	3.12 (0.11)	3.08 (0.13)	2.92 (0.12)	2.79 (0.12)
Wave III	4.25 (0.17)	4.31 (0.17)	4.11 (0.19)	3.89 (0.16)	4.25 (0.16)	3.94 (0.11)	3.87 (0.12)	3.68 (0.12)
Wave IV	5.42 (0.21)	5.31 (0.15)	5.18 (0.21)	4.94 (0.15)	5.27 (0.26)	5.12 (0.17)	5 (0.22)	4.84 (0.17)

Table A7: Means (and SEs) for click and tone ABRs in double KO and WT mice as presented in Chapter 5.

Mean (SE)	KIAA KO				WT				KIAA-Like KO			
Sound Level (dB SPL):	50	60	70	80	50	60	70	80	50	60	70	80
Amplitudes (fast):												
Wave I	1.07 (0.19)	1.64 (0.29)	2.08 (0.28)	2.43 (0.35)	0.83 (0.1)	1.48 (0.23)	1.96 (0.27)	2.44 (0.33)	1.13 (0.17)	1.56 (0.17)	2.09 (0.31)	2.09 (0.24)
Wave II	2.4 (0.3)	3.31 (0.34)	3.96 (0.29)	4.47 (0.42)	2.61 (0.17)	3.46 (0.29)	3.89 (0.21)	4.04 (0.37)	2.09 (0.27)	3.05 (0.29)	3.79 (0.3)	4.53 (0.34)
Wave III	1.5 (0.16)	2.42 (0.18)	3.1 (0.21)	4 (0.19)	1.66 (0.19)	2.8 (0.31)	3.13 (0.26)	3.97 (0.29)	1.02 (0.22)	1.75 (0.3)	2.32 (0.43)	2.8 (0.44)
Wave IV	1 (0.19)	1.18 (0.21)	1.61 (0.14)	1.3 (0.14)	1.15 (0.18)	1.48 (0.28)	1.62 (0.29)	1.16 (0.14)	1.35 (0.22)	1.92 (0.26)	1.67 (0.26)	1.71 (0.17)
Latencies (fast):												
Wave I	1.89 (0.03)	1.83 (0.02)	1.77 (0.02)	1.76 (0.03)	1.86 (0.03)	1.79 (0.02)	1.73 (0.02)	1.75 (0.02)	1.9 (0.02)	1.82 (0.02)	1.78 (0.02)	1.75 (0.02)
Wave II	2.62 (0.05)	2.53 (0.04)	2.47 (0.04)	2.44 (0.04)	2.6 (0.03)	2.51 (0.02)	2.43 (0.03)	2.37 (0.04)	2.68 (0.04)	2.53 (0.04)	2.43 (0.04)	2.33 (0.05)
Wave III	3.53 (0.05)	3.42 (0.03)	3.38 (0.03)	3.34 (0.03)	3.47 (0.03)	3.37 (0.03)	3.34 (0.02)	3.31 (0.02)	3.55 (0.05)	3.45 (0.05)	3.4 (0.05)	3.36 (0.04)
Wave IV	4.48 (0.06)	4.37 (0.06)	4.26 (0.06)	4.23 (0.05)	4.45 (0.04)	4.33 (0.04)	4.24 (0.03)	4.19 (0.03)	4.52 (0.06)	4.35 (0.06)	4.27 (0.05)	4.19 (0.05)
Amplitudes (slow):												
Wave I	1.1 (0.25)	1.73 (0.28)	2.51 (0.31)	3.28 (0.44)	1.13 (0.24)	1.78 (0.28)	2.38 (0.31)	3.05 (0.45)	1.22 (0.15)	1.73 (0.21)	2.27 (0.21)	2.83 (0.27)
Wave II	2.54 (0.36)	3.2 (0.26)	4.16 (0.39)	4.66 (0.48)	2.86 (0.16)	3.59 (0.26)	4.02 (0.27)	3.92 (0.4)	2.34 (0.2)	3.21 (0.28)	3.4 (0.36)	3.89 (0.34)
Wave III	1.73 (0.23)	2.57 (0.2)	3.21 (0.16)	4.22 (0.31)	1.82 (0.17)	2.75 (0.23)	3.53 (0.25)	4.05 (0.23)	1.08 (0.27)	1.41 (0.3)	2.32 (0.37)	2.7 (0.46)
Wave IV	0.83	1.6	1.45	1.22	0.81	1.41	1.38	1.64	1.14	1.93	1.82	1.66

	(0.17)	(0.17)	(0.22)	(0.16)	(0.15)	(0.19)	(0.12)	(0.1)	(0.23)	(0.32)	(0.34)	(0.24)
Latencies (slow):												
Wave I	1.94 (0.03)	1.85 (0.03)	1.78 (0.03)	1.74 (0.03)	1.88 (0.02)	1.8 (0.02)	1.73 (0.02)	1.7 (0.02)	1.9 (0.03)	1.84 (0.02)	1.75 (0.02)	1.69 (0.02)
Wave II	2.65 (0.05)	2.54 (0.04)	2.47 (0.04)	2.43 (0.03)	2.6 (0.03)	2.5 (0.03)	2.44 (0.03)	2.38 (0.04)	2.65 (0.05)	2.51 (0.04)	2.44 (0.03)	2.33 (0.05)
Wave III	3.54 (0.04)	3.44 (0.03)	3.36 (0.03)	3.29 (0.03)	3.49 (0.03)	3.39 (0.03)	3.3 (0.03)	3.24 (0.03)	3.57 (0.05)	3.46 (0.05)	3.34 (0.04)	3.27 (0.04)
Wave IV	4.52 (0.05)	4.35 (0.05)	4.26 (0.05)	4.16 (0.04)	4.51 (0.05)	4.31 (0.05)	4.19 (0.04)	4.1 (0.05)	4.5 (0.06)	4.31 (0.05)	4.19 (0.05)	4.08 (0.04)

Table A8: Means (and SEs) for click ABR results in single KO and WT mice as presented in Chapter 5.

Mean (+/- SE)	8ms probe delay		20ms probe delay		50ms probe delay	
	Double KO	WT	Double KO	WT	Double KO	WT
Probe Click:						
Amplitudes						
Wave I	0.34 (0.05)	0.37 (0.15)	0.57 (0.09)	0.39 (0.1)	0.6 (0.14)	0.77 (0.19)
Wave II	1.11 (0.17)	1.06 (0.14)	1.69 (0.18)	1.93 (0.25)	2.95 (0.26)	3.08 (0.42)
Wave III	0.28 (0.06)	0.5 (0.07)	0.5 (0.12)	1.11 (0.21)	1.2 (0.21)	2.36 (0.24)
Wave IV	0.43 (0.13)	0.56 (0.12)	0.35 (0.08)	0.28 (0.1)	0.5 (0.15)	0.42 (0.11)
Latencies						
Wave I	1.6 (0.08)	1.87 (0.1)	1.68 (0.06)	1.81 (0.08)	1.7 (0.05)	1.84 (0.07)
Wave II	2.51 (0.06)	2.74 (0.08)	2.58 (0.04)	2.57 (0.09)	2.41 (0.05)	2.53 (0.09)
Wave III	3.61 (0.09)	3.65 (0.08)	3.61 (0.06)	3.55 (0.08)	3.39 (0.03)	3.45 (0.08)
Wave IV	4.65 (0.09)	4.57 (0.08)	4.56 (0.11)	4.41 (0.1)	4.3 (0.04)	4.36 (0.08)
Reference click:						
Amplitudes						
Wave I	1.44 (0.24)	1.92 (0.34)	1.46 (0.18)	1.84 (0.4)	1.22 (0.18)	1.82 (0.38)
Wave II	2.77 (0.27)	3.06 (0.36)	2.99 (0.3)	3.04 (0.38)	2.89 (0.32)	3.09 (0.35)
Wave III	1.76 (0.25)	2.99 (0.36)	1.73 (0.27)	2.77 (0.35)	1.89 (0.26)	2.85 (0.33)
Wave IV	0.61 (0.07)	0.77 (0.12)	0.43 (0.11)	0.91 (0.15)	0.6 (0.11)	0.82 (0.13)
Latencies						
Wave I	1.67 (0.05)	1.82 (0.07)	1.69 (0.03)	1.79 (0.07)	1.69 (0.03)	1.83 (0.07)
Wave II	2.39 (0.03)	2.5 (0.08)	2.41 (0.03)	2.47 (0.07)	2.38 (0.04)	2.49 (0.07)
Wave III	3.29 (0.02)	3.36 (0.08)	3.31 (0.03)	3.34 (0.08)	3.28 (0.03)	3.37 (0.08)
Wave IV	4.14 (0.02)	4.23 (0.08)	4.21 (0.05)	4.19 (0.08)	4.15 (0.05)	4.23 (0.08)

Table A9: Means (and SEs) for masker-probe ABRs in double KO and WT mice as presented in Chapter 5.

Mean (SE)	KIAA KO	WT	KIAA-Like
Probe Click:			
Amplitudes			
Wave I	0.82 (0.1)	0.63 (0.13)	0.69 (0.13)
Wave II	1.22 (0.17)	1.6 (0.12)	1.06 (0.17)
Wave III	0.78 (0.15)	0.87 (0.14)	0.49 (0.14)
Wave IV	1.01 (0.19)	0.76 (0.11)	0.96 (0.29)
Latencies			
Wave I	1.85 (0.06)	1.84 (0.03)	1.81 (0.04)
Wave II	2.78 (0.08)	2.7 (0.04)	2.7 (0.05)
Wave III	3.7 (0.08)	3.62 (0.04)	3.63 (0.05)
Wave IV	4.74 (0.1)	4.58 (0.05)	4.64 (0.06)
Reference click:			
Amplitudes			
Wave I	1.94 (0.31)	1.76 (0.22)	1.88 (0.23)
Wave II	2.86 (0.2)	2.91 (0.2)	2.82 (0.18)
Wave III	2.37 (0.16)	2.31 (0.19)	1.63 (0.28)
Wave IV	1.31 (0.19)	1.51 (0.24)	1.81 (0.38)
Latencies			
Wave I	1.85 (0.06)	1.84 (0.03)	1.81 (0.04)
Wave II	2.78 (0.08)	2.7 (0.04)	2.7 (0.05)
Wave III	3.7 (0.08)	3.62 (0.04)	3.63 (0.05)
Wave IV	4.74 (0.1)	4.58 (0.05)	4.64 (0.06)

Table A10: Means (and SEs) for masker-probe ABRs in single KO and WT mice as presented in Chapter 5.